

**UCLA**

**UCLA Electronic Theses and Dissertations**

**Title**

Discovery and Characterization of Radiation Mitigator Yel002

**Permalink**

<https://escholarship.org/uc/item/45f395pv>

**Author**

Rivina, Yelena Olegovna

**Publication Date**

2013

Peer reviewed|Thesis/dissertation

UNIVERSITY OF CALIFORNIA

Los Angeles

Discovery and Characterization of Radiation Mitigator Yel002

A dissertation submitted in partial satisfaction of the  
requirements for the degree Doctor of Philosophy  
in Molecular Toxicology

by

Yelena Olegovna Rivina

2013

© Copyright by  
Yelena Olegovna Rivina

2013

## ABSTRACT OF THE DISSERTATION

Discovery and Characterization of Radiation Mitigator Yel002

by

Yelena Olegovna Rivina

Doctor of Philosophy in Molecular Toxicology

University of California, Los Angeles, 2013

Professor Robert H. Schiestl, Chair

The possibility of a radiation disaster from a nuclear detonation or accident has existed for over 50 years. This concern has been the the dominating influence of much of the basic research in radiobiology in the 1950-60s. The recent Fukushima accident was yet another reminder that of the dire need to develop novel therapies against radiation-induced toxicities. This dissertation describes our efforts to develop the novel radiation mitigator Yel002 starting from a phenotypic yeast-based DEL screen to the elucidation of its potential mechanism of action. Yel002 is small, biologically active, drug-like molecule that mitigates on average 75% of deaths in mice following an LD100/30 irradiation when administered at 24, 48, 72, 96, and 120 hours after the



exposure. Treatment with Yel002 following IR accelerates the recovery of the hematopoietic and immune systems possibly by preventing radiation-induced cell death and senescence of bone marrow stem cells and progenitors. Toxicity has not been observed in either *in vitro* or *in vivo* administrations. Overall, the Yel002 compound has much potential to become a stockpile therapy for radiation-induced lethality and cancer: it is highly effective when administered up to 24 hours post exposure, it reduces radiation-induced sequelae such as leukemia and appears to have an acceptable toxicity profile.

The Dissertation of Yelena Olegovna Rivina is approved.

William McBride

Hillary Godwin

Nicholas Cacalano

Robert H. Schiestl, Chair

University of California, Los Angeles

2013

*To my loving parents, Oleg and Lidiya,  
who have made great sacrifices for my success.*

## TABLE OF CONTENTS

Abstract of the Dissertation .....	ii
Acknowledgements .....	viii
VITA .....	xi
<b>Chapter 1: Introduction.....</b>	<b>1</b>
Background.....	2
Radiation Toxicity .....	4
Development of Radiation Mitigation Compound Yel002 .....	8
<b>Chapter 2: Cell cycle dependence of ionizing radiation-induced DNA deletions and antioxidant radioprotection in <i>Saccharomyces cerevisiae</i> .....</b>	<b>22</b>
Abstract.....	23
Introduction .....	23
Materials and Methods .....	24
Results .....	24
Discussion.....	26
References .....	28
<b>Chapter 3: Yeast DEL assay detects protection against radiation induced cytotoxicity and genotoxicity – adaptation of a microtiter plate version.....</b>	<b>30</b>
Abstract.....	31
Introduction .....	31
Materials and Methods .....	33
Results .....	34
Discussion.....	35
References .....	37

<b>Chapter 4: Yeloo2 mitigates acute hematopoietic radiation injury in mice.....</b>	<b>44</b>
Abstract.....	45
Introduction .....	45
Materials and Methods .....	49
Results .....	60
Discussion.....	67
References .....	97
<b>Chapter 5: Prevention of DNA double-strand breaks induced by radioiodide-(131)I in</b>	
<b>FRTL-5 thyroid cells .....</b>	<b>101</b>
Abstract.....	102
Introduction .....	102
Materials and Methods .....	103
Results .....	104
Discussion.....	106
References .....	107
<b>Chapter 6: Mouse Models for Efficacy Testing of Agents against Radiation</b>	
<b>Carcinogenesis — A Literature Review.....</b>	<b>108</b>
Preface .....	109
Abstract.....	115
Introduction .....	116
Materials and Methods .....	116
Results .....	117
Discussion.....	117
References .....	135
<b>Conclusion .....</b>	<b>153</b>

## TABLE OF CONTENTS

Abstract of the Dissertation.....	ii
Acknowledgements.....	viii
VITA.....	xi

### Chapter 1: Introduction

Background.....	1
Radiation Toxicity .....	3
Development of Radiation Mitigation Compound Yeloo2.....	7

### Chapter 2: Cell cycle dependence of ionizing radiation-induced DNA deletions and antioxidant radioprotection in *Saccharomyces cerevisiae*

Abstract.....	21
Introduction.....	21
Materials and Methods.....	22
Results.....	22
Discussion.....	24
References.....	26

### Chapter 3: Yeast DEL assay detects protection against radiation induced cytotoxicity and genotoxicity – adaptation of a microtiter plate version

Abstract.....	28
Introduction.....	28
Materials and Methods.....	30
Results.....	31
Discussion.....	31
References.....	34

**Chapter 4:** Yeloo2 mitigates acute hematopoietic radiation injury in mice

Abstract.....41  
Introduction.....41  
Materials and Methods.....45  
Results.....56  
Discussion.....63  
References.....93

**Chapter 5:** Prevention of DNA double-strand breaks induced by radioiodide-(131)I in FRTL-5 thyroid cells

Abstract.....97  
Introduction.....97  
Materials and Methods.....98  
Results.....99  
Discussion.....101  
References.....102

**Chapter 6:** Mouse Models for Efficacy Testing of Agents against Radiation

Carcinogenesis – A Literature Review

Preface.....103  
Abstract.....109  
Introduction.....110  
Materials and Methods.....110  
Results.....111  
Discussion.....111  
Conclusion.....128  
References.....129

**Conclusion.....147**

## **ACKNOWLEDGEMENTS**

Firstly, I thank my advisor and committee chair, Dr. Robert Schiestl, this very thesis would not have existed were it not for his unfailing optimism in science, constant inspiration and for giving me the freedom to learn on my own. With equal degree of appreciation, I graciously thank the members of my committee, Dr. William McBride, Dr. Nicholas Cacalano, and Dr. Hillary Godwin; they have supported my efforts with expert advice, constructive criticism and held me to highest standards of scientific pursuit. I also offer a special thank you to my LabAspire mentor, Dr. Sydney Harvey, for her unfailing dedication to my success.

I gladly offer thanks to my fellow members of the Schiestl Lab who have helped me throughout out the years. Zhanna Sobol, Kurt Hafer, Zorica Scuric, Aya Westbrook, Lynn Yamamoto, Ramune Reiline, Katrin Hacke, and Akos Szacmary, all have mentored, taught and challenged me intellectually. Additionally, I thank my fellow lab mates Aaron Chapman, Daniel Malkin, Bill Mahon, Rosario “Chayo” Mutti, Maisie Pascual and my volunteer students Sarkis Aroyan, Filbert Rosli and Maggie Martin for always offering a helping hand and a good laugh. I also reserve and present special gratitude to my friend and lab mate, Mike Davoren, together we were able to overcome challenges and develop creative solutions. Lastly, I am very pleased to thank Dr. Peter Guida and Dr. Dudley Goodhead for the opportunity to attend the NASA Space Radiation Summer School and for inspiring my continued pursuit of science.

Funding was made possible by LabAspire Public Health Laboratory Director training fellowship (2008 – 2012). Experimental work was supported by University of



California at Los Angeles Center for Medical Countermeasures grant U19

AI067769/NIAID.

Chapter 2 includes an article reprinted from *Radiation Research* **173**, 802–808 (2010), entitled “Cell cycle dependence of ionizing radiation-induced DNA deletions and antioxidant radioprotection in *Saccharomyces cerevisiae*” by Kurt Hafer, Leena Rivina, and Robert H. Schiestl. Kurt Hafer did the conceptualization and planning of the work while I humbly contributed labor and result interpretations. Reprinted with permission from Radiation Research Society.

Chapter 3 is also an article reprinted from *Radiation Research* **174**, 719–726 (2010), entitled “Yeast DEL assay detects protection against radiation induced cytotoxicity and genotoxicity – adaptation of a microtiter plate version” by Kurt Hafer, Yelena Rivina, and Robert H. Schiestl. My contribution to this manuscript included development of large-scale irradiation methodology, labor and result interpretation. Likewise, reprinted kind permission from Radiation Research Society.

Chapter 4 is a manuscript in preparation summarizing the highlights of my doctoral work – development and validation of radiation mitigator Yel002. This work could not have been possible without contribution from Ewa Micewicz, Michael Davoren, William McBride, Mo Kang, Andrew Norris, Xiaolu Cai, Dongjo Chang, Gang Deng, Michael E. Jung, Josephine Ratikan, Angeline Dang, and of course, Robert H. Schiestl. I am also much obliged to Nick Cacalano for his helpful comments and experimental suggestions. Additionally, I acknowledge Robert Damoiseaux, Kenneth Bradley, Richard Gatti, Aria Eshraghi and Kwanghee Kim. I was responsible for organizing most of the experiments, experimental design, screening and writing of the

manuscript resulting from this work. I offer many thanks to Colin McLean and Tristan Baptist for their support and training in our animal facility.

Chapter 5 includes an article reprinted from *Endocrinology* 2011 Mar; 152(3): 1130-5, entitled “Prevention of DNA double-strand breaks induced by radioiodide-(131)I in FRTL-5 thyroid cells” by Jerome M Hershman, Armen Okunyan, Yelena Rivina, Sophie Cannon and Victor Hogen. This work was done in collaboration with the West Los Angeles Veterans Affairs Medical Center. My contribution to this work included conceptualization, methodology development and experimental design.

Chapter 6 begins with a Preface section providing additional data on the activity of Yel002 in prevention of radiation-induced leukemogenesis, and results from a high throughput proteomics experiment conducted in collaboration with Dr. Jonathan Erde, without whom we would still be groping aimlessly in the dark for some validation of our hypothesis. Dr. Alexandra Miller from AFFRI kindly provided the leukemogenesis data. My contribution to this work included conceptualization, rationale, experimental design and data interpretation. This section rationalizes the inclusion of the article entitled “Mouse Models for Efficacy Testing of Agents against Radiation Carcinogenesis – A Literature Review” published by *International Journal of Environmental Research and Public Health* **2013**, 10(1), 107-143.

## VITA

### Education and Training

*March 2013*

Master's of Public Health in Environmental Health Sciences, University of California, Los Angeles

*May-June 2012*

NASA Space Radiation Summer School

*March 2007*

Bachelors' of Science in Biology and Psychology, University of Denver

### Patents

- COMPOUNDS AND COMPOSITIONS FOR MITIGATING TISSUE DAMAGE AND LETHALITY (US2011/046451)
- ASSAYS FOR MUTAGENESIS DETECTION (US20110065131)
- THERAPEUTIC AGENTS INTENDED TO MITIGATE/TREAT SYMPTOMS OF GENOMIC INSTABILITY DISORDERS (F5049-01201)

### Teaching

*January 2013*

Promotion to Teaching Fellow

*Spring 2012, 2013*

"Impact of Modern Lifestyle on Health": Independently developed and taught a seminar for undergraduates covering a diverse set of topics ranging from sleeping patterns to toxic exposures and their effects on human health.

*Fall – Winter 2012, 2013*

"Global Environment, Cluster Course": Designed exams, writing assignments and led discussion sections of undergraduate students.

*Spring 2011*

"Environmental Geology": Assisted in writing assignment and laboratory exercise design for undergraduates.

### Publications and Conference Presentations

1. Hershman, J.M., et al., *Prevention of DNA double-strand breaks induced by radioiodide-(131)I in FRTL-5 thyroid cells*. *Endocrinology*, 2011. **152**(3): p. 1130-5.
2. Hafer, K., Y. Rivina, and R.H. Schiestl, *Yeast DEL assay detects protection against radiation-induced cytotoxicity and genotoxicity: adaptation of a microtiter plate version*. *Radiat Res*, 2010. **174**(6): p. 719-26.

3. Hafer, K., L. Rivina, and R.H. Schiestl, *Cell cycle dependence of ionizing radiation-induced DNA deletions and antioxidant radioprotection in Saccharomyces cerevisiae*. *Radiat Res*, 2010. **173**(6): p. 802-8.
4. Kim, K., et al., *High throughput screening of small molecule libraries for modifiers of radiation responses*. *Int J Radiat Biol*, 2011.
5. Rivina L. and Schiestl RH. Mouse Models for Efficacy Testing of Agents Against Radiation Carcinogenesis –A Literature Review. *Int. J. Environ. Res. Public Health* **2013**, *10*(1), 107-143.
6. *Radiation mitigating compounds reduce radiation induced lethality and leukemia*. Yelena Rivina, R. H. Schiestl, University of California, Los Angeles, USA. 14<sup>th</sup> International Congress of Radiation Research. Warsaw, Poland, August 28 – September 1, 2011.
7. *Radiation mitigators: yeast-based screen identifies drug candidates*. Yelena O. Rivina, Robert H. Schiestl, University of California, Los Angeles, Los Angeles, CA. 56<sup>th</sup> Annual Meeting Radiation Research Society. Maui, Hawaii. September 25 – 29, 2010.
8. *NEXT GENERATION DEL ASSAY: RAPID AND ACCURATE ASSESSMENT OF TOXICITY*. Y. Rivina and R. H. Schiestl. Environmental Health Sciences, University of California, Los Angeles, Los Angeles, CA. Washington DC. March 6 – 10, 2011.

## Awards

### *June 2012*

NASA Space Radiation Summer School Outstanding Achievement Award  
 NASA BNL Summer Studies Slide Contest (3<sup>rd</sup> Place)

### *October 2008 – June 2012*

Public Health Laboratory Director Training Fellowship

### *May 2011*

14<sup>th</sup> International Congress of Radiation Research Travel Award sponsored by NIAID

### *September 2007*

Atlantic Richfield Company Fellowship (UCLA/SPH)

## **CHAPTER 1: Introduction**

## **Background**

Over the past 60 years the threat of exposure to ionizing radiation, which may include alpha particle and neutron radiation and electromagnetic gamma and X-rays [1], with potentially grave outcomes has increased dramatically. Global spread of nuclear energy reactors, nuclear weapons proliferation and the increase in funding and complexity of terrorist organizations with access to nuclear materials have all contributed to the amplification of exposure risk [2]. There have been concurrent efforts to develop therapies to counteract the damaging effects of radiation and much research has been done on antioxidants, melatonin, Tempol™ and Amifostine™ (WR2721). Currently, there are no safe and effective U.S. Food and Drug Administration (FDA)-approved radiation protectants and mitigators intended for use in case of a nuclear emergency or accident. Efficacy of the known agents is limited and their toxicity profiles are, in some instances, prohibitive for use on a population-based scale. Even the most widely studied and FDA-approved radiation-modulating drug, Amifostine, fails as a radioprotectant outside of a clinical setting due to severe side effects such as vomiting, allergic reactions and hypotension [3]. Most of the drug therapies developed in the 1950's and 1960's are free radical scavengers and only render protection against initial DNA and cell damage when administered prior to, but not after radiation exposures [4]. Therefore these agents will have limited or no efficacy in cases of general population exposure when the earliest drug intervention will be hours after the initial irradiation.

The September 11, 2001 terror attack once again brought the need for radiation protectants and mitigators to the forefront of national security and importance. There

was a realization that a nuclear terrorist attack is highly plausible but the adequate medical treatment options for mass exposure are absent. In 2004 as a part of the Project Bioshield Act several Centers for Medical Countermeasures against Radiation (CMCRs), including one at UCLA, were created with direct guidance from the National Institute for Allergy and Infectious Diseases (NIAD) and support from the National Cancer Institute (NCI). One of the main objectives for these centers was the development of novel radiation protectants [5]. In fact, the Office of Science and Technology Policy and the Homeland Security Council established Weapons of Mass Destruction Medical Countermeasures Subcommittee in the Spring of 2003 established the “development of radiation prophylaxis agents” as its top priority [6].

Since that time some progress has been made and a few novel radiation protection agents have been developed, none, however, have yet secured an FDA approval for the use as radiation mitigating therapies in cases of mass exposure. Among these novel agents are antibiotics tetracycline and flouoroquinolone [2], cell cycle modifying kinase inhibitor Ex-Rad™ [7], Toll-like receptor 5/NF-κB pathway stimulator derived from *Salmonella* [8], effectors of superoxide dismutase (SOD) pathways, select cytokines, and agents that decrease cytokine-activated cell death [9]. The most recently published agent HemaMax™ is a recombinant human interleukin-12 that mitigates radiation-induced death within the hematopoietic acute radiation syndrome doses [10].

The work described in this dissertation outlines our efforts to discover and characterize a novel radiation mitigator Yel002. This drug is currently being evaluated for fast-track development by the National Institute of Allergy and Infectious Diseases

as one of the potential stockpile drug therapies intended to mitigate and treat radiation-induced toxicity.

### *Radiation Toxicity*

Much of what is known about the effects of ionizing radiation on biological systems comes from animal studies, accounts of accidental exposures and *in vitro* experiments with irradiated cells [11]. These *in vitro* experiments have demonstrated that actively proliferating cells—such as stem cells in the hematopoietic system and intestinal epithelia—are much more sensitive to the effects of IR and their destruction is of much more consequence: potentially leading to death or carcinogenesis [12,13]. For example, a dose of 100Gy is necessary to destroy cell function in a non-proliferating cell

such as a muscle cell; less than 2Gy would be necessary to induce death in a proliferating cell. Loss of ability to reproduce indefinitely—reproductive death— in actively dividing tissues is equivalent to other death events such as necrosis or apoptosis [14].

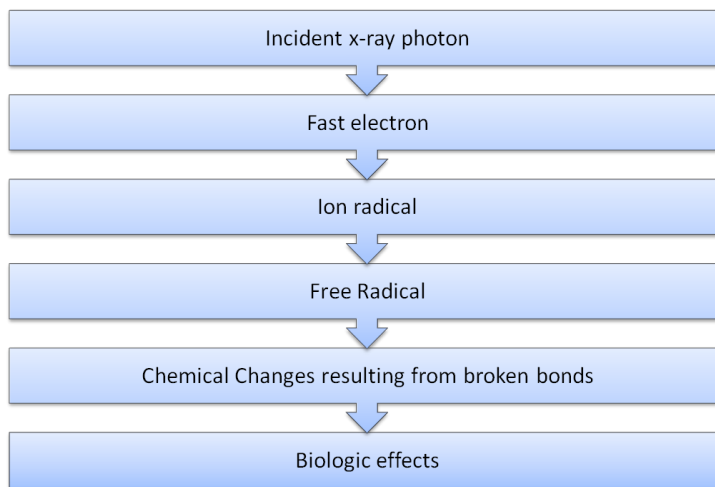


**Figure 1 Chain of events leading to a biologic response after exposure to an ionizing radiation event.**

There are two ways in which radiation affects the cell: direct and indirect action. In direct action photons or charged particles hit the targets within the cell and ionize it. In indirect action radiation generates free radicals within the cell that travel to the target such as the DNA. As ionizing radiation is absorbed by the biologic material the incident



rays ionize atoms with which they come into contact releasing fast electrons. These electrons in turn collide with water molecules generating an ion radical ( $\text{H}_2\text{O}^+$ ) and again with another water molecule to generate a highly reactive hydroxyl radical ( $\text{OH}\cdot$ ) which can diffuse and damage the DNA indirectly. Approximately two thirds of DNA damage associated with IR is attributed to hydroxyl radicals [14].

A large body of evidence points to the nucleus and mostly to DNA, as the main target and cause of cell killing following radiation exposure. Ionizing radiation-induced DNA damage may be base damage, DNA-protein cross-links, single-strand breaks (SSB) and double-strand breaks (DSB) [15]. Single-strand breaks are of little biological significance as the cell using the opposite strand as a template quickly and accurately repairs them. Of more serious consequence is a break in the two strands or breaks on opposite strands separated by only a couple of base pairs. This damage scenario can lead to the chromosome breaking in two and is believed to result in apoptosis or necrosis of the cell, carcinogenesis and/or mutations [14,16,17]. Number of DSBs increases proportionally with irradiation dose and can be induced by either free radicals or direct ionization. If not properly repaired DSBs may give rise to chromosome aberrations (one broken sister chromatid) and chromatid aberrations (two strands of chromatin are broken). These aberrations may either lead to cell death or carcinogenesis [12,13].

In addition to immediate induction of chromosomal aberrations and mutations, some cells retain a persistent genomic instability phenotype, defined as an increased rate of genetic alterations that may be observed in multiple progeny generations of the exposed parent cells. Such delayed effects also may include chromosomal aberrations,

micronuclei, gene mutations, microsatellite instability, changes in ploidy and decreased plating efficiency [15]. Loss of genome stability as described above is one of the recognized hallmarks of cancer [12,13,15,16,18].

At the whole organism level, exposure to ionizing radiation presents a serious risk and often multiple organ systems are affected. The severity of the injury and the ultimate prognosis is related to the total dose and the timing of the exposure [19-21]. In most mammals, including humans, three distinct causes of eventual death during the acute phase might be identified: cerebrovascular syndrome, gastrointestinal syndrome, and the hematopoietic syndrome. Within 24-48 hrs after total-body irradiation in excess of 100Gy death occurs due to severe damage of the cerebrovascular system with the suggested cause of death as the pressure buildup due to leakage of small vessels within the skull; gastrointestinal tract and the hematopoietic system are of course damaged but death occurs before the characteristic pathology is expressed.

In the even of whole body irradiation dose of 10Gy or more, death occurs within 3-10 days due to the gastrointestinal syndrome: depopulation of the intestinal epithelia due to necrosis or mitotic arrest of mucosal cells. Stem cells located in the crypts of the intestinal epithelia fold are ablated at this dose and eventually the entire villi population covering the tract is sloughed off without replacement; at the time of death the intestinal tract is usually completely free of cells.

At the doses of 2.5 to 5 Gy the hematopoietic syndrome sets in: actively proliferating precursor cells in the bone marrow are sterilized and consequently no new red and white blood cells as well as platelets are produced [22,23]. As the mature blood cells begin to die off without replacement a critical point is reached within a couple of

weeks after irradiation: up to 30-60 days in humans. However with a bone marrow transplant and infection control with antibiotics survival is still plausible [14].

Delayed effects, as described earlier, in the affected tissues are usually genomic instability leading to neoplastic malignancies. While the exact mechanism of radiation carcinogenesis is not yet entirely understood, ionizing radiation is considered a Group 1 carcinogen (known human carcinogen) by the Environmental Protection Agency and is often recognized as a “universal carcinogen,” meaning that it might induce cancer in any tissue of most species at all ages [13]. For example in leukemia, the most studied IR-induced neoplasm, incidence increases after both total body and localized radiation exposure [11,24]. Other cancers that have been linked to radiation-exposures are thyroid, breast, lung, bone and skin [14]. Huang *et al.* proposed that a failure to appropriately respond to ionizing radiation assault in the first place is a very important contributor to radiation-induced carcinogenesis [16].

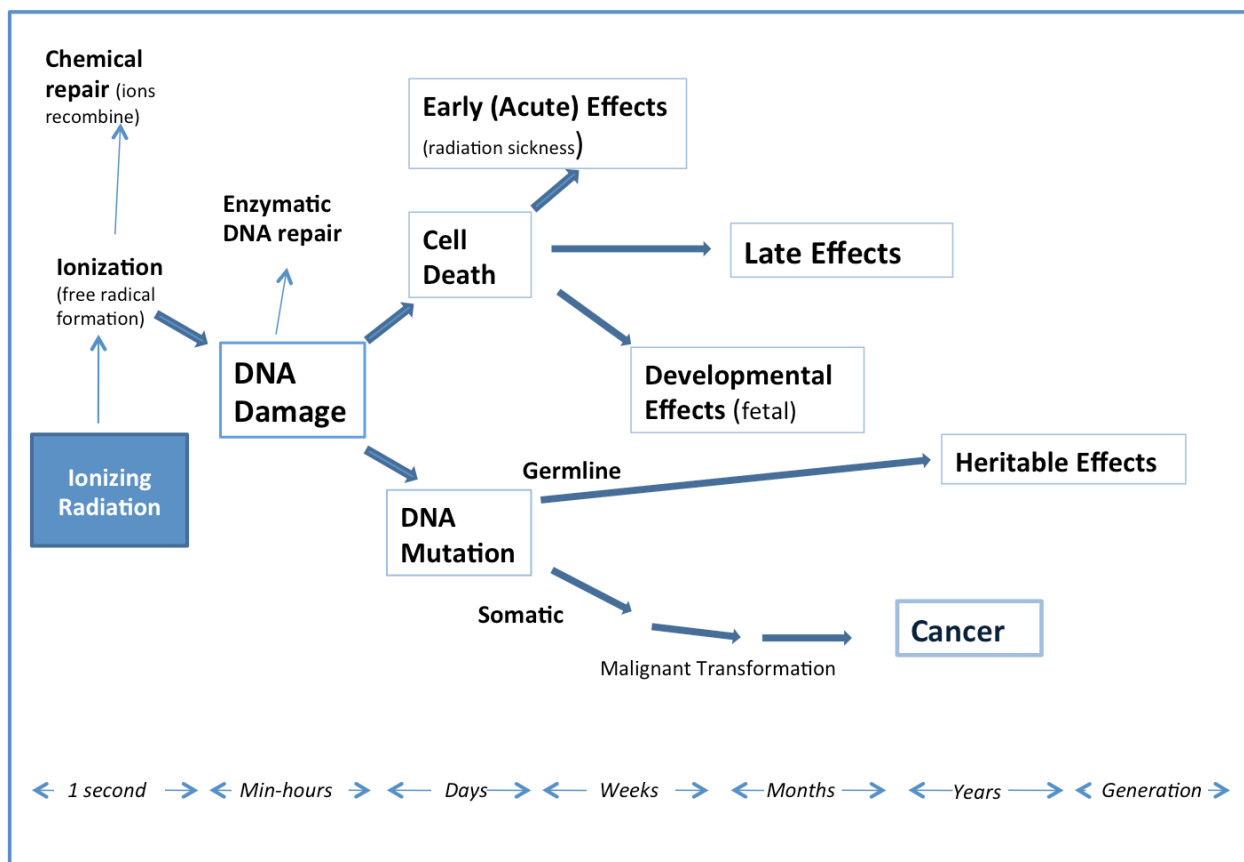


**Figure 2 Classic Paradigm of Radiation Injury": summary of generally accepted sequence of biological events following exposure to ionizing radiation. Illustration adopted from *Radiobiology for the Radiologist* (2006).**

## Development of Radiation Mitigation Compound Yel002

### *DEL Assay*

Ideally, a radiation-modulating drug does not only counteract early-onset radiation effects (i.e. cytotoxicity), but also prevents or ameliorates late-onset radiation effects (i.e. persistent genotoxicity and carcinogenesis). This carries an important pharmacological implication when it comes to the discovery and development of such drugs — a methodology aimed at uncovering radiation-modulating compounds must simultaneously detect both consequences of radiation exposure. There are a few high throughput assays reported in the literature that measure either cytotoxicity or

genotoxicity induced by ionizing radiation, but not both. Carmichael *et al.* developed one of the first cytotoxicity microwell semi-automatable assays by utilizing a tetrazolium-based compound MTT to measure cell proliferation capacities following IR [25]. A rapid genotoxicity  $\gamma$ -H2AX screening method tested five known radioprotectors against DNA breaks following IR [26]. Finally a method that detects antioxidant protection against IR-induced ROS was also recently described [27]. However, until the yeast-based DEL assay [28-42], there has never existed a method that could simultaneously demonstrate a given compound's ability to reduce IR-induced cytotoxicity and genotoxicity.

The yeast DEL assay in any of its adaptations is a unique tool that can simultaneously detect not only the protective and mitigating qualities against radiation-induced cell killing, but it can also evaluate the compound's ability to protect against genetic instability. Amenable to high throughput format and adaptable to a variety of radiation studies, this versatile assay can also be used to identify radiation sensitizers that are important for radiation oncology or in drug screens aimed at uncovering anti-mutagenic agents.

The original DEL assay construct comprises an inserted plasmid containing the *LEU2* gene and an internal *his3* fragments with terminal deletions at 3' and 5' of the *his3* allele at the *HIS3* locus resulting in a 6kb internal disruption flanked by two alleles of a *his3* duplication. The two *his3* alleles share 400bp of homology and can recombine to a functional *HIS3*<sup>+</sup> allele through intrachromosomal recombination [43]. A DEL (DNA deletion) event constitutes a restoration to the *HIS3*<sup>+</sup> phenotype after the deletion of an internal disruption. The assay in itself is very simple to use: RS112 cells uncover

intrachromosomal recombination events leading to gene reversions (called DEL events) upon treatment with compounds or agents of interest (e.g. UV and  $\gamma$ -rays, alkyl halides, etc). Plating treated RS112 cells onto complete media agar plates (+13) shows the extent of survival, and plating these cells onto selective histidine-deficient (-His) plates shows the number of reversion events. The DEL frequency is calculated as a fraction of revertants to the overall survival numbers—the degree of induced genetic instability (genotoxicity). A single DEL assay provides a methodology to independently assess both the cytotoxic and the genotoxic potential of the agents of interest. Over a period of 22 years the DEL assay has tested positive a variety of carcinogens, both mutagenic and non-mutagenic, and showed a much higher accuracy in detection of carcinogens compared to the currently-accepted gold-standard Ames assay [28-37,39-42,44].

As a part of our Center for Medical Countermeasures Against Radiation (CMCR), forming the UCLA Center for Biological Radiation Mitigators supported project, we further modified the DEL assay to suit the drug discovery needs of the program.

### *High Throughput Adaptation*

Hontzeas *et al.* modified the assay from its original agar-based format to a liquid microtiter high-throughput format and first adapted it for toxicity screening of large chemical libraries, capitalizing on the main DEL assay principle of gene reversion upon exposure to genotoxic events or agents [45]. A colorimetric indicator MTS tetrazolium salt (3-(4,5-dimethylthiazol-2-y)-5-(3-carboxymethoxyphenyl)-2-(4-sulphophenyl)-2H-tetrazolium, inner salt), that measured cell proliferation and reversion to the HIS3+

allele as a change in relative absorbance after an overnight incubation replaced the agar-based growth and colony counting to calculate the DEL events.

To achieve a simultaneous screen for geno- and cytotoxicity we divided the microwell plates (96- or 384-wells) into two: one side with complete +13 media and the other one with selective –His media. Into each well we dispensed 10,000 RS112 cells, set up a quadruplicate replication of the treatment and control wells and added MTS indicator. Growing cells metabolized MTS and produced a soluble product formazan detectable at 490 nm; thus, an increasing number of proliferating cells proportionally increased the amount of formazan in the growth media. Each side of the plates had treatment groups present as quadruplicates on each side of the plate in addition to untreated controls (Figure 1). Averaging of the absorbance of the four treatment wells in +13 media and dividing by the average absorbance in control wells yielded the extent of cytotoxicity. Dividing the averaged absorbance in –His media by the corresponding +13 treated wells uncovered the extent of genotoxicity; changes in the ratios of treated versus untreated wells yielded the fold-changes in the HIS+ growth. A Student's *t*-test comparing fold changes between groups determined significance.

The adaptation to the new high-throughput method was successful and turned out to be sensitive to various previously tested and newly tested toxic compounds with a high correlation between the agar-based and the liquid-based assays. In almost all cases the concentrations of the compounds detected by the HTS were the same as those detected by the agar-based assay [45].

The DEL assay in its HTS format provided a rapid, less labor-intensive, and more economic screening method of a large numbers of compound libraries for geno-

and cytotoxicities. However, the DEL high-throughput version suffered from concerns common to all high-volume rapid tests—it was less sensitive at lower concentration and had a higher false positive rate; the agar-based assay still proved to be superior in sensitivity to genotoxicity and was more accurate in differentiating between true genotoxicity versus false positives that are possible if the compounds are highly cytotoxic [45]. However, despite its minor fault the new assay adaptation proved to be uniquely suited for our search for radioprotectors and radiation mitigators.

Chapter 2 of this dissertation describes another essential improvement to the DEL assay was the identification of the most sensitive cell cycle stage to IR-induced geno- and cytotoxicity and antioxidant protection in the RS112 *Saccharomyces cerevisiae* cells [46]. The purpose of this optimization was to come as close as possible to the physiological sensitivities of IR-affected tissues such as the bone marrow and various epithelia [47,48].

Proportions of cells in each cell cycle stage were determined microscopically by a visual examination of samples taken from a continuous 30 hr liquid RS112 culture: from 0 to 4hrs cells turned out to be in the G<sub>0</sub>/G<sub>1</sub> stage, at 4hrs cells were predominantly in G<sub>2</sub>/S and after that cultures reverted to being predominantly G<sub>0</sub>/G<sub>1</sub>. Cells in G<sub>2</sub>/S were the most sensitive to radiation-induced cell-killing and DEL induction thus supporting similar observations in mammalian *in vitro* studies [49]. Of note, antioxidants L-ascorbic acid and DMSO protected cells against IR-induced DNA deletions in lag and early exponential stages but not in the non-dividing stationary cells. We concluded that the most sensitive phases of the cell cycle were also the phases at which radioprotection agents were most beneficial.



The implications for these findings are rather significant when it comes to developing radiation-modulating drugs for human and animal application: most sensitive tissues to IR-induced damage are cells that are not stationary G<sub>0</sub> cells but those that are actively proliferating, thus, allowing us to mimic even closer *in vitro* the events happening *in vivo* during and after IR exposure. The data obtained from these studies identified an optimal window of sensitivity to detect the most potent and most relevant radiation protectors in our screen for radiation protecting and mitigating drugs.

#### *HTS DEL utilization in radioprotection screening*

Incorporating the two innovations in the DEL assay we set out to verify that the assay was able to correctly identify radiation modulating compounds: known radiation protectors and synergistic sensitizers [50]. At the onset of these studies we ascertained that if the assay would be amenable to such a task we would then have a very powerful pharmacological tool.

Chapter 3 of this dissertation describes how based on the microtiter version of the DEL assay we created yet another effective DEL system for pharmacological and toxicological applications. The premise of this particular DEL HTS is the same as that of the toxicity-screen DEL HTS but it required a slight adaptation to incorporate ionizing radiation. First, the microwell-based DEL experiments demonstrated an incremental increase in DEL reversions and cell killing with an increasing  $\gamma$ -radiation exposure dose from 0 to 2000 Gy to verify the assay's sensitivity to radiation-induced toxicities in a microwell format. As with the original microwell adaptation, we have divided the microtiter plate into two regions (+13 and -His media), have allowed for a

quadruplicate well replication of the compound of interest being tested, and included treatment-free but irradiated controls. An additional modification was an inclusion of non-irradiated controls (Figure 1). RS112 cells bearing the DEL construct were dispensed into the wells of a microtiter plate after the addition of the appropriate media and compounds, irradiated, and followed by MTS addition. Reading of plates at 490 nm after an overnight incubation revealed the extent of cytotoxicity and genotoxicity by assessing survival in both media types for irradiated and un-irradiated controls and by comparing these read-outs with the drug-treated wells. Statistical significance was determined by comparing the relative absorbance changes in the wells as compared to controls [45,50].

After establishing an optimal induction dose at 2000 Gy, we then set out to evaluate the five known radioprotectors: N-acetyl-L-cysteine, L-ascorbic acid, DMSO, Tempol, and Amifostine, and one sensitizer 5-bromo-2-deoxyuridine (Figure 3). Our novel DEL design was able to correctly detect compounds that are radiation protectors and sensitizers and was able to almost perfectly correlate with the more-sensitive agar-based method. Thus, our new assay was able to accurately predict the previously-established behavior of the selected compounds and was therefore applicable as a high throughput screen with chemical libraries in search of novel radiation protection, mitigating and sensitizing agents.

### *In search of novel radiation drugs*

In the world of high-throughput assays for radiation protection, most of the assays are aimed only at identifying chemical agents that are capable of reducing

radiation-induced cell killing [25]. There also exists a method for rapidly establishing single and double DNA strand breaks with a  $\gamma$ H2AX assay [26]. However, none of the methods reported so far could simultaneously and rapidly identify both radiation-induced cytotoxicity and genotoxicity. This unique feature of the DEL assay renders it as the only methodology perfect for the use in the pharmacological search for radiation protectors, mitigators and sensitizers. The assay allows for a rapid screen of thousands of compounds from a variety of different chemical libraries and a selection system for compounds based on two independent endpoints: protection against IR-induced cell-killing and protection from genetic instability (determined as the reduction of DEL recombination frequencies). To differentiate between the two types of protections, as this assay picks up both mitigators and protectors, another DEL adaptation was developed in an agar-based method when there was a need to specifically select for radiation mitigating compounds.

The sum of DEL assay modifications that rendered it capable of uncovering radiation protectors, mitigators and sensitizers was a culmination of our optimization efforts. The system allows for a large volume high-throughput screen of chemical libraries capable of screening 384 compounds in 24 hrs in a relatively inexpensive setting with a high correlation between the activity in the DEL assay and mammalian assays *in vitro* and *in vivo*. This novel assay carried over the same design as was used to test radiation protectors with only a modification in the data processing for accuracy. Now the hits revealed their significance by comparing the relative potency of these hits to each other with a z-factor: an average of the specific treatment group read-out was compared to the overall plate average for the survival and recombination (DEL)[51].

Armed with a new and powerful tool we have been able to screen roughly 5,000 compounds in a short period of time. From the libraries that we have screened, approximately six positive hits for every 1000 compounds were identified in our HTS (*Rivina et al.* unpublished data). A radioprotective hit was generally a compound that showed an increase in survival (+13) z-factor of  $\geq 2$ , a DEL z-factor of  $\leq -2$ , and a gene reversion (-His) score of  $\leq -2$ . Positive hits from the initial screen were assembled into a new microtiter plate and re-screened. Roughly 17% were confirmed as true hits and studied further.

Subjecting positive hits to further scrutiny using the agar-based DEL radiation assay confirmed about 20% of the hits. In this test for radioprotection qualities yeast cells were pre-incubated and irradiated in the presence of the compound and then plated. Alternatively, we assessed the compound's mitigating potency by irradiating untreated cells and then adding the compounds of interest at various time points (i.e. 0, 10, 20, 30, 60 min). Our HTS screen does not distinguish between protectors and mitigators—because the cells are irradiated in the presence of the compounds and are incubated with them afterwards we had to test them for both qualities in separate assays. Compounds that have shown either radioprotective or radiation-mitigating activity were further tested in animals with significant correlation between *in vitro* and *in vivo* studies. Chapter 4 of this dissertation describes the positive outcomes of our screening efforts.

## *Radiation Mitigator Yel002*

Utilizing the modified DEL HTS assay we have uncovered a novel radiation mitigator Yel002. Yel002 mitigates radiation induced lethality and genomic instability. Chapters 4 and 5 of this dissertation describe the experiments and the obtained results that have demonstrated Yel002's activity in a variety of *in vitro* models and a C3H mouse model. While results presented in Chapter 4 validate Yel002 as a mitigator of radiation-induced lethality, Chapter 5 demonstrates Yel002's potential to mitigate radiation-induced genomic instability. Additionally, preface to Chapter 6 provides supplementary data on Yel002's prophylaxis of radiation-induced leukemogenesis.

## References

1. Fernandes, P.P.; Maniar, M.; Dash, A.K., Development and validation of a sensitive liquid chromatographic method for the analysis of a novel radioprotectant: On 01210.Na. *J Pharm Biomed Anal* **2007**, *43*, 1796-1803.
2. Kim, K.; Pollard, J.M.; Norris, A.J.; McDonald, J.T.; Sun, Y.; Micewicz, E.; Pettijohn, K.; Damoiseaux, R.; Iwamoto, K.S.; Sayre, J.W., *et al.*, High-throughput screening identifies two classes of antibiotics as radioprotectors: Tetracyclines and fluoroquinolones. *Clinical cancer research : an official journal of the American Association for Cancer Research* **2009**, *15*, 7238-7245.
3. Rades, D.; Fehlauer, F.; Bajrovic, A.; Mahlmann, B.; Richter, E.; Alberti, W., Serious adverse effects of amifostine during radiotherapy in head and neck cancer patients. *Radiother Oncol* **2004**, *70*, 261-264.
4. Seed, T.M., Radiation protectants: Current status and future prospects. *Health Phys* **2005**, *89*, 531-545.
5. Williams, J.P.; Brown, S.L.; Georges, G.E.; Hauer-Jensen, M.; Hill, R.P.; Huser, A.K.; Kirsch, D.G.; Macvittie, T.J.; Mason, K.A.; Medhora, M.M., *et al.*, Animal models for medical countermeasures to radiation exposure. *Radiation research* **2010**, *173*, 557-578.
6. Pellmar, T.C.; Rockwell, S., Priority list of research areas for radiological nuclear threat countermeasures. *Radiat Res* **2005**, *163*, 115-123.
7. Ghosh, S.P.; Perkins, M.W.; Hieber, K.; Kulkarni, S.; Kao, T.C.; Reddy, E.P.; Reddy, M.V.; Maniar, M.; Seed, T.; Kumar, K.S., Radiation protection by a new chemical entity, ex-rad: Efficacy and mechanisms. *Radiat Res* **2009**, *171*, 173-179.
8. Burdelya, L.G.; Krivokrysenko, V.I.; Tallant, T.C.; Strom, E.; Gleiberman, A.S.; Gupta, D.; Kurnasov, O.V.; Fort, F.L.; Osterman, A.L.; Didonato, J.A., *et al.*, An agonist of toll-like receptor 5 has radioprotective activity in mouse and primate models. *Science* **2008**, *320*, 226-230.
9. Greenberger, J.S., Radioprotection. *In Vivo* **2009**, *23*, 323-336.
10. Basile, L.A.; Ellefson, D.; Gluzman-Poltorak, Z.; Junes-Gill, K.; Mar, V.; Mendonca, S.; Miller, J.D.; Tom, J.; Trinh, A.; Gallaher, T.K., Hemamax, a recombinant human interleukin-12, is a potent mitigator of acute radiation injury in mice and non-human primates. *PloS one* **2012**, *7*, e30434.
11. Fajardo, L.F.; Berthrong, M.; Anderson, R.E., *Radiation pathology*. Oxford University Press: New York, 2001; p xv, 454 p.
12. Morgan, W.F., Non-targeted and delayed effects of exposure to ionizing radiation: I. Radiation-induced genomic instability and bystander effects in vitro. *Radiat Res* **2003**, *159*, 567-580.
13. Little, J.B., Radiation carcinogenesis. *Carcinogenesis* **2000**, *21*, 397-404.
14. Hall, E.J.; Giaccia, A.J., *Radiobiology for the radiologist*. 6th ed.; Lippincott Williams & Wilkins: Philadelphia, 2006; p ix, 546 p.
15. Huang, L.; Grim, S.; Smith, L.E.; Kim, P.M.; Nickoloff, J.A.; Goloubeva, O.G.; Morgan, W.F., Ionizing radiation induces delayed hyperrecombination in mammalian cells. *Mol Cell Biol* **2004**, *24*, 5060-5068.

16. Huang, L.; Snyder, A.R.; Morgan, W.F., Radiation-induced genomic instability and its implications for radiation carcinogenesis. *Oncogene* **2003**, *22*, 5848-5854.
17. Game, J.C.; Birrell, G.W.; Brown, J.A.; Shibata, T.; Baccari, C.; Chu, A.M.; Williamson, M.S.; Brown, J.M., Use of a genome-wide approach to identify new genes that control resistance of *saccharomyces cerevisiae* to ionizing radiation. *Radiat Res* **2003**, *160*, 14-24.
18. Lengauer, C.; Issa, J.P., The role of epigenetics in cancer. DNA methylation, imprinting and the epigenetics of cancer--an american association for cancer research special conference. Las croabas, puerto rico, 12-16 1997 december. *Mol Med Today* **1998**, *4*, 102-103.
19. Goans, R.E.; Wald, N., Radiation accidents with multi-organ failure in the united states. *BJR Suppl* **2005**, *27*, 41-46.
20. Lushbaugh, C.C.; Comas, F.; Hofstra, R., Clinical studies of radiation effects in man: A preliminary report of a retrospective search for dose-relationships in the prodromal syndrome. *Radiat Res Suppl* **1967**, *7*, 398-412.
21. Williams, J.P.; McBride, W.H., After the bomb drops: A new look at radiation-induced multiple organ dysfunction syndrome (mods). *Int J Radiat Biol* **2011**.
22. van Bekkum, D.W., Radiation sensitivity of the hemopoietic stem cell. *Radiat Res* **1991**, *128*, S4-8.
23. Gratwohl, A.; John, L.; Baldomero, H.; Roth, J.; Tichelli, A.; Nissen, C.; Lyman, S.D.; Wodnar-Filipowicz, A., Flt-3 ligand provides hematopoietic protection from total body irradiation in rabbits. *Blood* **1998**, *92*, 765-769.
24. Preston, D.L.; Kusumi, S.; Tomonaga, M.; Izumi, S.; Ron, E.; Kuramoto, A.; Kamada, N.; Dohy, H.; Matsuo, T.; Matsui, T., *et al.*, Cancer incidence in atomic bomb survivors. Part iii. Leukemia, lymphoma and multiple myeloma, 1950-1987. *Radiat Res* **1994**, *137*, S68-97.
25. Carmichael, J.; DeGraff, W.G.; Gazdar, A.F.; Minna, J.D.; Mitchell, J.B., Evaluation of a tetrazolium-based semiautomated colorimetric assay: Assessment of radiosensitivity. *Cancer Res* **1987**, *47*, 943-946.
26. Kataoka, Y.; Murley, J.S.; Baker, K.L.; Grdina, D.J., Relationship between phosphorylated histone h2ax formation and cell survival in human microvascular endothelial cells (hmec) as a function of ionizing radiation exposure in the presence or absence of thiol-containing drugs. *Radiat Res* **2007**, *168*, 106-114.
27. Meunier, S.; Desage-El Murr, M.; Nowaczyk, S.; Le Gall, T.; Pin, S.; Renault, J.P.; Boquet, D.; Creminon, C.; Saint-Aman, E.; Valleix, A., *et al.*, A powerful antiradiation compound revealed by a new high-throughput screening method. *ChemBiochem* **2004**, *5*, 832-840.
28. Aubrecht, J.; Rugo, R.; Schiestl, R.H., Carcinogens induce intrachromosomal recombination in human cells. *Carcinogenesis* **1995**, *16*, 2841-2846.
29. Brennan, R.J.; Schiestl, R.H., Diaminotoluenes induce intrachromosomal recombination and free radicals in *saccharomyces cerevisiae*. *Mutat Res* **1997**, *381*, 251-258.
30. Brennan, R.J.; Schiestl, R.H., Positive responses to carcinogens in the yeast del recombination assay are not due to selection of preexisting spontaneous revertants. *Mutation research* **1998**, *421*, 117-120.

31. Brennan, R.J.; Schiestl, R.H., Chloroform and carbon tetrachloride induce intrachromosomal recombination and oxidative free radicals in *saccharomyces cerevisiae*. *Mutat Res* **1998**, *397*, 271-278.
32. Brennan, R.J.; Swoboda, B.E.; Schiestl, R.H., Oxidative mutagens induce intrachromosomal recombination in yeast. *Mutat Res* **1994**, *308*, 159-167.
33. Carls, N.; Schiestl, R.H., Evaluation of the yeast del assay with 10 compounds selected by the international program on chemical safety for the evaluation of short-term tests for carcinogens. *Mutation research* **1994**, *320*, 293-303.
34. Galli, A.; Schiestl, R.H., Salmonella test positive and negative carcinogens show different effects on intrachromosomal recombination in g2 cell cycle arrested yeast cells. *Carcinogenesis* **1995**, *16*, 659-663.
35. Galli, A.; Schiestl, R.H., Effects of salmonella assay negative and positive carcinogens on intrachromosomal recombination in g1-arrested yeast cells. *Mutat Res* **1996**, *370*, 209-221.
36. Galli, A.; Schiestl, R.H., Hydroxyurea induces recombination in dividing but not in g1 or g2 cell cycle arrested yeast cells. *Mutat Res* **1996**, *354*, 69-75.
37. Kirpnick, Z.; Homiski, M.; Rubitski, E.; Repnevskaya, M.; Howlett, N.; Aubrecht, J.; Schiestl, R.H., Yeast del assay detects clastogens. *Mutation research* **2005**, *582*, 116-134.
38. Kirpnick-Sobol, Z.; Reliene, R.; Schiestl, R.H., Carcinogenic cr(vi) and the nutritional supplement cr(iii) induce DNA deletions in yeast and mice. *Cancer Res* **2006**, *66*, 3480-3484.
39. Schiestl, R.H., Nonmutagenic carcinogens induce intrachromosomal recombination in yeast. *Nature* **1989**, *337*, 285-288.
40. Schiestl, R.H., Nonmutagenic carcinogens induce intrachromosomal recombination in dividing yeast cells. *Environ Health Perspect* **1993**, *101 Suppl 5*, 179-184.
41. Schiestl, R.H.; Chan, W.S.; Gietz, R.D.; Mehta, R.D.; Hastings, P.J., Safrole, eugenol and methyleugenol induce intrachromosomal recombination in yeast. *Mutation research* **1989**, *224*, 427-436.
42. Schiestl, R.H.; Gietz, R.D.; Mehta, R.D.; Hastings, P.J., Carcinogens induce intrachromosomal recombination in yeast. *Carcinogenesis* **1989**, *10*, 1445-1455.
43. Schiestl, R.H.; Igarashi, S.; Hastings, P.J., Analysis of the mechanism for reversion of a disrupted gene. *Genetics* **1988**, *119*, 237-247.
44. Brennan, R.J.; Schiestl, R.H., Persistent genomic instability in the yeast *saccharomyces cerevisiae* induced by ionizing radiation and DNA-damaging agents. *Radiat Res* **2001**, *155*, 768-777.
45. Hontzeas, N.; Hafer, K.; Schiestl, R.H., Development of a microtiter plate version of the yeast del assay amenable to high-throughput toxicity screening of chemical libraries. *Mutat Res* **2007**, *634*, 228-234.
46. Hafer, K.; Rivina, L.; Schiestl, R.H., Cell cycle dependence of ionizing radiation-induced DNA deletions and antioxidant radioprotection in *saccharomyces cerevisiae*. *Radiat Res* **2010**, *173*, 802-808.
47. Till, J.E.; Mc, C.E., A direct measurement of the radiation sensitivity of normal mouse bone marrow cells. *Radiat Res* **1961**, *14*, 213-222.



48. Warren, S., Effects of radiation on normal tissues. *CA Cancer J Clin* **1980**, *30*, 350-355.
49. Pawlik, T.M.; Keyomarsi, K., Role of cell cycle in mediating sensitivity to radiotherapy. *Int J Radiat Oncol Biol Phys* **2004**, *59*, 928-942.
50. Hafer, K., Rivina, Y., Schiestl, R.H. , Yeast del assay detects protection against radiation induced cytotoxicity and genotoxicity--adaptation of a microtiter plate version. . *Radiat Res* **2010**, *In print*.
51. Zhang, J.H.; Chung, T.D.; Oldenburg, K.R., A simple statistical parameter for use in evaluation and validation of high throughput screening assays. *J Biomol Screen* **1999**, *4*, 67-73.

**CHAPTER 2: Cell cycle dependence of ionizing radiation-induced DNA deletions and antioxidant radioprotection in *Saccharomyces cerevisiae***

## Cell Cycle Dependence of Ionizing Radiation-Induced DNA Deletions and Antioxidant Radioprotection in *Saccharomyces cerevisiae*

Kurt Hafer, Leena Rivina and Robert H. Schiestl<sup>1</sup>

Departments of Radiation Oncology, Pathology, and Environmental Health, David Geffen School of Medicine at UCLA and UCLA School of Public Health, Los Angeles, California

---

Hafer, K., Rivina, L. and Schiestl, R. H. Cell Cycle Dependence of Ionizing Radiation-Induced DNA Deletions and Antioxidant Radioprotection in *Saccharomyces cerevisiae*. *Radiat. Res.* 173, 802–808 (2010).

The yeast DEL assay is an effective method for measuring intrachromosomal recombination events resulting in DNA deletions that when occurring in mammalian cells are often associated with genomic instability and carcinogenesis. Here we used the DEL assay to measure  $\gamma$ -ray-induced DNA deletions throughout different phases of yeast culture growth. Whereas yeast survival differed by only up to twofold throughout the yeast growth phase, proliferating cells in lag and early exponential growth phases were tenfold more sensitive to ionizing radiation-induced DNA deletions than cells in stationary phase. Radiation-induced DNA deletion potential was found to correlate directly with the fraction of cells in S/G<sub>2</sub> phase. The ability of the antioxidants L-ascorbic acid and DMSO to protect against radiation-induced DNA deletions was also measured within the different phases of yeast culture growth. Yeast cells in lag and early exponential growth phases were uniquely protected by antioxidant treatment, whereas nondividing cells in stationary phase could not be protected against the induction of DNA deletions. These results are compared with those from mammalian cell studies, and the implications for radiation-induced carcinogenesis and radioprotection are discussed. © 2010 by Radiation Research Society

### INTRODUCTION

Ionizing radiation exposure produces a variety of DNA damages in cells, which includes strand crosslinks, base damages, single-strand breaks (SSBs) and double-strand breaks (DSBs) (1). Cells respond to this damage through complex molecular signaling pathways that can activate cellular responses such as DNA repair, gene expression, growth arrest and apoptosis (2). Cells sustaining radiation-induced damage may exhibit delayed effects such as genomic instability and may ultimately become carcino-

genic (3). Both acute DNA damage induced by radiation and the subsequent cellular responses are influenced by a variety of factors, including radiation quality, dose rate, dose fractionation, cell/tissue type, cell cycle phase and cell environment physiology [for a comprehensive review, see ref. (4)].

Throughout the 1920s to 1940s, early studies aimed at determining sensitivity to radiation throughout the cell cycle were performed in a variety of organisms. The results of these pioneering studies lacked agreement as to which cell cycle stage is the most radiosensitive and as a whole were inconclusive (5). In 1961, in studies made possible by the development of the *in vitro* clonogenic survival assay of Puck and Marcus 5 years previously (6), Terasima and Tolmach definitively measured the clonogenic radiosensitivity of HeLa cells synchronized by mitotic harvest throughout the cell cycle (7). HeLa cells in M phase were the most sensitive to X-ray cell killing, G<sub>1</sub> and G<sub>2</sub> were the most radioresistant, and S-phase cells were intermediately sensitive. These results have been reproduced in other mammalian cell lines generally yielding the same variation in cell cycle radiosensitivity (8). In 1961 and 1962, Dewey and Humphrey reported measurements of the sensitivity of mouse fibroblasts to  $\gamma$ -ray-induced chromosomal aberrations (9, 10); similar to the earlier observation (7), cells irradiated in S and G<sub>2</sub> phases were up to twofold more sensitive to chromosomal aberrations than G<sub>1</sub> cells. These results were later reproduced in numerous follow-up studies using multiple cell types and collectively established G<sub>2</sub> to be the most sensitive to radiation-induced aberrations (11–14).

Likewise, the genotoxic effects of radiation also vary with cell cycle position. Multiple attempts were made in the 1970s to determine a relationship between radiation-induced mutation sensitivity and cell cycle phase (15–17), but no firm conclusions were established until 1980, when H. J. Burki published his study using synchronized CHO cells. Here G<sub>1</sub> was demonstrated to be the most sensitive cell cycle phase for X-ray-induced *Hprt* mutations for each dose between 1 and 8 Gy, early S phase to be slightly less radiosensitive, and late S phase

<sup>1</sup> Address for correspondence: Department of Radiation Oncology, David Geffen School of Medicine at UCLA, 650 Charles E. Young Drive South, 71-295 CHS, Los Angeles, CA 90095; e-mail: rschiestl@mednet.ucla.edu.

to be relatively resistant (18). These results were upheld by later studies reporting  $G_1$  to be the most sensitive phase for mutation induction by radiation (19–22).

The results from experiments aimed at quantifying cell cycle phase sensitivity in yeast have thus far offered mixed correlations with results from *in vitro* mammalian cell studies. Budding yeast cells in S and M phase are more resistant to radiation cell killing than nonbudding cells in  $G_1$  (23, 24), in opposition to that observed in mammalian cell cultures (7, 8). Proliferating yeast cells (predominant in  $S/G_2$ ) exhibit greater X-ray-induced chromosomal loss (monosomy) than stationary ( $G_1/G_0$ )-phase yeast cells (25). Yeast cells are most sensitive to radiation-induced mutations in the  $G_1$  phase, less sensitive in early S, and least sensitive in late  $S/G_2$  (26), well modeling that observed in mammalian cell studies (18–22).

Here we use the yeast DEL assay to measure the sensitivity of radiation-induced DNA deletions with respect to cell cycle phase. The DEL assay is an efficient system for measuring intrachromosomal recombination events characterized by deletion of 6 kb of genomic DNA (27). The RS112 yeast strain carries an internal disruption cassette at the genomic *his3* locus; deletion here restores wild-type *HIS3* and phenotypic histidine prototrophy. The DEL assay was established previously as a marker for DNA deletions, a subset of genome rearrangements that, when occurring in mammalian cells may be involved in carcinogenesis (28, 29). In validating studies, the DEL assay detected 47 of 50 EPA-listed carcinogens, and for 60 compounds of known carcinogenic activity, it correlated 92% positively with animal carcinogenicity data (30). Ionizing radiation is a potent inducer of DNA deletion events using the DEL assay (28, 31, 32). Here we observed that DNA deletions are significantly more strongly induced in yeast by radiation when cells are in the  $S/G_2$  phase compared to  $G_1/G_0$ , which may be important for the best mode of use of the assay. Furthermore, we observed that antioxidant treatment uniquely protected proliferating yeast cells but not stationary cells from radiation-induced DNA deletions.

## MATERIALS AND METHODS

### *Yeast Strain, Media and Reagents*

The diploid *S. cerevisiae* strain RS112 (MATa/MAT $\alpha$  ura3-52/ura3-52 leu2-3,112/leu2- $\Delta$ 98 trp5-27/TRP5 arg4-3/ARG4 ade2-40/ade2-101 ilv1-92/ILV1 HIS3::pRS6/*his3* $\Delta$ 200 LYS2/*lys2*-801) was used to measure DNA intrachromosomal recombination events at the *his3* locus. Synthetic complete (SC or +13) medium was prepared as yeast nitrogen base 0.67%, glucose 2%, agar 2% plus the following amino acids and bases per 900 ml of distilled water: 60 mg each of adenine sulfate, L-isoleucine, L-leucine, L-lysine-HCl, L-tyrosine, 45 mg of L-arginine-HCl, L-histidine-HCl, L-methionine, uracil, 90 mg of L-tryptophan. SC medium lacking histidine (-his) was made as above but without addition of histidine. SC medium lacking leucine (-leu) was made as above but without leucine, and the

following was added per 900 ml of distilled water after autoclaving: 18 mg uracil, 36 mg adenine sulfate, and 18 mg L-histidine. For liquid medium preparation, agar was not added.

L-Ascorbic acid (CAS No. A-0278) and DMSO (CAS No. D2650) were purchased from Sigma.

### *$\gamma$ Irradiation*

Yeast cells were irradiated with 1000 Gy in a Mark I irradiator (J. L. Shepherd and Associates, Glendale, CA) with a  $^{137}\text{C}$   $\gamma$ -ray source at dose rate of  $\sim$ 16.1 Gy/min.

### *Yeast Proliferation and DEL Assay*

The yeast DEL assay was used to score radiation-induced cell killing, DNA deletions and radioprotection using agar plates. Individual clones of RS112 were grown on -leu plates for 56 h at 30°C and then up to 4 weeks at 4°C. A single clone of RS112 was inoculated in  $\sim$ 7 ml -leu medium at 30°C and at subsequent times in 2- to 6-h intervals for 30 h and aliquots were taken and resuspended in distilled water to measure cell density, cell cycle composition, and radiation-induced deletion events. Yeast cells were sonicated for  $\sim$ 8 min prior to scoring cell density and cell cycle distribution. Cell density was measured with a hemocytometer. Cell cycle was assessed by scoring budding yeast (S and  $G_2$ ) and nonbudding yeast ( $G_1$  and  $G_0$ ); an average of 266 cells was scored for each individual measurement at each time.

Radiation-induced deletion events were measured as follows: Cells were exposed to 1000 Gy  $\gamma$  rays. Then irradiated cells were plated at 200,000 per -his and 1,000 per +13 plate and unirradiated control cells were plated 100,000 per -his and 100 per +13 plate, each in duplicate. Plates were then incubated at 30°C for 48 h, after which colonies were counted. Survival was calculated by dividing the number of colonies counted on +13 plates by the number of cells plated and the plating efficiency obtained from unirradiated control yeast measurements. The number of colonies scored on -his plates was used to calculate the number of deletion events per 10,000 surviving yeast. The measurements at 0 and 30 min were generated by suspending individual clones directly in either 1 ml water or 1 ml -leu liquid medium, respectively. Both were irradiated  $\sim$ 30 min after inoculation, but the former measurement was considered as time 0 since yeast cells do not proliferate while in water. Experiments without radioprotector measurement were performed in quadruplicate at each time.

For experiments done with L-ascorbic acid (1 mM) and DMSO (1% v/v), two aliquots were taken at each time for irradiation, and compounds were added to a single aliquot  $\sim$ 20 min prior to  $\gamma$ -ray treatment; both antioxidant-treated and nontreated samples were exposed simultaneously to  $\gamma$  rays, and deletion recombination and survival were measured as above. Samples were taken 4–30 h after inoculation. Experiments with radioprotectors were performed in triplicate with control experiments performed in parallel, also in triplicate. Statistical significance was calculated using the two-tailed Student's *t* test.

## RESULTS

### *Yeast Proliferation and Radiation-Induced Cytotoxicity and Genotoxicity*

Yeast proliferation was measured in liquid cultures for 30 h after inoculation. Single clones comprising of  $\sim$ 10<sup>6</sup> cells were inoculated in 7 ml -leu medium, and yeast density was measured every 4 h for 24 h and again at 30 h. This time window included the lag, exponential and stationary phases of yeast growth (Fig. 1A, Fig. 2).

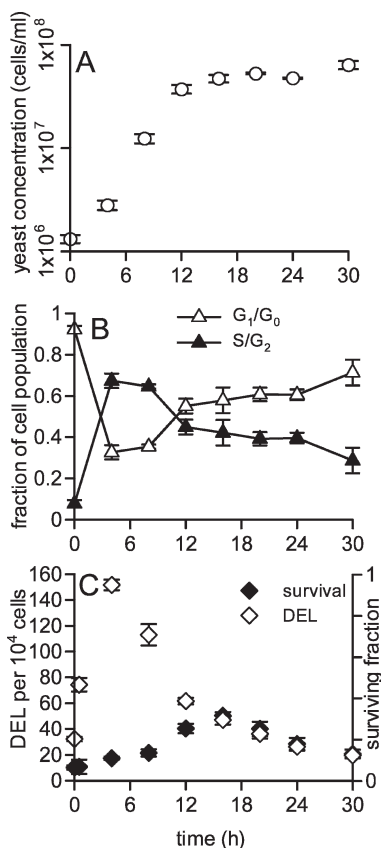


**FIG. 1.** Panel A: Yeast cell density measured in cell cultures as a function of time after inoculation. Panel B: The fractions of cells in G<sub>1</sub>/G<sub>0</sub> and S/G<sub>2</sub> in the same cultures. G<sub>1</sub>/G<sub>0</sub> cells were measured by scoring nonbudding yeast and S/G<sub>2</sub> cells were measured by scoring budding yeast cells. Panel C: Radiation-induced cell killing and homologous DNA deletion (DEL) events per 10<sup>4</sup> surviving cells in cell cultures irradiated with 1000 Gy at different times after inoculation. For all panels, each point is the mean of four independent experiments ± SEM.

Cell cycle composition was also measured at the same time for 30-h yeast culture growth. Nonbudding yeast observed via microscopy were classified as G<sub>1</sub> or G<sub>0</sub> phase and budding yeast as S or G<sub>2</sub> phase. Initial cultures at time zero were comprised predominantly (>90%) of G<sub>1</sub>/G<sub>0</sub> cells, after 4 h of growth, yeast cultures were comprised predominantly (~75%) of S and G<sub>2</sub> cells (Fig. 1B). With time, the fraction of cells in S and G<sub>2</sub> diminished as cells entered stationary phase characterized by being primarily in G<sub>0</sub> and/or G<sub>1</sub> phases.

At each time, aliquots of yeast cultures were exposed to 1000 Gy  $\gamma$  rays and radiation cell killing and DNA deletion events (DEL) were measured. Both end points demonstrated measurable changes in magnitude throughout the three phases of yeast growth. Prior to inoculation, 1000 Gy  $\gamma$  rays induced 32.3 deletion events per 10<sup>4</sup> surviving cells (Fig. 1C). Four-hour cultures, in

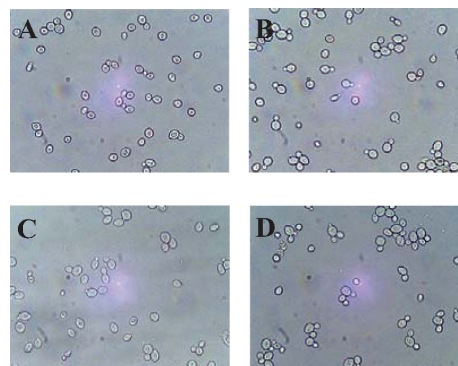


**FIG. 2.** Representative images of budding and non-budding yeast from 0-, 2-, 8- and 30-h cultures are presented in panels A, B, C and D, respectively.

which the greatest fraction of cells were in S/G<sub>2</sub>, were the most sensitive to deletion events induced by 1000 Gy, with 152 induced events per 10<sup>4</sup> surviving cells. Between 4 and 30 h, as yeast populations began to reaccumulate in G<sub>1</sub> and G<sub>0</sub> phases, the sensitivity of radiation-induced deletion events decreased correspondingly. After 30 h growth, yeast cultures were well into stationary phase (Fig. 1A) were comprised mostly of G<sub>0</sub> cells (Fig. 1B), and only 19.5 deletion events per 10<sup>4</sup> cells were induced by radiation.

The magnitude of radiation-induced cytotoxicity was also measured throughout the first three phases of cell growth. Yeast cultures just entering stationary phase were the most resistant to  $\gamma$ -ray-induced cell killing (Fig. 1C). Yeast in lag phase and in the end of stationary phase were most sensitive to radiation cytotoxicity. The difference between the maximum and minimum sensitivity of yeast to radiation cytotoxicity throughout 30 h of culture growth was approximately twofold.

#### Radioprotection and Yeast Culture Growth

The ability of antioxidants DMSO and L-ascorbic acid to protect against cell killing and induction of DNA deletions by radiation was determined throughout yeast growth. DMSO (1%) offered some protection against 1000 Gy  $\gamma$ -ray induced DNA deletions in 4-, 8- and 12-h cultures, with  $P = 0.061$ ,  $P = 0.047$  and  $P = 0.16$ , respectively. At these times, cells are in the exponential growth phase. DMSO did not protect at other times when cells were in stationary phase (Fig. 3A). DMSO also uniquely protected against 1000-Gy-induced cytotoxicity after 4 and 8 h of growth ( $P < 0.01$  at both times), but protection against cytotoxicity was not observed at later times.

Yeast cells incubated with 1 mM ascorbic acid during radiation exposure exhibit a response that is similar to that observed with DMSO but reduced in magnitude. Ascorbic acid reduced  $\gamma$ -ray-induced DNA deletions

CELL CYCLE-DEPENDENT RADIATION TOXICITY IN YEAST

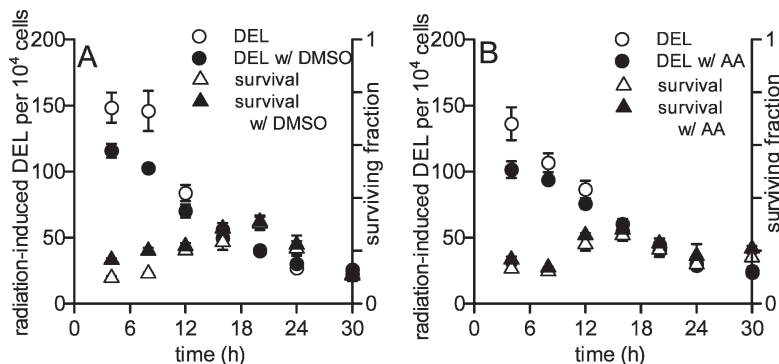


**FIG. 3.** Protection against 1000 Gy  $\gamma$ -ray-induced cell killing and DNA deletions in yeast culture grown for 4 to 30 h by DMSO (panel A) and ascorbic acid (panel B). Protection against deletion events was generally present only during stages of yeast exponential growth and not during stationary phase. Each measurement is the mean of three independent experiments  $\pm$  SEM.

early in exponential yeast growth at 4 and 8 h, but this was not significant ( $P < 0.07$  and  $P = 0.16$ , respectively). No protective trend was observed as cells entered stationary phase (Fig. 3B). Protection against cell killing by ascorbic acid was similarly strongest after 4 h and 8 h of growth ( $P = 0.10$  and  $P = 0.037$ , respectively), but significant protection was not observed at other times when yeast cells were in stationary phase.

**DISCUSSION**

Radiation cytotoxicity and genotoxicity were measured throughout yeast culture growth. Radiation cell killing varied by as much as twofold throughout the first three phases of yeast growth (Fig. 1C). Cells were most resistant to radiation cell killing when cultures were entering stationary phase; such resistance did not correlate with cell cycle. Induction of DNA deletion by radiation varied approximately eightfold throughout the phases of yeast growth, and cells were most sensitive to radiation-induced deletions when cultures were in exponential growth, when most cells are in S/G<sub>2</sub> phase. For measurements taken throughout the first 30 h of cell growth, the magnitude of radiation-induced DNA deletions correlated positively with the fraction of cells in S/G<sub>2</sub> (Fig. 4). The correlation of sensitivity to DNA deletion after irradiation with the fraction of cells in S/G<sub>2</sub> is highly significant ( $P < 0.0001$ ) using a Pearson test ( $r = 0.775$  with 68 degrees of freedom).

The variation of the radiation sensitivity of yeast with growth phase observed here complements that reported in previous studies. In multiple studies, budding yeast cells have been observed to be more resistant to radiation inactivation than nonbudding yeast (23, 24, 33). Generally, exponentially growing yeast cells are more resistant to radiation cell killing than cells in stationary phase or G<sub>1</sub> (34). Similarly, medium-starved cells (presumed to be in G<sub>0</sub> or G<sub>1</sub>) are more sensitive to

radiation inactivation than nonstarved yeast (33, 35). Here yeast cells in late exponential growth are most resistant to radiation cell killing, supporting the observations of Tippins and Parry (34). Furthermore, cells in late stationary phase were most sensitive to radiation cell killing, paralleling the heightened radiosensitivity of medium-starved yeast observed by Raju *et al.* (33) and Laser (35).

Previous reports related the relationship between radiation-induced recombination to cell cycle stage. In synchronized yeast cells, the magnitude of both X-ray-induced intra- and intergenic recombination was greatest in G<sub>1</sub> cells, lower in S and least in G<sub>2</sub> (36). Using arrested cells, X-ray-induced homologous recombination (HR) is greater in G<sub>1</sub> than G<sub>2</sub>, but sister chromatid recombination induction is higher in G<sub>2</sub> than G<sub>1</sub> (37). Cells arrested in S and G<sub>2</sub> phases are more sensitive to  $\gamma$ -ray-induced deletion events than cells arrested in the G<sub>1</sub> phase (32) in agreement with our present data. Here, using dividing cells, cultures were comprised predomi-

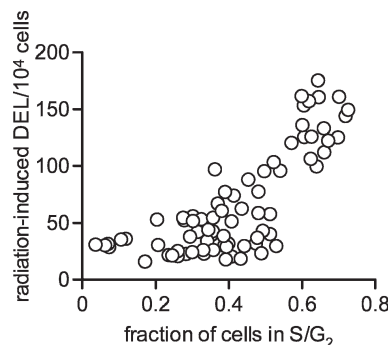


**FIG. 4.** Radiation-induced DNA deletions (DEL) per 10<sup>4</sup> surviving cells as a function of the fraction of cells in S/G<sub>2</sub> for 70 independent measurements. Cultures with more cells in S/G<sub>2</sub> were more susceptible to radiation-induced DNA deletions. This correlation was highly significant ( $P < 0.0001$ ) as calculated by Pearson test.



**TABLE 1**  
**Comparison of Yeast and Mammalian Cells for Cell Cycle Dependence of Sensitivity to Ionizing Radiation for Cell Killing and Genotoxicity**

	Yeast	Mammalian cells
Cell killing	$G_1 > S$ and $G_2$ (23, 24)	$M > S > G_1$ and $G_2$ (7, 8)
Chromosomal aberrations	No experimental data	$G_2 > S > G_1$ (9–14)
Mutation induction	$G_1 > \text{early S} > \text{late S}$ and $G_2$ (26)	$G_1 > \text{early S} > \text{late S}$ (18–22)
Homologous DNA deletions	$S$ and $G_2 > G_1$ and $G_0$ (this study)	No experimental data

*Notes.* Cell cycle phase sensitivity to ionizing radiation was tabulated for measurements performed in yeast and mammalian cell systems. The cell cycle phases are listed in order of most sensitive to least sensitive to radiation exposure.

nantly of S/G<sub>2</sub>-phase cells were as much as eightfold more sensitive to  $\gamma$ -ray-induced deletions than cultures comprised of G<sub>0</sub> and G<sub>1</sub> cells (Fig. 1).

The severe susceptibility of dividing cells to radiation-induced intrachromosomal recombination compared to nondividing cells observed here is noteworthy. First, the effects of radiation-induced damage fixation in different periods of the cell cycle or different phases of cell growth is biologically relevant. Throughout the body, many cells are nondividing (G<sub>0</sub>) while others are constantly dividing; this is well modeled by cell cultures in log growth. Thus studies of the effects of radiation on cells *in vitro* in exponentially dividing cells may not always be relevant to the effects of radiation on tissue *in vivo*. Second, the cellular response and repair of DNA damage, specifically DSBs, is regulated by cyclin-dependent kinases (CDKs) and thus is dependent on cell cycle stage (38). Cells in G<sub>1</sub> repair DSBs using the non-homologous end-joining (NHEJ) pathway, whereas cells in S and G<sub>2</sub> repair DSBs predominantly by HR (39). These repair pathways are highly conserved and remain dependent on the cell cycle in both yeast (40) and mammalian cells (41, 42). In agreement with this are our data on the yeast sensitivity to radiation-induced deletion events that correlate with the S/G<sub>2</sub> cell cycle stage (Figs. 1 and 4) since deletion events are formed primarily through homologous intrachromosomal (deletion) recombination (28).

The capacity of antioxidants to protect against radiation-induced damages exclusively in dividing cell cultures may have implications for radioprotection in humans. Whereas cell cycle-specific sensitivity to radiation-induced toxicities has been well investigated, studies of cell cycle-dependent radioprotection capacity have been sparse thus far. Here dividing cells were protected with antioxidant treatment against radiation-induced DNA deletions, yet nondividing cells were not protected under the same conditions (Fig. 3). Antioxidants protect against radiation primarily by reducing indirect oxidative base damage caused by radiolytic ROS (43). Base damage lesions have been shown previously to induce deletion events when cells are allowed to undergo DNA replication (44). Thus the observation that proliferating cell cultures are better protected by antioxidant treatment against DNA

deletion events is fitting and may have implications for radioprotection against carcinogenesis. The yeast DEL assay is a model for studying radiation-induced homologous DNA deletions (28, 31, 32). Genome rearrangements, specifically including DNA deletions between repetitive elements, are present in many if not most human cancers [for review, see ref. (45)]. Using the DEL assay to qualify antioxidant protection against DNA deletions offers a system for measuring radioprotection against particular genomic rearrangement events involved in carcinogenesis. That observed here (Fig. 3) suggests that rapidly dividing cells are more sensitive to radiation carcinogenesis but are also uniquely protectable with antioxidant treatment against the same. This suggestion is complemented in part by the atomic bomb epidemiological studies in which human tissues comprised of rapidly proliferating cells were observed to be more susceptible to radiation carcinogenesis than slowly dividing tissues (46, 47).

Currently, we are using the yeast DEL assay in a high-throughput format (48) to screen for novel radioprotectors. The data reported here are important for determining the optimal window of sensitivity for screening with the DEL assay. Furthermore, the traditional DEL assay protocol using agar plates use 17 h of incubation with the chemicals to be tested, which encompasses several generations of cell division (49), including the most sensitive phase as determined here. If rapidly dividing yeast cells are hypersensitive to chemically induced deletion recombination like they are to ionizing radiation-induced deletion recombination, this may be one of the reasons why the DEL assay detects carcinogens with greater sensitivity than other genotoxicity assays (30).

Finally, a comparison can be made between cell cycle sensitivity to radiation damages measured in mammalian and yeast *in vitro* systems. Specific cell cycle stage sensitivity to radiation-induced cell killing, chromosomal aberrations, mutation induction and homologous DNA deletions is tabulated with experimental data from yeast and mammalian cells in Table I. Conflicting results exist for cell cycle stage dependence on radiation cell killing, yet analogous results exist for mutation induction. Radiation cell killing likely has little relevance to cancer, but mutation induction and intrachromosomal homologous deletion events are both associated with

carcinogenesis. Both yeast and mammalian *in vitro* cultures are most susceptible to radiation mutations early in the cell cycle, but yeast in later stages of the cell cycle are most sensitive to homologous DNA deletion formation. Cell cycle sensitivity to radiation-induced homologous DNA deletions in mammalian cells (50) is thus far undetermined, but studies of this are warranted.

#### ACKNOWLEDGMENTS

KH was funded in part by an NIH National Institute of Biomedical Imaging and Bioengineering training grant and a NASA Graduate Student Researchers Program (GSRP) research fellowship. This work was supported by project 1 to RHS of NIH grant 1 U19 AI 67769-01 to William McBride.

Received: November 10, 2008; accepted: September 17, 2009; published online: November 17, 2009

#### REFERENCES

1. J. F. Ward, DNA damage produced by ionizing radiation in mammalian cells: identities, mechanisms of formation, and reparability. *Prog. Nucleic Acid Res. Mol. Biol.* **35**, 95–125 (1988).
2. R. K. Schmidt-Ullrich, P. Dent, S. Grant, R. B. Mikkelsen and K. Valerie, Signal transduction and cellular radiation responses. *Radiat. Res.* **153**, 245–257 (2000).
3. K. Suzuki, M. Ojima, S. Kodama and M. Watanabe, Radiation-induced DNA damage and delayed induced genomic instability. *Oncogene* **22**, 6988–6993 (2003).
4. J. P. Pouget and S. J. Mather, General aspects of the cellular response to low- and high-LET radiation. *Eur. J. Nucl. Med.* **28**, 541–561 (2001).
5. A. H. Sparrow, X-ray sensitivity changes in meiotic chromosomes and the nucleic acid cycle. *Proc. Natl. Acad. Sci. USA* **30**, 147–155 (1944).
6. T. T. Puck and P. I. Marcus, Action of X-rays on mammalian cells. *J. Exp. Med.* **103**, 653–666 (1956).
7. T. Terasima and L. J. Tolmach, Changes in X-ray sensitivity of HeLa cells during the division cycle. *Nature* **190**, 1210–1211 (1961).
8. E. J. Hall, *Radiobiology for the Radiologist*, 3rd ed. Lippincott, Philadelphia, 1988.
9. W. C. Dewey and R. M. Humphrey, Relative radiosensitivity of different phases in the life cycle of L-P59 mouse fibroblasts and ascites tumor cells. *Radiat. Res.* **16**, 503–530 (1962).
10. W. C. Dewey and R. M. Humphrey, Relative radiosensitivity of different phases in the life cycle of L-P59 mouse fibroblasts. *Radiat. Res.* **14**, 461 (1961).
11. E. H. Y. Chu, N. H. Giles and K. Passano, Types and frequencies of human chromosome aberrations induced by X-rays. *Proc. Natl. Acad. Sci. USA* **47**, 830–839 (1961).
12. T. C. Hsu, W. C. Dewey and R. M. Humphrey, Radiosensitivity of cells of Chinese hamster *in vitro* in relation to the cell cycle. *Exp. Cell Res.* **27**, 441–452 (1962).
13. W. C. Dewey and R. M. Humphrey, Restitution of radiation-induced chromosomal damage in Chinese hamster cells related to the cell's life cycle. *Exp. Cell Res.* **35**, 262–276 (1964).
14. W. C. Dewey, R. M. Humphrey and B. A. Sedita, Cell cycle kinetics and radiation-induced chromosomal aberrations studies with C14 and H3 labels. *Biophys. J.* **6**, 247–260 (1966).
15. C. F. Arlett and J. Potter, Mutation to 8-azaguanine resistance induced by gamma-radiation in Chinese hamster cell line. *Mutat. Res.* **13**, 59–65 (1971).
16. J. H. Carlson, W. C. Dewey and L. E. Hopwood, X-ray-induced mutants resistant to 8-azaguanine. II. Cell cycle dose response. *Mutat. Res.* **34**, 465–480 (1976).
17. M. Watanabe and M. Horikawa, Analyses of differential sensitivities of synchronized HeLa S3 cells to radiations and chemical carcinogens during the cell cycle. *Mutat. Res.* **44**, 413–426 (1977).
18. H. J. Burki, Ionizing radiation-induced 6-thioguanine-resistant clones in synchronous CHO cells. *Radiat. Res.* **81**, 76–84 (1980).
19. J. P. O'Neill and K. B. Flint, X-ray induction of 6-thioguanine-resistant mutants in division arrested, G<sub>0</sub>/G<sub>1</sub> phase Chinese hamster ovary cells. *Mutat. Res.* **150**, 443–450 (1985).
20. D. J. Grdina and C. P. Sigdestad, Chemical protection and cell-cycle effects on radiation-induced mutagenesis. *Cell Prolif.* **25**, 23–29 (1992).
21. H. Tauchi, N. Nakamura and S. Sawada, Cell cycle dependence for the induction of 6-thioguanine-resistant mutations: G<sub>2</sub>/M stage is distinctively sensitive to <sup>252</sup>Cf neutrons but not to <sup>60</sup>Co gamma-rays. *Int. J. Radiat. Biol.* **63**, 465–481 (1993).
22. S. B. Chernikova, K. L. Lindquist and M. M. Elkind, Cell cycle-dependent effects of wortmannin on radiation survival and mutation. *Radiat. Res.* **155**, 826–831 (2001).
23. C. A. Beam, R. K. Mortimer, R. G. Wolfe and C. A. Tobias, The relation of radioresistance to budding in *Saccharomyces cerevisiae*. *Arch. Biochem. Biophys.* **49**, 110–122 (1954).
24. E. N. Langguth and C. A. Beam, Repair mechanisms and cell cycle dependent variations in X-ray sensitivity of diploid yeast. *Radiat. Res.* **53**, 226–234 (1973).
25. J. M. Parry, D. Sharp, R. S. Tippins and E. M. Parry, Radiation-induced mitotic and meiotic aneuploidy in the yeast. *Mutat. Res.* **61**, 37–55 (1979).
26. S. L. Kelly, C. Merrill and J. M. Parry, Cyclic variations in sensitivity to X-irradiation during meiosis in *Saccharomyces cerevisiae*. *Mol. Gen. Genet.* **191**, 312–318 (1983).
27. R. H. Schiestl, Nonmutagenic carcinogens induce intrachromosomal recombination in yeast. *Nature* **337**, 285–288 (1989).
28. R. J. Brennan and R. H. Schiestl, Persistent genomic instability in the yeast *Saccharomyces cerevisiae* induced by ionizing radiation and DNA-damaging agents. *Radiat. Res.* **155**, 768–777 (2001).
29. A. J. Bishop and R. H. Schiestl, Homologous recombination and its role in carcinogenesis. *J. Biomed. Biotechnol.* **2**, 75–85 (2002).
30. W. W. Ku, J. Aubrecht, R. J. Mauthe, R. H. Schiestl and A. J. Fornace, Jr., Genetic toxicity assessment: employing the best science for human safety evaluation Part VII: Why not start with a single test: a transformational alternative to genotoxicity hazard and risk assessment. *Toxicol. Sci.* **99**, 20–25 (2007).
31. R. H. Schiestl, R. D. Gietz, R. D. Mehta and P. J. Hastings, Carcinogens induce intrachromosomal recombination in yeast. *Carcinogenesis* **10**, 1445–1455 (1989).
32. A. Galli and R. H. Schiestl, On the mechanism of UV and gamma-ray-induced intrachromosomal recombination in yeast cells synchronized in different stages of the cell cycle. *Mol. Gen. Genet.* **248**, 301–310 (1995).
33. M. R. Raju, M. Gnanapurani, B. Stackler, U. Madhvanath, J. Howard, J. T. Lyman, T. R. Manney and C. A. Tobias, Influence of linear energy transfer on the radioresistance of budding haploid yeast cells. *Radiat. Res.* **51**, 310–317 (1972).
34. R. S. Tippins and J. M. Parry, A comparison of the radiosensitivity of stationary, exponential, and G<sub>1</sub> phase wild type and repair deficient yeast cultures: supporting evidence for stationary phase yeast cells being in G<sub>0</sub>. *Int. J. Radiat. Biol.* **41**, 215–220 (1982).
35. H. Laser, Some observations on irradiation effects in yeast. *Radiat. Res.* **16**, 471–482 (1962).
36. R. E. Esposito, Genetic recombination in synchronized cultures of *Saccharomyces cerevisiae*. *Genetics* **59**, 191–210 (1967).



37. L. C. Kadyk and L. H. Hartwell, Replication-dependent sister chromatid recombination in rad1 mutants of *Saccharomyces cerevisiae*. *Genetics* **133**, 469–487 (1993).
38. G. Ira, A. Paellicoli, A. Balijja, X. Wang, S. Fiorani, W. Carotenuto, G. Liberi, D. Bressan, L. Wan and M. Foiani, DNA end resection, homologous recombination and DNA damage checkpoint activation require CDK1. *Nature* **431**, 1011–1017 (2004).
39. Y. Aylon, B. Liefshitz and M. Kupiec, The CDK regulates repair of double-strand breaks by homologous recombination during the cell cycle. *EMBO J.* **23**, 4868–4875 (2004).
40. C. Zierhut and J. F. Diffley, Break dosage, cell cycle stage and DNA replication influence DNA double strand break response. *EMBO J.* **27**, 1875–1885 (2008).
41. F. Delacote and B. S. Lopez, Importance of the cell cycle phase for the choice of the appropriate DSB repair pathway, for genome stability maintenance: the trans-S double-strand break repair model. *Cell Cycle* **7**, 33–38 (2008).
42. M. Shrivastav, L. P. De Haro and J. A. Nickoloff, Regulation of DNA double-strand break repair pathway choice. *Cell Res.* **18**, 134–147 (2008).
43. W. F. Blakely, A. F. Fuciarelli, B. J. Wegher and M. Dizdaroglu, Hydrogen peroxide-induced base damage in deoxyribonucleic acid. *Radiat. Res.* **121**, 338–343 (1990).
44. A. Galli and R. H. Schiestl, Cell division transforms mutagenic lesions into deletion-recombinagenic lesions in yeast cells. *Mutat. Res.* **429**, 13–26 (1999).
45. A. Varshavsky, Targeting the absence: Homozygous DNA deletions as immutable signposts for cancer therapy. *Proc. Natl. Acad. Sci. USA* **104**, 14935–14940 (2007).
46. D. L. Preston, S. Kusumi, M. Tomonaga, S. Izumi, E. Ron, A. Kuramoto, N. Kamada, H. Dohy, T. Matsui and K. Mabuchi, Cancer incidence in atomic bomb survivors. Part III: Leukemia, lymphoma and multiple myeloma, 1950–1987. *Radiat. Res.* **137** (Suppl.), S68–S97 (1994).
47. D. L. Preston, E. Ron, S. Tokuoka, S. Funamoto, N. Nishi, M. Soda, K. Mabuchi and S. Kodama, Solid cancer incidence in atomic bomb survivors: 1958–1998. *Radiat. Res.* **168**, 1–64 (2007).
48. N. Hontzeas, K. Hafer and R. H. Schiestl, Development of a microtiter plate version of the yeast DEL assay amenable to high-throughput toxicity screening of chemical libraries. *Mutat. Res.* **634**, 228–234 (2007).
49. R. J. Brennan and R. H. Schiestl, Detecting carcinogens with the yeast DEL assay. *Methods Mol. Biol.* **262**, 111–124 (2004).
50. J. Aubrecht, R. E. Rugo and R. H. Schiestl, Carcinogens induce intrachromosomal recombination in human cells. *Carcinogenesis* **16**, 2841–2846 (1995).

**CHAPTER 3: Yeast DEL assay detects protection against radiation induced  
cytotoxicity and genotoxicity – adaptation of a microtiter plate  
version**



Published in final edited form as:

*Radiat Res.* 2010 December ; 174(6): 719–726. doi:10.1667/RR2059.1.

## Yeast DEL Assay Detects Protection against Radiation-Induced Cytotoxicity and Genotoxicity: Adaptation of a Microtiter Plate Version

Kurt Hafer, Yelena Rivina, and Robert H. Schiestl<sup>1</sup>

Departments of Radiation Oncology, Pathology and Environmental Health, David Geffen School of Medicine at UCLA and UCLA School of Public Health, Los Angeles, California

### Abstract

The DEL assay in yeast detects DNA deletions that are inducible by many carcinogens. Here we use the colorimetric agent MTS to adapt the yeast DEL assay for microwell plate measurement of ionizing radiation-induced cell killing and DNA deletions. Using the microwell-based DEL assay, cell killing and genotoxic DNA deletions both increased with radiation dose between 0 and 2000 Gy. We used the microwell-based DEL assay to assess the effectiveness of varying concentrations of five different radioprotectors, N-acetyl-L-cysteine, L-ascorbic acid, DMSO, Tempol and Amifostine, and one radiosensitizer, 5-bromo-2-deoxyuridine. The microwell format of the DEL assay was able to successfully detect protection against and sensitization to both radiation-induced cytotoxicity and genotoxicity. Such radioprotection and sensitization detected by the micro-well-based DEL assay was validated and compared with similar measurements made using the traditional agar-based assay format. The yeast DEL assay in microwell format is an effective tool for rapidly detecting chemical protectors and sensitizers to ionizing radiation and is automatable for chemical high-throughput screening purposes.

### INTRODUCTION

Ionizing radiation exposure in humans produces an array of different DNA damages that may lead to carcinogenesis if misrepaired (1). Humans regularly receive ionizing radiation exposure from a variety of sources including environmental (2), medical (3) and occupational exposures (4). A threat of significantly greater radiation exposure exists from a radiological accident or emergency situation (5). Whereas the risk of radiation-induced cancer from low-dose exposure is still uncertain (6) and controversial (7-11), the cancer risk resulting from exposures greater than ~10 cSv is well established.

Much focus has been directed on the development and use of nontoxic radioprotectors that have the potential to reduce both the acute and chronic epidemiological risks associated with radiation exposure. Many plant extracts and antioxidants have well-described and characterized radioprotective properties [for reviews, see refs. (12) and (13)]. Since approximately two-thirds of damage by low-LET radiation is caused indirectly through the radiolytic production of reactive oxygen species (ROS), the scavenging of ROS by antioxidants offers a potent mechanism for protection against  $\gamma$  and X rays (14). However, high-LET radiations such as  $\alpha$  particles, accelerated neutrons and heavy ions cause DNA damage predominately via direct action; thus antioxidant protection against high-LET

© 2010 by Radiation Research Society.

<sup>1</sup> Address for correspondence: Department of Radiation Oncology, David Geffen School of Medicine at UCLA, 650 Charles E. Young Drive South, 71-295 CHS, Los Angeles, CA 90095; rschiestl@mednet.ucla.edu.

radiation is substantially less efficient (15). Pharmacological agents including immunomodulators, cytokines, protease inhibitors, endotoxins and antiapoptosis drugs have been reported to provide effective protection against radiation damage *in vivo* (16-19) and may offer stronger protection against high-LET radiation damage than antioxidants. Cells also have inducible biological protection against radiation (20), and pharmacological activation of this pathway may offer an additional approach to radiation protection.

Multiple methods for rapidly assessing the efficacy of radioprotective compounds and assays amenable for screening of new radioprotective compounds have been reported. A semi-automatable microwell-based assay using the tetrazolium-based agent MTT was first reported to quantify radioprotection *in vitro* by measuring cellular proliferation after radiation exposure. This assay takes between 3–14 days depending on the cell growth rate and is able to quantify the protective and sensitive effects of antioxidant and 5-bromo-2-deoxyuridine (BrdU) treatment against radiation-induced cytotoxicity (21). A method capable of rapidly evaluating radioprotection against  $\gamma$ -H2AX focus formation has also been reported; five previously established radioprotectors were used to validate the method by their capacity to reduce  $\gamma$ -H2AX focus formation *in vitro* measured by flow cytometry (22). A high-throughput method that can uniquely identify antioxidant compounds that protect against radiation-induced ROS has also been described (23). Thus far, no method has been reported that can rapidly characterize protection against radiation-induced genotoxicity.

The yeast DEL assay is an efficient *in vitro* system for detecting DNA deletion events (24). The yeast RS112 strain has a 6-kb internal disruption at the *his3* locus, and deletion of this disruption and subsequent restoration to wild-type *his3* is scored as a DNA deletion event. A deletion frequency is then used in the calculation of the DEL score: a ratio of cells growing on –His medium to the number of cells plated on –His and adjusted for the overall plating efficiency:  $(\text{DEL} \times [(\text{colonies on } -\text{His}) / ((\text{cells plated on } -\text{His}) * (\text{colonies on } +13 / \text{cells plated on } +13))] \times 10,000)$ . A DEL event has previously been established as a measurement of genotoxicity and has been suggested to be a marker for genomic instability and carcinogenesis. An observed DEL event, reversion to a functional HIS3 gene, is a consequence of a homologous recombination and an excision of an internal disruption segment. It is deemed as an indicator of a successful DNA repair activity in response to a spectrum of various DNA lesions within this construct (25,26). Of 50 EPA-listed carcinogens, 47 induced DNA deletion events using the yeast DEL assay, and for 60 compounds of known carcinogenic activity, the DEL assay positively correlates 92% with animal carcinogenicity data (27). The correlation between carcinogen exposure and DEL event induction is so strong that the yeast DEL assay has recently been proposed as a single test system for evaluating suspected carcinogenic risk (28).

Ionizing radiation has previously been described as a potent inducer of yeast deletion events using this model (25,29,30). Here we use the yeast DEL assay for microwell-based detection of radiation-induced DNA deletion events. We also use the DEL assay for rapid characterization of radioprotectors based upon their ability to protect against DNA deletion events in yeast. We validate this method using six previously established radioprotective and radiosensitive compounds. We propose that the microwell-based yeast DEL assay is uniquely capable of simultaneously measuring radio-protection against both radiation-induced genotoxicity and cytotoxicity and is amenable for high-throughput screening purposes.

## MATERIALS AND METHODS

### Yeast Strains, Medium and Reagents

The diploid *S. cerevisiae* strain RS112 (MATa/MATa ura3-52/ura3-52 leu2-3,112/leu2-Δ98 trp5-27/TRP5 arg4-3/ARG4 ade2-40/ade2-101 ilv1-92/ILV1 HIS3::pRS6/his3Δ200 LYS2/lys2-801) was used to measure DNA intrachromosomal recombination events (DEL events) at the his3 locus. Synthetic complete (SC or +13) medium was prepared as yeast nitrogen base 0.67%, glucose 2%, agar 2% plus the following amino acids and bases per 900 ml of distilled water: 60 mg each of adenine sulfate, L-isoleucine, L-leucine, L-lysineHCl, L-tyrosine, 45 mg each of L-arginine-HCl, L-histidine-HCl, L-methionine, uracil, 90 mg of L-tryptophan. SC medium lacking histidine (–his) was made as above but without addition of histidine. SC medium lacking leucine (–leu) was made as above but without leucine, and the following was added per 900 ml of distilled water after autoclaving: 18 mg uracil, 36 mg adenine sulfate, and 18 mg L-histidine. For liquid medium preparation, agar was not added.

The following compounds were purchased from Sigma: L-ascorbic acid (CAS No. A-0278), DMSO (CAS No. D2650), and BrdU (CAS No. B5002). N-acetyl-L-cysteine was purchased from Alfa Aesar (CAS No. 616-91-1), Tempol from Calbiochem (CAS No. 581500), and Amifostine (WR-1065) from the NCI Chemical Carcinogen Repository (CAS No. 345308/4). MTS tetrazolium compound [3-(4,5-dimethylthiazol-2-yl)-5-(3-carboxymethoxyphenyl)-2-(4-sulfophenyl)-2H-tetrazolium, inner salt] was purchased from Promega (CAS No. G358B).

### γ Irradiation

Yeast cells were irradiated with 2000 Gy in a Mark I irradiator (J. L. Shepherd and Associates, Glendale, CA) with a cesium-137 γ-ray source. A dose rate of ~33.3 Gy/min was used.

### DEL Assay

The yeast DEL assay was used to score radioprotection and sensitization using agar plates. A single clone of RS112 was inoculated in ~7 ml –leu medium at 30°C for 4 h prior to irradiation; for experiments with radioprotectors and radiosensitizers, compounds were added to individual inoculation medium 2 h prior to irradiation with the exception of BrdU, which was added 4 h prior. After irradiation yeast cells were plated 200,000 per –his plate and 1,000 per +13 plate in duplicate for 2000 Gy-exposed samples and 100,000 per –his plate and 100 per +13 plate in duplicate for sham-exposed samples. Plates were incubated at 30°C for 48 h and then colonies were counted. Cytotoxicity (i.e. survival) was calculated by dividing the number of colonies counted on the +13 plates by the number of cells plated and the plating efficiency obtained for parallel measurements made using unirradiated controls. The number of colonies scored on –his plates was used to calculate the number of DEL events per 10,000 surviving yeast as described above. Each compound treatment experiment was performed in triplicate simultaneously, and untreated-irradiated control samples were always run concurrently in parallel (also in triplicate).

The yeast DEL assay was adapted for microwell measurement of radiation-induced toxicity. Similarly, a single RS112 clone was inoculated in ~6 ml –leu medium for 16 h prior to 2000 Gy irradiation. Compounds were added to individual inoculation medium 2 h prior to irradiation with the exception of BrdU, which was added 6 h prior. After irradiation, 100,000 yeast cells were placed into each of 12 microwells: six microwells containing 100 μl of +13 liquid medium and six microwells containing 100 μl of –his liquid medium. Then 18 μl of MTS reagent was added to each well. For each experiment, untreated/unirradiated controls, untreated-irradiated, and compound-treated/unirradiated controls were run in

parallel. Ninety-six-well plates were incubated stationary for ~16 h at 30°C, after which colorimetric readings were taken at 490 nm using a Molecular Devices SpectraMax M5 microplate reader (Sunnyvale, CA). Cytotoxicity was determined by measuring yeast proliferation in +13 medium relative to proliferation in +13 medium of control treated yeast cells. Genotoxicity (DEL events) was determined as described previously (27) by dividing the colorimetric value of yeast measured in –his medium-containing wells by that measured in +13-containing wells.

## RESULTS

### Quantification of Radioprotection and Sensitization with DEL Assay

The DEL assay was used to measure protection against and sensitization to radiation-induced genotoxicity and cytotoxicity for six different compound treatments using the agar plate format. Yeast exposure to 2000 Gy  $\gamma$  rays produced an average of 84–201 DEL events per 10,000 surviving cells in six separate experiments; this is a significant induction over unirradiated control yeast, which exhibited fewer than 1 DEL event per 10,000 clones (Table 1). The surviving fraction and number of DEL events were scored for irradiated yeast treated with 1 mM N-acetyl-L-cysteine (NAC), 1 mM L-ascorbic acid (vitamin C), 1 mM Tempol, 1% DMSO, 50  $\mu$ M 5-bromo-2-deoxyuridine (BrdU), and 10 mM WR-1065; untreated cells were irradiated in parallel and compared with each compound-treatment experiment. The radioprotectors NAC, vitamin C, DMSO and WR-1065 each provided protection of varying significance against radiation-induced DEL events and cell killing at the concentrations used compared to control experiments (Table 1). Tempol protected against genotoxicity but sensitized yeast to cytotoxicity. BrdU sensitized yeast to  $\gamma$ -ray-induced DEL and cell killing.

### Microwell-Based Measurement of Radiation DEL Response

We adapted the DEL assay for microwell plate measurement of radiation-induced cytotoxicity and genotoxicity. Yeast cells were irradiated with 0, 50, 150, 250, 500, 1000 and 2000 Gy, and proliferation was measured 16 h later in microwells containing both +13 and –his liquid medium using the MTS colorimetric reagent. Proliferation of cells in either medium increased the relative 490-nm absorbance from 0 to 16 h. Yeast proliferation in +13 medium diminished with increased radiation dose, indicative of radiation cytotoxicity (Fig. 1A). Cells that undergo DNA deletion events and revert to wild-type *his3* are able to grow in medium lacking histidine. Absolute yeast proliferation in –his medium increased with between 0 and 250 Gy and was fairly level between 250 and 2000 Gy (Fig. 1A), but growth in –his medium relative to proliferation in +13 medium increased incrementally across the entire dose range (Fig. 1B).

### Microwell-Based Measurement of Radioprotection and Radiosensitization with the DEL Assay

The yeast microwell-based DEL assay was used with the five radioprotectors and one radiosensitizer to evaluate the assay's ability to detect radioprotection and radiosensitization. Yeast samples were cultured with various concentrations of NAC, vitamin C, Tempol, WR-1065, DMSO and BrdU and irradiated as above. Proliferation in microwells that contained +13 medium and –his medium was measured with MTS to score cytotoxicity and genotoxicity resulting from the radiation exposure.

The microwell format of the yeast DEL assay accurately detected chemical protection and sensitization to radiation-induced cytotoxicity and genotoxicity. One and 5 mM NAC, 0.1, 0.5 and 1 mM ascorbic acid, 10 mM WR-1065, and 0.1 and 1% DMSO each protected against the cytotoxicity of 2000 Gy as measured by greater yeast proliferation in +13

medium compared to proliferation of untreated yeast exposed to 2000 Gy (Fig. 2A). Concentrations of 0.02, 0.05, 0.1 and 1 mM Tempol and 0.1 mM BrdU caused slight radiosensitization to 2000 Gy by the same standard; 0.2 mM BrdU, which caused only slight cytotoxicity in unirradiated yeast, resulted in extreme radiosensitization when combined with 2000 Gy (Fig. 2A). Similarly, 1 and 5 mM NAC, 0.1, 0.5 and 1 mM ascorbic acid, 0.1 and 1 mM Tempol, and 0.1 and 1% DMSO each protected against radiation-induced DNA deletions, and 0.02 to 0.2 mM BrdU provided sensitization to radiation-induced deletions as measured by yeast proliferation in *-his* medium relative to proliferation in *+13* medium (Fig. 2B). A concentration of 10 mM WR-1065 did not significantly protect yeast against radiation-induced DNA deletions (Fig. 2B). Consistently across multiple experiments, WR-1065 was by itself genotoxic to unirradiated yeast.

## DISCUSSION

Here the yeast DEL assay has been used in microwell-based format to rapidly determine the protective and sensitizing effects of chemicals against radiation-induced cytotoxicity and genotoxicity. The assay was used with six radioprotectors and radiosensitizers, and both protection against and sensitization to radiation and DNA deletion events were detectable by this assay.

The yeast DEL assay is a powerful method for detecting the genotoxicity of carcinogens, including radiation (28). Recently, the yeast DEL assay was adapted to microwell format and was shown to be capable of simultaneously assessing the cytotoxicity and genotoxicity of 13 different chemical compounds (27). Here we used the DEL assay in microwell format to rapidly detect chemical protection and sensitization to the cytotoxicity and genotoxicity induced in cells by radiation. Reduced cellular proliferation after radiation exposure has been a standard measurement of cytotoxicity by multiple microwell-based proliferation assays with various mammalian cell types (21,31-33). We build upon this colorimetric proliferation model as the basis for measuring radiation-induced genotoxicity in yeast. All proliferating cells of the strain RS112 will grow in *+13* complete medium, but only cells that have undergone a 6-kb deletion of genomic DNA and restoration to wild-type *his3* will grow in *-his* medium. The relative frequency of growth in *-his* medium then can be used to derive a relative DEL event score and thus establish the extent of genotoxicity and its fluctuation with different chemical entities. A measure of genotoxicity, a calculated DEL score, can be considered separately from cytotoxicity because it assesses the recombination frequency only in the fractions that survive irradiation. The ratio of yeast growth in *-his* medium to that in *+13* medium and adjusted to survival has been used as a standardized measurement of DEL genotoxicity in both agar plate assays (24,29) and liquid microwell assays (27). Here the microwell plate format of the DEL assay is capable of detecting both increased cytotoxicity and genotoxicity with radiation doses between 0 and 2000 Gy (Fig. 1). This response correlates well with similar dose responses observed in previous studies in which the DEL assay was used to measure radiation cell killing and DNA deletion events using agar plates (25,29,30). The DEL assay can accurately distinguish a purely genotoxic compound from a purely cytotoxic one because a DEL score is a ratio of irradiated cells proliferating in a selective medium to nonirradiated cells in selective medium and adjusted with a survival coefficient derived from cells in complete medium. Seeding all treated and control wells with the same cell density also allows for a direct comparison between the wells. Yeast cocultured with various concentrations of radioprotectors and radiosensitizers exhibited differences in radiotoxicity measurable 16 h after 2000 Gy exposure using the microwell-based DEL assay. NAC, ascorbic acid and DMSO each protected against both radiation cytotoxicity and genotoxicity in yeast (Fig. 2); such results are consistent with previous studies in which these agents protected from radiation cell killing and genotoxic mutation induction at the *hprt* and *CD59* loci *in vitro* (34-37). Tempol and WR-1065 offered

mixed results (Fig. 2A and B). Whereas Tempol has been shown to protect against clonogenic cell killing and mutation induction at the *xprt* and *hprt* loci in mammalian cells (38,39), in the yeast system used here Tempol offered protection against radiation-induced DNA deletions but no protection against cell killing; in fact, it behaved as a radiosensitizer. The observed lack of protection observed against cell killing by Tempol may be due to the fact the concentrations used were 1/50 and 1/500 of that which provided cytotoxic protection in mammalian cell experiments. The radioprotective effect of WR-1065 in yeast is also interesting; at 10 mM, it protected well against cytotoxicity, but no significant protection was observed against DEL events. This result is likely due to the fact 10 mM WR-1065 was by itself genotoxic to yeast cells. In previous reports, WR-1065 has been postulated to function through separate mechanisms at different concentrations to protect against radiation-induced genotoxicity and cytotoxicity (40-42). BrdU sensitized yeast to radiation, increasing both cytotoxic and genotoxic responses to 2000 Gy (Fig. 2); these results are consistent with those of others (43,44).

A comparison can be made between radioprotection and sensitization measured using the microwell- and agar-based yeast DEL methods. Overall, for the six concentrations of chemicals tested for protection and sensitization using both assay formats, the results correlated well (Table 2). NAC at 1 mM, 1 mM ascorbic acid, and 1% DMSO each provided radioprotection against cell killing and DNA deletions using both assay formats; 1 mM Tempol protected against radiation-induced DEL events at the expense of increased radio-cytotoxicity similarly under both assay formats. Conversely, 10 mM WR-1065 protected against radiation-induced cell killing and DEL events using the agar-based format; this was not fully correlated by microwell-based measurements in which the same concentration of WR-1065 protected against cell killing but offered nonsignificant protection against DEL events. BrdU at 50  $\mu$ M sensitized yeast cells to radiation-induced cell killing and deletions using both formats. Overall, a positive qualitative correlation was observed between the two DEL assay formats for 12 out of 12 of the paired cytotoxic and genotoxic measurements (Table 2). Still, radioprotection and radiosensitization differed quantitatively between assay formats.

A perfect correlation between the two DEL assay formats should not necessarily be expected. Two reasons may account for the differences in radioprotection observed between the two assay formats. First, both yeast (25) and mammalian cells (45) exhibit delayed effects to radiation; ROS have been implicated in such delayed effects (46-48), and scavenging these ROS with antioxidant administration after radiation exposure has been shown to protect against these delayed effects (34-36). In the microwell-based format, the antioxidants are present before, during and after radiation exposure; in the agar-based format, these radioprotectors are present only before and during radiation exposure and are not present to scavenge ROS after irradiation, thus possibly accounting for some of the quantitative differences in radioprotection between these two assay formats. Second, because the two assay formats measure two different end points, proliferation and clonogenicity, one would not expect the levels of relative protection to be the same for these two end points. Proliferation assays have been demonstrated to correlate imperfectly with a clonogenic response (32), and this likely is likely to be another reason for the difference between the two assay formats.

A comparison can be made between microwell DEL assay format and other microwell plate assays, notably the MTT assay, which has been used to detect radioprotection and sensitization. The MTT assay has frequently been used to quantify cellular proliferation responses to radiation (21) and toxic chemical (49) treatments. Thus far these tetrazolium-based assays have been used only to measure cytotoxicity as indicated by reduced cellular proliferation after radiation treatment. Here we used a similar tetrazolium agent (MTS)



together with the yeast DEL assay. Whereas previous methods scored only cytotoxicity to radiation, this is the first example of a microwell-based assay capable of measuring both ionizing radiation-induced cytotoxicity and genotoxicity simultaneously *in vitro*. MTT assessment of radio-cytotoxicity in mammalian cells takes between 3–14 days depending on the growth rate of the cell line used (21), yet radiation-induced genotoxicity and cytotoxicity can be assessed with the microwell DEL assay only 16–18 h after exposure.

Here a microwell-based format of the yeast DEL assay was used to measure radiation damage in yeast. The DEL assay is unique in that it can rapidly and simultaneously measure cyto- and genotoxicity. It is possible that the mechanism that confers cytotoxic protection is different and possibly independent from that which confers genotoxic protection. In our subsequent studies we plan to screen a library of yeast mutants deficient in various repair mechanisms against compounds that show either genotoxic or cytotoxic properties or both to potentially identify and differentiate the above-mentioned mechanisms. Genotoxic protection against radiation-induced DNA deletion events in yeast may serve as a unique model for protection against radiation carcinogenesis because the DEL assay has been demonstrated to be strongly correlated with the cancer-causing activity of chemicals (28). Six different compounds were used to evaluate the ability of the assay to detect radioprotectors and radiosensitizers. NAC, ascorbic acid, DMSO, Tempol and WR-1065 were observed to protect against DNA deletion events in yeast, each to different degrees. The yeast DEL assay in microwell format is capable of measuring radioprotection and is suitable for detecting radioprotectors in high-throughput screening applications.

## Acknowledgments

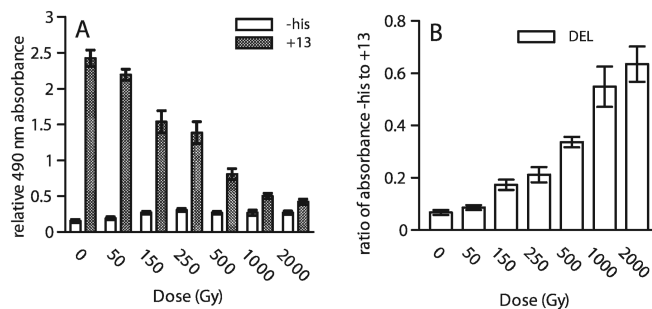
KH was partially funded by a National Institute of Biomedical Imaging and Bioengineering training grant. This research was supported by project 1 to RHS of NIH grant 1 U19 AI 67769-01 to William McBride.

## REFERENCES

1. Pouget JP, Mather SJ. General aspects of the cellular response to low- and high-LET radiation. *Eur. J. Nucl. Med.* 2001; 28:541–561. [PubMed: 11357507]
2. Moeller DW. Environmental health physics: 50 years of progress. *Health Phys.* 2005; 88:676–696. [PubMed: 15891461]
3. Aroua A, Trueb P, Vader JP, Valley JF, Verdun FR. Exposure of the Swiss population by radiodiagnosics: 2003 review. *Health Phys.* 2007; 92:442–448. [PubMed: 17429302]
4. Wakeford R. Occupational exposure, epidemiology and compensation. *Occup. Med. (Lond.)*. 2006; 56:173–179. [PubMed: 16641502]
5. Bushberg JT, Kroger LA, Hartman MB, Leidholdt EM Jr, Miller KL, Derlet R, Wraa C. Nuclear/radiological terrorism: emergency department management of radiation casualties. *J. Emerg. Med.* 2007; 32:71–85. [PubMed: 17239736]
6. Brenner DJ, Doll R, Goodhead DT, Hall EJ, Land CE, Little JB, Lubin JH, Preston DL, Preston RJ, Zaider M. Cancer risks attributable to low doses of ionizing radiation: assessing what we really know. *Proc. Natl. Acad. Sci. USA.* 2003; 100:13761–13766. [PubMed: 14610281]
7. Puskin JS. What can epidemiology tell us about risks at low doses? *Radiat. Res.* 2008; 169:122–124. [PubMed: 18159960]
8. Mossman KL. Economic and policy considerations drive the LNT debate. *Radiat. Res.* 2008; 169:245. [PubMed: 18220464]
9. Leonard BE. Common sense about the linear no-threshold controversy—give the general public a break. *Radiat. Res.* 2008; 169:245–246. [PubMed: 18220465]
10. Feinendegen LE, Paretzke H, Neumann RD. Two principal considerations are needed after low doses of ionizing radiation. *Radiat. Res.* 2008; 169:247–248. [PubMed: 18220467]
11. Tubiana M, Arengo A, Averbek D, Masse R. Low-dose risk assessment. *Radiat. Res.* 2007; 167:742–744. [PubMed: 17523853]

12. Jagetia GC. Radioprotective potential of plants and herbs against the effects of ionizing radiation. *J. Clin. Biochem. Nutr.* 2007; 40:74–81. [PubMed: 18188408]
13. Weiss JF, Landauer MR. Radioprotection by antioxidants. *Ann. NY Acad. Sci.* 2000; 899:44–60. [PubMed: 10863528]
14. Borek C. Antioxidants and radiation therapy. *J. Nutr.* 2004; 134:3207S–3209S. [PubMed: 15514309]
15. Ito A, Nakano H, Kusano Y, Hirayama R, Furusawa Y, Murayama C, Mori T, Katsumura Y, Shinohara K. Contribution of indirect action to radiation-induced mammalian cell inactivation: dependence on photon energy and heavy-ion LET. *Radiat. Res.* 2006; 165:703–712. [PubMed: 16802871]
16. Hosseinimehr SJ. Trends in the development of radioprotective agents. *Drug Discov. Today.* 2007; 12:794–805. [PubMed: 17933679]
17. von Hofe E, Brent R, Kennedy AR. Inhibition of X-ray-induced exencephaly by protease inhibitors. *Radiat. Res.* 1990; 123:108–111. [PubMed: 2371376]
18. Ainsworth EJ. From endotoxins to newer immunomodulators: survival-promoting effects of microbial polysaccharide complexes in irradiated animals. *Pharmacol. Ther.* 1988; 39:223–241. [PubMed: 3059368]
19. Burdelya LG, Krivokrysenko VI, Tallant TC, Strom E, Gleiberman AS, Gupta D, Kurnasov OV, Fort FL, Osterman AL, Gudkov AV. An agonist of toll-like receptor 5 has radioprotective activity in mouse and primate models. *Science.* 2008; 320:226–230. [PubMed: 18403709]
20. Bonner WM. Low-dose radiation: thresholds, bystander effects, and adaptive responses. *Proc. Natl. Acad. Sci. USA.* 2003; 100:4973–4975. [PubMed: 12704228]
21. Carmichael J, DeGraff WG, Gazdar AF, Minna JD, Mitchell JB. Evaluation of a tetrazolium-based semiautomated colorimetric assay: assessment of radiosensitivity. *Cancer Res.* 1987; 47:943–946. [PubMed: 3802101]
22. Kataoka Y, Murley JS, Baker KL, Grdina DJ. Relationship between phosphorylated histone H2AX formation and cell survival in human microvascular endothelial cells (HMEC) as a function of ionizing radiation exposure in the presence or absence of thiol-containing drugs. *Radiat. Res.* 2007; 168:106–114. [PubMed: 17723002]
23. Meunier S, Desage-El Murr M, Nowaczyk S, Le Gall T, Pin S, Renault JP, Boquet D, Creminon C, Saint-Aman E, Mioskowski C. A powerful antiradiation compound revealed by a new high-throughput screening method. *Chembiochem.* 2004; 5:832–840. [PubMed: 15174167]
24. Schiestl RH. Nonmutagenic carcinogens induce intrachromosomal recombination in yeast. *Nature.* 1989; 337:285–288. [PubMed: 2643057]
25. Brennan RJ, Schiestl RH. Persistent genomic instability in the yeast *Saccharomyces cerevisiae* induced by ionizing radiation and DNA-damaging agents. *Radiat. Res.* 2001; 155:768–777. [PubMed: 11352758]
26. Bishop AJ, Schiestl RH. Homologous recombination and its role in carcinogenesis. *J. Biomed. Biotechnol.* 2002; 2:75–85. [PubMed: 12488587]
27. Hontzeas N, Hafer K, Schiestl RH. Development of a microtiter plate version of the yeast DEL assay amenable to high-throughput toxicity screening of chemical libraries. *Mutat. Res.* 2007; 634:228–234. [PubMed: 17707690]
28. Ku WW, Aubrecht J, Mauthe RJ, Schiestl RH, Fornace AJ Jr. Genetic toxicity assessment: employing the best science for human safety evaluation Part VII: Why not start with a single test: a transformational alternative to genotoxicity hazard and risk assessment. *Toxicol. Sci.* 2007; 99:20–25. [PubMed: 17548889]
29. Schiestl RH, Gietz RD, Mehta RD, Hastings PJ. Carcinogens induce intrachromosomal recombination in yeast. *Carcinogenesis.* 1989; 10:1445–1455. [PubMed: 2665967]
30. Galli A, Schiestl RH. On the mechanism of UV and gamma-ray-induced intrachromosomal recombination in yeast cells synchronized in different stages of the cell cycle. *Mol. Gen. Genet.* 1995; 248:301–310. [PubMed: 7565592]
31. Slavotinek A, McMillan TJ, Steel CM. Measurement of radiation survival using the MTT assay. *Eur. J. Cancer.* 1994; 30A:1376–1382. [PubMed: 7999428]

32. Banasiak D, Barnetson AR, Odell RA, Mameghan H, Russell PJ. Comparison between the clonogenic, MTT, and SRB assays for determining radiosensitivity in a panel of human bladder cancer cell lines and a ureteral cell line. *Radiat. Oncol. Investig.* 1999; 7:77–85.
33. Hellweg CE, Arenz A, Baumstark-Khan C. Assessment of space environmental factors by cytotoxicity bioassays. *Acta Astronaut.* 2007; 60:525–533.
34. Koyama S, Kodama S, Suzuki K, Matsumoto T, Miyazaki T, Watanabe M. Radiation-induced long-lived radicals which cause mutation and transformation. *Mutat. Res.* 1998; 421:45–54. [PubMed: 9748497]
35. Ueno A, Vannais D, Lenarczyk M, Waldren CA. Ascorbate, added after irradiation, reduces the mutant yield and alters the spectrum of CD59<sup>2</sup> mutations in A(L) cells irradiated with high LET carbon ions. *J. Radiat. Res. (Tokyo)*. 2002; 43(Suppl.):S245–249. [PubMed: 12793767]
36. Waldren CA, Vannais DB, Ueno AM. A role for long-lived radicals (LLR) in radiation-induced mutation and persistent chromosomal instability: counteraction by ascorbate and RibCys but not DMSO. *Mutat. Res.* 2004; 551:255–265. [PubMed: 15225598]
37. Zhou H, Randers-Pehrson G, Geard CR, Brenner DJ, Hall EJ, Hei TK. Interaction between radiation-induced adaptive response and bystander mutagenesis in mammalian cells. *Radiat. Res.* 2003; 160:512–516. [PubMed: 14565832]
38. Hahn SM, Krishna CM, Samuni A, DeGraff W, Cuscela DO, Johnstone P, Mitchell JB. Potential use of nitroxides in radiation oncology. *Cancer Res.* 1994; 54:2006s–2010s. [PubMed: 8137329]
39. DeGraff WG, Krishna MC, Kaufman D, Mitchell JB. Nitroxide-mediated protection against X-ray- and neocarzinostatin-induced DNA damage. *Free Radic. Biol. Med.* 1992; 13:479–487. [PubMed: 1459474]
40. Grdina DJ, Shigematsu N, Dale P, Newton GL, Aguilera JA, Fahey RC. Thiol and disulfide metabolites of the radiation protector and potential chemopreventive agent WR-2721 are linked to both its anti-cytotoxic and anti-mutagenic mechanisms of action. *Carcinogenesis.* 1995; 16:767–774. [PubMed: 7728953]
41. Grdina DJ, Nagy B, Hill CK, Wells RL, Peraino C. The radioprotector WR1065 reduces radiation-induced mutations at the hypoxanthine-guanine phosphoribosyl transferase locus in V79 cells. *Carcinogenesis.* 1985; 6:929–931. [PubMed: 4006082]
42. Murley JS, Grdina DJ. The effects of cycloheximide and WR-1065 on radiation-induced repair processes: a mechanism for chemoprevention. *Carcinogenesis.* 1995; 16:2699–2705. [PubMed: 7586189]
43. Limoli CL, Corcoran JJ, Milligan JR, Ward JF, Morgan WF. Critical target and dose and dose-rate responses for the induction of chromosomal instability by ionizing radiation. *Radiat. Res.* 1999; 151:677–685. [PubMed: 10360787]
44. Ling LL, Ward JF. Radiosensitization of Chinese hamster V79 cells by bromodeoxyuridine substitution of thymidine: enhancement of radiation-induced toxicity and DNA strand break production by monofilar and bifilar substitution. *Radiat. Res.* 1990; 121:76–83. [PubMed: 2300671]
45. Morgan WF. Non-targeted and delayed effects of exposure to ionizing radiation: I. Radiation-induced genomic instability and bystander effects in vitro. *Radiat. Res.* 2003; 159:567–580. [PubMed: 12710868]
46. Redpath JL, Gutierrez M. Kinetics of induction of reactive oxygen species during the post-irradiation expression of neoplastic transformation in vitro. *Int. J. Radiat. Biol.* 2001; 77:1081–1085. [PubMed: 11683978]
47. Rugo RE, Schiestl RH. Increases in oxidative stress in the progeny of X-irradiated cells. *Radiat. Res.* 2004; 162:416–425. [PubMed: 15447041]
48. Laurent C, Pouget JP, Voisin P. Modulation of DNA damage by pentoxifylline and alpha-tocopherol in skin fibroblasts exposed to gamma rays. *Radiat. Res.* 2005; 164:63–72. [PubMed: 15966766]
49. Carmichael J, DeGraff WG, Gazdar AF, Minna JD, Mitchell JB. Evaluation of a tetrazolium-based semiautomated colorimetric assay: assessment of chemosensitivity testing. *Cancer Res.* 1987; 47:936–942. [PubMed: 3802100]

**FIG. 1.**

Panel A: Yeast proliferation 16 h after exposure to 2000 Gy is measured in microwells containing +13 and -his medium using the MTS colorimetric reagent. Increased relative absorbance from 0 to 16 h correlated with cell proliferation. Yeast proliferation in +13 medium decreased markedly with increased dose, whereas yeast growth in -his medium, indicative of deletion of 6 kb genomic DNA and reversion to wild-type *his3*, increased slightly with dose up to 250 Gy before leveling off. Panel B: The ratio of yeast proliferation in -his medium to that in +13 medium, indicative of relative DEL induction, increased incrementally across the entire dose range. The experiment was carried out using six repeats for each treatment group, and the results are presented as means  $\pm$  SD.

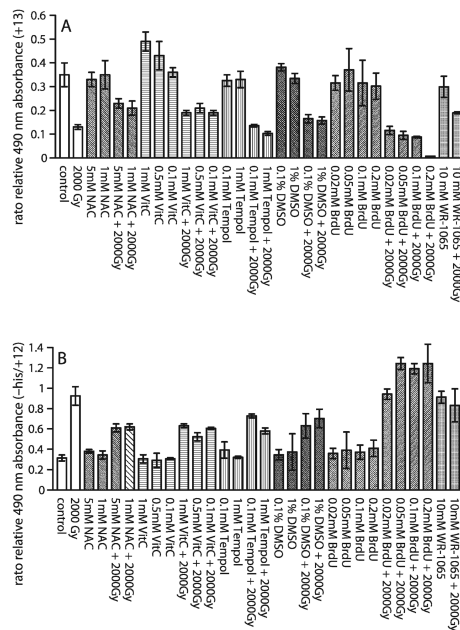


**FIG. 2.** Panel A: Yeast proliferation of samples irradiated with 2000 Gy and cocultured with different concentrations of five radioprotectors and one radiosensitizer measured in +13 medium containing microwells using MTS colorimetric reagent. Increased relative absorbance from 0 to 16 h correlated with cell proliferation. Protection and sensitization to radiation-induced cytotoxicity was observed. Panel B: The ratio of yeast proliferation measured in -his medium to that measured in +13 medium for yeast cocultured with five radioprotectors and one radiosensitizer and exposed to 2000 Gy. Results are from six individual experiments each carried out using at least six repeats for each treatment group and normalized to the untreated controls; the results are presented as means  $\pm$  SD.

**TABLE 1**  
Effects of Treatment of Irradiated Yeast with Various Radioprotectors and Radiosensitizers

	Control			With compound treatment		
	DEL	$\sigma$	Survival	DEL	$\sigma$	Survival
NAC (1 mM)	146.8	6.1	10.4%	123.8**	3.8	14.4%*
Vitamin C (1 mM)	136.1	12.4	13.2%	101.3 <sup>A</sup>	6.2	16.7% <sup>A</sup>
Tempo (1 mM)	200.8	13.7	8.4%	163.5 <sup>A</sup>	9.6	6.6%**
WR-1065 (10 mM)	83.5	13.1	4.0%	42.0**	4.0	9.4%**
DMSO (1%)	148.2	11.4	9.8%	115.8 <sup>A</sup>	5.3	16.6%**
BrdU (50 $\mu$ M)	112.3	2.6	12.3%	158.1*	3.7	8.5%*

Notes: Results are presented as the average of three individual experiments for each measurement, and control experiments were always run in parallel with compound-treated experiments. Unirradiated control yeast cells exhibited an average DEL induction of  $0.85 \pm 0.27$  averaged across all experiments. The DEL induction measured in unirradiated compound-treated cells did not differ significantly from control cells for any experiment (data not shown). DEL is the number of DNA deletion events per 10,000 surviving yeast and  $\sigma$  is the SEM. Significance calculated using a Student's *t* test:

<sup>A</sup>  $P \leq 0.10$

\*  $P < 0.05$

\*\*  $P < 0.01$ .

**TABLE 2**

Effects of Radiosensitizers and Radioprotectors Determined by Microwell and Agar Plates Methods

	Microwell method		Agar plate method	
	DEL change	Proliferation change	DEL change	Survival change
NAC (1 mM)	-32.9% **	91.7% **	-15.6% **	39.2% *
Vitamin C (1 mM)	-31.6% **	46.2% **	-25.6% ^	26.1% ^
Tempol (1 mM)	-37.2% **	-20.4% **	-18.6% ^	-21.4% **
WR-1065 (10 mM)	-9.9%	45.9% **	-49.7% **	135.7% **
DMSO (1%)	-24.0% **	21.2% **	-21.9% ^	68.7% **
BrDU (50 μM)	34.5% **	-27.0% **	40.8% *	-30.5% *

Notes. Values are presented as percentage difference between compound-treated and untreated control measurements each performed and irradiated in parallel. A comparison can be made between the radioprotection and radiosensitization measured by using both methods. Significance calculated using a Student's *t* test:

^  $P \leq 0.10$

\*  $P < 0.05$

\*\*  $P < 0.01$ .

## **CHAPTER 4: Yeloo2 mitigates acute hematopoietic radiation injury in mice**



## **ABSTRACT**

Exposure to ionizing radiation (IR) either through a radiological accident or terrorist attack is a grave public health concern, that demands appropriate pharmacological intervention in order to reduce mass casualties. Here we present a novel small molecule radiation mitigator, designated Yel002, with an established dose-modifying factor of 1.15. Yel002 rescued on average 75% (range 66% - 90%) of mice when first injected at 24 hours after lethal irradiation (8 Gy, LD100/30), without any supportive care. Yel002 mitigated radiation-induced hematopoietic syndrome by accelerating the recovery of the hematologic and immune system components. By day 13 Yel002-treated animals began to show signs of bone marrow recovery through increased white blood cell and platelet counts. Furthermore, Yel002 significantly reduced radiation-induced senescence in primary normal human oral keratinocytes (NHOKs) by enhancing the phosphorylation state of Rb and through reduced cellular concentrations of cyclin-dependent kinase inhibitor p21<sup>WAF1</sup>. Our data suggest that treatment with Yel002 affects the phosphatidylinositol 3-kinase/protein kinase B (PI3K/Akt) signaling pathway, potentially activating its pro-survival activity. Yel002's efficacy against acute radiation syndrome, with a protracted time of administration following exposure, renders it a potential stockpile therapy against acute radiation syndrome.

## **INTRODUCTION**

Recent events have again reminded us that the threat of exposure to ionizing radiation either from a radiation accident or a nuclear attack is a real possibility with grave consequences. This realization also highlights a lack of safe and reliable chemotherapeutic

agents intended to treat radiation injury on a mass scale. In 2005 the Center for Medical Countermeasures against Radiation was established at UCLA. Within the CMCR we have set out to develop novel radiation effect modulating compounds suitable for a variety of exposure scenarios (i.e. attacks on nuclear power stations, detonation of a “dirty bomb,” detonation of a nuclear weapon or hidden radiation-exposure device) [1].

Early lethality associated with exposure to high-intensity radiation is usually due to acute radiation syndrome (ARS). ARS can be subdivided into three somewhat overlapping conditions – cerebrovascular, gastrointestinal (GI), and hematopoietic syndromes. Each of these is associated with a specific range of radiation doses and a characteristic time of death. Death due to the cerebrovascular syndrome occurs within 24-48 hours following doses in excess of 100 Gy. At intermediate doses of 5 – 12 Gy lethality occurs within 9 – 10 days due to the destruction of the gastrointestinal mucosa. In the lower exposure range of 2.5 to 5 Gy, death occurs due to bone marrow or hematopoietic syndrome destruction, between several weeks to two months without medical intervention [1]. According to data obtained from nuclear accidents, approximately 50% of exposed individuals will die within 60 day after a 4 Gy ionizing radiation (IR) exposure without targeted medical intervention [2].

While therapeutic intervention in cases of cerebrovascular syndrome is limited to providing final comforts, intervention for patients with gastrointestinal and hematopoietic syndromes has the potential to save lives. In a hospital setting a bone marrow transplant for patients diagnosed with the hematopoietic syndrome along with antibiotic treatment has been shown to be beneficial, albeit the window of efficacy is very small, ending around 8 Gy [1]. Additionally, Saha et al. showed that bone marrow-derived stromal cells,

including mesenchymal, endothelial, and macrophage cell population administered intravenously might also benefit individuals with radiation-induced GI syndrome [3]. The challenge, however, is to develop radiation mitigation interventions suitable for utilization in settings outside of a sterile hospital environment. Furthermore, it is likely that medical attention and administration of radiation mitigating therapies will most likely be delayed 24 hours or more until appropriate medical personnel are mobilized [4], thus necessitating that mitigating therapy be efficacious on a protracted administration schedule.

A few pharmacological approaches aimed at mitigating radiation-induced gastrointestinal and hematopoietic syndromes are currently at different stages of drug development and evaluation. Among them are a few cytokines and small molecules. One of the most recent additions is a human recombinant interleukin-12 (IL-12), HemaMax™, which rescued on average 65% of animals following 9 Gy (LD100/30) with a single administration dose at 24 hours after irradiation. Additionally, HemaMax™ rescued 70% of non-human primates exposed to LD50/30 dose of IR on the same drug administration dose [5]. The next most efficacious therapy is a small cyclin-dependent kinase inhibitor that increased mouse survival from about 12.5% to roughly 62.5% when administered 20 hours after irradiation [6]. Limited efficacy was also reported with the use of human recombinant growth hormone when injected up to 12 hours after irradiation in mice and non-human primate models [7]. Furthermore, toll-like receptor 5 agonist CBLB502, injected prior to high-intensity IR exposure, protected up 87% of mice and increased non-human primate survival from 25% to 64% (injected 45 min prior to exposure) [8]. To our best knowledge, there have been no published reports on small molecule drugs capable of

mitigating radiation-induced acute hematopoietic syndrome in 75% of animals lethality irradiated (LD100/30) when administered at 24 hours post-IR exposure.

Here we report a novel radiation mitigator Yel002 with a dose-modifying factor (DMF) of 1.15 for acute radiation syndrome within the hematopoietic syndrome radiation doses when administered at 24hrs post-irradiation followed by additional 4 doses every 24 hours. Yel002 was uncovered in a phenotypic DEL high throughput screen (DEL HTS) that was designed to discern molecules that modulated radiation-induced cyto- and genotoxicity in *Saccharomyces cerevisiae* [9]. Radiomitigating activity of Yel002 was next validated in murine cells and in vivo with C3H/Kam mice without demonstrating any overt toxicity. Yel002 mitigates IR-associated lethality by accelerating the recovery of the hematopoietic and immune system components without use of supportive care such as antibiotics. Notably, by day 13 following irradiation, white blood cell and platelet counts in Yel002-treated animals are nearly five times and 1.7 times higher respectively than those of control animals. We have also previously reported that Yel002 administration to thyroid cells 30 to 60 minutes after incubation with radioiodide-(131)I reduced DNA double strand breaks in thyroid cells [10].

Precise binding target of Yel002 within the cell remains elusive; however, Kinexus™ pathway activation microarray screening revealed a perturbation of the pro-survival facet of the PI3K/Akt signaling cascade. Subsequently, we were able to validate the importance of the PI3K/Akt pathway with a qRT-PCR that demonstrated a Yel002-associated suppression of PI3K inhibitor PI3KIP1.

## **MATERIALS and METHODS**

### **Mice**

C3Hf/Kam mice were bred and maintained in a strict defined-flora, pathogen-free environment in the American Association of Laboratory Animal Care–accredited animal facilities of the Department of Radiation Oncology, University of California at Los Angeles. The University of California at Los Angeles Animal Care and Use Committee approved all experiments, which were done in accordance with all local and national guidelines for the care and use of animals.

### **Animal survival assay**

Male mice, 8 to 12 weeks old, received TBI (LD100/30) from a Gamma Cell 40 irradiator ( $^{137}\text{Cs}$  source; Atomic Energy of Canada) at a dose rate of ca 67 cGy/min. To identify radiomitigators, mice were given five, daily, subcutaneous injections, starting 24 h after TBI (5x24 treatment protocol). Injections were made with Yel002 or CJ010 (75 mg/kg) dissolved in pre-warmed 1 N saline. Additional supportive care, such as antibiotics, was not provided. Mice were monitored for 30 days using standard criteria for humane euthanasia as an endpoint.

### **Differential blood counts**

C3H mice were irradiated as described above with 6 Gy and treated with Yel002 (75mg/kg) on the 5x24 treatment protocol. On days 7, 10, 13, and 16, 60  $\mu\text{L}$  of blood was taken supra-orbitally and analyzed using a HemaVet™ 950 hematology system (Drew Scientific, Waterbury, CT) [11].

## Cell lines and irradiation

A CD4<sup>+</sup>CD8<sup>+</sup> murine T lymphocyte cell line (Til-1) was cultured in DMEM with 10% fetal bovine serum and 1% antibiotic-antimycotic solution (Corning, Tewksbury, MA).

Normal human oral keratinocytes (NHOKs) were isolated from primary human specimens as previously described by Kang et al. [12]. Detached oral keratinocytes were cultured in Keratinocyte Growth Medium (KGM) (Cambrex, East Rutherford, NJ) in collagen-treated flasks. The cumulative population doublings (PDs) and replication kinetics were determined based on the number of NHOK harvested at every passage [13].

For mitigators, cells were irradiated (with X-ray irradiator at a dose of 2 Gy) 1 h before compound loading. Cell viability was determined at 24 h post-irradiation by luminescence-based measurement of ATP production (ATPlite reagent; Perkin-Elmer) with a SpectraMax M5 microplate reader (Molecular Devices).

## High-throughput screening of libraries

DEL high throughput screening for radiation-modulating agents was used to screen Asinex™ targeted libraries as previously described [9,14]. In brief, *Saccharomyces cerevisiae* Rs112 cells were inoculated into media lacking leucine (-Leu) and grown overnight with slight agitation. Plateaued cells were then re-suspended in fresh -Leu media and incubated for an additional 4 hours to synchronize the cells in S/G2 phase [15]. Synchronized cells were dispensed into 384-well target plates with Asinex™ compounds (15 μM) having previously speed-vaced DMSO. One-half of the plate contained full media (+13) and the second half contained media lacking histidine (-His). Each compound was represented in quadruplicate in each growth media type. Plates were then irradiated with

2000 Gy in upright orientation. Following irradiation, MTS compound [3-(4,5-dimethylthiazol-2-yl)-5-(3-carboxymethoxyphenyl)-2-(4-sulfophenyl)-2H-tetrazolium] was added (CellTiter 96<sup>®</sup> AQueous One Solution Cell Proliferation Assay, Promega Corp., Madison, WI) and plates were incubated at 30° C for 17 hrs. After incubation plates were read with a SpectraMax M5 microplate reader (Molecular Devices, Sunnyvale, CA) at 490 nm. Data were averaged and Z-scores for survival, DEL, and -His were calculated for each compound as previously reported [14].

Ten thousand Til-1 cells were dispensed into each well of 384-well plates using a Multidrop384 (Thermo Scientific). To identify radioprotectors, cells were preincubated with compounds for 3 h before irradiation (2 Gy). For mitigators, cells were irradiated 1 h before compound loading. Cell viability was determined at 24 h post-irradiation by luminescence-based measurement of ATP production (ATPlite reagent; Perkin-Elmer) with a SpectraMax M5 microplate reader (Molecular Devices, Sunnyvale, CA). Each compound was represented four times and the average was used for data processing. The Z' factor (10) for the assay was >0.5. To qualify for validation, the average values for the compound normalized to the vehicle controls had to be >130%.

### **Plate-based DEL validation**

Rs112 cells were grown in -Leu media, synchronized and irradiated with 2000 Gy at the density of  $2 \times 10^6$  cells/ml. After 30 min post-irradiation Yel002, hit molecules or the analogs (15  $\mu$ M) were added to the irradiated cultures and incubated with gentle agitation. After a 17-hr incubation cells were counted and plated at appropriate densities onto +13

and –His agar plates. Plates were then incubated for 72 hrs and counted. Survival was calculated as a percentage of cells surviving from the number of cells plated. DEL events were calculated as the number of revertants to functional his3 gene from the surviving fractions [14-17].

## **Proteomics**

Til-1 cells were irradiated with 2 Gy and treated with Yel002 (15uM) 1 h later. At 2h following irradiation protein lysates of cells were prepared as outlined in “Protein extract preparation, immunoprecipitation, and Western blot analysis.” Lysis buffer, supplemented with protease and phosphatase inhibitors, were supplied by Kinexus Bioinformatics (Vancouver, BC, Canada). Kinexus performed subsequent dye labeling, hybridization, and analysis of the Kinex antibody array.

## **Immunohistochemistry**

NHOKs were lysed with lysis buffer (1% Triton X–100, 20mM Tris-HCl (pH7.5), 150mM NaCl, 1mM EDTA, 1mM EGTA, 2.5mM sodium pyrophosphate, 1mM  $\beta$ -glycerolphosphate, 1mM sodium orthovanadate and PMSF) and sonicated. Whole cell lysates (40-50  $\mu$ g) were run on SDS-PAGE and transferred onto Immobilon protein membrane (Millipore, Billerica, MA). Immobilized proteins were incubated with primary antibodies against p21<sup>WAF1</sup>, p16<sup>INK4A</sup> from EMD Biosciences, Inc. (San Diego, CA, USA); pRb, p-pRb<sup>807/811</sup>, PCNA and GAPDH from Santa Cruz Biotechnology (Santa Cruz, CA); and Bmi-1



(F-6) from Upstate (Charlottesville, VA). Following incubation with primary antibodies, the membrane was probed with appropriate secondary antibodies. Results were normalized to GAPDH levels and quantitated with Scion Image software (Frederick, MD).

### **RNA sequencing (RNA-seq) and Quantitative real-time PCR (qRT-PCR)**

Total RNA was isolated from Til-1 cells using the RNeasy Mini Kit (Qiagen, Valencia, CA) with the optional column DNA digestion with Rnase-Free Dnase (Qiagen) to eliminate any traces of genomic DNA. cDNA libraries were prepared from 5 µg of total RNA with TruSeq™ RNA kit (Illumina, San Diego, CA) and sequenced on Illumina HiSeq 2000 with single-end-sequencing length of 50 nt. Data was analyzed with Ingenuity™ Pathway Analysis software (Redwood City, CA).

Real-time PCR was performed in triplicates with LC480 SYBR Green I master (Roche, Indianapolis, IN) employing universal cycling conditions on Roche LightCycler (Roche). For normalization GAPDH expression was used. The following primers for Tgfβ3, Pik3ip1, and Chac1 were used:

5' – GGG GTG GAG CCA CAC ATT TA – 3' - Tgfβ3-forward

5' – CTC CTT CGG GTG CTT CAG TT – 3' - Tgfβ3-reverse

5' – TTG GAC ACT GGC TGT TGA GT – 3' - Pik3ip1-forward

5' – CAG CCA AAACCT TCC TTC CC – 3' - Pik3ip1-reverse

5' – GCC CTG TGG ATT TTC GGG TA – 3' – Chac1-forward

5' – CAC TCC AGG ATA CGA GTG CC – 3' - Chac1-reverse

## Yel002 and Analog Synthesis

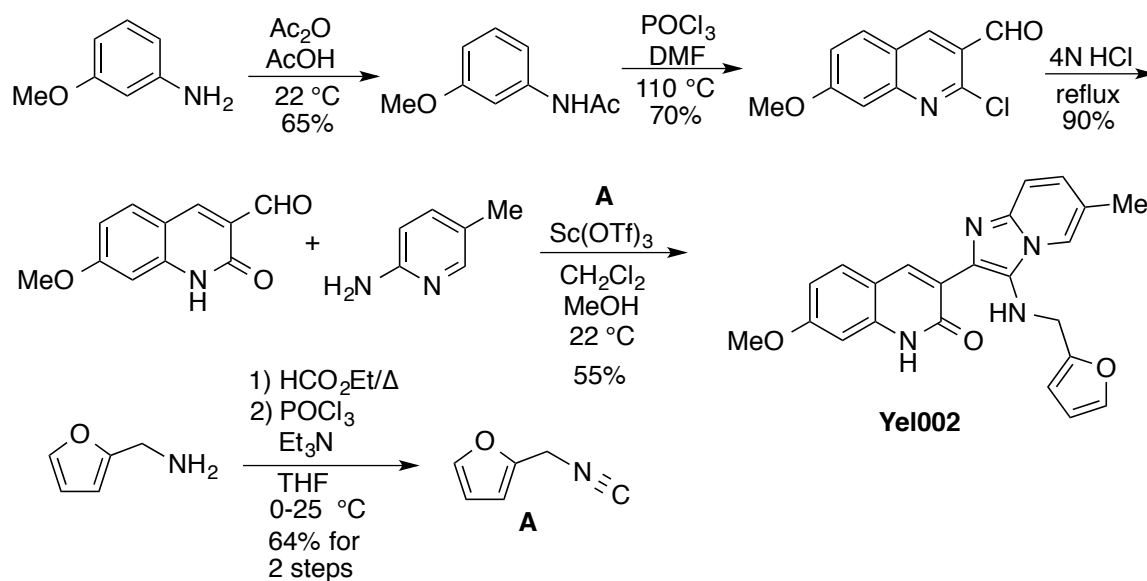


**Figure 1.** Schematic representation of Yel002 synthesis

The preparation of the most active imidazo[1,2-a]pyridine, **Yel002**, is described in detail. All of the other analogs, **CJ001-CJ008**, were made by a similar route utilizing the appropriate aldehyde, amine, and isonitrile.

### 2-(Isocyanomethyl)furan [18].

A solution of furfurylamine (2.8 mL, 30.9 mmol) in ethyl formate (ACS reagent grade, 5.1 mL) was refluxed overnight. After cooling to  $22\text{ }^\circ\text{C}$ , the reaction mixture was concentrated under reduced pressure to give the corresponding N-(furan-2-ylmethyl)formamide, which was used directly in the next step. To a solution of the crude formamide (30.9 mmol) in dry THF (77 mL) was dropwise added triethylamine (17.4 mL 123 mmol) at  $0\text{ }^\circ\text{C}$ , and  $\text{POCl}_3$  (3.2 mL, 34.0 mmol) in dry THF (8.0 mL) was added over 45

min. The reaction was stirred at 0 °C for 2 h and for 1 h at 22 °C. The reaction mixture was poured into cold water, and the organic layer was extracted three times with diethyl ether. The combined organic fractions were washed with brine, dried over MgSO<sub>4</sub>, and concentrated under reduced pressure. The crude isonitrile was purified via flash column chromatography on silica gel, eluting with ethyl acetate/hexanes 1:5 to afford the isonitrile in 65% yield. <sup>1</sup>H NMR (CDCl<sub>3</sub>, 400 MHz) δ 7.42 (s, 1H), 6.38 (s, 2H), 4.60 (s, 2H).

### **N-(3-Methoxyphenyl)acetamide.**

Acetic anhydride (5.0 mL) was added to a solution of m-anisidine (5 g, 39.8 mmol) in acetic acid (5.0 mL) cooled with an ice-water bath. The reaction was allowed to warm up to 22 °C and was stirred for 3h. The reaction was quenched with 50 mL of a 1:1 mixture of ice and water, and the resulting mixture was stirred for 20 min. The solid formed was filtered and washed with water. The material was pure enough to be used in the next step. <sup>1</sup>H NMR (CDCl<sub>3</sub>, 400 MHz) δ 7.27 (br, 1H), 7.21 (s, 1H), 7.20 (dd, 1H, J = 8.0, 8.4 Hz), 6.95 (d, 1H, J = 8.0 Hz), 6.66 (d, 1H, J = 8.4 Hz), 3.80 (s, 3H), 2.17 (s, 3H).

### **7-Methoxy-2-oxo-1,2-dihydroquinoline-3-carbaldehyde [19].**

Dimethylformamide (DMF, 4.2 mL, 21.6 mmol) was cooled to 0 °C and phosphoryl oxychloride (14.3 ml, 151 mmol) was added dropwise. To this solution was added the acetanilide (3.57 g, 21.6 mmol) and after it stirred for 5 min, the solution was heated to 110 °C for 4 h. The reaction mixture was poured into ice-water (150 ml) and stirred for 30 min at 0-10 °C. The product, the chloroquinolinecarbaldehyde, was filtered off and washed with water (100 ml). A suspension of this aldehyde (1.15 g, 6.81 mmol) in 4N aq. HCl

solution (25 mL) was heated with reflux for 3h. The mixture was added dropwise to ice-water (150 mL) and then the mixture was stirred for 30 min at 22 °C. The precipitate was filtered off, washed with water, and dried to give 7-methoxy-2-oxo-1,2-dihydroquinoline-3-carbaldehyde in 63% yield. <sup>1</sup>H NMR (DMSO-d<sub>6</sub>, 400 MHz) δ 12.03 (s, 1H), 10.14 (s, 1H), 8.40 (s, 1H), 7.80 (d, 1H, J = 8.8 Hz), 6.85 (dd, 1H, J = 8.8, 2.4 Hz), 6.79 (d, 1H, J = 2.4 Hz), 3.83 (s, 3H).

### **3-(3-((Furan-2-ylmethyl)amino)-6-methylimidazo[1,2-a]pyridin-2-yl)-7-methoxyquinolin-2(1H)-one, Yel002.**

An Ugi three-component coupling was used [20]. To a stirring mixture of 7-methoxy-2-oxo-1,2-dihydroquinoline-3-carbaldehyde (1.02 g, 5.05 mmol), 6-amino-3-picoline (0.551 g, 5.05 mmol), scandium triflate (125 mg, 0.252 mmol) in dichloromethane/methanol (1/1, 25 mL) was added 2-(isocyanomethyl)furan (5.55 mmol, 0.595 g). The reaction was stirred for 12 h at 22 °C. The reaction mixture was concentrated under reduced pressure, and then ethyl acetate (10 mL) was added. After the mixture had stirred for 30 min at 0-5 °C, the precipitate was filtered off, washed with cold ethyl acetate (5 mL) and dried under reduced pressure to furnish in 55% yield the desired compound, 3-(3-((furan-2-ylmethyl)amino)-6-methylimidazo[1,2-a]pyridin-2-yl)-7-methoxyquinolin-2(1H)-one, **Yel002**, as a yellow solid. <sup>1</sup>H NMR (DMSO-d<sub>6</sub>, 400 MHz) δ 11.97 (s, 1H), 8.33 (s, 1H), 7.89 (s, 1H), 7.68 (d, 1H, J = 8.8 Hz), 7.33 (d, 1H, J = 8.8 Hz), 7.21 (d, 1H, J = 1.2 Hz), 7.01 (dd, 1H, J = 9.6, 1.2 Hz), 6.82 (m, 2H), 6.33 (t, 1H, J = 6.8 Hz), 6.08 (dd, 1H, J = 3.2, 1.6 Hz), 5.96 (d, 1H, J = 3.2 Hz), 3.96 (d, 2H, J = 6.8 Hz), 3.80 (s, 3H), 2.28 (s, 3H). <sup>13</sup>C NMR (DMSO-d<sub>6</sub>, 125 MHz) δ 161.8, 161.1, 153.2, 142.3, 140.3, 139.7, 138.1, 130.3, 129.8, 128.3, 127.0,

123.9, 120.9, 120.4, 116.4, 114.4, 111.9, 110.5, 107.7, 97.8, 55.7, 43.8, 18.1.; HRMS (ESI)  
calcd for C<sub>23</sub>H<sub>20</sub>N<sub>4</sub>O<sub>3</sub> (M+H<sup>+</sup>): 401.1614, Found: 400.1616.

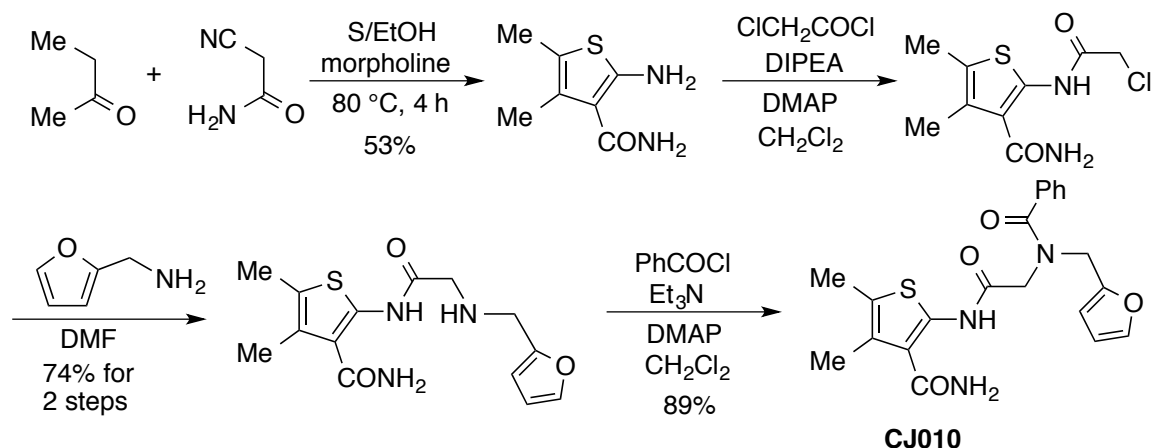


**Figure 2.** Schematic representation of CJ010 synthesis

The preparation of the most active 2-amidothiophene-3-carboxamide, **CJ010**, is described in detail. The other analogs, **CJ009-CJ014**, were all made by a similar route utilizing the appropriate ketone, amine, and acid chloride.

### **2-Amino-4,5-dimethylthiophene-3-carboxamide.[21]**

To a well-stirred suspension of 2-butanone (9.05 mL, 0.1 mol), sulfur (3.21 g, 0.1 mol) and cyanoacetamide (8.49 g, 0.1 mol) in ethanol (30 mL) was added all at once an excess of morpholine (44.2 mL, 0.5 mol). The mixture was stirred at 80 °C for 4 h. After the mixture was cooled to 22 °C, the precipitate was filtered off. Most of the solvents were evaporated and then the residue was extracted with ethyl acetate (3 × 100 mL). The combined organic phase was washed with water and brine and dried over anhydrous MgSO<sub>4</sub>. Flash column chromatography on silica gel eluting with 50/1

dichloromethane/methanol gave the Gewald cyclization product 2-amino-4,5-dimethylthiophene-3-carboxamide (9.02 g, 53%). <sup>1</sup>H NMR (500 MHz, MeOD) δ 2.15 (s, 3H), 2.13 (s, 3H). <sup>13</sup>C NMR (125 MHz, MeOD) δ 171.3, 160.0, 141.7, 128.9, 115.8, 14.2, 12.3.

**2-(2-((Furan-2-ylmethyl)amino)acetamido)-4,5-dimethylthiophene-3-carboxamide.**

To a solution of 2-amino-4,5-dimethylthiophene-3-carboxamide (1.022 g, 6.0 mmol) and (4-dimethylamino)pyridine (DMAP, 102 mg) in anhydrous dichloromethane (50 mL) and diisopropylethylamine (DIPEA, 5.5 mL) cooled to 0 °C was added slowly a solution of chloroacetyl chloride (1.95 mL, 24 mmol). The reaction mixture was allowed to warm slowly to 22 °C and was stirred overnight. The mixture was concentrated and the resulting residue was extracted with ethyl acetate (3 × 50 mL). The combined organic phase was washed with water and brine and dried over anhydrous MgSO<sub>4</sub>. The organic phase was evaporated and the crude product was dissolved in dimethylformamide (DMF, 15 mL) and furfurylamine (1.61 mL, 18 mmol) was added to the mixture. The mixture was stirred at 22 °C overnight and then extracted with ethyl acetate (3 × 50 mL). The combined organic phase was washed with water and brine and dried over anhydrous MgSO<sub>4</sub>. Flash column chromatography on silica gel eluting with 1/1 hexane/ethyl acetate gave the desired 2-(2-((furan-2-ylmethyl)amino)acetamido)-4,5-dimethylthiophene-3-carboxamide (1.36 g, 74%). <sup>1</sup>H NMR (500 MHz, CDCl<sub>3</sub>) δ 12.42 (br s, 1H), 7.27 (s, 1H), 6.22 (s, 1H), 6.19 (s, 1H), 6.18 (s, 1H), 3.78 (s, 2H), 3.40 (s, 2H), 2.21 (s, 3H), 2.20 (s, 3H). <sup>13</sup>C NMR (125 MHz, CDCl<sub>3</sub>) δ 169.0, 168.1, 152.8, 143.4, 141.8, 125.4, 124.0, 115.6, 110.0, 107.3, 50.9, 45.6, 13.9, 12.3.

## **2-(2-(N-(Furan-2-ylmethyl)benzamido)acetamido)-4,5-dimethylthiophene-3-carboxamide, CJ010.**

To a solution of 2-(2-((furan-2-ylmethyl)amino)acetamido)-4,5-dimethylthiophene-3-carboxamide (0.614 g, 2.0 mmol) and DMAP (62 mg) in anhydrous dichloromethane (10 mL) and TEA (1.0 mL) cooled to 0 °C was added slowly a solution of benzoyl chloride (0.237 mL, 2.0 mmol) in anhydrous dichloromethane (3.0 mL). The reaction mixture was allowed to warm slowly to 22 °C and was stirred overnight. The mixture was concentrated and the resulting residue was extracted with ethyl acetate (3 × 20 mL). The combined organic phase was washed with water and brine and dried over anhydrous MgSO<sub>4</sub>. Flash column chromatography on silica gel eluting with 60/1 dichloromethane/methanol gave the desired compound, **CJ010** (0.732 g, 89%). <sup>1</sup>H NMR (500 MHz, CDCl<sub>3</sub>) δ 12.31 (br s, 1H), 7.63 (br s, 2H), 7.40 (br s, 3H), 7.33 (m, 1H), 6.27 (m, 1H), 6.22 (s, 1H), 6.16 (br s, 1H), 4.64 (s, 2H), 4.29 (s, 2H), 2.25 (s, 3H), 2.23 (s, 3H). <sup>13</sup>C NMR (125 MHz, CDCl<sub>3</sub>) δ 172.2, 168.4, 166.2, 149.3, 144.3, 142.8, 135.2, 129.7, 128.3, 127.0, 125.4, 124.5, 115.4, 110.3, 109.3, 48.1, 47.2, 13.8, 12.2. HR-MS (ESI) Calcd for [C<sub>21</sub>H<sub>21</sub>N<sub>3</sub>O<sub>4</sub>S + H]<sup>+</sup> 412.1331, found 412.1316.

## **Statistical Analyses**

Statistical analyses were performed through a variety of tests including Student's t-test,  $\chi$ -squared, and Z-score calculations in Microsoft Excel and GraphPad software (La Jolla, CA).

## RESULTS

### Yel002 mitigates radiation-induced death in yeast and murine cells

#### *Yeast-based DEL High Throughput Assay*

Utilizing DEL high throughput assay we screened over 5,000 small molecule compounds from the Asinex™ library to uncover 6 novel agents (Yel002, Yel001, and Compounds A, B, C and D) that modulate radiation response in *Saccharomyces cerevisiae* tester strain RS112. Exposure to 2000 Gy of gamma rays and subsequent 16-hour incubation with these compounds reduced radiation-induced genotoxicity and increased survival (Table 1). Proliferation was measured in microwells containing both +13 and -his liquid media using colorimetric indicator MTS [9]. Increased proliferation in either media correlated with increased absorbance at 490 nm within the incubation period. Cell survival was assessed as an increase in absorbance in the +13 media (Survival z-score), while reduction in genotoxicity as a decrease in -his media (-His z-score) when compared to irradiated but untreated controls. Decrease in -his proliferation was considered a measure of genotoxicity because RS112 cells that underwent DNA deletions and subsequent repair restored the wild-type his3 gene and ability to grown in media lacking histidine. We also used a second and more accurate genotoxicity parameter, the DEL event z-score, that was calculated as a fraction of surviving cells that have undergone the reversion to a functional his3 gene. An ideal radiation-modulating (protecting or mitigating) molecule would have had a high positive survival z-score and low DEL/-his z-score. The eventual lead molecule, Yel002, was not the most potent radiation-modulating compound (DEL z-score: -7.19, Survival z-score: 4.38, and -His z-score: -4.69), but above our set threshold z-scores of 3.5 for survival and -3.5 for both DEL and -His.



### *Plate-Based DEL Assay*

We used a more sensitive plate-based DEL assay to confirm the efficacy against radiation-induced toxicity of the six compounds identified in our high throughput screen. RS112 cells were irradiated with 2000 Gy and treated with the compounds at 30 minutes after exposure for incubated them for 17hrs [14]. After the incubation cells were plated on differential media: +13 media to evaluate overall survival and -his to establish the number of genomic instability events. All six compounds were efficacious in mitigating radiation-induced geno- and cytotoxicity (Figure 3). Addition of Yel002 increased the fraction of surviving cells from 3.46% to 5.50% and decreased the number of DEL events from 12.38 to 4.47 per 10,000 surviving cells;  $P = .0114$  (survival) and  $P < .0001$  (DEL). Control surviving fraction average was 26.2% and background DEL induction was 1.3 events per 10,000 surviving cells.

### *Murine Lymphocyte Assays*

The Asinex™ library from which the 6 lead compounds originated was also tested in a high throughput assay with murine T lymphocyte cell line (Til-1). One hour following a 2 Gy irradiation, compounds were loaded onto cells and after 24hrs viability was assessed with luminescence-based measurement of ATP production. Yel002 and Compound (C) have provided some mitigation activity against radiation-induced lethality at 104.7% and 117.4% respectively, but not above the statistical significance threshold of 130%. Other compounds might have experienced slight synergy with radiation: Yel001 -97.5%, Compound (A) - 78.7%, Compound (B) - 91.2%, Compound (D) - 62.5%.

We repeated the experiment with varying concentrations of Yel002: 50, 10, 1, 0.1, 0.01 and 0.001  $\mu\text{M}$  administered 1 hr after 2 Gy. Yel002 concentrations of .001 and .01  $\mu\text{M}$  had no effect on the reproductive survival of Til-2. Optimal survival was observed between 10 and 50  $\mu\text{M}$  (Figure 4A).

## **Yel002 mitigates radiation-induced lethality in vivo by rescuing the hematopoietic system**

### *Yel002 increases survival after lethal irradiation*

Prior to the transition from in vitro to in vivo experiments, we investigated compound toxicity in a small pilot study in which animals were injected 5, 25 and 150 mg/kg of the new compounds subcutaneously. Despite the fact that the compounds originated from a library of small biological active optimized for oral drug delivery, a small pilot study to estimate the administration dose was still necessary. Animals did not display any adverse reactions to the drugs either immediately or at long term, and had normal lifespans. Additional long-term and reproductive toxicity study was later conducted with weekly subcutaneous Yel002 injections of 75mg/kg for over 12 months. No obvious toxicity was noted. Likewise, weekly subcutaneous injections with Yel002 during pregnancy did not have any adverse effects on the offspring: litter size, pup weights and health were not affected by the drug administration.

In the first set of in vivo studies, C3H mice were injected with the compounds at 1hr and 24hrs prior to radiation exposure (8 Gy, LD100/30). In this radioprotection experiment, all animals died within the period of 12 to 25 days after exposure. However, compounds A, D, Yel001 and Yel002 demonstrated some potential life extension at Day 14

post irradiation and were therefore used in subsequent mitigation experiments. In a small (n=3) mitigation study 66.7% of lethally irradiated animals (8Gy) were rescued after 75mg/kg administration of either Yel001 or Yel002 at 24, 48, 72, 96 and 120hrs after irradiation (5x24 treatment schedule). In a full-scale mitigation study (n=8) with identical experimental conditions, Yel002 and Yel001 respectively rescued 100% and 50% of the animals past Day 30 (Figure 4B). Averaged over several experiments, Yel002 rescued approximately 75% of lethality irradiated C3H mice.

To establish Yel002's dose modifying factor (DMF) within the hematopoietic syndrome dose ranges, we exposed groups of C3H mice to various doses ranging from 7 Gy to 9.1 Gy and subcutaneously treated with Yel002 at 75mg/kg and 5x24 treatment schedule. Administration of Yel002 at 9.1 Gy did not provide any benefit, but for all other doses it did, the calculated DMF was 1.15 (Figure 5).

#### *Yel002 aides in rapid hematopoietic system recovery following irradiation*

All animal experiments evaluating Yel002's efficacy against radiation-induced toxicity and death were carried out within the hematopoietic dose ranges of 6 Gy to 9.1 Gy. To track the rescue of the hematopoietic system following exposure to gamma rays and Yel002 therapy, we collected blood from irradiated (IR) and treated (IR+Yel002) C3H mice and conducted differential blood count analysis during the well-established recovery period of 7 to 16 days post-exposure. Animals were irradiated at 6 Gy as blood collections from 8 Gy irradiated animals caused spontaneous death even in the treated mice.

By Day 7 after irradiation, both the irradiated controls and irradiated and Yel002-treated animals had overall reduced white blood cell counts (WBC), 1.55 K/uL and 1.07

K/uL, respectively, compared to unirradiated control count of 13.85 K/uL. On Days 13 and 16 WBC counts went up to 3.95 K/uL and 6.09 K/uL in Yel002 animals versus .84 K/uL and 2.32 K/uL in untreated animals (Figure 6A). All types of white blood cells measured exhibited the same pattern of radiation toxicity and recovery with Yel002 administration. On Days 7 and 10 counts of neutrophils (NE), lymphocytes (LY), monocytes (MO), eosinophils (EO) and basophiles (BA) plummeted in both the IR and IR+Yel002 animals. However, by Day 13 and Day 16 Yel002 treated animals began to show signs of recovery and counts of almost all white blood cell types were higher than those of the non-treated animals. In those samples EO and BA on Day 13, and LY on Day 16 had p-values below 0.05 (Table 2).

Administration of Yel002 by Day 16 ameliorated signs of thrombocytopenia observed in irradiated animals to nearly non-irradiated control levels: 223.75 K/uL in IR+Yel002 animals, 120.75 K/uL in IR versus 267.50 K/uL non-irradiated controls (Table 2). Yel002 injections did not affect red blood cell counts, hematocrit percentages or hemoglobin concentration in irradiated animals (Table 2 and Figure 6B). However, in a repeat experiment with a larger dose of 7 Gy, red blood cells counts were significantly higher in animals treated with Yel002 on Day 17 after exposure (data not shown).

### **Yel002 mitigates radiation-induced cell senescence**

Cell senescence, or reproductive death, is another potential consequence of radiation exposure. To test whether Yel002 mitigates radiation-induced cell senescence, we irradiated (5 Gy) primary human keratinocytes – cells that are known to senesce naturally and with radiation – and followed their growth in culture for 2 week with Yel002

(5uM and 10uM dissolved in DMSO). On Day 14 cells grown in the presence of Yel002 at 10uM had 5 times as many cells as the control treated with DMSO carrier (Figure 7). Replicative senescence in non-irradiated primary human keratinocytes cultured with Yel002 was also reduced (data not shown).

We validated molecular markers of senescence with Western Blots. On Day 9 in irradiated and non-irradiated cells we saw a surge in hyperphosphorylated retinoblastoma-associated protein (Rb) and decrease in cyclin-dependent kinase inhibitor 1 (p21<sup>Cip1/WAF1</sup>) and cyclin-dependent kinase inhibitor 2A (p16<sup>INK4A</sup>) (Figure 8).

### **Lead Molecule Optimization**

In our attempt to produce a more potent radiation mitigator, 14 analogs were synthesized based on the structures of Yel001 and Yel002. In a plate-based DEL screen only CJ010 showed efficacy against radiation-induced lethality and genomic instability. Following a 2000 Gy irradiation administration of CJ010 reduced the average number of DEL events per 10,000 surviving cells to 1.54 versus 15.07 in irradiated controls. CJ010 also increased average survival from 7.49% to 36.60%. In comparison, Yel002 increased survival to 11.59% and reduced DEL events down to 2.12/10,000 surviving cells (Figure 9). CJ010 has also mitigated radiation-induced lethality in mice on the 5x24 treatment protocol and is currently being developed as a possible second lead agent (data not shown; manuscript in preparation).

## **Yel002 may modulate survival in cells through PI3K/Akt signaling**

Further development of Yel002 as a potential drug, in part, depends on its mechanism of action (MOA). Unlike traditional drug development efforts, Yel002 was uncovered in a phenotypic screen without a defined protein or signaling pathway thus leaving us with a herculean task of establishing its MOA after the lead molecule was selected. In one of our futile attempts to establish Yel002's MOA, we synthesized a biotinylated Yel002 and incubated it with whole cell lysates from yeast, mice and human, but failed to uncover Yel002's binding target (data not shown).

We screened a murine lymphocyte cell line (Til-1) for differentially activated signaling pathways following a 1-hour incubation with Yel002 using Kinex protein expression and phosphorylation profiling antibody microarray. Over 800 different antibodies are printed on the Kinex microarray chip: 530 of these antibodies are pan-specific and 270 are phosphor-specific, intended to identify changes in cell signaling proteins. Our screen revealed 110 altered protein expression or phosphorylation sites in response to Yel002 with Z-score ratio parameter set at 1.5 (Supplementary Table 1). Among the effected signal transduction pathways are extracellular signal-regulated kinase/mitogen-activated protein kinase (ERK/MAPK) (Arrestin b1, CaMK4, Caveolin 2, Cdc25, Erk5, FAK, Fos, IkbA, JNK 1/2/3, KHS, MAPKAPK2, MEK1, MEK2, MKP2, MST3, p38g, Pak3, PKC<sub>z/l</sub>, RIP/RICK, RSK1/2, STAT1/2, TAK1)[22], NF-κB (Erk5, Hsp90a/b, IkbA, IKKg (NEMO), PKA Ca/b, PKCq, PKC<sub>z/l</sub>, TBK1, TRADD), TGF-β (CDK1/2, Cofilin 1, FAK, Fos, p38g, PKBa/b, PKCq, ROKa/b, SMAD1/5/8, TAK1), TNF-α (FasL, MAPKAPK2, SODD) and PI3K/Akt (Arrestin b1, BMX (Etk), CREB1, Caspase 3, e14E, FAK, Hsp90a/b, HspBP1, IKKg (NEMO), IR, IRS1, Mcl1, p38g, PI4KCB, PKBa (Akt1), PKBb (Akt2), PKCq, PKC<sub>z/l</sub>, PP2A/Ca,

PTEN, S6Kb1, TBK1) [23,24]. Additionally, we repeated the experiment with a 2 Gy irradiation followed by a 1 hr incubation with Yel002. We set the statistical threshold at z-score ratio at 1.5 ( $P < .05$ ) between cells irradiated and treated with Yel002 versus irradiated control cells. We observed a similar pattern of pathway perturbations, especially in the case of PI3K/Akt (4E-BP1, Bcl2, Bcl-xL, DNA-PK, eIF4E, FAK, GSK3a + GSK3b, IR, PKBa (Akt1), PKCm (PKD), PTEN, S6Kb1) (Supplementary Table 2).

To examine the effects of Yel002 on gene transcription, we incubated Til-1 cells with Yel002 for 7hrs with or without 2 Gy irradiation, harvested mRNAs and performed RNA sequencing analysis (RNA-seq). In non-irradiated samples treated with Yel002, 123 genes had a fold change of at least 1.5 ( $P < .005$ ) when compared to controls (Supplemental Table 3). In the irradiated samples, 35 genes were differentially affected by irradiation and Yel002 addition (Supplemental Table 4). Among these 35 genes were Tgf $\beta$ 3 (Transforming growth factor beta 3), Pik3ip1 (Phosphoinositide-3-kinase-interacting protein 1) and Chac1 (Botch, Cation transport regulator-like protein 1). A subsequent qRT-PCR detected a slight, but significant suppression of both of these genes in non-irradiated: 36.4 versus 34.3 copies of Pik3ip1 (p-value = .018), and 34.7 versus 32.7 copies of Chac1 ( $P = .001$ ) for control and Yel002-treated samples, respectively (Figure 10). Both genes have documented involvement in apoptosis. Tgf $\beta$ 3 expression changes were not significant.

## **Discussion**

The severity of the injury and the ultimate prognosis of total-body irradiation are related to the total dose and the timing of the exposure [25-27]. In most mammals, including humans, three distinct causes of eventual death during the acute phase can be

identified: cerebrovascular syndrome, gastrointestinal syndrome, and hematopoietic syndrome. Cerebrovascular syndrome reports are linked to extremely high exposure doses of >60 Gy, with death imminent within 24-48 hours. At smaller TBI doses of >10 Gy depopulation of the intestinal epithelia, due to necrosis or mitotic arrest of mucosal cells, leads to death within 3-10 days without therapeutic intervention. A few novel agents are currently being developed for the mitigation of gastrointestinal syndrome; among them are HemaMax™ [5] and toll-like receptor 5 agonist, CBLB502[8]. The most radiation-sensitive cells in the body are the cells of the hematopoietic and the immune systems. After as little as >2 Gy of TBI, lymphocyte counts plummet within days, followed by platelet and granulocyte depletion. Red blood cells have longer lifespans, and therefore severe anemia develops at a later time point, within a couple of weeks [28,29]. At doses of 2.5 to 5 Gy, death due to hematopoietic syndrome occurs because actively proliferating precursor cells in the bone marrow are sterilized, and consequently components of the hematopoietic system are not replaced. Within 30-60 days in humans and 12-30 days in mice, mature blood cells begin to die off and without therapeutic intervention death ensues. Bone marrow transplant, infection control, and antibiotic administration can promote survival [30]; however, population-scale implementation of these therapeutic interventions is impractical and cost-prohibitive. In the event of large-scale radiation exposure due to a nuclear accident or attack radiation mitigator administration will most likely take place in the field outside of a hospital setting, and not until several hours after the initial exposure. This setting necessitates stable and easy-to-administer radiation mitigators with potent activity when administered at 24 hours or longer after the initial exposure.



Here we presented a novel radiation mitigator Yel002 that rescued on average 75% of mice following an 8 Gy irradiation (LD100/30) without additional supportive care. Notably, Yel002 mitigated radiation-induced hematopoietic toxicity with the first administered injection 24 hours after irradiation followed by 4 additional treatments at 48, 72, 96, and 120 hours after. Yel002 mediated survival by promoting regeneration of the hematopoietic system potentially by reducing radiation-induced senescence or apoptosis among the hematopoietic stem cells and their progenitors.

Taken together, our experiments suggest that Yel002 acts via the PI3K/Akt signaling cascade (Figure 11). At one hour after administration of Yel002 to murine lymphocytes Kinexus microarrays screen detected perturbations – increase or decrease in protein levels or degree of phosphorylation – in PI3K/Akt downstream substrates and its upstream effectors. It is imperative to keep in mind that the results of large high throughput screens, such as the Kinexus microarray or the RNA-seq experiments, represent only a snapshot of the cell's activity at a particular time point. Such experiments can demonstrate patterns and tendencies, but not necessarily elucidate the exact mechanism of action. It is of no surprise then that within the same PI3K/Akt signaling pathway we have observed both activating and deactivating components. Nevertheless, because Yel002 promotes survival in irradiated cells and mice, and decreases radiation-induced cell senescence via p21<sup>Cip1/WAF1</sup> suppression, we can infer that Yel002 affects the pro-survival facets of PI3K/Akt signaling pathway and its downstream substrates [31,32]. The precise target and chain of events within the pathway, however, remains elusive.

The phosphatidylinositol 3-kinase (PI3K) signaling pathway through its downstream serine/threonine-specific Protein Kinase B (PKB/Akt) substrates affects a

variety of functions in the cell including cell growth, metabolism, motility and survival; it has been implicated in a diverse set of diseases ranging from cancer to type-2 diabetes. The PI3K/Akt cascade is highly conserved from simple eukaryotes, such as yeast, to mammals, and its regulation is tightly controlled. PI3K regulatory subunit p110 maintains a low degree of activation in quiescent cells and directly interacts with activated receptor tyrosine kinases (e.g. insulin and growth factor receptors) and adaptor proteins. Downstream activation of Akt is mediated by 3-phosphoinositide-dependent protein kinase 1 (PDK1) in response to stimulated PI3K. Phosphorylation of Akt at Threonine-308 (T308) within the “activation loop,” and at a second site in the carboxyl terminal domain on Serine-473, must be activated by the Rictor kinase part of the mammalian target of rapamycin (mTORC2) [33] incites its catalytic activity resulting in phosphorylation of many downstream substrates that regulate cell cycle, cell growth and survival [34].

Incubation with Yel002 directly increased the abundance of Akt1 and Akt2, but reduced phosphorylation levels on T308 on Akt1. Akt exists in three isoforms (Akt1, Akt2, and Akt3), and despite sequence homology in some signaling cascades Akt1 and Akt2 might act in complementary opposite manner [34]; in some instances stimulation and activation of the same receptor might activate either Akt1 or Akt2 and result in entirely divergent effects [35]. Decreases in phosphorylation at T308 might have been a consequence of elevated PP2A, a regulatory phosphatase as a part of the negative feedback loop [23,36]. Literature suggests that increases in Akt concentration predictably increase phosphorylation of its substrates [34]. Thus, we inferred that Yel002 largely activates the PI3K/Akt pathway, despite the observed dephosphorylation in the activating loop.

Our screens did not register direct perturbation in the PI3K, PDK1 nor mTOR concentrations or their respective phosphorylation states. While mTOR itself was not changed, its downstream substrates – ribosomal protein S6 kinase beta-1 (S6Kb1) and eukaryotic translation initiation factor 4E (eIF4E) – were affected [37]. Additionally, levels of PI3K negative regulator PTEN rose after Yel002 incubation. Increase in both PP2A and PTEN might be a part of the negative feedback loop reacting to the potential activation of PI3K/Akt signaling cascade.

Yel002 affected a handful of pro-survival substrates within the Akt signaling pathway, among them increase in the inhibitor of apoptosis MCL-1 and decrease in the overall abundance of Caspase-3 and Caspase-6. Unfortunately, the Kinexus microarray does not provide information on activation or cleavage state of these caspases, therefore we cannot definitively conclude if these were inactivated via degradation. These will be investigated in detail in our further studies. Furthermore, we observed an increase in Akt-activating upstream effector TANK binding kinase 1 (TBK1), which stimulates pro-survival signaling independent of the canonical PI3K/PDK1 and mTOR pathways [38]. However, another important pro-survival substrate, cyclic AMP-responsive element-binding protein 1 (CREB1), was deactivated through dephosphorylation on its activating serine sites (S129 and S133) [39,40].

One-hour incubation with Yel002 might also promote survival by activating the NF- $\kappa$ B pathway possibly even downstream of PI3K/Akt [41-43]. While we didn't detect changes on the NF- $\kappa$ B molecule directly, there were changes in protein levels of I $\kappa$ B $\alpha$  and IKK $\gamma$ /NEMO, regulators of NF- $\kappa$ B activity. I $\kappa$ B $\alpha$  is one of the NF- $\kappa$ B inhibitory proteins that keeps NF- $\kappa$ B inactive in the cytoplasm. Activated NF- $\kappa$ B is released from its inhibitory

proteins and translocates to the nucleus where it initiates transcription. I $\kappa$ B $\alpha$  itself is one of the transcriptional targets of activated NF- $\kappa$ B that is resynthesized upon NF- $\kappa$ B stimulation. Newly synthesized I $\kappa$ B $\alpha$  binds NF- $\kappa$ B, creating a negative feedback loop within one hour of NF- $\kappa$ B activation, corresponding to the time in which we detected the I $\kappa$ B $\alpha$  surge [44]. Observed reduction of IKK $\gamma$ /NEMO might also be a part of internal NF- $\kappa$ B regulation. Recent study by Shibata et al. reported negative NF- $\kappa$ B regulation through NEMO degradation via NSFL1 cofactor p47 (p47)[45].

There are conflicting reports regarding the role of PI3K/Akt pathway in cell senescence. Miyauchi et al. reported that Akt activity increases with cellular senescence and that inhibition of Akt prolonged the lifespan of primary human endothelial cells [46]. In a more recent study Liu and colleagues demonstrated that a decrease in Akt activity is linked to increased senescence and self-renewal of human skin-derived precursors [47]. Heron-Milhavet and colleagues reported that Akt1, but not Akt2, is required for proliferation in vitro by cyclin-dependent kinase inhibitor p21<sup>Cip1/WAF1</sup> (p21) phosphorylation and its subsequent re-localization to the cytoplasm. Akt2, on the other hand, is essential for cell cycle exit via p21 stabilization and concentration increase [48]. Moreover, in complex breast cancer tumor microenvironments, Akt1 activation promotes cell survival while Akt2 activation inhibits growth [49]. Late-passage and senescent cells show accumulation of p16<sup>INK4A</sup> [50] and p21<sup>Cip1/WAF1</sup> [51]. Because primary human keratinocytes grown in the presence of Yel002 showed a significant reduction in both of these proteins, and an increase in pRb consistent with non-senescent, cycling cells, we concluded that Yel002 affects pro-cycling Akt involvement.

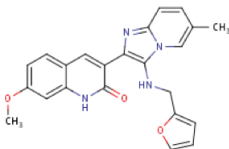
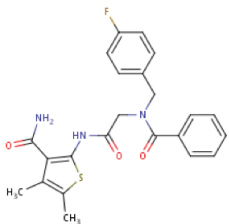
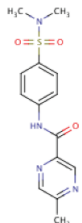
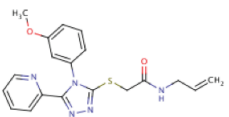
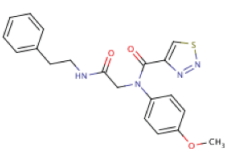
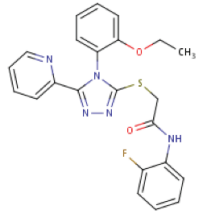
Moreover, we were able to demonstrate the importance of PI3K/Akt signaling on a transcriptional level. After 7 hours of incubation with Yel002, Til-1 cells showed suppressed mRNA levels of PI3K inhibitor PI3KIP1. PI3K interacting protein 1, is a novel negative PI3K regulator that binds to its p110 subunit and decreases PI3K activity in vitro and in vivo. Decreased PI3KIP1 was also linked to aberrant PI3K activity in murine and human hepatocellular carcinomas [52,53]. Another pro-apoptotic gene, *chac1/mgc4504* (cation transport regulator-like protein 1)[54], was downregulated by Yel002 treatment further supporting its pro-survival activity in cells.

To summarize, Yel002 was uncovered in a phenotypic yeast-based screen that simultaneously assessed compounds for their ability to modulate radiation-induced genotoxicity and cytotoxicity. Yel002 treatment of irradiated cells increased survival and reduced the number of cells that underwent gene deletion to reconstitute a functional *his3* gene. Reduction in DEL events in the mitigation treatment protocol, where the drug is added sometime after the IR, may be interpreted in two different ways. In the first scenario, reduction in His<sup>+</sup> colonies after IR and subsequent Yel002 administration might truly be a reduction in genomic instability. Alternatively, treatment of irradiated RS112 yeast cells with Yel002 30 minutes after exposure might indicate that Yel002 does not necessarily mitigate genomic instability in yeast cells, but rather that Yel002 steers the cells towards an alternative repair mechanism. Restoration of the functional *his3* gene in RS112 is a product of homologous recombination (HR) repair following a DNA double-strand break (DSB) [55,56], thus, a reduction in detectable His<sup>+</sup> colonies might indicate a potential decrease in HR repair, but an increase in non-homologous end-joining (NHEJ). Of

note, Yel002's proposed mechanism of action via PI3K/Akt has been reported to suppress HR in favor of NHEJ, contributing to radioresistance [57].

Yel002 represents an important addition to the radiation mitigating drug development pipeline. In addition to mitigating lethality associated with exposure to gamma radiation, Yel002 also reduces DNA double strand breaks induced with a common nuclear exposure byproduct, radioiodide-(131)I [10]. Yel002's ability to modulate cell senescence in response to IR might also find potential application in the clinical setting as a mitigator of normal tissue damage in patients undergoing radiation therapy.

**Table 1. Six Novel Radiation-Modulating Compounds**

	<b>DEL z-score</b>	<b>Survival z-score</b>	<b>-His z-score</b>
<p><b>Compound Yeloo2</b></p> 	-7.19	4.38	-4.69
<p><b>Compound Yeloo1</b></p> 	-3.68	3.14	-2.66
<p><b>Compound (A)</b></p> 	-6.41	4.30	-3.94
<p><b>Compound (B)</b></p> 	-5.83	4.10	-2.96
<p><b>Compound (C)</b></p> 	-4.61	7.55	-2.03
<p><b>Compound (D)</b></p> 	-4.52	3.12	-2.32

**Table 1. Six hit molecules uncovered with DEL HTS.** Yeast RS112 cells were synchronized to G2/S phase and irradiated with 2000 Gy in 384-well microtiter plates. Half of the plate contained full media (+his) and the other half contained media lacking histidine (-his). Following irradiation colorimetric MTS agent was loaded into the wells and incubated at 30° C for 16 hrs. After incubation absorbance was measured at 490 nm and z-scores were calculated for each compound represented in quadruplicate in each type of media. Compounds with survival z-scores above 2.0 and -his and DEL z-scores below -2.0 (p <.005) were considered for a re-test.



**Figure 3. Six hit molecules mitigate radiation-induced cell death and genomic instability in *S. cerevisiae***

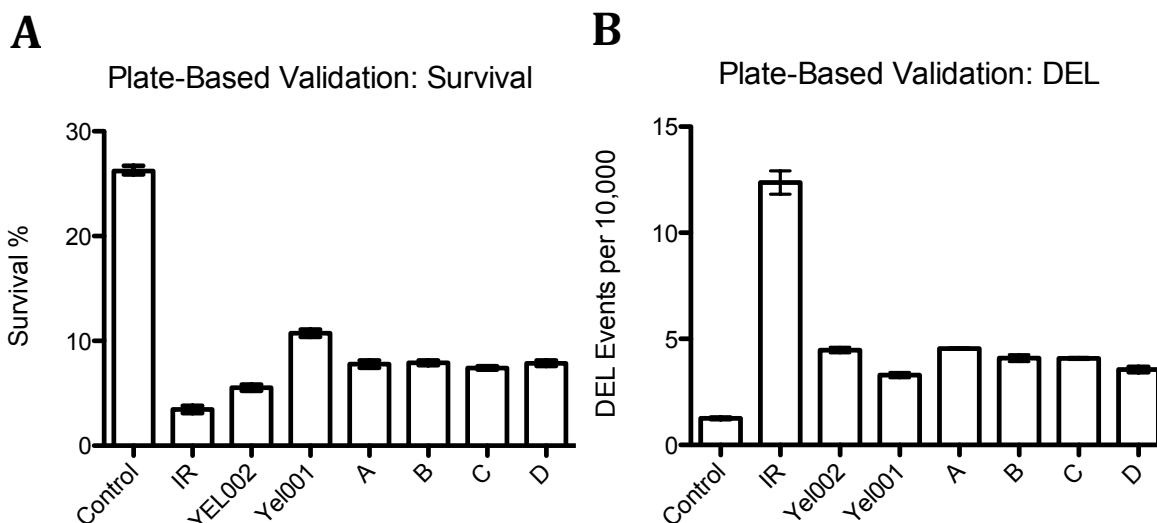


**Figure 3.** Six hit molecules mitigate radiation-induced cell death and genomic instability in *S. cerevisiae* when added 30 min after irradiation. RS112 cells were grown overnight, synchronized to G2/S phase and exposed to 2000 Gy IR. Thirty minutes after exposure hit compounds (15  $\mu$ M) were added to irradiated cells and incubated with agitation for 17 hrs. After incubation cells were plated on  $-$ His or  $+13$  agar media and incubated for 72hrs. Colonies were then counted and appropriate surviving fractions and DEL events calculated. **A.** Treatment with hit molecules of RS112 cells exposed to 2000 Gy mitigated cell death. Survival was calculated as the percentage of individual colonies on  $+13$  media from the number of cells plated (Student-t test, all molecules  $P < .05$ ). **B.** Treatment with hit molecules reduced deletion events were also reduced with hit molecule administration. DEL events were calculated as fractions of surviving cells that have undergone a reversion to a functional *his3* gene and produced colonies on  $-his$  media (Student-t test, all molecules  $P < .05$ ).

**Figure 4. Yel002 mitigates radiation-induced death *in vitro* and *in vivo***

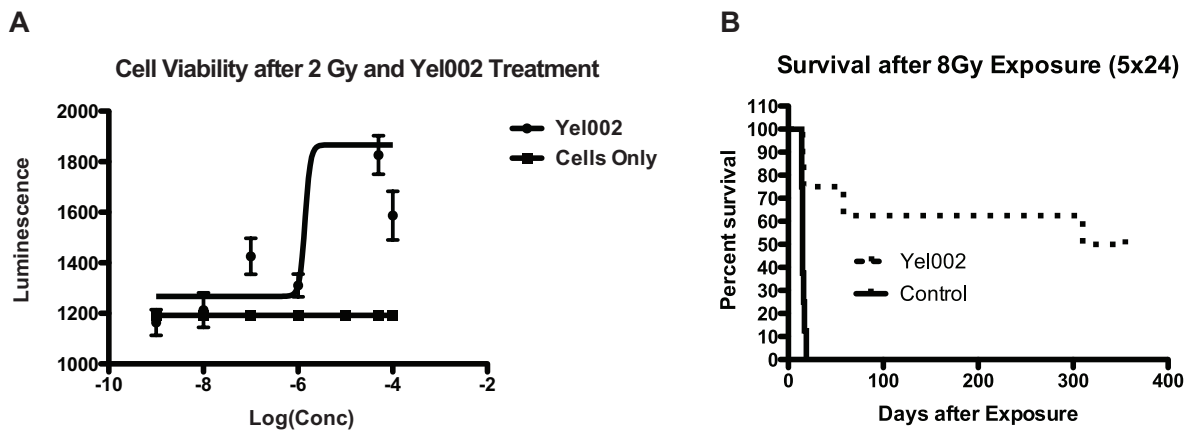


**Figure 4.** Administration of Yel002 mitigates radiation-induced death *in vitro* and *in vivo*. **A.** Til-1 lymphocytes were irradiated with 2 Gy and 1 hr later treated with Yel002. Dose-response curve was generated with 100, 50, 10, 1, 0.1, .01 and .001  $\mu\text{M}$ . Viability was measured with luminescence-based measurement of ATP production (ATPlite™) at 24 hrs. Optimal mitigation was achieved with concentrations between 10 and 50  $\mu\text{M}$  (Student t-test,  $P < .05$ .) **B.** Male C3H mice at 8 weeks old ( $n = 8$ ) were irradiated with 8 Gy (LD100/30) and treated with Yel002 (75mg/kg) in 1N saline at 24 hrs after IR. Additional subcutaneous (s.c.) injections were made at 48, 72, 96 and 120 hrs later (5x24 treatment protocol). Control animals were injected with saline carrier. At 30 days post-IR 75% of Yel002-treated animals were alive while 100% of control animals have died (X-square test,  $P = .0019$ ). Within 1 year the number of surviving animals decreased to 50%. Remaining mice after had normal 2.5-year lifespans.

**Figure 5. Dose-modifying curve**

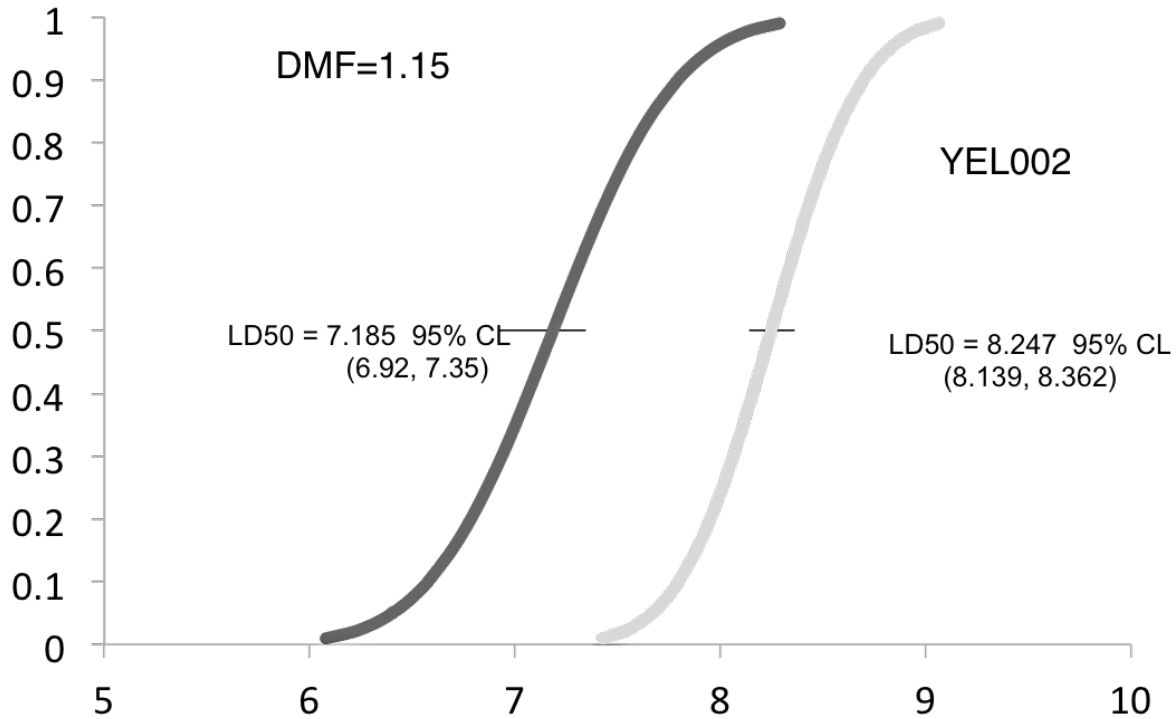


**Figure 5.** Yel002 has a Dose-Modifying Factor (DMF) of 1.15 for IR within the hematopoietic syndrome range. C3H mice (n=8 per group with matched controls) were exposed to increasing doses of gamma radiation (7.0 to 9.0 Gy) and treated with Yel002 (75mg/kg) s.c. on the 5x24 drug administration protocol. Controls received 1N saline carrier injections. Statistical calculations predict a DMF of 1.15 at LD50.

**Table 2. Yeloo2 mitigates radiation-induced hematopoietic system damage**

	Day 7	Day 10	Day 13	p-value <sub>D13</sub>	Day 16	p-value <sub>D16</sub>
WBC-6Gy (K/uL)	1.55	0.66	0.84		2.32	
WBC-6Gy+Yel002 (K/uL)	1.07	0.77	3.95	.03	6.09	.03
NE#-6Gy (K/uL)	0.61	0.18	0.13		0.69	
NE#-6Gy+Yel002 (K/uL)	0.34	0.20	1.47	.03	2.73	.03
LY#-6Gy (K/uL)	0.58	0.37	0.62		1.22	
LY#-6Gy+Yel002 (K/uL)	0.54	0.44	1.93	.03	2.26	.06
MO#-6Gy (K/uL)	0.11	0.05	0.04		0.14	
MO#-6Gy+Yel002 (K/uL)	0.06	0.08	0.20	.01	0.32	.04
EO#-6Gy (K/uL)	0.17	0.05	0.04		0.19	
EO#-6Gy+Yel002 (K/uL)	0.09	0.04	0.26	.06	0.56	.04
BA#-6Gy (K/uL)	0.08	0.01	0.02		0.08	
BA#-6Gy+Yel002 (K/uL)	0.04	0.01	0.09	.11	0.22	.05
RBC-6Gy (M/uL)	7.21	5.37	5.11		5.18	
RBC-6Gy+Yel002(M/uL)	6.62	7.31	5.94	.07	6.59	.17
HB-6Gy (g/dL)	11.30	8.20	8.45		8.40	
HB-6Gy+Yel002(g/dL)	9.98	11.68	9.40	.16	10.70	.17
PLT-6Gy (K/uL)	104.75	84.75	75.75		120.75	
PLT-6Gy+Yel002 (K/uL)	134.5	96.25	129.29	.05	223.75	.04
HCT-6Gy (%)	37.95	27.43	25.73		27.23	
HCT-6Gy+Yel002(%)	34.60	38.05	30.78	.12	37.08	.12

**Table 2.** Yeloo2 mitigates radiation-induced hematopoietic system damage after a 6 Gy irradiation. C3H mice (n=4) were irradiated with 6 Gy and treated with Yeloo2 (75mg/kg) s.c. on the 5x24 treatment protocol. Starting at Day 7 after irradiation animals were bled supraorbitally and differential blood counts were obtained with HemaVet™ analytical instrument. Statistical significance was calculated with Student’s t-test.

**Figure 6. Yel002 accelerates recovery of the hematopoietic system**

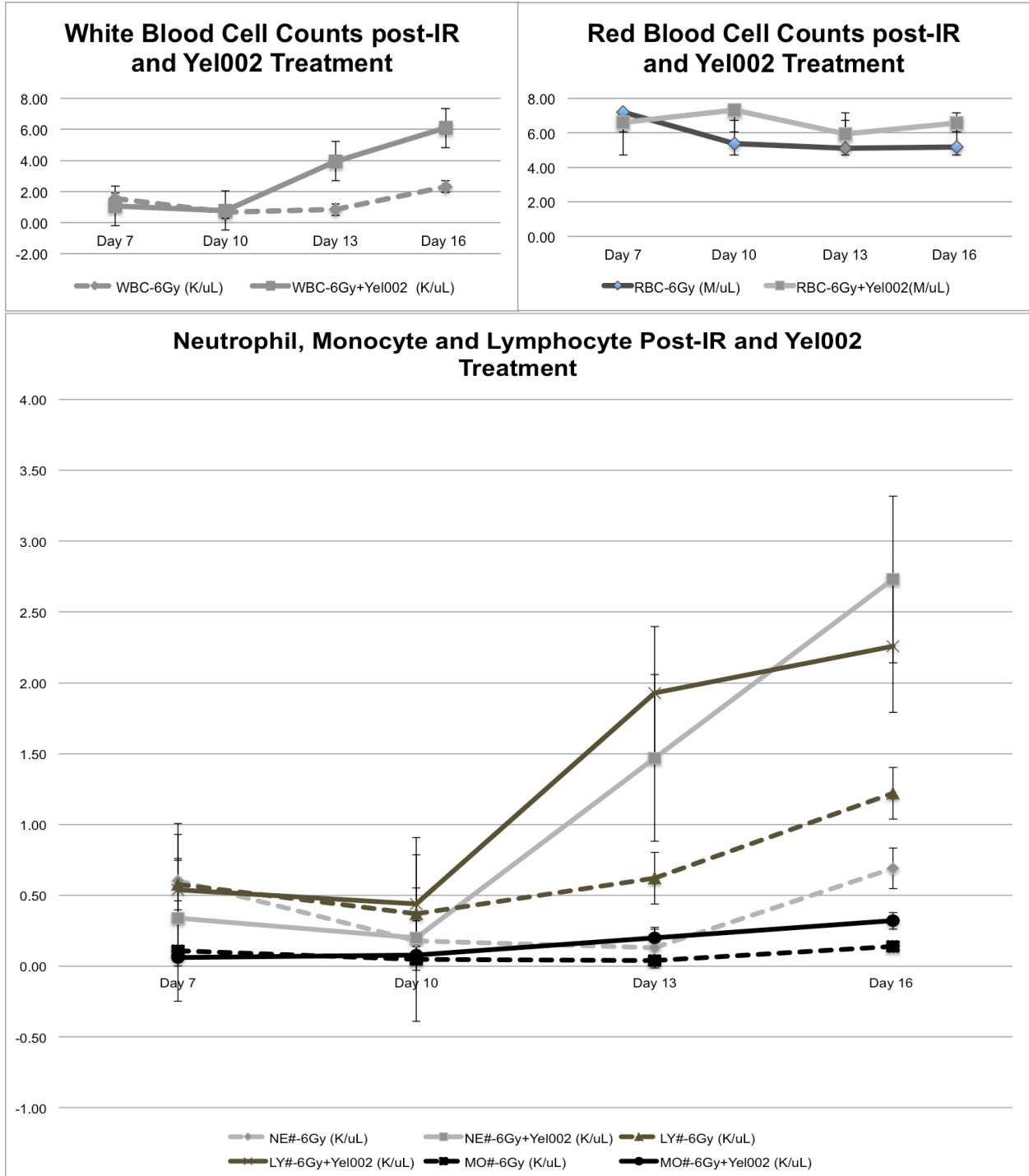


**Figure 6.** Yeloo2 mitigates radiation-induced hematopoietic system damage after a 6 Gy irradiation. C3H mice (n=4) were irradiated with 6 Gy and treated with Yeloo2 (75mg/kg) s.c. on the 5x24 treatment protocol. Starting at Day 7 after irradiation animals were bled supraorbitally and differential blood counts were obtained with HemaVet™ analytical instrument. Statistical significance was calculated with Student's t-test. **A.** On days 13 and 16 the overall white blood cell (WBC) counts in the Yeloo2-treated group were higher than the non-treated controls suggesting a more rapid recovery. **B.** Treatment with Yeloo2 didn't significantly affect the red blood cell (RBC) counts in animals irradiated with 6 Gy. **C.** Irradiated animals treated with Yeloo2 had significantly larger counts of neutrophils (NE), monocytes (MO), eosinophils (EO), and basophils (BA) between days 13 and 16 (Refer to Table 2).

**Figure 7. Yel002 reduces radiation-induced senescence**

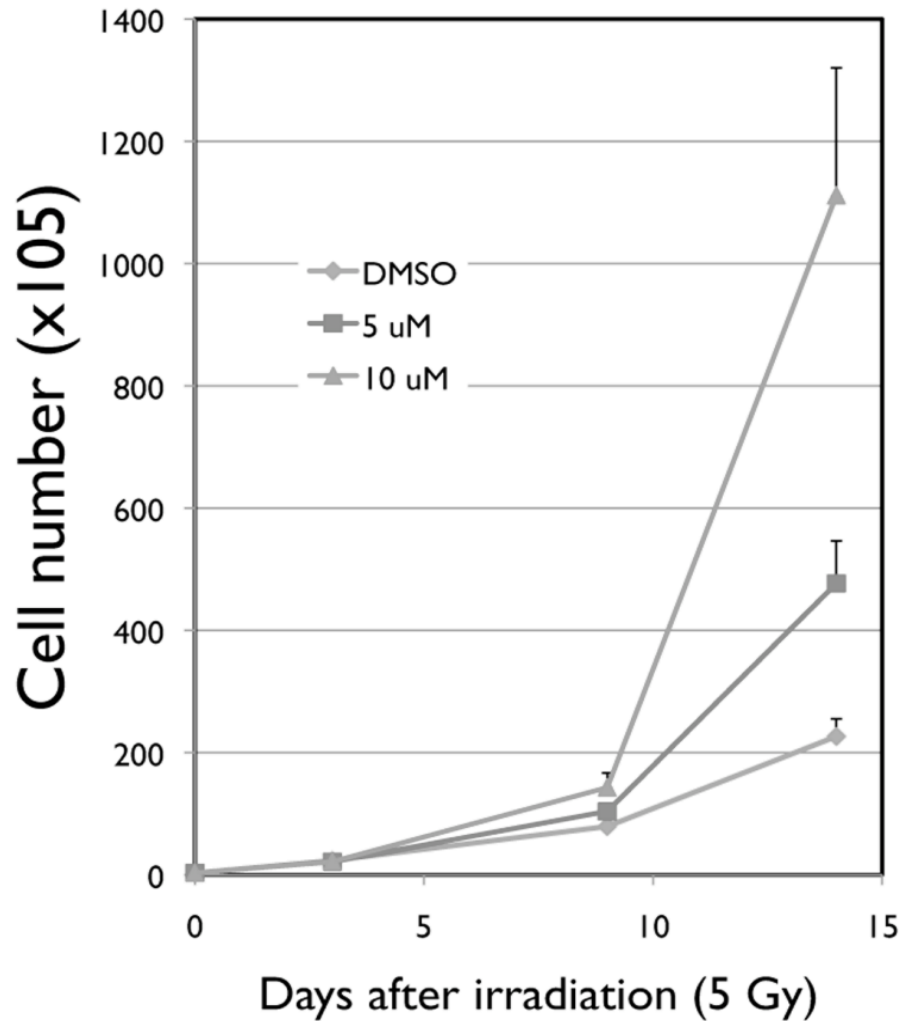


**Figure 7.** Coculturing of primary normal human oral keratinocytes (NHOK) after a 5 Gy irradiation reduced radiation-induced cell senescence and promoted cells replication. NHOK were harvested from patients undergoing oral surgery and irradiated. One hour following irradiation Yel002 was added to the irradiated NHOKs either at 5 or 10  $\mu$ M. Cells were harvested and counted on days 3, 9, and 14. By day 14, cells grown in the presence of Yel002 had exceeded the number of cells in non-treated groups multiple-fold.

**Figure 8. Incubation with Yel002 reduced senescence-associated proteins**

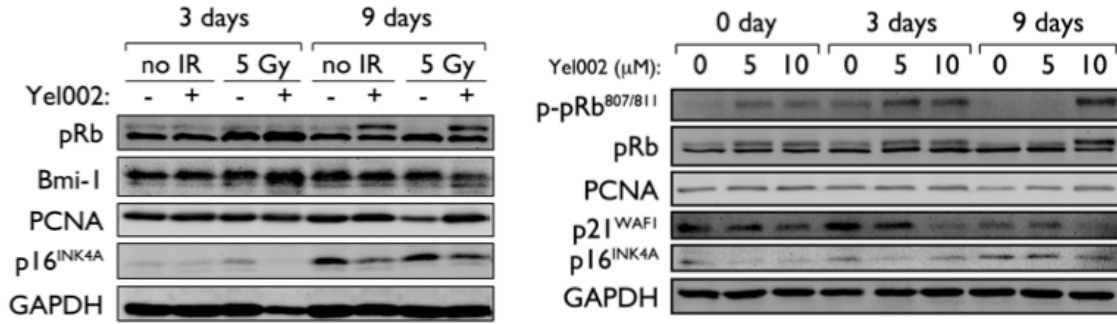


**Figure 8.** Incubation of Yel002 decreased senescence-associated proteins and promoted cell cycling via phosphorylation of Rb in irradiated and non-irradiated NHOK cells. **A.** Co-culture of NHOKs with Yel002 (10 μM) following a 5 Gy irradiation increased phosphorylation of Rb and reduced concentrations of p16<sup>INK4A</sup> in irradiated NHOKs. **B.** Yel002 appears to affect Rb, p21<sup>WAF1</sup>, and p16<sup>INK4A</sup> in a concentration-dependent manner in unirradiated NHOKs. In the case of p21<sup>WAF1</sup>, Yel002 appears to have a stronger suppressive effect over prolonged incubation period. Suppressive effect on p16<sup>INK4A</sup> appears to wear-off over time. Phosphorylation of Rb, however, continued to increase with extended Yel002 treatment.



**Figure 9. Lead molecule optimization with DEL Assay**

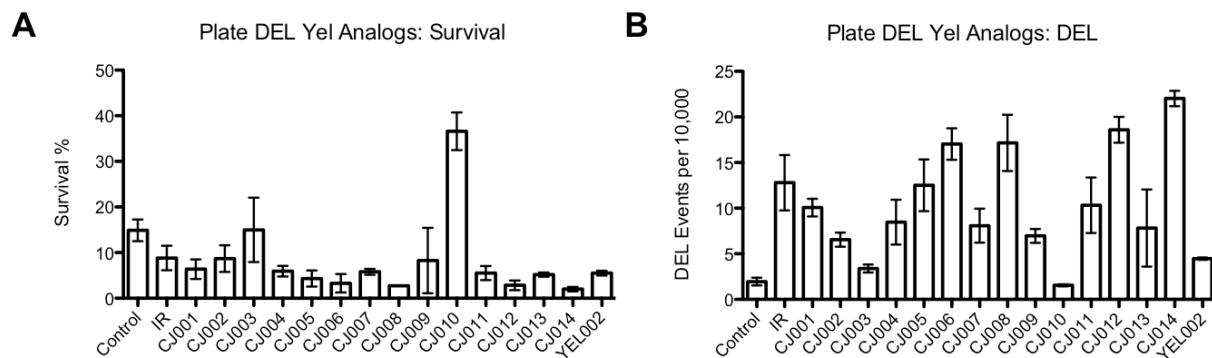


**Figure 9.** Only one analog based on lead molecules Yel001 and Yel00, CJ010, reduced genomic instability and increased survival after 2000 Gy irradiation in RS112 cells. RS112 cells were grown overnight, synchronized to G2/S phase and exposed to 2000 Gy IR. Thirty minutes after exposure analog compounds (15  $\mu$ M) were added to irradiated cells and incubated with agitation for 17 hrs. After incubation cells were plated on –His or +13 agar media and incubated for 72hrs. Colonies were then counted and appropriate surviving fractions and DEL events calculated. **A.** Treatment with either CJ010 or Yel002 of RS112 cells exposed to 2000 Gy mitigated cell death. Survival was calculated as the percentage of individual colonies on +13 media from the number of cells plated (Student-t test, CJ010:  $P = .0003$ , Yel002:  $P = .01$ ). **B.** Likewise, only Treatment with CJ010 or Yel002 reduced deletion events were also reduced with hit molecule administration. DEL events were calculated as fractions of surviving cells that have undergone a reversion to a functional *his3* gene and produced colonies on –his media (Student-t test, CJ010:  $P = .003$ , Yel002  $P = .01$ ).

**Figure 10. Yel002 suppresses pro-apoptotic genes *PI3KI1* and *Chac1***

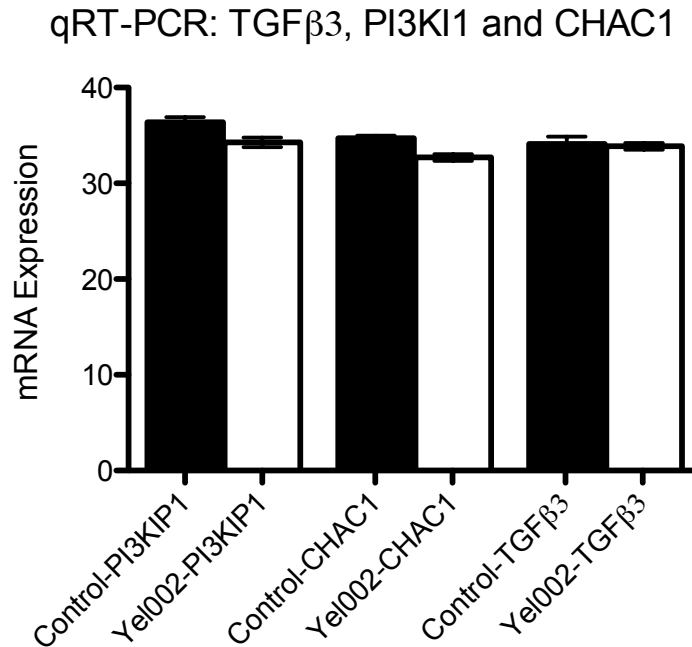


**Figure 10.** Seven-hour incubation with Yel002 suppresses pro-apoptotic genes *PI3KI1* and *Chac1*. Til-1 cells were incubated with Yel002 (15μM) for 7 hours after which mRNA was harvested and converted into cDNA libraries. Quantitative PCR (qRT-PCR) was used to enumerate relative number of mRNA copies of *PI3KIP1* and *Chac1* genes. Yel002 significantly suppressed both of the genes (Student's t-test,  $P_{PI3KIP1} = .02$  and  $P_{CHAC1} = .001$ ). Changes in *Tgfb3* were not significant ( $P=.78$ ).

**Figure 11. Proposed mechanism of Action of Yel002**

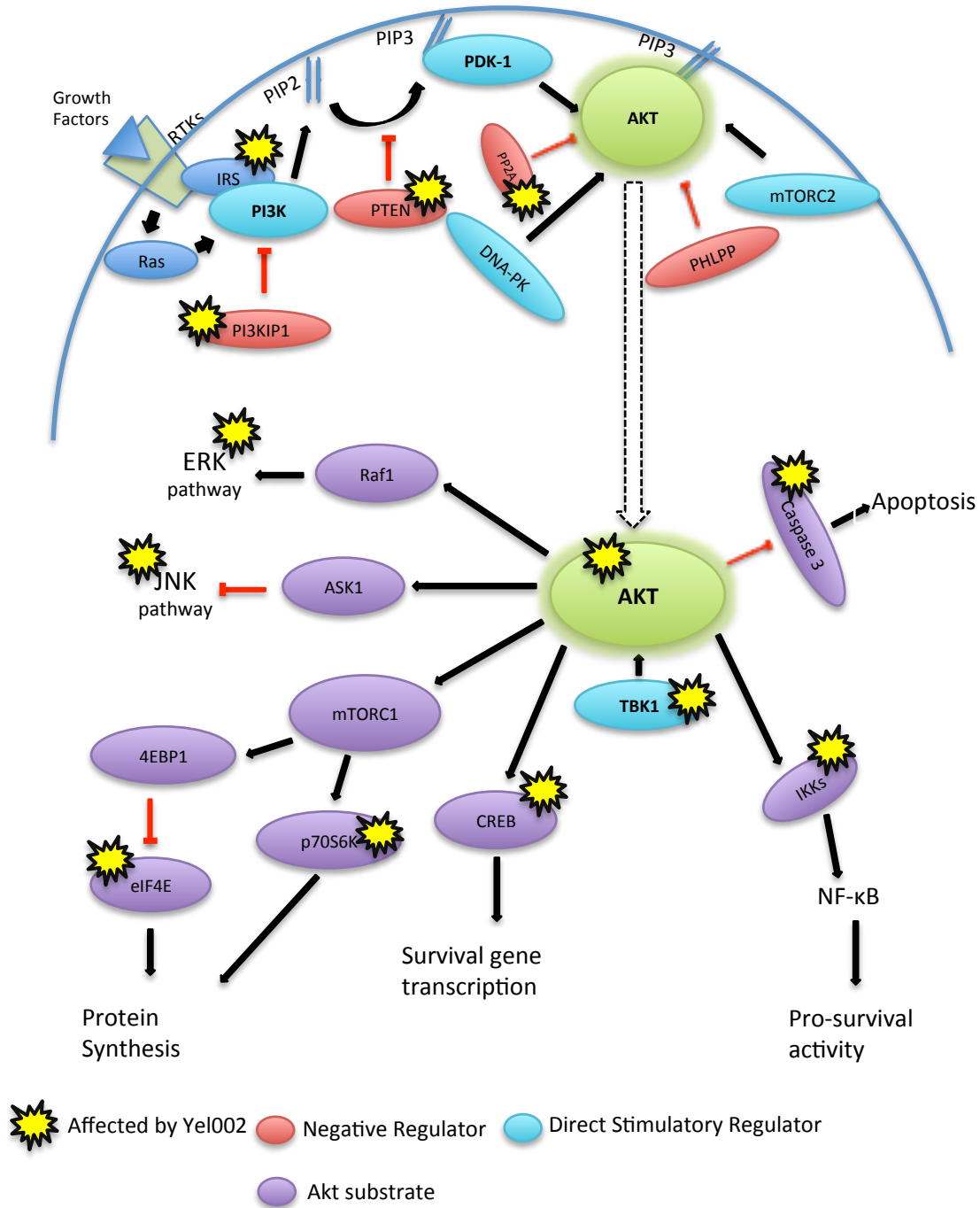


**Figure 11.** Yel002 modulates response to ionizing radiation via the PI3K/Akt pathway. Collectively, the data from the Kinexus protein microarray and the validated qRT-PCR experiment indicate that Yel002 affects the PI3K/Akt signaling cascade in a pro-survival manner. The pattern of perturbations in the mouse lymphocytes incubated with Yel002

(15  $\mu\text{M}$ ) also point to an activation of the NF- $\kappa\text{B}$  signaling. The exact binding target of Yel002 remains to be established.

**Supplementary Table 1. Yel002 Affects Protein Expression and Phosphorylation in Non-Irradiated Cells**

Target Protein	Phospho site (human)	Z-score ratio (Yel002 vs. Control)	Target Protein	Phospho site (human)	Z-score ratio (Yel002 vs. Control)
Arrestin b1	Pan-specific	-1.97	ErbB2 (HER2)	Pan-specific	1.54
B23 (NPM)	T234/T237	-1.86	Erk5	Pan-specific	-1.5
BMX (Etk)	Pan-specific	-1.94	Erk5	T218+Y220	-1.73
Btk	Y223	-1.54	FAK	S722	-1.81
Caldesmon	S789	1.62	FAK	S732	-1.59
CaMK4	Pan-specific	-1.72	FasL	Pan-specific	-1.78
CAS	Pan-specific	-3.17	Fos	T232	-1.92
CASK/Lin2	Pan-specific	-1.66	GFAP	S8	-1.68
CASP1	Pan-specific	-1.68	Histone H3	T12	1.7
CASP3	Pan-specific	-1.73	Hsp90a/b	Pan-specific	-2.16
CASP6	Pan-specific	-1.71	Hsp90b	Pan-specific	-1.66
Caveolin 2	Pan-specific	-3.18	HspBP1	Pan-specific	-1.8
Cdc25C	S216	-2.73	IkBα	Pan-specific	1.57
CDK1/2	Y15	-2.06	IKKg (NEMO)	Pan-specific	-2.15
CDK2	Pan-specific	-2.09	IR	Pan-specific	-1.9
CDK6	Pan-specific	-1.51	IRS1	Y612	-1.56
Cofilin 1	Pan-specific	-2.25	JNK1/2/3	T183 + Y185	-1.64
Cofilin 1	S3	-1.72	KHS	Pan-specific	1.71
COX2	Pan-specific	-2.21	Ksr1	Pan-specific	2.75
CPG16/CaMKinase VI	Pan-specific	-2.47	LATS1	Pan-specific	2.42
CREB1	S129+S133	-1.79	Lck	Pan-specific	1.78
CREB1	S133	-1.52	Lck	Y505	1.72
Crystallin aB	Pan-specific	-1.78	MAPKAPK2	Pan-specific	1.74
Crystallin aB	Pan-specific	-1.58	MAPKAPK2	T222	1.64
Csk	Pan-specific	-2.21	MAPKAPK2a + MAPKAPK2b	T334	2.04
eEF2K	Pan-specific	2.75	MARK	Pan-specific	1.51
EGFR	Y1197	2.23	Mcl1	Pan-specific	1.52
eIF4E	S209	-1.94	MEK1 (MAP2K1)	Pan-specific	1.57

(Supplementary Table 1 continued)

Target Protein	Phospho site (human)	Z-score ratio (Yel002 vs. Control)	Target Protein	Phospho site (human)	Z-score ratio (Yel002 vs. Control)
MEK2 (MAP2K2)	T394	-1.61	RSK1/2	S380/S386	3.32
MKP2	Pan-specific	-2.07	S6Kb1	Pan-specific	2.92
MST3	Pan-specific	-1.8	S6Kb1	T252	2.12
p38g MAPK (Erk6)	Pan-specific	1.57	S6Kb1	T444+S447	1.82
PACSIN1	Pan-specific	1.83	S6Kb1	T412	-1.78
PAK3	Pan-specific	1.68	Smad1/5/8	S463+S465/S463+S465/S465+S467	1.55
PI4KCB	Pan-specific	1.68	SMC1	S957	1.86
PKA Ca/b	Pan-specific	-2.25	SODD	Pan-specific	2.03
PKBa (Akt1)	Pan-specific	2.32	STAT1a + STAT1b	Pan-specific	2.75
PKBa (Akt1)	T308	-2.59	STAT2	Y690	3.28
PKBb (Akt2)	Pan-specific	1.59	Synapsin 1	S9	1.68
PKCq	Pan-specific	-1.87	TAK1	Pan-specific	2.15
PKCz/l	T410/T412	-2	TAK1	Pan-specific	1.89
PKG1	Pan-specific	1.67	Tau	S516	2.87
PKR1	Pan-specific	-2.42	Tau	S516+S519	3.67
PKR1	T451	-2.28	Tau	S713	2.31
PP2A/Ca + PP2A/Cb	Pan-specific	-2.17	Tau	S721	3.37
PTEN	Pan-specific	1.71	Tau	S519	2.4
PTP1B	Pan-specific	-2.11	Tau	S739	2.1
PTP1C	Pan-specific	-1.71	TBK1	Pan-specific	2.12
Pyk2	Y579	-1.72	TRADD	Pan-specific	2.58
Rb	Pan-specific	-1.99	Tyk2	Pan-specific	1.8
Rb	S807+S811	-2.54	Tyrosine Hydroxylase	S18	1.75
RIP2/RICK	Pan-specific	-2.56	Vrk1	Pan-specific	2.22
ROKa (ROCK2)	Pan-specific	1.62	YSK1	Pan-specific	1.6
ROKb (ROCK1)	Pan-specific	-1.69	ZIPK	Pan-specific	2.14
RONa	Pan-specific	-1.66			

**Supplementary Table 1.** One-hour incubation with Yel002 affected the total concentration and phosphorylation states of 110 proteins in non-irradiated murine lymphocytes. TIL-1 cells were incubated for 1 hr with Yel002 (15  $\mu$ M) prior to total protein harvest. The samples were then shipped to Kinexus™ where the proteins were stained, applied onto antibody microarray chips and readouts were analyzed. Here we compared Z-score ratios of Yel002-treated and untreated samples with a threshold of 1.5 ( $P < .05$ ).

**Supplementary Table 2. Yel002 Affects Protein Expression and Phosphorylation in Irradiated Cells**

Target Protein	Phospho site (human)	Z-ratio (IR+Yel002 vs. IR)	Target Protein	Phospho site (human)	Z-ratio (IR+Yel002 vs. IR)
4E-BP1	T70	-5.67	GRK2 (BARK1)	S670	-1.77
B23 (NPM)	T234/T237	-1.89	GRK3 (BARK2)	Pan-specific	-1.58
Bcl2	Pan-specific	-2.19	GroEL	Pan-specific	-1.53
Bcl-xL	Pan-specific	-2.28	Grp94	Pan-specific	-1.84
BLNK	Y84	-1.91	GSK3a + GSK3b	Pan-specific	-2.58
BMX (Etk)	Pan-specific	-2.40	Haspin	Pan-specific	-1.58
BRD2	Pan-specific	-1.51	Histone H2B	S15	-2.46
Btk	Pan-specific	-1.61	IkBa	Pan-specific	3.13
Btk	Y223	-2.26	IKKb	Pan-specific	1.54
Calnexin	Pan-specific	-2.54	IR	Pan-specific	-1.55
CDK1/2	Y15	-1.52	JNK1	Pan-specific	-1.69
DAPK2	Pan-specific	2.13	JNK2/3	Pan-specific	1.61
DNAPK	Pan-specific	1.57	JNK3	Pan-specific	2.19
eEF2K	Pan-specific	4.38	Jun	Pan-specific	2.29
EGFR	Y1197	2.49	Jun	S63	-1.70
EGFR	Y1197	2.70	Jun	S73	3.37
eIF4E	Pan-specific	3.14	Kit	Y730	1.58
ErbB2 (HER2)	Pan-specific	2.75	Kit	Y936	2.13
ErbB2 (HER2)	Y1248	2.72	LATS1	Pan-specific	2.61
Erk1 + Erk2	Pan-specific	1.57	Lck	Pan-specific	3.17
Erk1 + Erk2	Pan-specific	2.11	Lck	Y505	2.44
Erk1 + Erk2	[T202+Y204] + [T185+Y187]	1.63	LIMK1	Pan-specific	4.58
Erk2	Pan-specific	1.81	Lyn	Y508	2.11
Erk5	Pan-specific	-2.29	LATS1	Pan-specific	2.61
Erk5	T218+Y220	-2.19	Lck	Pan-specific	3.17
ERP57	Pan-specific	-1.96	Lck	Y505	2.44
FAK	Y576	-1.72	LIMK1	Pan-specific	4.58
FAK	S722	-2.00	Lyn	Y508	2.11
FAK	S910	-1.75	MAK	Pan-specific	1.60
FasL	Pan-specific	-1.51	MAPKAPK2a + MAPKAPK2b	T334	2.09
FKBP52	Pan-specific	-1.87	MARCKS	S159+S163	2.66
FKHRL1	T32	-1.84	MEK1 (MAP2K1)	Pan-specific	2.03
GAP-43	S41	-1.62	MEK1 (MAP2K1)	T386	1.51

(Supplementary Table 2 continued)

Target Protein	Phospho site (human)	Z-ratio (IR+Yel002 vs. IR)	Target Protein	Phospho site (human)	Z-ratio (IR+Yel002 vs. IR)
MAK	Pan-specific	1.60	PKM2	Pan-specific	1.71
MAPKAPK2a + MAPKAPK2b	T334	2.09	Plk2	Pan-specific	1.54
MARCKS	S159+S163	2.66	PP5C	Pan-specific	-1.86
MEK1 (MAP2K1)	Pan-specific	2.03	PP6C	Pan-specific	-1.64
MEK1 (MAP2K1)	T386	1.51	PRK1 (PKN1) + PRK2 (PKN2)	T774 + T816	-2.23
MEK2 (MAP2K2)	T394	-1.60	PSD-95	Pan-specific	-1.91
MEK3 (MAP2K3)	S218	-1.93	PTEN	S380+T382+S385	-2.58
MEK3/6 (MAP2K3/6)	S218/S207	-1.90	PTP1B	Pan-specific	-2.70
MEK5 (MAP2K5)	Pan-specific	-1.77	PTP1D	S580	-1.82
MKP2	Pan-specific	-1.95	TPD1	Pan-specific	-1.55
MLK3	T277+S281	-1.73	Rab5	Pan-specific	-1.59
PDGFRa/b	Y572+Y574/Y579+Y581	-1.80	Rac1	Pan-specific	-2.08
PKA Ca/b	Pan-specific	-2.41	RIP2/RICK	Pan-specific	-1.80
PKBa (Akt1)	T308	-1.76	RIPK1	Pan-specific	1.76
PKCd	T507	1.55	ROKa (ROCK2)	Pan-specific	-1.56
PKCg	Pan-specific	1.53	ROKb (ROCK1)	Pan-specific	-2.12
PKCh	S674	1.60	RSK1/2	S380/S386	-2.45
PKCm (PKD)	S910	1.55	S6Kb1	T412	2.75
PKCq	T538	1.52	Smad2/3	Pan-specific	-2.51
PKCz	Pan-specific	1.71	VHR	Pan-specific	-1.76
PKCz/l	T410/T412	1.93			

**Supplementary Table 2.** One-hour incubation with Yel002 affected the total concentration and phosphorylation states of 110 proteins in irradiated murine lymphocytes. Til-1 cells irradiated with 2 Gy and incubated for 1 hr with Yel002 (15  $\mu$ M) prior to total protein harvest. The samples were then shipped to Kinexus™ where the proteins were stained, applied onto antibody microarray chips and readouts were analyzed. Here were compared Z-score ratios of Yel002-treated and untreated irradiated samples with a threshold of 1.5 ( $P < .05$ ).

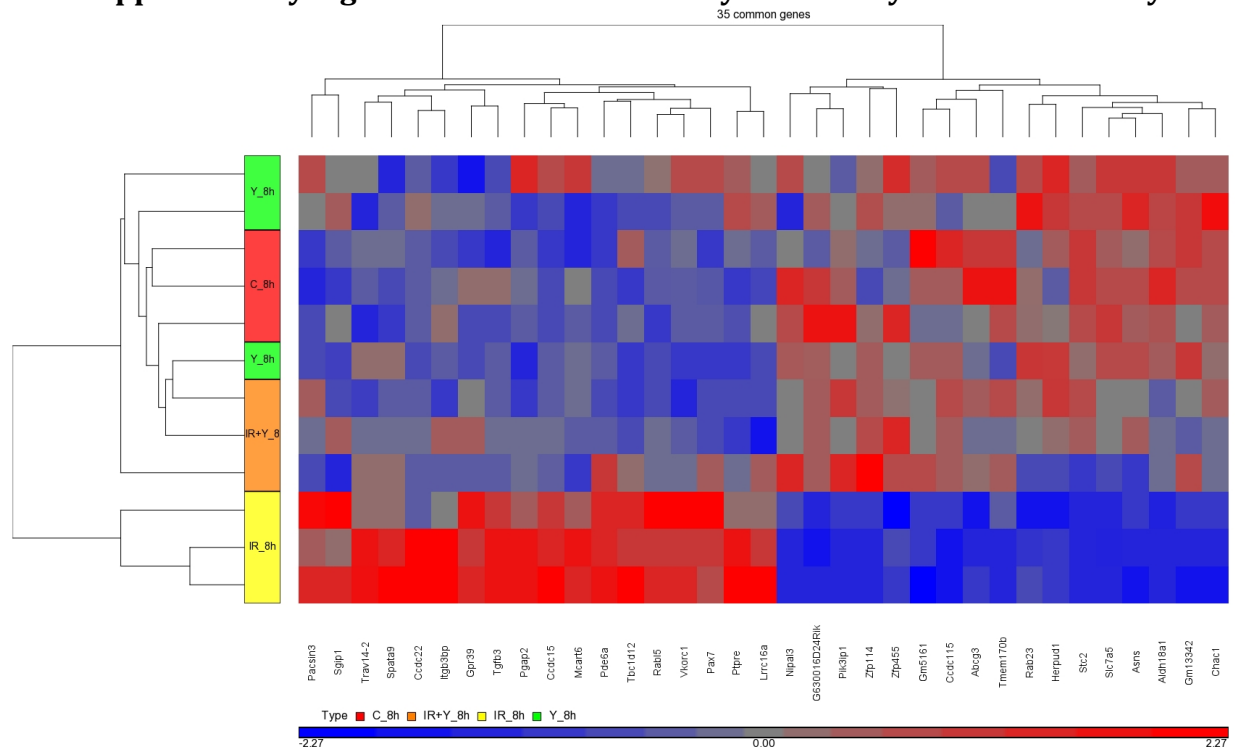


**Supplementary Table 3. Genes Affected by Yel002 after IR**

Genes	Fold Change (IR+Y_8h vs. IR_8h)	Genes	Fold Change (IR+Y_8h vs. IR_8h)	Genes	Fold Change (IR+Y_8h vs. IR_8h)
Trav14-2	-2.31	Rabl5	-1.53	Gm5161	1.59
Pde6a	-1.77	Ccdc22	-1.64	Zfp455	2.07
Pacsin3	-1.52	Tgfb3	-1.53	Zfp114	2.96
Spata9	-1.86	Sgip1	-1.64	Asns	1.66
Mcart6	-2.50	Ptpre	-1.58	Stc2	1.72
Ccdc15	-1.59	Pgap2	-1.60	Slc7a5	1.70
Gpr39	-1.52	Nipal3	1.50	Aldh18a1	1.64
Vkorc1	-2.05	Herpud1	1.59	Tmem170b	1.79
Itgb3bp	-1.84	Ccdc115	1.57	Chac1	2.11
Pax7	-1.53	Pik3ip1	1.62	G630016D24Rik	2.53
Lrrc16a	-1.98	Rab23	1.53	Abcg3	2.32
Tbc1d12	-1.76	Gm13342	1.58		

**Supplementary Table 3.** Yel002 administration differentially affects 35 genes in murine lymphocytes after a 2 Gy irradiation. Til-1 cells were irradiated and 1 h later Yel002 (15  $\mu$ M) was administered. Til-1 cells were incubated with Yel002 (15  $\mu$ M) for 7 hours after which mRNA was harvested and converted into cDNA libraries. Genes presented in this table were significantly and differentially affected by Yel002 incubation in irradiated cells (1.5 fold difference threshold;  $P < .005$ ).

## Supplementary Figure 1. Genes differentially affected by Yel002 after 2 Gy



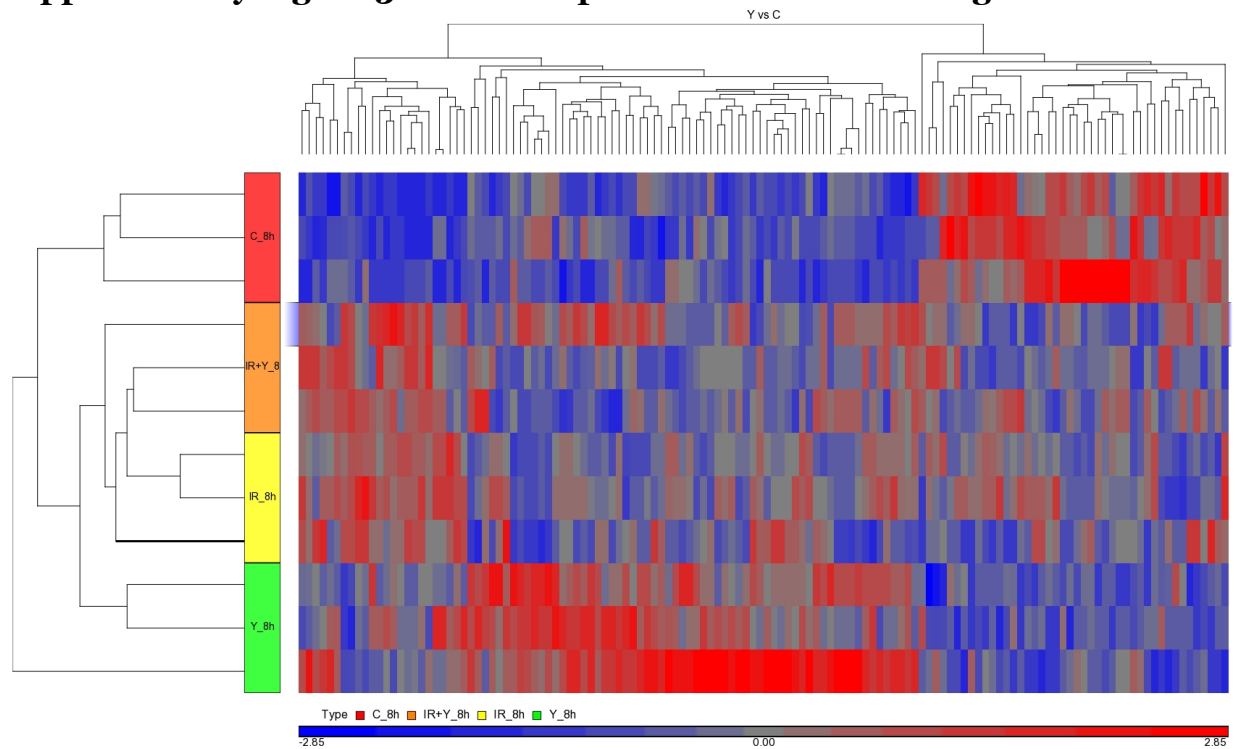
**Supplementary Figure 1.** Incubation with Yel002 for 7 hrs following irradiation differentially affected 35 genes – if the gene was up-regulated in the irradiated cells, then the treatment with Yel002 returned the expression to normal levels and vice versa. Til-1 cells were treated with Yel002 and after the incubation mRNAs were harvested and converted to cDNA libraries. Libraries were subsequently sequenced and analyzed with Ingenuity™ pathway analysis software. Significance threshold was set at 1.5 fold change ( $P < .005$ ).

**Supplementary Table 4. Genes Affected by Yeloo2 Treatment**

Genes	Fold Change (Y_8h vs. C_8h)	Genes	Fold Change (Y_8h vs. C_8h)	Genes	Fold Change (Y_8h vs. C_8h)
Phlda3	-1.54	Zfp26	1.51	9430038I01Rik	2.34
Cd80	-4.55	Zfp428	0.66	Fam69b	0.55
Acot5	2.23	Elmod2	1.63	Txnrd2	0.56
Acot2	1.76	Gm5662	1.94	H2-Ke6	1.55
Acot1	1.85	Gm4425	3.22	Mfsd12	1.74
Trbj2-4	1.73	Gm2035	1.72	Spag1	1.59
Col15a1	-1.55	Efna2	2.29	Accs	1.69
Rhob	1.96	Cd2	0.62	LOC100862027	0.42
41522	1.61	Ern1	1.70	Sle37a3	0.54
Tmem170b	-1.76	1110007C09Rik	1.98	H2-Ke6	1.57
Cyb5b	1.54	Naip2	1.57	H2-Ke6	1.57
Gm2056	3.38	Prkd2	1.70	LOC100862432	1.88
Slc16a5	1.65	Fgfbp3	0.26	Hspbap1	1.58
Tsga14	1.59	4930523C07Rik	0.55	Numbl	0.57
Tmem68	1.68	Hmgcs1	1.53	Ttc30b	0.57
Lss	1.51	BC024978	1.85	F2	1.66
Cpt1a	1.80	Nkrf	1.53	Sgsh	0.57
Lamb3	1.80	Rex2	1.58	Grk4	1.99
Dnahc14	4.32	Casp9	1.53	Glp1r	0.53
ND4L	1.50	Rgp1	1.59	Golt1b	0.61
Cd160	1.52	Ccbl2	0.63	Acn9	1.94
Lrrc28	1.88	Zfp566	1.63	Hpca	0.62
Mocs3	2.66	Pecam1	1.61	Gm8332	1.52
Scel	1.97	D630037F22Rik	1.57	Gm2046	1.95
Atf5	1.57	Fnip2	1.86	Trbj2-5	1.95
Ccdc57	-1.87	Coro2b	1.97	Crebl2	0.49
Obfc1	2.07	Trp53bp2	1.63	Ptprn	1.72
Naip2	1.69	Anxa4	0.55	H2-Ke6	1.56
Eif1a	1.56	Lmcd1	0.55	Psen2	0.62
6230427J02Rik	-1.89	LOC100039029	1.56	1600002K03Rik	2.79
Dscc1	-1.70	Polr2f	0.64	Bnip1	1.60
Cd2	-1.87	Grin3b	0.54	Fbxo6	1.50
Erlin1	-1.64	LOC100041824	2.80	1500031L02Rik	1.56
Tmem203	1.57	Gm20267	0.40	Ier3	0.56
Fdps	1.58	Myh11	1.62	Mmaa	0.63
Xrcc6bp1	-1.59	Ifi30	1.79	LOC100861993	0.52
Sc4mol	1.61	Bscl2	1.68	Dmpk	0.62
Pard6b	-1.80	Fam18b	1.57	Morn2	1.97
Mrpl51	1.54	LOC100862448	1.84	Gm8300	1.68
Gm5215	-4.29	Rhbdd2	0.65	LOC671917	1.51
9930104L06Rik	-1.52	Glyctk	1.67	Agbl3	2.03

**Supplementary Table 4.** Following 7-hr incubation with Yeloo2 123 genes were significantly up- or down-regulated on transcriptional level. Til-1 cells were incubated with Yeloo2 (15  $\mu$ M) for 7 hours after which mRNA was harvested and converted into cDNA libraries. Genes presented in this table were significantly affected by Yeloo2 incubation ( $P < .005$ ).

### Supplementary Figure 3: Yel002 expression versus control gene cluster



**Supplementary Figure 3.** Yel002 expression versus control gene cluster. A seven-hour incubation of Til-1 lymphocytes with Yel002 (15  $\mu$ M) affected the expression of 123 genes. Til-1 cells were treated with Yel002 and after the incubation mRNAs were harvested and converted to cDNA libraries. Libraries were subsequently sequenced and analyzed with Ingenuity™ pathway analysis software.

## References

1. Hall, E.J.; Giaccia, A.J., Radiobiology for the radiologist. 7th ed.; Wolters Kluwer Health/Lippincott Williams & Wilkins: Philadelphia, 2012; p p.
2. Donnelly, E.H.; Nemhauser, J.B.; Smith, J.M.; Kazzi, Z.N.; Farfan, E.B.; Chang, A.S.; Naeem, S.F., Acute radiation syndrome: Assessment and management. Southern medical journal **2010**, 103, 541-546.
3. Saha, S.; Bhanja, P.; Kabarriti, R.; Liu, L.; Alfieri, A.A.; Guha, C., Bone marrow stromal cell transplantation mitigates radiation-induced gastrointestinal syndrome in mice. PloS one **2011**, 6, e24072.
4. Williams, J.P.; Brown, S.L.; Georges, G.E.; Hauer-Jensen, M.; Hill, R.P.; Huser, A.K.; Kirsch, D.G.; Macvittie, T.J.; Mason, K.A.; Medhora, M.M., et al., Animal models for medical countermeasures to radiation exposure. Radiation research **2010**, 173, 557-578.
5. Basile, L.A.; Ellefson, D.; Gluzman-Poltorak, Z.; Junes-Gill, K.; Mar, V.; Mendonca, S.; Miller, J.D.; Tom, J.; Trinh, A.; Gallaher, T.K., Hemamax, a recombinant human interleukin-12, is a potent mitigator of acute radiation injury in mice and non-human primates. PloS one **2012**, 7, e30434.
6. Johnson, S.M.; Torrice, C.D.; Bell, J.F.; Monahan, K.B.; Jiang, Q.; Wang, Y.; Ramsey, M.R.; Jin, J.; Wong, K.K.; Su, L., et al., Mitigation of hematologic radiation toxicity in mice through pharmacological quiescence induced by cdk4/6 inhibition. The Journal of clinical investigation **2010**, 120, 2528-2536.
7. Chen, B.J.; Deoliveira, D.; Spasojevic, I.; Sempowski, G.D.; Jiang, C.; Owzar, K.; Wang, X.; Gesty-Palmer, D.; Cline, J.M.; Bourland, J.D., et al., Growth hormone mitigates against lethal irradiation and enhances hematologic and immune recovery in mice and nonhuman primates. PloS one **2010**, 5, e11056.
8. Burdelya, L.G.; Krivokrysenko, V.I.; Tallant, T.C.; Strom, E.; Gleiberman, A.S.; Gupta, D.; Kurnasov, O.V.; Fort, F.L.; Osterman, A.L.; Didonato, J.A., et al., An agonist of toll-like receptor 5 has radioprotective activity in mouse and primate models. Science **2008**, 320, 226-230.
9. Hontzeas, N.; Hafer, K.; Schiestl, R.H., Development of a microtiter plate version of the yeast del assay amenable to high-throughput toxicity screening of chemical libraries. Mutation research **2007**, 634, 228-234.
10. Hershman, J.M.; Okunyan, A.; Rivina, Y.; Cannon, S.; Hogen, V., Prevention of DNA double-strand breaks induced by radioiodide-(131)i in frtl-5 thyroid cells. Endocrinology **2011**, 152, 1130-1135.
11. Kim, K.; Pollard, J.M.; Norris, A.J.; McDonald, J.T.; Sun, Y.; Micewicz, E.; Pettijohn, K.; Damoiseaux, R.; Iwamoto, K.S.; Sayre, J.W., et al., High-throughput screening identifies two classes of antibiotics as radioprotectors: Tetracyclines and fluoroquinolones. Clinical cancer research : an official journal of the American Association for Cancer Research **2009**, 15, 7238-7245.
12. Kang, M.K.; Guo, W.; Park, N.H., Replicative senescence of normal human oral keratinocytes is associated with the loss of telomerase activity without shortening of telomeres. Cell growth & differentiation : the molecular biology journal of the American Association for Cancer Research **1998**, 9, 85-95.

13. Kim, R.H.; Lieberman, M.B.; Lee, R.; Shin, K.H.; Mehrazarin, S.; Oh, J.E.; Park, N.H.; Kang, M.K., Bmi-1 extends the life span of normal human oral keratinocytes by inhibiting the tgf-beta signaling. *Experimental cell research* **2010**, 316, 2600-2608.
14. Hafer, K.; Rivina, Y.; Schiestl, R.H., Yeast del assay detects protection against radiation-induced cytotoxicity and genotoxicity: Adaptation of a microtiter plate version. *Radiation research* **2010**, 174, 719-726.
15. Hafer, K.; Rivina, L.; Schiestl, R.H., Cell cycle dependence of ionizing radiation-induced DNA deletions and antioxidant radioprotection in *saccharomyces cerevisiae*. *Radiation research* **2010**, 173, 802-808.
16. Brennan, R.J.; Schiestl, R.H., Positive responses to carcinogens in the yeast del recombination assay are not due to selection of preexisting spontaneous revertants. *Mutation research* **1998**, 421, 117-120.
17. Carls, N.; Schiestl, R.H., Evaluation of the yeast del assay with 10 compounds selected by the international program on chemical safety for the evaluation of short-term tests for carcinogens. *Mutation research* **1994**, 320, 293-303.
18. Kercher, T.; Rao, C.; Bencsik, J.R.; Josey, J.A., Diversification of the three-component coupling of 2-aminoheterocycles, aldehydes, and isonitriles: Efficient parallel synthesis of a diverse and druglike library of imidazo- and tetrahydroimidazo[1,2-a] heterocycles. *Journal of combinatorial chemistry* **2007**, 9, 1177-1187.
19. Meth-Cohn, O.N., B.; Tarnowski, B., A versatile new synthesis of quinolines and related fused pyridines, part 5. The synthesis of 2-chloroquinoline-3-carbaldehydes. *J. Chem. Soc., Perkin Trans* **1981**, 1520-1530.
20. Blackburn, C.; Guan, B.; Fleming, P.; Shiosaki, K.; Tsai, S., Parallel synthesis of 3-aminoimidazo[1,2-a]pyridines and pyrazines by a new three-component condensation. *Tetrahedron Lett* **1998**, 39, 3635-3638.
21. Kovalenko, S.A.; Vlasov, S.V.; Chernykh, V.P., Synthesis of 5-methyl-4-oxo-2-(coumarin-3-yl)-n-aryl-3,4-dihydrothieno[2,3-d]-pyrimidine-6-carboxamides. *Heteroatom Chem* **2007**, 18, 341-346.
22. Roskoski, R., Jr., Erk1/2 map kinases: Structure, function, and regulation. *Pharmacological research : the official journal of the Italian Pharmacological Society* **2012**, 66, 105-143.
23. Hemmings, B.A.; Restuccia, D.F., Pi3k-pkb/akt pathway. *Cold Spring Harbor perspectives in biology* **2012**, 4, a011189.
24. Zhou, H.; Li, X.M.; Meinkoth, J.; Pittman, R.N., Akt regulates cell survival and apoptosis at a postmitochondrial level. *The Journal of cell biology* **2000**, 151, 483-494.
25. Goans, R.E.; Wald, N., Radiation accidents with multi-organ failure in the united states. *BJR Suppl* **2005**, 27, 41-46.
26. Lushbaugh, C.C.; Comas, F.; Hofstra, R., Clinical studies of radiation effects in man: A preliminary report of a retrospective search for dose-relationships in the prodromal syndrome. *Radiat Res Suppl* **1967**, 7, 398-412.
27. Williams, J.P.; McBride, W.H., After the bomb drops: A new look at radiation-induced multiple organ dysfunction syndrome (mods). *Int J Radiat Biol* **2011**.
28. van Bekkum, D.W., Radiation sensitivity of the hemopoietic stem cell. *Radiat Res* **1991**, 128, S4-8.

29. Gratwohl, A.; John, L.; Baldomero, H.; Roth, J.; Tichelli, A.; Nissen, C.; Lyman, S.D.; Wodnar-Filipowicz, A., Flt-3 ligand provides hematopoietic protection from total body irradiation in rabbits. *Blood* **1998**, 92, 765-769.
30. Hall, E.J.; Giaccia, A.J., *Radiobiology for the radiologist*. 6th ed.; Lippincott Williams & Wilkins: Philadelphia, 2006; p ix, 546 p.
31. Cataldi, A.; Di Giacomo, V.; Rapino, M.; Zara, S.; Rana, R.A., Ionizing radiation induces apoptotic signal through protein kinase cdelta (delta) and survival signal through akt and cyclic-nucleotide response element-binding protein (creb) in jurkat t cells. *The Biological bulletin* **2009**, 217, 202-212.
32. Li, H.F.; Kim, J.S.; Waldman, T., Radiation-induced akt activation modulates radioresistance in human glioblastoma cells. *Radiation oncology* **2009**, 4, 43.
33. Sarbassov, D.D.; Guertin, D.A.; Ali, S.M.; Sabatini, D.M., Phosphorylation and regulation of akt/pkb by the rictor-mtor complex. *Science* **2005**, 307, 1098-1101.
34. Manning, B.D.; Cantley, L.C., Akt/pkb signaling: Navigating downstream. *Cell* **2007**, 129, 1261-1274.
35. Heron-Milhavet, L.; Khouya, N.; Fernandez, A.; Lamb, N.J., Akt1 and akt2: Differentiating the aktion. *Histology and histopathology* **2011**, 26, 651-662.
36. Andjelkovic, M.; Jakubowicz, T.; Cron, P.; Ming, X.F.; Han, J.W.; Hemmings, B.A., Activation and phosphorylation of a pleckstrin homology domain containing protein kinase (rac-pk/pkb) promoted by serum and protein phosphatase inhibitors. *Proceedings of the National Academy of Sciences of the United States of America* **1996**, 93, 5699-5704.
37. Fingar, D.C.; Richardson, C.J.; Tee, A.R.; Cheatham, L.; Tsou, C.; Blenis, J., Mtor controls cell cycle progression through its cell growth effectors s6k1 and 4e-bp1/eukaryotic translation initiation factor 4e. *Molecular and cellular biology* **2004**, 24, 200-216.
38. Ou, Y.H.; Torres, M.; Ram, R.; Formstecher, E.; Roland, C.; Cheng, T.; Brekken, R.; Wurz, R.; Tasker, A.; Poverino, T., et al., Tbk1 directly engages akt/pkb survival signaling to support oncogenic transformation. *Molecular cell* **2011**, 41, 458-470.
39. Du, K.; Montminy, M., Creb is a regulatory target for the protein kinase akt/pkb. *The Journal of biological chemistry* **1998**, 273, 32377-32379.
40. Li, X.Y.; Zhan, X.R.; Liu, X.M.; Wang, X.C., Creb is a regulatory target for the protein kinase akt/pkb in the differentiation of pancreatic ductal cells into islet beta-cells mediated by hepatocyte growth factor. *Biochemical and biophysical research communications* **2011**, 404, 711-716.
41. Kim, A.H.; Khursigara, G.; Sun, X.; Franke, T.F.; Chao, M.V., Akt phosphorylates and negatively regulates apoptosis signal-regulating kinase 1. *Molecular and cellular biology* **2001**, 21, 893-901.
42. Ozes, O.N.; Mayo, L.D.; Gustin, J.A.; Pfeffer, S.R.; Pfeffer, L.M.; Donner, D.B., Nf-kappab activation by tumour necrosis factor requires the akt serine-threonine kinase. *Nature* **1999**, 401, 82-85.
43. Romashkova, J.A.; Makarov, S.S., Nf-kappab is a target of akt in anti-apoptotic pdgf signalling. *Nature* **1999**, 401, 86-90.
44. Alberts, B.; Wilson, J.H.; Hunt, T., *Molecular biology of the cell*. 5th ed.; Garland Science: New York, 2008; p xxxiii, 1601, 1690 p.

45. Shibata, Y.; Oyama, M.; Kozuka-Hata, H.; Han, X.; Tanaka, Y.; Gohda, J.; Inoue, J., P47 negatively regulates ikk activation by inducing the lysosomal degradation of polyubiquitinated nemo. *Nature communications* **2012**, *3*, 1061.
46. Miyachi, H.; Minamino, T.; Tateno, K.; Kunieda, T.; Toko, H.; Komuro, I., Akt negatively regulates the in vitro lifespan of human endothelial cells via a p53/p21-dependent pathway. *The EMBO journal* **2004**, *23*, 212-220.
47. Liu, S.; Liu, S.; Wang, X.; Zhou, J.; Cao, Y.; Wang, F.; Duan, E., The pi3k-akt pathway inhibits senescence and promotes self-renewal of human skin-derived precursors in vitro. *Aging cell* **2011**, *10*, 661-674.
48. Heron-Milhavet, L.; Franckhauser, C.; Rana, V.; Berthenet, C.; Fisher, D.; Hemmings, B.A.; Fernandez, A.; Lamb, N.J., Only akt1 is required for proliferation, while akt2 promotes cell cycle exit through p21 binding. *Molecular and cellular biology* **2006**, *26*, 8267-8280.
49. Maroulakou, I.G.; Oemler, W.; Naber, S.P.; Tschlis, P.N., Akt1 ablation inhibits, whereas akt2 ablation accelerates, the development of mammary adenocarcinomas in mouse mammary tumor virus (mmtv)-*erbB2/neu* and mmtv-polyoma middle t transgenic mice. *Cancer research* **2007**, *67*, 167-177.
50. Hara, E.; Smith, R.; Parry, D.; Tahara, H.; Stone, S.; Peters, G., Regulation of p16<sup>cdkn2</sup> expression and its implications for cell immortalization and senescence. *Molecular and cellular biology* **1996**, *16*, 859-867.
51. Stein, G.H.; Drullinger, L.F.; Soulard, A.; Dulic, V., Differential roles for cyclin-dependent kinase inhibitors p21 and p16 in the mechanisms of senescence and differentiation in human fibroblasts. *Molecular and cellular biology* **1999**, *19*, 2109-2117.
52. He, X.; Zhu, Z.; Johnson, C.; Stoops, J.; Eaker, A.E.; Bowen, W.; DeFrances, M.C., Pik3ip1, a negative regulator of pi3k, suppresses the development of hepatocellular carcinoma. *Cancer research* **2008**, *68*, 5591-5598.
53. Zhu, Z.; He, X.; Johnson, C.; Stoops, J.; Eaker, A.E.; Stoffer, D.S.; Bell, A.; Zarnegar, R.; DeFrances, M.C., Pi3k is negatively regulated by pik3ip1, a novel p110 interacting protein. *Biochemical and biophysical research communications* **2007**, *358*, 66-72.
54. Mungrue, I.N.; Pagnon, J.; Kohanim, O.; Gargalovic, P.S.; Lusic, A.J., Chac1/mgc4504 is a novel proapoptotic component of the unfolded protein response, downstream of the atf4-atf3-chop cascade. *Journal of immunology* **2009**, *182*, 466-476.
55. Schiestl, R.H.; Igarashi, S.; Hastings, P.J., Analysis of the mechanism for reversion of a disrupted gene. *Genetics* **1988**, *119*, 237-247.
56. Schiestl, R.H.; Gietz, R.D.; Mehta, R.D.; Hastings, P.J., Carcinogens induce intrachromosomal recombination in yeast. *Carcinogenesis* **1989**, *10*, 1445-1455.
57. Xu, N.; Lao, Y.; Zhang, Y.; Gillespie, D.A., Akt: A double-edged sword in cell proliferation and genome stability. *Journal of oncology* **2012**, *2012*, 951724.



**CHAPTER 5: Prevention of DNA double-strand breaks induced by  
radioiodide-(131)I in FRTL-5 thyroid cells**

## Prevention of DNA Double-Strand Breaks Induced by Radioiodide-<sup>131</sup>I in FRTL-5 Thyroid Cells

Jerome M. Hershman, Armen Okunyan, Yelena Rivina, Sophie Cannon, and Victor Hogen

Endocrinology and Diabetes Division, West Los Angeles Veterans Affairs Medical Center and University of California, Los Angeles, School of Medicine, Los Angeles, California 90073

Radioiodine-131 released from nuclear reactor accidents has dramatically increased the incidence of papillary thyroid cancer in exposed individuals. The deposition of ionizing radiation in cells results in double-strand DNA breaks (DSB) at fragile sites, and this early event can generate oncogenic rearrangements that eventually cause cancer. The aims of this study were to develop a method to show DNA DSBs induced by <sup>131</sup>I in thyroid cells; to test monovalent anions that are transported by the sodium/iodide symporter to determine whether they prevent <sup>131</sup>I-induced DSB; and to test other radioprotective agents for their effect on irradiated thyroid cells. Rat FRTL-5 thyroid cells were incubated with <sup>131</sup>I. DSBs were measured by nuclear immunofluorescence using antibodies to p53-binding protein 1 or  $\gamma$ H2AX. Incubation with 1–10  $\mu$ Ci <sup>131</sup>I per milliliter for 90 min resulted in a dose-related increase of DSBs; the number of DSBs increased from a baseline of 4–15% before radiation to 65–90% after radiation. GH3 or CHO cells that do not transport iodide did not develop DSBs when incubated with <sup>131</sup>I. Incubation with 20–100  $\mu$ M iodide or thiocyanate markedly attenuated DSBs. Perchlorate was about 6 times more potent than iodide or thiocyanate. The effects of the anions were much greater when each was added 30–120 min before the <sup>131</sup>I. Two natural organic compounds recently shown to provide radiation protection partially prevented DSBs caused by <sup>131</sup>I and had an additive effect with perchlorate. In conclusion, we developed a thyroid cell model to quantify the mitogenic effect of <sup>131</sup>I. <sup>131</sup>I causes DNA DSBs in FRTL-5 cells and had no effect on cells that do not transport iodide. Perchlorate, iodide, and thiocyanate protect against DSBs induced by <sup>131</sup>I. (*Endocrinology* 152: 1130–1135, 2011)

Radioiodine-131 released from nuclear reactor accidents has dramatically increased the incidence of papillary thyroid cancer in exposed individuals, especially young children who were exposed in the Marshall Islands or in areas affected by the Chernobyl catastrophe (1–3). For prevention of radiation-induced thyroid cancer, the Food and Drug Administration in 2001 recommended that potentially exposed people take potassium iodide tablets that contain 100 mg iodide per day to block thyroid uptake of the <sup>131</sup>I (<http://www.fda.gov/downloads/Drugs/GuidanceComplianceRegulatoryInformation/Guidances/ucm080542.pdf>). based on the work of Braverman and colleagues (4). The deposition of ionizing radiation in cells results in double-strand DNA breaks (DSBs) at fragile sites, and this

early event can generate oncogenic rearrangements that eventually cause the cancer (5, 6).

Ionizing radiation causes double-strand breaks in DNA that lead to downstream activation of repair processes within cells (7). The two main pathways for repair of DSBs are nonhomologous end-joining and homologous recombination. Nonhomologous end joining is the main pathway by which cells repair damage from ionizing radiation because it does not require a template for repair and involves limited processing of the damaged ends before religation of the DSBs (7). This process is more likely to result in rearrangements leading to oncogenic mutations than repair by homologous recombination. The presence of  $\gamma$ H2AX (histone H2AX, which is phosphorylated at

ISSN Print 0013-7227 ISSN Online 1945-7170  
Printed in U.S.A.

Copyright © 2011 by The Endocrine Society

doi: 10.1210/en.2010-1163 Received October 5, 2010. Accepted November 29, 2010.

First Published Online December 29, 2010

Abbreviations: 53BP1, P53-binding protein-1; DSB, double-strand DNA break; FBS, fetal bovine serum; NIS, sodium/iodide symporter.

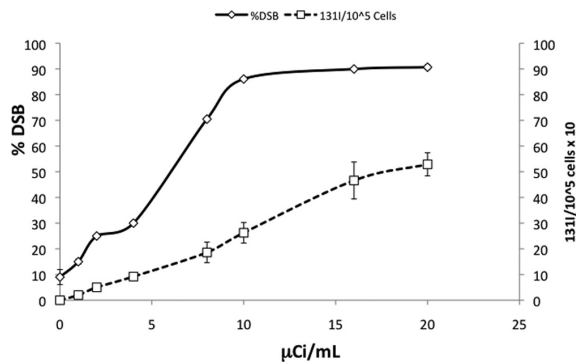


**FIG. 1.**  $^{131}\text{I}$ -induced DSBs in FRTL-5 cells detected by  $\gamma\text{H2AX}$  immunostaining, 90 min incubation. The solid line shows the relationship of DSBs with concentration of  $^{131}\text{I}$  in the incubation medium; there was no increase of DSB at  $^{131}\text{I}$  concentrations greater than 10  $\mu\text{Ci/mL}$ . The dashed line shows the  $^{131}\text{I}$  taken up by cells (microcuries per  $10^5$  cells) at each concentration of  $^{131}\text{I}$ .

serine 139 located in the carboxy terminal tail) is accepted as a specific indicator for the presence of DSBs (8). P53-binding protein-1 (53BP1) is another component of the DNA repair system for nonhomologous end joining of DSBs that accumulates in the nucleus after DSBs caused by ionizing radiation (9, 10).

The goals of this study were: 1) to develop a method to show DSBs induced by  $^{131}\text{I}$  in thyroid cells; 2) to test monovalent anions that are transported by the sodium/iodide symporter (NIS) to determine whether they prevent  $^{131}\text{I}$ -induced DSB; and 3) to test other radioprotective or mitigating agents for their effect on irradiated thyroid cells.

## Materials and Methods

FRTL-5 rat thyroid cells were cultured in Coon's modified F-12 medium (Sigma, St. Louis, MO) supplemented with six hormones (TSH, 1 U/liter; insulin, 246 mU/liter; somatostatin, 10  $\mu\text{g/liter}$ ; hydrocortisone, 10 nM; transferrin, 5 mg/liter; glycyl-histidyl-lysine, 2.5  $\mu\text{g/liter}$ ), 5% calf serum and antibiotics (6H

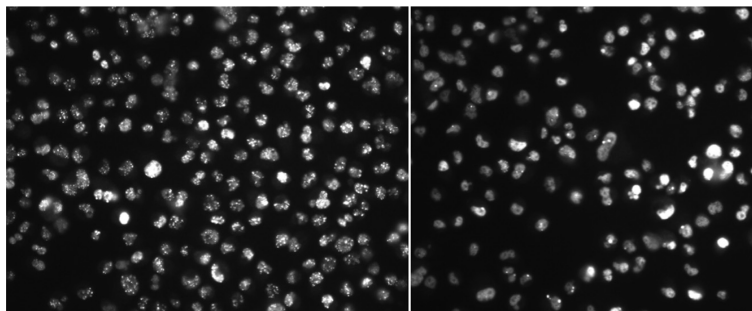


**FIG. 2.** FRTL cells were incubated with 10  $\mu\text{Ci/mL}$  for 90 min. Left panel shows that 91% had positive 53BP1 nuclear immunostaining indicating DSBs. Right panel shows that 4.3% of control FRTL-5 cells not incubated with  $^{131}\text{I}$  had positive 53BP1 nuclear immunostaining.

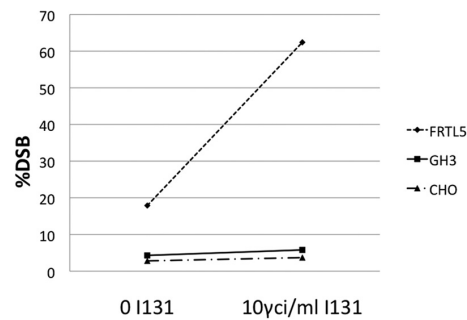


**FIG. 3.**  $^{131}\text{I}$  (10  $\mu\text{Ci/mL}$ , 90 min) caused a marked increase of DSBs in FRTL-5 cells detected by 53BP1 immunostaining ( $P < 0.01$ ) but did not induce DSBs in Chinese hamster ovary (CHO) cells or GH3 cells that do not transport iodide.

medium) as previously described (11). Cells were maintained in a 5%  $\text{CO}_2$ -95% air atmosphere at 37 C with a change of medium every second day and passed every 7 d. For the experiments, cells were then transferred to LabTek chamber slides that were ionized for cell adherence (Thermo Fisher Scientific, Los Angeles, CA).

To prepare cells for irradiation with  $^{131}\text{I}$ , when the cells in the 75- $\text{cm}^2$  flask were approximately 75% confluent, they were resuspended into 1 ml 6H, and 25  $\mu\text{l}$  containing approximately  $10^5$  cells was added into each well with 475  $\mu\text{l}$  6H. Cells were allowed approximately 45 min to adhere. They were then incubated with  $^{131}\text{I}$ -iodide (Mallinkrodt, Commerce, CA), usually for 90 min. The radioactive medium was removed, and the cells were rinsed three times with 500  $\mu\text{l}$  of PBS and then incubated in 500  $\mu\text{l}$  4% paraformaldehyde for 15 min. The cells were then rinsed three times more with PBS, once with 0.5% Triton X-100, and again three times with PBS. Then 500  $\mu\text{l}$  of 10% fetal bovine serum (FBS) was added to the wells to block nonspecific binding, and the cells were incubated overnight at 4 C (or, alternatively, 1 h at room temperature). Chemicals were obtained from Sigma unless stated otherwise.

The primary antibody (53BP1 rabbit antibody) (Santa Cruz Biotechnology, Santa Cruz, CA), used to indicate DSBs, was prepared in 10% FBS at a 1:800 dilution. In some experiments  $\gamma\text{H2AX}$  was used as the primary antibody (Santa Cruz Biotechnology). The cells were incubated in the primary antibody (200  $\mu\text{l/well}$ ) for 1 h at room temperature. The primary antibody was removed and the cells were rinsed once with 0.1% Triton X-100 and twice with PBS and then incubated in 10% FBS to block nonspecific binding for 1 h at room temperature. The secondary antibody (Alexa Fluor 488 goat antirabbit IgG antibody; Invitrogen Molecular Probes, Eugene OR), used to produce immunofluorescence, was prepared in 10% FBS at a 1:500 dilution. The cells were incubated with this antibody (200  $\mu\text{l/well}$ ) for 45 min at room temperature. They were then washed three times with 500  $\mu\text{l}$  of PBS and mounted with coverslips using 10  $\mu\text{l}$  of 4',6'-diamino-2-phenylindole/well.

Nuclear immunofluorescence was viewed using a Zeiss Axioskop 2 plus fluorescent microscope (New York, NY). Approximately 100–150 cells were counted in each well; when the number of positive nuclear foci was five or more, the cells

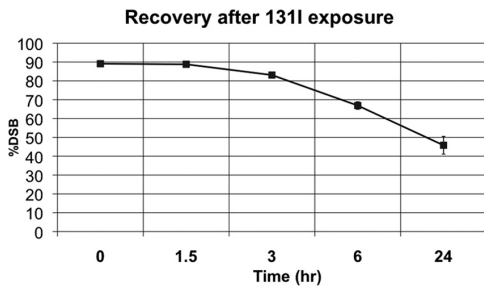


**FIG. 4.** Recovery from DSBs induced by exposure to <sup>131</sup>I. FRTL-5 cells were incubated in 10 μCi <sup>131</sup>I per milliliter. The DSB of cells not incubated with <sup>131</sup>I was 10% (basal DSB). The DSB at 0 time shown here is the maximum DSB after the 90-min incubation. After the removal of the <sup>131</sup>I, the incubation was continued for 24 h and immunostaining for 53BP1 was performed at various times (*P* < 0.05 at 6 h and *P* < 0.01 at 24 h compared with 0 time).

were considered to have significant DNA damage indicative of a DSB. Each condition was studied in duplicate wells and the mean number of DSB ± SD was calculated. Each experiment

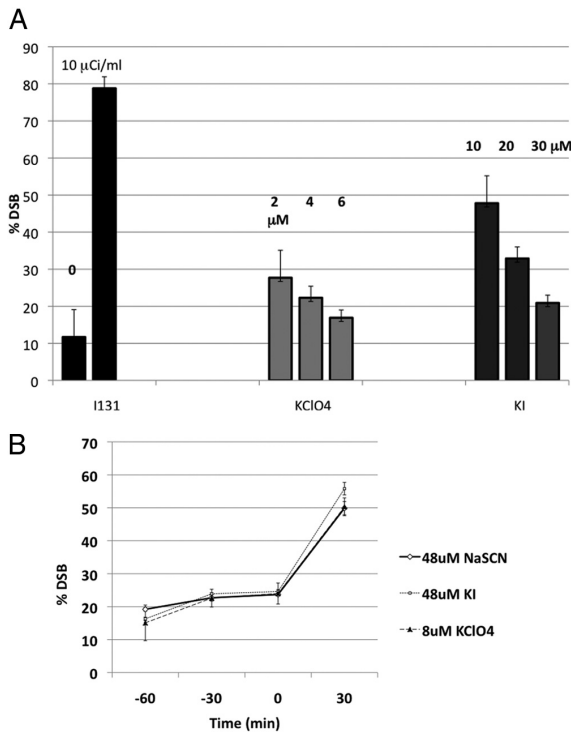


**FIG. 5.** A, Inhibition of DSBs caused by perchlorate (2, 4, or 6 μM) or iodide (10, 20, or 30 μM). FRTL-5 cells were incubated with 10 μCi per milliliter <sup>131</sup>I for 90 min; anions were added at 0 time; basal DSB was 11.7%. Perchlorate and iodide caused a dose-related reduction of DSBs by a multiple comparison test (*P* < 0.01). B, Inhibition of DSBs by anions (90 min incubation, 10 μCi/ml <sup>131</sup>I). Basal DSB was 11%; maximum DSB with no anion was 84%. Anions added 60, 30, and 0 min before <sup>131</sup>I were similarly effective in preventing DSBs (*P* < 0.01); anions added 30 min after <sup>131</sup>I were less effective (*P* < 0.05) compared with no anion.

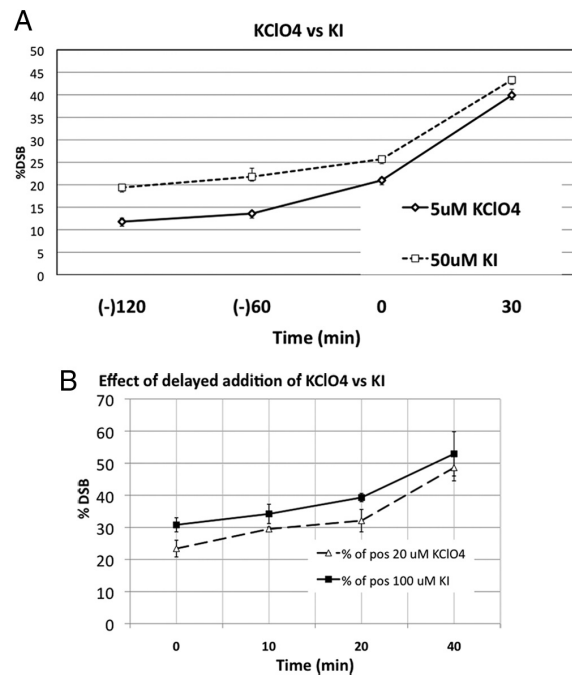


**FIG. 6.** A, Inhibition by KClO<sub>4</sub> and KI using 53BP1 (90 min incubation with <sup>131</sup>I; basal DSB, 8.1%; maximum DSB, 86.5%). Perchlorate or iodide added after 30 min incubation was less protective than when added 120, 60, or 0 min before <sup>131</sup>I (*P* < 0.05). B, Perchlorate or iodide was added at various times shown after incubation with <sup>131</sup>I (basal DSB, 11%; maximum DSB, 76%). Addition of the anion at 40 min was less protective than when added at 0 time (*P* < 0.01).

was repeated, usually three times with close agreement of results.

Statistical significance between groups was determined by an unpaired two-tailed Student's *t* test, Tukey-Kramer multiple comparison test, or Dunnett multiple comparison test, as appropriate, using InStat3 for the Mac (GraphPad Software, Inc., La Jolla, CA).

The radioactive uptakes by the cells were determined by counting an aliquot of the supernatant in triplicate after the 90-min incubation in a scintillation counter. The mean uptake was 30.7 ± 12.4% (sd).

## Results

### Induction of DSBs by <sup>131</sup>I

Figure 1 shows that incubation of FRTL-5 cells with <sup>131</sup>I for 90 min resulted in a dose-related increase in DSBs detected by γH2AX immunostaining at doses of 1–20 μCi <sup>131</sup>I per milliliter. There was a dose-related increase in the uptake of <sup>131</sup>I by the FRTL-5 cells (Fig. 1). Figure 2 shows that incubation of cells with 10 μCi <sup>131</sup>I per milliliter for 90 min caused 91% of the cells to be positive for DSBs, compared with only 4.3% of cells being positive for DSB when they were not incubated with <sup>131</sup>I (*P* < 0.01). We found similar effects of <sup>131</sup>I using the PCCL3 rat thyroid

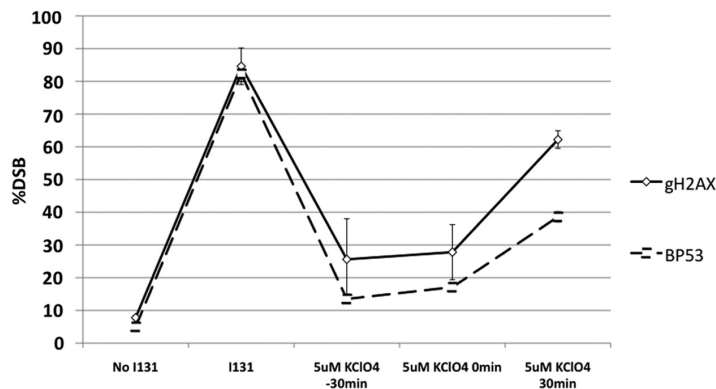


**FIG. 7.** Comparison of 53BP1 and  $\gamma$ H2AX (90 min incubation with  $^{131}\text{I}$ ). Results are qualitatively similar in basal state and at maximum DSBs but differ slightly during incubation with perchlorate that inhibits  $^{131}\text{I}$ -induced DSBs.

cell line kindly provided by Jacques Dumont (Universite Libre de Bruxelles, Bruxelles, Belgium) (data not shown).

To determine whether the DSBs induced by  $^{131}\text{I}$  might be caused by a bystander effect that was not due to transport of the  $^{131}\text{I}$  into the cell, studies were performed with two cell lines that do not transport iodide, CHO cells and GH3 rat pituitary cells. Figure 3 shows that there was no induction of DSBs by  $^{131}\text{I}$  in these cell lines in contrast with the effect of  $^{131}\text{I}$  on FRTL-5 cells.

To determine whether the FRTL-5 cells recovered from the DSBs induced by  $^{131}\text{I}$ , cells were incubated with  $^{131}\text{I}$  for 90 min, the  $^{131}\text{I}$  was removed, the cells were washed twice with medium, and the incubation was continued for 24 h. There was only partial recovery to the baseline state of DSBs at 24 h (Fig. 4). To determine whether incubation with  $10\ \mu\text{Ci}\ ^{131}\text{I}$  per milliliter compromised cell viability, FRTL-5 cells were incubated in flasks for 90 min with  $^{131}\text{I}$  rather than in the LabTek chamber slides (Thermo Fisher Scientific, Los Angeles, CA). The  $^{131}\text{I}$  was removed, the cells were washed twice, and the incubation was continued with passage of the cells two times over 7 d. Study of cell viability by flow cytometry using 7-amino actinomycin D showed no impairment of viability in comparison with control cells not incubated with  $^{131}\text{I}$  (12).

### Prevention of DSBs by monovalent anions and other compounds

Studies were performed to assess the relative effect of monovalent anions for prevention of DSBs induced by  $^{131}\text{I}$ . We compared iodide, perchlorate, and thiocyanate, monovalent anions that are transported by the NIS. Figure 5A shows the dose-related reduction of DSBs caused by perchlorate and iodide. Numerous comparisons were performed to determine the relative efficacy of perchlorate, iodide, and thiocyanate as inhibitors of  $^{131}\text{I}$ -induced DSBs. The concentrations of these

anions chosen for the experiment in Fig. 5B were selected to produce similar effects. The results show that iodide and thiocyanate are similar in blocking potency and perchlorate is about 6-fold more potent than the other anions. In various experiments, the relative effect of perchlorate compared with iodide for blocking DSBs varied from 4- to 20-fold, although the 6-fold relative potency, perchlorate/iodide, shown in Fig. 5B was repeatable in several experiments.

Figure 6A shows that preincubation with stable iodide or perchlorate was more effective in prevention of DSBs than addition of the inhibitor after a

30-min incubation with  $^{131}\text{I}$ . In this experiment, perchlorate was more than 10 times as potent as iodide for prevention of DSBs. Figure 6B shows that delayed addition of the inhibitory anion resulted in a time-dependent loss of the inhibitory effect.

$\gamma$ H2AX is a well-established indicator of radiation damage. Figure 7 shows that results obtained with  $\gamma$ H2AX were very similar to those found using 53BP1 as the indicator of DSBs. Several experiments with  $\gamma$ H2AX gave results similar to those using 53BP1 as the indicator of DSBs.

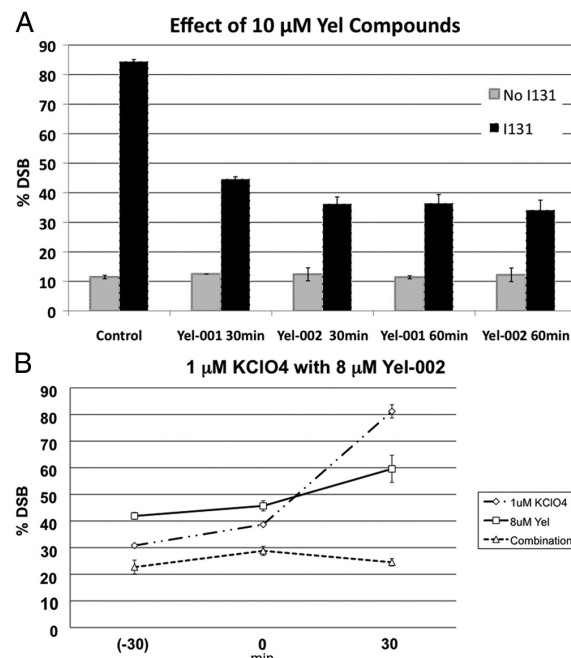


**FIG. 8.** A, Yel-001 and -002 are radioprotective when added before  $^{131}\text{I}$  ( $P < 0.05$  for each comparison). B, Yel-002 blocked DSBs and had an additive effect with  $1\ \mu\text{M}\ \text{KClO}_4$  (90 min incubation,  $10\ \mu\text{Ci/ml}\ ^{131}\text{I}$ ; basal DSB was 4.1%; maximum DSB with no anion was 88%).

Yel-001 and Yel-002 are natural organic compounds that have been shown to protect against radiation-induced injury. Figure 8A shows that the addition of these compounds 30–60 min after exposure to <sup>131</sup>I (in a 90 min incubation) reduced the percent of DSBs. Figure 8B shows that the combination of Yel-002 and 1  $\mu$ M perchlorate was additive in prevention of DSBs. Ciprofloxacin, tetracycline, and tilorone, shown by others to confer radioprotection (13), did not prevent DSBs induced by <sup>131</sup>I in FRTL-5 cells (data not shown).

## Discussion

Our results show that uptake of <sup>131</sup>I causes DNA DSBs in FRTL-5 rat thyroid cells in a dose-related manner and that this does not occur in cell lines that do not actively transport iodide. Our work is the first demonstration *in vitro* that <sup>131</sup>I causes DNA DSBs in thyroid cells. Others have shown that external radiation can cause DNA DSBs in primary cultures of human thyroid cells (14) and in the PCCL3 rat thyroid cell line (15). In contrast with the nearly complete loss of DSBs found by Galleani *et al.* (14) in human primary culture cells 24 h after external irradiation, we noted that there was a significant persistence of DSBs 24 h after removal of the <sup>131</sup>I. This persistence of radiation-induced foci suggests the persistence of disorganized chromatin regions (16). The differences between results could be attributable to a higher radiation dose in our study or the fact that we used a rat cell line.

Perchlorate was about 6-fold more potent than iodide or thiocyanate in prevention of DSBs. A study of perchlorate transport into FRTL-5 cells indicated that the affinity of NIS for perchlorate is much greater than that for iodide (11). Van Sande *et al.* (17) calculated that the relative IC<sub>50</sub> of perchlorate/iodide for inhibition of radioiodide transport in FRTL-5 cells was 0.6:51. However, our data show that perchlorate is much less effective for blockade of DSBs than suggested by this ratio. Perhaps iodide has a special effect as a radioprotective agent in addition to prevention of radioiodide uptake. Iodide has been shown to reduce the mRNA and protein of the NIS in the thyroids of rats exposed to large amounts of iodide (18). Perhaps this effect of iodide plays a role in its radioprotective effect, although the rapid prevention of DSB by iodide *in vitro* makes this mechanism speculative.

Our data also show that maximum prevention of <sup>131</sup>I-induced DSBs by competing monovalent anions requires addition of the anion to the incubation medium before the radioiodide exposure and that addition after incubation with the <sup>131</sup>I has begun results in progressive loss of the radioprotective effect with the time of delay. Yel-001 and Yel-002 are examples of compounds under development

for mitigation of the effects of ionizing radiation. Our study showed that the mitigating effects of these compounds are additive with those of anions that compete for NIS. The exact mechanisms of action of the Yel compounds are yet to be determined; however, *in vivo* and *in vitro* data (not reported yet) point to DNA repair up-regulation processes and rescue from cell death after genotoxic injuries.

The lack of induction of DSBs in cells that do not transport <sup>131</sup>I or in whom the transport is blocked by competitive anions requires an explanation. The  $\beta$ -radiation of the <sup>131</sup>I has an average energy of 190 keV and penetration of about 1 mm in tissue or water (19). Yet there is an absence of significant bystander effect that could produce detectable DSBs from penetration of this radiation into the cells in this study. One possible explanation is the fact that the cells are grown in a monolayer, which exposes the cells to less of the <sup>131</sup>I that is dispersed uniformly in the medium. Another factor is that the FRTL-5 cells transport a high proportion of the <sup>131</sup>I into the cell, thereby increasing the radiation to the DNA in the nucleus.

In recent years, there has been an increase in the frequency of papillary thyroid cancer (20). The basis for the increase is unknown. The model developed for this study could provide a method for screening compounds that could be thyroid carcinogens by measuring their induction of DSBs as a precursor to neoplasia. However, proof of principle will require validation by suitable studies in experimental animals.

In summary, we have developed a cell model using FRTL-5 rat thyroid cells that concentrate <sup>131</sup>I, which results in DSBs that are visualized with 53BP1 or  $\gamma$ H2AX. Preincubation with perchlorate, iodide, or thiocyanate prevents the DSB. Addition of the anions after exposure to <sup>131</sup>I is less effective in prevention of DSBs. These data provide a basis for studies of radioprotection against DSBs induced by <sup>131</sup>I in animals and studies to refine the prevention of thyroid cancer resulting from nuclear fallout.

## Acknowledgments

The authors are grateful for the advice and guidance of William McBride.

Address all correspondence and requests for reprints to: Jerome M. Hershman, M.D., Endocrinology-111D, West Los Angeles Veterans Affairs Medical Center, Los Angeles, California 90073. E-mail: jhershmn@ucla.edu.

This work was supported by a research grant from the University of California, Los Angeles, Center of Biological Radioprotectors and the National Institutes of Health.

Disclosure Summary: The authors have nothing to disclose.



## References

1. Land CE, Bouville A, Apostoaeci I, Simon SL 2010 Projected lifetime cancer risks from exposure to regional radioactive fallout in the Marshall Islands. *Health Phys* 99:201–215
2. Williams D 2008 Radiation carcinogenesis: lessons from Chernobyl. *Oncogene* 27(Suppl 2):S9–S18
3. Walsh L, Jacob P, Kaiser JC 2009 Radiation risk modeling of thyroid cancer with special emphasis on the Chernobyl epidemiological data. *Radiat Res* 172:509–518
4. Sternthal E, Lipworth L, Stanley B, Abreau C, Fang SL, Braverman LE 1980 Suppression of thyroid radioiodine uptake by various doses of stable iodide. *N Engl J Med* 303:1083–1088
5. Ito T, Seyama T, Iwamoto KS, Hayashi T, Mizuno T, Tsuyama N, Dohi K, Nakamura N, Akiyama M 1993 *In vitro* irradiation is able to cause RET oncogene rearrangement. *Cancer Res* 53:2940–2943
6. Santoro M, Thomas GA, Vecchio G, Williams GH, Fusco A, Chiappetta G, Pozharskaya V, Bogdanova TI, Demidchik EP, Cherstvoy ED, Voscoboinik L, Tronko ND, Carss A, Bunnell H, Tonnachera M, Parma J, Dumont JE, Keller G, Höfler H, Williams ED 2000 Gene rearrangement and Chernobyl related thyroid cancers. *Br J Cancer* 82:315–322
7. Burdak-Rothkamm S, Prise KM 2009 New molecular targets in radiotherapy: DNA damage signalling and repair in targeted and non-targeted cells. *Eur J Pharmacol* 625:151–155
8. Ohnishi T, Mori E, Takahashi A 2009 DNA double-strand breaks: their production, recognition, and repair in eukaryotes. *Mutat Res* 669:8–12
9. Wang B, Matsuoka S, Carpenter PB, Elledge SJ 2002 53BP1, a mediator of the DNA damage checkpoint. *Science* 298:1435–1438
10. Doil C, Mailand N, Bekker-Jensen S, Menard P, Larsen DH, Peppercok R, Ellenberg J, Panier S, Durocher D, Bartek J, Lukas J, Lukas C 2009 RNF168 binds and amplifies ubiquitin conjugates on damaged chromosomes to allow accumulation of repair proteins. *Cell* 136:435–446
11. Tran N, Valentin-Blasini L, Blount BC, McCuiston CG, Fenton MS, Gin E, Salem A, Hershman JM 2008 Thyroid-stimulating hormone increases active transport of perchlorate into thyroid cells. *Am J Physiol Endocrinol Metab* 294:E802–E806
12. Steensma DP, Timm M, Witzig TE 2003 Flow cytometric methods for detection and quantification of apoptosis. *Methods Mol Med* 85:323–332
13. Kim K, Pollard JM, Norris AJ, McDonald JT, Sun Y, Micewicz E, Pettijohn K, Damoiseaux R, Iwamoto KS, Sayre JW, Price BD, Gatti RA, McBride WH 2009 High-throughput screening identifies two classes of antibiotics as radioprotectors: tetracyclines and fluoroquinolones. *Clin Cancer Res* 15:7238–7245
14. Galleani J, Miranda C, Pierotti MA, Greco A 2009 H2AX phosphorylation and kinetics of radiation-induced DNA double strand break repair in human primary thyrocytes. *Thyroid* 19:257–264
15. Driessens N, Versteijne S, Ghaddab C, Burniat A, De Deken X, Van Sande J, Dumont JE, Miot F, Corvilain B 2009 Hydrogen peroxide induces DNA single- and double-strand breaks in thyroid cells and is therefore a potential mutagen for this organ. *Endocr Relat Cancer* 16:845–856
16. Suzuki M, Suzuki K, Kodama S, Watanabe M 2006 Phosphorylated histone H2AX foci persist on rejoined mitotic chromosomes in normal human diploid cells exposed to ionizing radiation. *Radiat Res* 165:269–276
17. Van Sande J, Massart C, Beauwens R, Schoutens A, Costagliola S, Dumont JE, Wolff J 2003 Anion selectivity by the sodium iodide symporter. *Endocrinology* 144:247–252
18. Eng PH, Cardona GR, Fang SL, Previti M, Alex S, Carrasco N, Chin WW, Braverman LE 1999 Escape from the acute Wolff-Chaikoff effect is associated with a decrease in thyroid sodium/iodide symporter messenger ribonucleic acid and protein. *Endocrinology* 140:3404–3410
19. 1970 Radiological health handbook. Washington, DC: U.S. Government Printing Office
20. Enewold L, Zhu K, Ron E, Marrogi AJ, Stojadinovic A, Peoples GE, Devesa SS 2009 Rising thyroid cancer incidence in the United States by demographic and tumor characteristics, 1980–2005. *Cancer Epidemiol Biomarkers Prev* 18:784–791



**Share Your Career News!**  
*Endocrine News* would like to consider your news  
 for its Smart Moves section.

endocrineneews@endo-society.org.

**CHAPTER 6: Mouse Models for Efficacy Testing of Agents against Radiation  
Carcinogenesis – A Literature Review**



## PREFACE

A cell's encounter with ionizing radiation may end in one of a few ways: it may die via necrosis or apoptosis, it may experience replicative senescence and lose its ability to divide, or it may incorrectly repair the sustained DNA damage and embark on a journey of carcinogenesis. The first two scenarios fall under the umbrella of deterministic effects – the effects whose severity increases with dose past a cell-specific threshold. Radiation-induced carcinogenesis, on the other hand, belongs to the stochastic effect category where the gravity of the effect is independent of the dose of exposure and without a threshold.

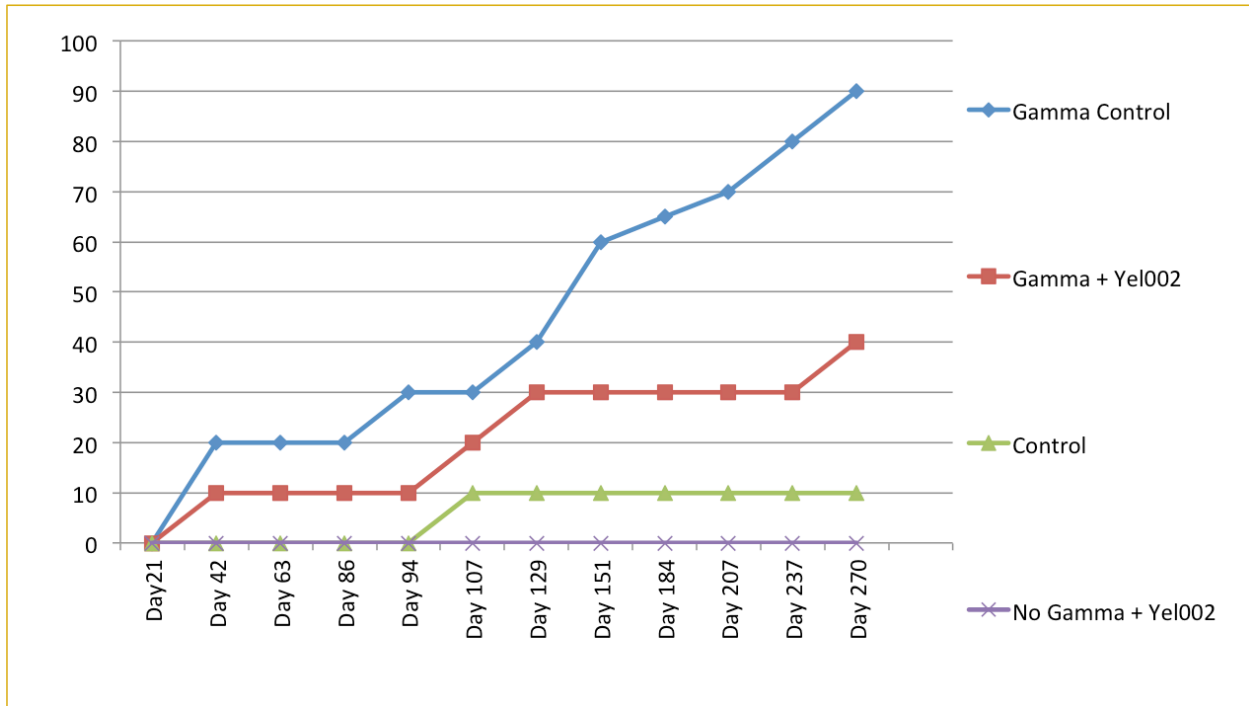
Over the last eight years our primary focus at the Center for Medical Countermeasures against Radiation at UCLA has been to identify radiation-mitigating therapies against acute radiation syndrome (ARS) and prevention of lethality. While we did not pursue the development of agents aimed at reducing radiation-induced cancer we were highly cognizant of that fact that an optimal radiation mitigator will not only reduce early lethality from ARS, but will also mitigate radiation late effects, such as cancer. Radiation-induced carcinogenesis and leukemogenesis are the most important effects of low-dose exposure to ionizing radiation, especially for those exposed at a relatively young age [1]. Our data suggest that Yel002 might be a “complete” radiation mitigator reducing both the acute radiation syndrome effects and radiation carcinogenesis.

We have previously demonstrate that in vitro treatment with Yel002 mitigated DNA double strand breaks (DSB) in rat thyroid cells induced with a radioactive iodine isotope, I-131 [2]. This finding bears tremendous significance in the context of radiation mitigation from a radiological accident or a nuclear detonation. Radioactive iodine is a significant

nuclear fallout byproduct and a major public health threat. For example, following the Chernobyl accident individuals located hundreds of miles away from the imploded nuclear plant, were still susceptible to radioactive iodine exposure. Those exposed had experienced an unprecedented increase in hypothyroidism and thyroid cancers [1,3,4]. While an in vivo validation of the observed effects remains to be completed, the ability of Yel002 to reduce iodine-induced DNA damage in thyroid cells is a very promising additional facet to Yel002's mitigation capacity.

Radiation-induced leukemia has the shortest latent period following exposure and its development is highly age-dependent. Leukemia is also one of the common secondary cancers in radiotherapy patients [1]. Experiments conducted in collaboration with Dr. Alexandra Miller from the Armed Forces Radiobiology Research Institute (AFFRI) have demonstrated that administration of Yel002 reduced radiation-induced leukemia in DBA/2 mouse model. In brief, 15 DBA/2 mice per group were irradiated with  $^{60}\text{Co}$  (3.5 Gy, 0.6 Gy/min). Twenty-four hours later mice were transplanted intravenously with ( $5 \times 10^6$ ) FDC-P1 cells to induce leukemia [5,6] and immediately injected with Yel002 (25 mg/kg) with additional injections every 24 hours for 4 days. Leukemogenesis was monitored with blood draws every 21 days. Treatment with Yel002 reduced the incidence of radiation-induced leukemia from 90% in control animals to 40%. Additionally, Yel002 administration prolonged the latency of the disease by 21 days. Of note, Yel002 administration to unirradiated animals reduced the spontaneous leukemogenesis frequency from 10% down to 0% (Preface Figure 1).

### Preface Figure 1: Yel002 mitigates radiation-induced leukemogenesis



**Preface Figure 1.** Administration with Yel002 to irradiated mice decreases penetrance rates and prolongs latency of leukemia. DBA/2 mice irradiated and transplanted with pre-leukemic FDC-P1 cells developed leukemia in 90% of the animals versus 40% in Yel002-treated mice by Day 270 ( $P < .05$ ). Yel002 was administered along with the cells.

Yel002 appears to promote genomic stability following radiation assaults possibly by up-regulating cell's DNA repair capacity. In collaboration with Dr. Jonathan Erde we have conducted a high throughput proteomics assay in immortalized human lymphoblast that revealed an increase in DNA repair enzymes following a 24 hr incubation with Yel002 (15  $\mu\text{M}$ ). In brief, cells were lysed and proteins extracted, solubilized, and digested by eFASP with 0.2% DCA. The resulting peptides from eFASP were separated based on isoelectric point and hydrophilicity using ERLIC on a polyWAX LP column. Fractions were pooled based on the 215 nm UV-Vis absorbance trace, yielding 25 to 30 fractions. Each fraction was injected onto a reverse phase 219 column and separated by UPLC on a

nanoACQUITY. Eluting peptides were analyzed by LC-MSE on a Synapt HDMS. Raw data files produced for all fractions of a sample were merged and searched using PLGS. DECO was utilized to correct peptide ion volume data for any peptide found in multiple ERLIC fractions. Expression Analysis was used for data normalization prior to further processing. Threshold for protein up-regulation was set at a natural log ratio greater than 0.45, with a p-value of up-regulation greater than 0.95. A relative PLGS score was also assigned. Proteins with PLGS score above 100 were considered significant, corresponding to p-values < .05.

Yel002 incubation enriched components of the ataxia telangiectasia mutated (ATM) Signaling pathway (p-value=5.75E-05), including components of DSB repair by homologous recombination (p-value=7.08E-04) and non-homologous recombination (p-value= 4.47E-05). Among them were ATM (PLGS score 604), NBN/nibrin/NBS1 (PLGS score 678), and RAD50 (PLGS score 713) proteins.

ATM is a master regulator responsible for genomic integrity that is activated following a recognized DNA damage site. Cells lacking a functional ATM are deficient in DNA damage response (DDR) and are prone to cancer [7-9]. The first step in DNA DSB repair is recognition of the damage site mediated by Mre11 protein that tethers broken DNA ends together and activates ATM. ATM in turn, activates the MRN complex composed of Mre11, Rad50 and Nbs1 proteins. Activated MRN complex has over 30 known downstream substrates involved in DNA damage response [8,10,11].

Additionally, three other DNA repair accessory proteins were significantly upregulated APEX1, DDB1, and XRCC4. APEX nuclease 1 is involved in base excision repair pathway by catalyzing pre-processed cleavage of the phosphodiester bond in the backbone

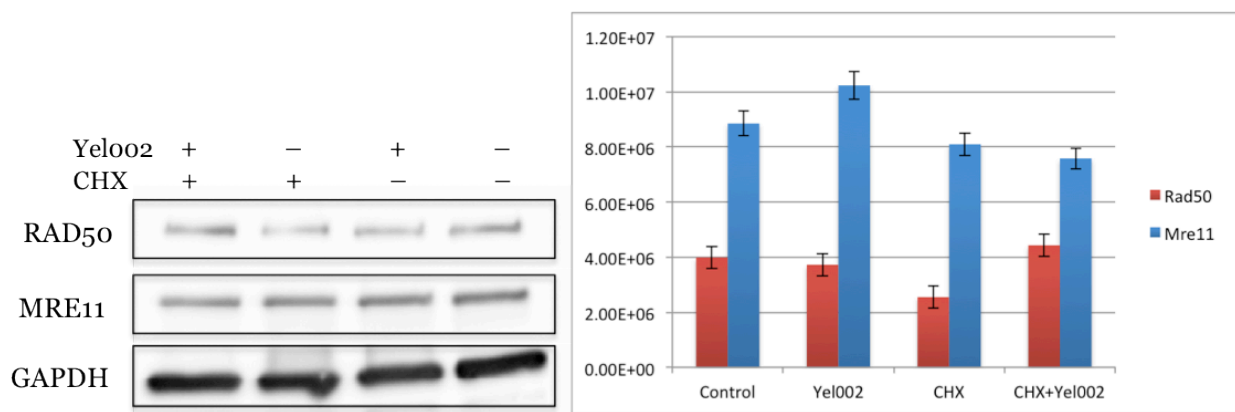
near the site of damage (37). Damage-specific DNA binding protein 1 (DDB1) is implicated in transcriptional control over other DNA repair proteins and repair itself. Its major function is the recognition of ultraviolet (UV) - induced DNA damage, and activation of its repair (40). Lastly, XRCC4 stands for X-ray repair complementing defective repair in Chinese hamster cells 4 and is imperative for proper non-homologous end-joining (NHEJ) repair and important for V(D)J recombination [12].

High throughput proteomic experiments revealed a possible mechanism of genomic stabilization through an increase in protein involved in DNA repair. The data, however, posed a new question: is the increase in protein concentration due to de novo protein synthesis or due to the stabilization of the existing proteins? Our RNA-seq experiments, described in Chapter 4, didn't detect any DNA repair gene mRNAs after a 7-hr incubation with Yel002, which suggested that the increase that we observed after 24 hrs of exposure was most likely due to the stabilization of these enzymes. To further investigate our hypothesis we incubated the same human lymphoblastoid cells with Yel002 (15  $\mu$ M) for 24 hrs with and without a protein synthesis inhibitor cyclohexamide (CHX, 25  $\mu$ M). Following the incubation cells were lysed with RIPA lysis buffer supplemented with a protease inhibitor cocktail. Whole cell lysates were then run on an SDS gel and immobilized on a membrane (See Chapter 4 for detailed description). Membrane was probed with anti-RAD50 (#3427) and anti-MRE11 (#4847) antibodies (Cell Signaling Technology, Inc., Danvers, MA). Protein amounts were normalized to GAPDH in each treatment group.

Western blot data suggest that MRE11 is most likely synthesized de novo following a 24 hr incubation with Yel002 because we did not detect an increase in MRE11 amounts

following an incubation with CHX and Yel002, but did see an increase in MRE11 amounts in cells incubated with Yel002 alone ( $P < .05$ ). Situation with RAD50 is a bit more interesting. No increase in RAD50 was detected after Yel002 incubation alone. However, there was a significant increase in RAD50 amount in the Yel002+cyclohexamide group compared to cyclohexamide alone potentially suggesting a stabilization of the protein (Preface Figure 2). Further investigations are certainly needed to clarify the status of RAD50 and additional DNA repair enzymes.

**Preface Figure 2. Effect of Yel002 incubation on RAD50 and MRE11**



**Preface Figure 2.** Incubation of human lymphoblastoid cells with Yel002 (15  $\mu$ M) for 24 hrs differentially affects the total amount of two components of the MRN complex. Yel002 appears to stimulate de novo synthesis of MRE11 but not RAD50. Increase in RAD50 protein concentration following a co-incubation of Yel002 with cyclohexamide (CHX, 25  $\mu$ M) might be partially explained by the protein’s stabilization in response to Yel002.

Taken together, our data suggest that Yel002 might be effective in mitigation and prophylaxis of radiation-induced carcinogenesis and leukemogenesis. To begin exploring this application of Yel002 I have compiled a review article examining and evaluating available animal models of radiation-induced cancers.

Review

## Mouse Models for Efficacy Testing of Agents against Radiation Carcinogenesis—A Literature Review

Leena Rivina <sup>1,\*</sup> and Robert Schiestl <sup>1,2,3</sup>

<sup>1</sup> Department of Environmental Health Sciences, University of California, Los Angeles, 650 Charles E. Young Dr. South, CHS 71-295, Los Angeles, CA 90095, USA

<sup>2</sup> JCCC Healthy and At-Risk Populations Program Area, Department of Pathology and Laboratory Medicine, University of California, Los Angeles, 650 Charles E. Young Dr. South, CHS 71-295, Los Angeles, CA 90095, USA; E-Mail: rschiestl@mednet.ucla.edu

<sup>3</sup> Department of Radiation Oncology, University of California, Los Angeles, 650 Charles E. Young Dr. South, CHS 71-295, Los Angeles, CA 90095, USA

\* Author to whom correspondence should be addressed; E-Mail: yrivin@ucla.edu;  
Tel.: +1-310-267-2593; Fax: +1-310-267-2578.

Received: 6 October 2012; in revised form: 26 November 2012 / Accepted: 11 December 2012 /  
Published: 27 December 2012

---

**Abstract:** As the number of cancer survivors treated with radiation as a part of their therapy regimen is constantly increasing, so is concern about radiation-induced cancers. This increases the need for therapeutic and mitigating agents against secondary neoplasias. Development and efficacy testing of these agents requires not only extensive *in vitro* assessment, but also a set of reliable animal models of radiation-induced carcinogenesis. The laboratory mouse (*Mus musculus*) remains one of the best animal model systems for cancer research due to its molecular and physiological similarities to man, small size, ease of breeding in captivity and a fully sequenced genome. This work reviews relevant *M. musculus* inbred and F<sub>1</sub> hybrid animal models and methodologies of induction of radiation-induced leukemia, thymic lymphoma, breast, and lung cancer in these models. Where available, the associated molecular pathologies are also included.

**Keywords:** radiation carcinogenesis; animal models; radiation protectors; radiation mitigators; secondary cancers

---

## **1. Introduction**

The number of people diagnosed with cancer each year is growing, as is the number of post-therapy survival rates. Approximately one in two people in the United States will be diagnosed with cancer at some point in their lifetime and about half of them will receive radiation as a part of their therapy regimen [1,2]. Radiation is either administered as a sole curative/palliative agent, in combination with chemotherapeutic drugs, molecular targeted therapy, immunotherapy, or as a part of immune suppression procedure for bone marrow, stem cell and organ transplantation [3]. However, normal healthy tissues are inadvertently exposed to radiation, which may result in a variety of acute toxicities or chronic secondary malignancies. One of such malignancies is radiation-induced cancer [4,5].

In recent years, rapid technological advances in radiation oncology have enabled radiation to be targeted much more precisely to tumor sites reducing some unnecessary exposure of healthy surrounding tissues and increasing both the maximum tolerated doses and the therapeutic ratio [6,7]. However, collateral exposure of normal tissue and potential subsequent malignancy is still unavoidable. Development of biological therapies to supplement technological advances in radiation oncology would present a powerful solution and may further revolutionize the field.

There are three potential classes of agents intended to modulate normal tissue damage: (1) radiation protectors, agents given prior to radiation exposure; (2) radiation mitigators, agents given post-exposure (PE) but prior to the onset of symptoms; and (3) therapies, or agents administered after the onset of symptoms [8]. To date, Amifostine™ is only agent approved by the Food and Drug Administration (FDA) intended to protect normal tissues during irradiation [9]. To increase the number of available radiation modulating therapies, National Cancer Institute (NCI) in collaboration with the National Institute of Allergy and Infectious Diseases (NIAID) have put forth an algorithm for preclinical and clinical development for agents aimed at decreasing the adverse effects of cancer therapy, including radiation [10]. One of the imperative parts of the proposed algorithm is accurate selection of animal models for therapeutic activity validation. For in-depth review on the selection of NIAID-recommended animal models for the testing of therapies designed to mitigate or treat non-cancer toxicities associated with radiation exposures one can refer to Williams *et al.* [11]. The purpose of this work is to review select inbred mouse models that may be used in preclinical settings to test the efficacy of agents intended to protect, mitigate, or treat radiation-induced carcinogenesis.

## **2. Methods**

### *2.1. Research Strategy*

*Mus musculus*, the laboratory mouse, is one of the best models available for the study of cancer initiation, progression and corresponding pathologies. The laboratory mouse has undergone a significant evolution in its complexity enabling it to mimic more and more precise aspects of the most multifaceted disease of all—cancer. In the researcher's arsenal today are murine models ranging from carcinogen-inducible tumors to xenograft models transplanted with human neoplastic cells to humanized mice that express human genes. New generations of genetically engineered mice (GEM) have been imbued with the ability to accurately recapitulate pathophysiological and underlining molecular features of many human cancers [12]. Genetically homogenous inbred mice used in



environmentally inducible cancer studies are increasingly neglected in favor of GEMs, often because the inbred mice develop tumors at low frequencies and with variable latencies. Despite these flaws, however, inbred mice are indispensable in the discovery of novel oncogenes, tumor suppressors and preclinical assessment of toxic or therapeutic effects of innumerable agents [13].

We have set out to identify inbred mouse models of radiation-induced (RI) cancers intended for assessment of efficacy in protecting, mitigating or treating these malignancies. We have concentrated on models of leukemia, lung and breast cancers, as these have been identified as the most commonly arising secondary cancers post radiation therapy [5]. Lymphoma has also been included, despite its unconfirmed status as a radiation-induced malignancy in man.

## *2.2. Inclusion Criteria*

The scope of this review is limited to murine models of radiation-induced leukemogenesis, lymphomagenesis, breast and lung carcinogenesis following exposure to low-LET gamma- and X-ray radiations with a high total dose and dose-rate. Inductions with high-LET radiation, genetically engineered mice and models that required supplemental treatment are outside of the scope of this work. Only inbred mice whose cancers are inducible with either a single total body irradiation (TBI) or fractionated targeted exposures are described, the only exception being an orthograft radiation chimera model of breast cancer. Lastly, only murine models mimicking underlying molecular pathologies observed in man are included.

## **3. Results and Discussion**

### *3.1. Radiation-Induced Leukemia*

Leukemia was one of the few cancers recognized as a radiation-induced malignancy quite early in the development of the field of radiation biology. Before any radiation safety standards were introduced, many X-ray workers, mostly physicists and engineers, developed leukemia after working near accelerators and other ionizing radiation (IR) sources. However, much more than anecdotal correlation between radiation exposure and increased leukemia incidence and mortality began emerging as the reports from Life Span Study cohorts following Japanese atom-bomb survivors and patients receiving high doses of therapeutic radiation for cervical cancers, tinea capitis and ankylosing spondylitis began to be published [5,14–19]. In a large study conducted by Boice and colleagues, the risk of secondary malignancies following radiation treatment for the uterine cervix carcinoma established as a sharp increase in leukemia incidence following irradiation [20]. In the last decades, more reliable data from the Chernobyl disaster on excess risk estimates of leukemia in adults and children also began to emerge, providing a more complete data set on age-dependence, doses and latencies [21–24].

Despite the differences in exposure scenarios, irradiation dose-rates and doses, and radiation quality components, there are salient features common to all reported IR-induced leukemias. Acute and chronic myeloid leukemia (AML and CML, respectively) are the two most common radiation-induced cancers observed in the adult human population [15,16,18,25–27]. Children exposed at 5–9 years of age appear to be more susceptible to acute lymphocytic leukemia (ALL), while older children are more

likely to develop AML. Chronic lymphocytic leukemia (CLL) does not seem to be influenced by radiation [14]. The risk of developing leukemia is highest within the first decade following exposure and begins to decrease as time goes on, but never quite returns to baseline risk [15,16,21,26,28]. In some reports, sex differences have been reported in radiation-induced leukemia instances [16,18,21,25].

Epidemiological data, however, cannot tell the whole story about radiation-induced leukemogenesis. The use of mouse models becomes imperative to study the mechanism of induction, improve diagnostics, and further radiation protection, therapy and mitigation efforts. Today a few established IR-induced leukemogenesis murine models exist: RF [29,30], SJL/J [31], CBA [32,33], and C3H/He [34]. Table 1 summarizes the optimal methods of induction and the associated myeloid leukemia (ML) frequencies.

**Table 1.** Induction of myeloid leukemia in mice with low-LET ionizing radiation.

Malignancy	Mouse Strain	Age	Sex	Mode of Induction	Latency	Spontaneous Frequency	Induced Frequency	Ref.
Myeloid Leukemia	RF (RF/J, RFM)	8 weeks	Male	4.25 Gy	4–12 months	2–4%	50–90%	[30]
Myeloid Leukemia	SJL/J	8–10 weeks	Female	3–3.5 Gy	12 months	0 %	10–30%	[31]
Myeloid Leukemia	C3H/He	8–10 weeks	Male	2.84 Gy	1.5–18 months	<1%	25%	[34]
Myeloid Leukemia	(CBA/Ca, CBA/Cne, CBA/H)	12–15 weeks	Male	3 Gy	18–24 months	<1%	~25%	[32,33]

### 3.1.1. RF Mouse

The RF mouse was developed at the Rockefeller Institute as a general-purpose stock from A, R, and S strains [30,35,36]. Its propensity for radiation-induced leukemogenesis has been extensively studied by Upton and colleagues [37]. One of the earliest accounts of leukemogenesis in these mice dates back to 1936 with detonation experiments conducted by Furth and colleagues [38]. Myelogenous or myeloid leukemia (ML) in the RF model is inducible with a single dose of ionizing radiation and has been proposed as a valid counterpart to human AML, particularly due to its prolonged preclinical period with diagnosable pre-cancerous tissue lesions [30].

Background incidence of myeloid leukemia in RF mice is 2–4% and appears later in life, at around 18–24 months of age [39]. Exposure of 8-week old RF males to 1.5 Gy increases ML frequency to about 40% while *in utero* and neonatal exposures actually decrease ML induction [29,40]. At the dose of 4.25 Gy ML incidence increases to 50–90%, with a latency period of 4–12 months [30,37,41]. As early as 12 weeks post exposure, an enlarged spleen and liver accumulate young myeloid cells. Clinically, RF leukemia presents with infiltration to peribronchial areas, lymph nodes, and gastrointestinal lymphoid organs. However, at the same dose the induction of thymic lymphoma also increases to about 25%, which can potentially interfere with accurate ML diagnosis and modeling of

the human disease [30]. Upton *et al.* have also demonstrated a sex difference in susceptibility to TL and ML: females are more susceptible to TL, while males are more likely to develop ML [29].

Hayata *et al.* reported that, similarly to radiation-induced leukemia in the SJL/J mouse [42], myeloid leukemia in the RF model exhibits partial deletion of chromosome #2 along with other genomic instabilities including loss of the Y-chromosome [43]. Some researchers have suggested that the protracted latency of ML in RF mice correlates with the data from Japanese A-bomb survivors and children exposed in the Chernobyl disaster, with the corresponding peak incidence in leukemia 5–10 years following the irradiation event [16,21,25,44]. One drawback of the RF mouse model is the fact that it often presents with mixed hematopoietic tumors of myeloid leukemia and thymic lymphoma [29].

### 3.1.2. SJL/J Mouse

Developed in the 1960s by Murphy, the SJL/J strain is known for its high spontaneous frequency of reticulum cell neoplasms (type B, RCN B) [45,46] that occur at roughly 380 days of age in both males and females. The histological pattern observed in the RCN B was similar to that of Hodgkin's disease in human beings, leading to the proposal for its use as an investigative model of such lesions [47].

Single exposure of 8–10-week old female SJL/J mice to 3.0–3.5 Gy of whole-body irradiation induces myeloid leukemia in 10–30% of treated animals within a year. However, Haran-Ghera and Kotler have also observed that SJL/J exposure to fractionated X-rays induces lymphosarcomas [47]. Consistent with AML diagnosis, leukemic infiltrations are observed in the bone marrow, lymph nodes, spleen and liver [31]. The frequency of radiation-induced acute myeloid leukemia (RI-AML) increases with age up to about 12 weeks during the time of irradiation. Such an increase is possibly explained by the sensitivity of the developing mononuclear phagocytic system [48].

While radiation appears to initiate the progression of RI-AML, this multiphase malignancy often requires additional promoting factors for tumor development [49]. Preleukemic cells and the characteristic chromosome 2 deletions are observed in the overwhelming majority of bone marrows of IR-treated mice prior to overt AML clinical presentation (90–120 days) [50,51]. Additionally, administration of corticosteroids following irradiation increases RI-AML incidence to 50–70% [31]. Administration of growth factors, especially colony stimulating factor-1 (CSF-1), decreases latency and increases frequency to 75% [49,52]. In fact, 2–4 months prior to RI-AML onset, preleukemic RJL/L mice have significantly elevated CSF-1 levels as compared to mice that fail to develop RI-AML or those that develop RCN B. RI-AML cells *in vitro* synthesize significant amounts of CSF-1, further supporting CSF-1 necessity for leukemia progression in addition to IR [48].

Clinical presentation of RI-AML in SJL/J mouse resembles that of secondary leukemias observed in man [31]. Patients in remission after radiation and steroid treatment for Hodgkin's disease often develop AML similar to those described in SJL/J mice [53–55]. Additionally, elevated circulating levels of CSF-1 have been reported in neoplastic malignancies including AML and appear to be associated with poor prognosis [56–59], further supporting the use of the SJL/J mouse for the study of CSF-1's role in cancer.

### 3.1.3. C3H Mouse

Strong developed the C3H strain in 1920 from a cross of the Bragg Albino mouse and the DBA mouse, specifically selecting for elevated incidence of mammary tumors (MT). Ninety percent of unfostered pups (pups remaining with mother postpartum) develop mammary tumors by 11 months of age. Fostering the offspring or transferring fertilized ova to a mammary tumor virus-free surrogate significantly reduces tumor frequency [35,36]. Fostered C3H/He substrain has a high incidence of spontaneous hepatomas later in life [34,60].

X-irradiation of 8–10 week old male C3H/He mice with 3 Gy TBI induces myeloid leukemia in 23.9% of exposed animals, with myelomonocytic leukemia being the most prevalent subtype. Dose-response curves for C3H mice are similar to those for RFM and CBA mice: there is a proportional increase in the frequency of leukemia induction until a critical dose of around 3 Gy, after which the incidence spontaneously drops off [32]. Spontaneous incidence of leukemia is less than 1% [34].

Yoshida *et al.* reported a significant sex difference, with females being less susceptible to RI-ML than males of the same age. Administration of the synthetic glucocorticoid prednisolone following irradiation of C3H/He mice increases the incidence of ML to 38.5% in a similar fashion to that of SJL/J mice [31]. The mechanism of induction is suspected to involve suppression and promotion of hematopoietic recovery. Reducing daily caloric intake by roughly a third eliminates spontaneous ML entirely and decreased the incidence of RI-ML to 7.9% when the restriction started before 6 weeks of age or to 10.7% when the restriction started post exposure (PE) at 10 weeks of age [61]. Caloric restriction also promoted PE longevity via insulin pathway modulation [62]. Chronic inflammation may also be implicated as an exacerbating and possibly a leukemogenesis-promoting factor. In later studies Yoshida demonstrated that inducing chronic low-level inflammation by inserting a cellulose acetate membrane increases RI-ML incidence to 35.9% [63].

As with the RFM and SJL/J mice, partial deletion of chromosome 2 has been implicated in RI-AML in C3H/He mice [43,64]. As early as 24 h PE, during the first metaphase, chromosome 2 deletions are detectable in the bone marrow in the C3H/He mouse, suggesting that chromosome 2 deletions act in the initiation stages of leukemogenesis [65]. Some researchers have compared human Ph<sup>1</sup> chromosome transformations in chronic myeloid leukemia to mouse chromosome 2 aberrations in its incidence and disease specificity [66,67].

### 3.1.4. CBA Mouse

The CBA mouse is a cross between a Bragg albino female and a DBA male originally developed by Strong in 1920 with low mammary tumor incidence. Males of CBA/Ca substrain tend to have a shorter lifespan than CBA/Ca females [35,36]. Both CBA/Ca and CBA/H are direct substrains of the original CBA mouse derived in the United Kingdom [68,69].

A 3.0 Gy TBI irradiation with either gamma- or X-rays of 12-week old male CBA/H mice results in 25% induction of myeloid leukemia. Infiltration of the sternal bone marrow, liver, and spleen are observed and serve as diagnostic endpoints [32,33]. As previously mentioned, the dose-response curve is curvilinear, implying a threshold dose similar to that of man—leukemia is rarely observed in cases with high exposure [70,71].

As with the other mouse models of RI-ML, chromosome 2 aberrations have been reported and correlated with myeloid leukemia in the CBA mouse [69,72,73]. From as early as 20 hours to as late as 24 months PE, expansion of cells carrying chr2 lesions is observed in 20–25% of irradiated mice [74]. Bouffler *et al.*, however, weren't able to conclude that the induction of chr2 aberrations and presence of an aberrant chr2 clone can accurately predict development of RI-AML in CBA mice [75]. Aberrations on chromosome 4 in about 50% of CBA/H mice diagnosed with typical AML were also reported. Cleary *et al.* have identified the *Lyr2*/TLSR5 allele as a likely mutation candidate for radiation-induced hematopoietic malignancies including the myeloid and lymphoid mouse leukemias [76]. Susceptibility to RI-AML in CBA/H has also been linked to an 8% decrease in DNA-methylation not observed in the AML-resistant strain C57Bl/6 [77].

The CBA mouse is the current favorite RI-AML model for human AML for a few reasons: (1) it has a low spontaneous frequency of AML, (2) it has a favorable mean latency of 18 months, and (3) morphologically CBA AML resembles the human malignancy [68,78]. Dekkers *et al.* have also suggested that the two-step mutation model of RI-AML in CBA/H, extrapolated from X-ray and neutron data, has application in animal modeling of human RI-AML [79].

### 3.1.5. ML-Associated Molecular Pathologies

For over 30 years, deletions on chromosome 2 have been linked to AML in murine models across multiple strains (RF, C3H/He, CBA, and SJL/J) [42,43,64]. Due to the specific nature of the chromosome aberrations on chr2, the loss of a tumor suppressor gene seemed a more likely scenario than an oncogene activation [80]. In 2004 Cook and colleagues identified the *sfpi* gene encoding a transcription factor PU.1 from the 2 Mbp commonly deleted region on chr2 [80–82].

PU.1/*Sfpi-1* is an important player in hematopoiesis and is involved in promotion, differentiation and regulation of all hematopoietic lineages. It's essential for terminal myeloid (macrophages and neutrophils) cell differentiation and stem cell maintenance [83–87]. In mice, PU.1 function is important for leukemic transformations in myeloid cells; in humans its importance in such transformations is still actively debated [81,88,89]. PU.1 has a DNA binding domain, engages in protein-protein interactions and has regulatory phosphorylation sites imperative for its function [90].

In addition to the loss of PU.1 on one chr2, the second copy of PU.1 is often inactivated by point mutations in the DNA binding region [81,88]. Homozygous conditional knockdown of PU.1 (expressing ~20% of WT levels) induces AML in mice by 3–8 months of age [91] and myeloid leukemia when inactivated in adult mice [92]. In transgenic mice expressing oncoprotein PML-PAR, loss of genomic region coding for PU.1 is a common secondary event in leukemogenesis [93]. Upregulation of *c-Myc* has also been reported in AML cells accompanying PU.1 deficiencies [94]. Cook *et al.* have demonstrated that expression of PU.1 at WT levels in promyelocytic leukemia cells inhibited clonogenic growth, forced monocytic differentiation, and induced apoptosis. All of these findings suggest that suboptimal expression of PU.1 can provoke and promote leukemogenesis by blocking maturation of the cell [81,87]. Peng *et al.* have also suggested that quantification of PU.1-deleted bone marrow cells may be used as a surrogate marker for RI-AML [95].

In humans a homologue of PU.1 exists on chromosome 11 [87] and is expressed at low levels in most AML cases [96]. However, direct inactivation by deletion of PU.1 is very rare [88,89]. Cook

proposes that other mechanism of PU.1 inactivation in human AML might be at play: the gene might be silenced epigenetically, through protein-protein interaction or via interaction with a mutated receptor (*i.e.*, Flt3 cytokine receptor that are found in 25% of human AML) [81]. Interestingly, Finnon *et al.* have recently shown that *Flt3*-ITD and *Sfpi1*/PU.1 mutations are mutually exclusive in murine radiation-induced AML without any overt phenotypic differences [97]. The group has not reported actual levels of PU.1 in these RI-AMLs, so it is plausible that the PU.1 depression is still involved in these malignancies.

It remains unclear, however, whether radiation is responsible for one or both genomic events observed in RI-AML: deletion of PU.1 on chr2 and *Sfpi1* mutations in its DNA-binding domain. Data suggests that IR induces chr2 deletions [51,64,95], but it remains undetermined whether the deletion is a result of direct DNA damage or induced through delayed genomic instability [98–100]. Radiation, however, is not a likely candidate for the direct alteration of the second PU.1 allele in RI-AML cells, as IR does not induce point mutations observed in *Sfpi1* [81,88,94]. Point mutations are the most common type of spontaneous mutations and evidence suggest that *Sfpi1* mutations are of spontaneous origin [101,102].

Ban and Kai demonstrated that replicative stress applied to hematopoietic stem cells (HSC) surviving 3 Gy radiation contributes to the HSC's accelerated aging, thus decreasing replicative fidelity of the genome and increasing the rate of mutation accumulation, including mutations in the remaining copy of the *Sfpi1* gene. A mathematical model fitted to experimental data from cobblestone area forming cells (CAFC) and colony forming unit-granulocyte/macrophages (CFU-G/M) on *ex vivo* bone marrows revealed that irradiated HSCs cycle as much as ten times more quickly than those from unexposed animals [102]. Such increase in cycling is thought to also appear *in vivo* after irradiation.

Hirouchi *et al.* have recently challenged the commonly accepted paradigm that the HSC is the target cell of RI-AML [78] and concluded that AML stem cells can arise from long-lived HSCs as well as the short-lived multipotent progenitors (MPPs) and common myeloid progenitors (CMPs) that have acquired self-renewal potential. The cell surface phenotypes and gene expression profiles of AML stem cells in the study closely resembled those of normal CMPs rather than those of HSCs [103].

In addition to chr2, critical loci on chromosomes 8, 13, and 18 have also been identified. On chr18 resides *Rbbp8* gene that encodes for the CtIP protein. CtIP is upregulated in response to X-ray exposure in the RI-AML-sensitive CBA mice but not in the RI-AML-resistant C57BL/6 and is a suspected tumor suppressor. Aberrant human chromosome segments bearing *Rbbp8* gene have been reported in many cancers including AML [104].

### *3.2. Radiation-Induced Lymphoma*

Debate is still ongoing regarding the causal effect of ionizing radiation on lymphomagenesis in man. While Hartge and colleagues concluded that IR probably causes lymphoma and a small increase in risk between radiotherapy and lymphoma has been identified [105,106], a plethora of investigators tend to disagree. Some investigators found the link between non-Hodgkin's lymphoma (NHL) and radiotherapy extremely weak, and no association at all between IR and Hodgkin's disease [16,107–109]. Recent data, however, seem to suggest that the causal link is real. Richardson *et al.* have published data supporting a strong link between ionizing radiation and lymphoma mortality among radiation

workers exposed at the Savannah River Site in South Carolina. The basis for disagreement among researchers appears to be the disease’s protracted latency and obscure mechanism of induction [110].

Historically, in rodent pathology classification no distinction was made between lymphomas and lymphocytic leukemias. Malignant lymphomas in mice can be placed into six subdivisions with further modifiers depending on the site of the tumor—thymic, mesenteric, and leukemic [111]. Most of the time murine lymphoma is diagnosed phenotypically: labored breathing, hunched posture, and the enlargement of spleen and lymph nodes are indications of fulminant malignancy. Mice with labored breathing but without enlarged spleens and lymph nodes are usually classified as thymic lymphomas [112]. Immunological markers and morphologic criteria are also commonly used in more specific diagnosis [113–115]. Immunophenotypes of thymic lymphoma in mice closely resemble their counterparts in humans despite the fact that there is no direct human analog of thymic lymphoma [115].

Thymic lymphoma (TL) in mice has been extensively studied as a model of radiation-induced carcinogenesis since it was first described by Kaplan *et al.* in 1953 [116]. In addition to C57BL/6 and other C57BL substrains, BALB/c and NSF are also susceptible to RI-TL [117,118] (See Table 2 for summary).

**Table 2.** Induction of thymic lymphoma in mice with low-LET ionizing radiation.

Malignancy	Mouse Strain	Age	Sex	Mode of Induction	Latency	Spontaneous Frequency	Induced Frequency	Ref.
Thymic Lymphoma	C57BL (C57BL/6, C57BL/6J)	4–6 weeks	Male, Female	4 fractions of ~1.7 Gy once a week	3–6 months	<1%	>90%	[116, 119, 120]
Thymic Lymphoma	BALB/c (BALB/cHeA)	4 weeks	Male, Female	4 exposures ~1.7 Gy once a week for 4 weeks	2.5–9.5 months	5–6% females; 0% males	77 % (Females) 86% (Males)	[112, 117]
Thymic Lymphoma	NFS	4 weeks	Male, Female	4 fractions ~1.7 Gy once a week for 4 weeks	3–6 months	>1% within 12 months	90% (females) 89% (males)	[121, 122]

### 3.2.1. C57BL Mouse

C57BL mice were developed in 1921 as a cross between female 57 and male 52 from Miss Abbie Lanthrop stock. It is one of the most widely used mouse stocks in the laboratory. Up to 7% of C57BL/6 mice develop spontaneous leukemia [36,123].

As early as 1949, Sacher and Brues were able to induce thymic lymphoma in mice with X-ray radiation [124]. In 1952 Kaplan *et al.* published a seminal paper identifying optimal fractionation periods for TL induction at 8-day intervals for 4 weeks in C57BL mice that results in 93% disease penetrance within ~250 days following the first irradiation. Females were identified to be slightly but significantly more susceptible than males to TL at 58% *versus* 47%, respectively. Lungs and peripheral lymph nodes seem to be affected in the majority of murine lymphoma cases [119]. TL with similar

frequencies and latency periods can be induced in C57BL/6, C57BL/10 and C57BL/Ka substrains of C57BL [120,125,126].

Radiation-induced thymic lymphoma (RI-TL) is highly asynchronous and lymphoma cells have been often staged by the presence of MEL-14<sup>hi</sup> (lymphocyte homing receptor), H-2K<sup>hi</sup> (histocompatibility antigen), and IL-2R<sup>+</sup> (interleukin 2 receptor) surface markers on thymus cortical cells. In the normal adult thymus less than 3% of the cells in the cortex express MEL-14<sup>hi</sup> or IL-2R<sup>+</sup> [127,128] and the presence of MEL-14<sup>hi</sup> may signify appearance of a leukemic clone [129]. Additionally, most of the TL tumors bear T-lymphocyte specific antigens Thy-1, Lyt-1, and Lyt-2 [130,131].

The most detected early chromosome abnormality observed in IR-induced thymic lymphoma in C57BL mice is trisomy of chromosome 15, detected in 65–71% of case [132,133]. Chromosome 15 trisomy is one of the most common cytogenic abnormalities in murine cancers as it leads to amplification of the oncogene *myc*, deregulation of which might be important in TL [134,135]. Alteration of *myc* expression through a translocation is observed in nearly all Burkitt's lymphoma (BL) cases in man. *Myc* is an oncogene and a transcriptional factor regulating apoptosis; its deregulation has been observed in many cancers in addition to BL [136]. Activation of *N-ras* and *K-ras* has also been reported in just over 50% of RI-TL case in C57BL/6J [128,137]. Inactivation of tumor suppressor *p53* does not seem to be a salient feature of RI-TL in C57BL/6 mice [135] but transgenic *p53* knockout mice do exhibit higher frequency of RI-TL and implicate another tumor suppressor *Pten* [138].

### 3.2.2. BALB/c Mouse

BALB/c is an inbred strain acquired by Bagg in 1913 and further expanded by Snell in 1932, who has subsequently added the /c designation to reflect the “color” homozygous color locus. It is among one of the most commonly used strains and purportedly does not develop lymphatic leukemia, but is sensitive to radiation lethality [36].

Following the Kaplan *et al.* methodology, thymic lymphoma can be induced in BALB/c mice with fractionated radiation (1.7 Gy/fraction, four fractions total) beginning at 4 weeks of age in both male and female mice at 86% and 77%, respectively. Later in life, females exhibit a spontaneous frequency of lymphoma at 5.5% but males do not. The mean latency for both sexes is ~5 months after IR [112,117].

The majority of studies on the mechanism of lymphomagenesis have been historically worked out either in C57BL/6 and its substrains or in hybrids that have included a BALB/c parent mated with a strain resistant to radiation-induced lymphoma. Recently, however, the inbred BALB/c mice have been used to demonstrate the role of microRNA (miRNA) in radiation-induced lymphomagenesis. Liu *et al.* concluded that in RI-TL tissues tumor suppressor gene *Big-h3* is downregulated while miR-21 is upregulated. MiR-21 is likely to directly target *Big-h3* by inhibiting translation in a 3' UTR dependent manner [139]. 3' UTR dependent manner assumes a specific binding of miRNA to mRNA targets in the 3' untranslated region (3' UTR) [140].



### 3.2.3. NFS Mouse

NFS is an inbred strain derived from the outbred NIH Swiss-Webster introduced to Japan in 1972. Maintained in sister-brother mating its current designation is NFS or NIH Swiss/S. The strain is also available in the United States [118].

Thymic lymphoma in NFS mice is induced in the same fashion as in BALB/c and C57BL mice: 4 weekly irradiations of 1.7 Gy beginning at one month of age. Both males and females are susceptible with comparable frequencies but the latency in males is longer (167 vs. 208 days). Spontaneous frequency is also low at less than 10% at 600 days of age [118]. Thymectomy on pre-irradiated NSF animals reduces the incidence of TL but increases the incidence of nonthymic lymphomas and leukemias in 67% of treated mice. Nonthymic lymphomas were predominantly observed in the spleen and mesentery lymph nodes and were most likely of B-cell origin [121]. Perhaps, thymectomies prior to irradiation might provide for a more relevant model of human lymphoma.

### 3.2.4. TL-Associated Molecular Pathologies

From the 1980s on the use of hybrid models in radiation-induced thymic lymphoma studies became more common as it allowed for easier detection of underlying molecular pathologies. Popular hybrids included (C57BL/6J × BALB/c)<sub>F1</sub>, B6C3F1 (C57BL/6J × C3H)<sub>F1</sub>, C3B6F1 (C3H × C57BL/6)<sub>F1</sub>, (BALB/c × MSM)<sub>F1</sub> [122], (C57BL/6J × RF/J)<sub>F1</sub> [141], (C57BL/6J × DBA)<sub>F1</sub>, CBA/H × C57BL/6 [142,143] and the CXS series of recombinant inbred strains derived from TL-susceptible BALB/cHeA and TL-resistant STS/A [112]. The frequencies of RI-TL in the hybrids between highly susceptible strains and those with low susceptibilities (e.g., BALB/c × MSM) are usually between the expected frequencies of the parental strains. However, at times the hybrid mice require higher radiation doses in the four weekly fractions, *i.e.*, 2.5 Gy instead of the usual 1.7 Gy [122]. The use of these hybrids has elucidated the importance of such molecular players as *Ikaros/Znfla1* [144,145], *BCL11B/Rit1* [146], *p73* [147], *p19/ARF* [148], and inactivation of *p15/INK4b(Cdkn2b)* and *p16/INK4a(Cdkn2a)* [149] in radiation-induced lymphomagenesis. *Ikaros/Znfla1* protein is encoded by the *Ikzf1* gene and has many functions including immune system development and regulation of hematopoietic differentiation. In recent years downregulation of *Ikaros* activity has been established as the most clinically relevant tumor suppressor in B-cell acute lymphoblastic leukemia (B-ALL) and its downregulation associated with poor prognosis [150]. *BCL11B/Rit1* (B-cell CLL/lymphoma 11b) belongs to the largest family of transcription factors, the Kruppel-like C2H2 type zinc finger transcription proteins, and is involved in T-cell differentiation. *BCL11B* is also a tumor suppressor and is reportedly downregulated in 10–16% of T-cell acute lymphoblastic leukemias (T-ALL) [151,152]. *p73* is a member of the *p53*, pro-apoptotic tumor suppressor family [153]. Low levels of *p73* mRNA have been reported in non-Hodgkin's lymphoma (NHL) but not in reactive hyperplasia patients. *p73* inactivation in NHL cases appears to be due to aberrant methylation of its promoter [154]. Inactivation of cyclin dependent kinase inhibitors from the INK4 family (*ARF*, *p15*, and *p16*) have been reported in Non-Hodgkin's and Burkitt's lymphoma cases [155,156]. Table 3 summarizes the most relevant molecular pathologies observed in radiation-induced thymic lymphoma in mice.

**Table 3.** Relevant molecular pathologies in murine RI leukemia and lymphoma.

Mouse Strain	Malignancy	Molecular Pathology	Role in Cancer	Ref.
RF; SJL/J; C3H/He; CBA	Myeloid Leukemia	Chr2 deletions: loss of <i>PU.1/Sfpi1</i> on one chr2 copy; inactivation on the second copy	Oncogene and transcriptional regulator of myeloid promoters PU.1 suppression linked to leukemic transformation in mice and men	[80–82, 88, 89]
C57BL	Thymic Lymphoma	Trisomy of chr15: <i>myc</i> implicated	Oncogene and transcription regulator of many cell events including apoptosis —Almost ubiquitous deregulation in Burkitt’s lymphoma	[131–134]
Hybrids between C57BL/6, C3H, BALB/c, MSM, and RF/J, CBA, DBA, and the CTX	Thymic Lymphoma	Loss of <i>Ikaros/Znfn1a1</i> activity	Gene expression regulation and chromatin remodeling in hematopoietic differentiation One of the most clinically- relevant tumor suppressors in acute lymphoblastic leukemia (B-ALL)	[144,145] [121,150]
		Loss of <i>BCL11B/Rit1</i> activity	Transcription factor and tumor suppressor Linked to T-cell acute lymphoblastic leukemia (T-ALL)	[146,151, 152]
		Loss of <i>p73</i> activity	<i>p53</i> family tumor suppressor Abrogated expression in non-Hodgkin’s lymphoma	[147,153, 154]
		Loss of <i>p19/ARF</i> , <i>p15/INK4b</i> ( <i>Cdkn2b</i> ) and <i>p16/INK4a</i> ( <i>Cdkn2a</i> ) activity	Cyclin dependent kinase inhibitors that restrict cell cycle progression at G <sub>1</sub> Non-Hodgkin’s and Burkitt’s lymphomas	[142,148, 149,155, 156]

Transgenic expression of activated *Notch1* in murine lymphocytes induces lymphomagenesis [157]. Activation of *Notch1* and inactivation of *Notch2*, paired with overexpression of *c-Myc* and defective *Znfn1a1/Ikaros* has been reported in 81.25% of RI-TL suggesting their molecular collaboration in lymphomagenesis [158]. Additionally, the use of hybrids has elucidated recurring chromosomal aberrations on chromosomes 4, 11 and 12, but these aberrations do not appear ubiquitously in all hybrids (e.g., BALB/C × MSM does not show LOH on chr 4 but C57BL/6J × RF/J does) [143]. Saito *et al.* have reported a specific susceptibility locus near *D4Mit12* on chromosome 4, as well as loci at *D2Mit15* (chr2) and *D5Mit15* (chr5). [122]. Piskorowska and colleagues identified additional susceptibility loci at a sex-dependent locus on chr10 (*D10Mit134*), and chr12 (*D12Mit52I*) [159].

Hybrids between C57BL/6 and C3H (C3B6F1 and B6C3F) share similar aberrations resulting in copy-number reduction and allelic loss at *Ikaros* and *Bcl1b* but not at the *Cdkn2a/Cdk2b* and *Pten* when compared to their parental strains. Interestingly, *Ikaros* and *Bcl1b* alterations are due to multilocus deletions, while *Cdkn2a/Cdk2b* and *Pten* show uniparental disomy. In these specific mice,

*Ikaros* appears to be lost first followed by *Bcl11l* at a later time, in contrast with BALB/c × MSM hybrids where the order is reversed [132]. Rearrangements within the T-cell receptor alpha, *Tcra*, are also more common in these C57BL/6 and C3H hybrids as compared to those of the T-cell receptor beta, *Tcrb*, although both aberrations are observed. Allelic loss of *Tcrb*, a more strictly regulated allele, suggests that increased aberrant V(D)J rearrangement or increases in illegitimate V(D)J recombination might be important in IR-induced lymphomagenesis and may be the basis for strain differences in susceptibility to RI-TL [132]. Deficiencies in V(D)J activity have also been associated with intragenic deletion in *BCL11B* and *Notch1* in human lymphoid malignancies [160–162].

Kominami and Niwa have expanded the idea of an indirect mechanism of RI-TL, where IR may contribute to induction through genomic instability, but does not necessarily target thymocytes for the promotion of TL [163]. Fractionated total body irradiation leads to thymocyte apoptosis and that in turn leads to differentiation arrest and population regeneration by the damaged but surviving thymocytes with tumorigenic potential [124,164–166]. Transplantation or intravenous infusion of unirradiated bone marrow into an irradiated host reduces lymphomagenesis possibly by restoring the thymic microenvironment and preventing clonal expansion of irradiated T-cell precursors. Similarly, bone marrow shielding protects against RI-TL possibly through the same thymus repopulation mechanism. Inversely, transplantation of a non-irradiated thymus into an irradiated animal can develop into full TL [165,167–169]. Additionally, Muto and colleagues demonstrated that intrathymic (i.t.) and intraperitoneal (i.p.) injections of thymocytes from irradiated donors 4 months post-IR into unirradiated hosts results in T-type lymphomas of the donor type. At one month post-IR only intrathymic injections result in donor-type lymphomas in the recipient host suggesting the necessity of the thymus for further promotion in these “prelymphoma cells.” Identical experiments but with bone marrow cell injections did not induce lymphomas in recipients indicating that the bone marrow might not be the site of origin of the prelymphoma cells [170]. Furthermore, RF mice subjected to thymectomy prior to irradiation have a reduced incidence of TL down to 1% from 32% [29]. Collectively, all of these findings suggest that IR targets additional cells and tissues, not only the thymocytes, at the origin of this malignancy and that the thymic environment plays an important role in TL promotion.

Notch ligands and receptors appear to at least partially mediate the interaction between thymus tissues and hematopoietic progenitors leading to lymphoma [163]. Further contributing to the indirect model of lymphomagenesis might be alterations in regulation of reactive oxygen species (ROS) in surviving thymocytes, leading to the accumulation of ROS-induced mutations [171,172]. Tamura *et al.* have identified a candidate susceptibility gene *Mtf-1* (metal responsive transcription factor-1) and later demonstrated that a certain variant of *MTF-1*, found in susceptible BALB/c mice, is linked to more proliferating premature thymocytes with higher ROS levels than in the strain of mice resistant to RI-TL [173,174]. *MTF-1* is activated by heavy metals and is involved in post-radiation signaling pathways regulating intracellular ROS [175].

While thymic lymphoma is a malignancy observed in mice but not in man, radiation-induced lymphomagenesis models can offer important insight into the progression of hematopoietic neoplasias in humans as well. *Ikaros*, identified in RI-TL mice, has also been implicated in human acute lymphoblastic leukemia (ALL), the most common hematopoietic malignancy among children [144,176–179]. Tsuji *et al.* demonstrated the contribution of illegitimate V(D)J recombination

to *Notch1* 5'-deletions in radiation-induced thymic lymphoma, deregulation of which is thought to be involved in etiology of B- and T-cell human lymphomagenesis [180]. *Notch1*, a diverse master regulator responsible for a plethora of cellular processes, is itself an important player in both RI-TL and T-cell acute lymphoblastic leukemia [181]. Similarly, *PTEN* [182] and *CDKN2A/CDKN2B* have been proposed as candidates for initiation and/or progression of human ALL [183,184]. A new target gene, *EPHA7*, has been recently uncovered in the RI-TL mouse model and correlated with human T-cell lymphoblastic leukemia/lymphoma (T-LBL). *EPHA7* is inactivated in 100% of T-LBL in mice and 95.23% of humans by either loss of heterozygosity, promoter hypermethylation or a combination of both [185].

### *3.3. Radiation-Induced Lung Cancer*

In most industrialized nations, including the United States, lung carcinoma accounts for about a quarter of all cancer deaths, with the majority of cases being attributable to tobacco smoke [186]. Of the cancers associated with radiation, lung carcinoma was one of the first to be identified due to its high mortality [187]. Historically, data on radiation's contribution to lung carcinogenesis has primarily come from three groups of exposed individuals: (1) underground miners exposed to alpha radiation through radon-222 and radon-220 inhalation, (2) patients treated with IR for neoplastic and non-neoplastic malignancies, (3) and the Japanese atomic bomb survivors [4,188,189]. Minimal latency for gamma and X-ray exposed patients appears to be 9–10 years with a persistent increase in risk remaining over 25 years after exposure. Females tend to be considerably more susceptible to radiation-induced lung cancer than men when researchers have accounted for the confounding factor of smoking. Based on the data from Japanese survivors, adenocarcinoma appears to be the most common type of lung cancer in the exposed population, and no correlation is apparent between age at time of exposure and malignancy risk [4,190,191]. Travis and colleagues have reported a significant increase in all histopathological types of lung cancer in Hodgkin's disease patients treated with radiation up to 40 Gy or more after controlling for smoking. The incidence of secondary lung cancers in Hodgkin's patients peaks at 5–9 years following radiation therapy [192–194]; the reason for this shorter latency remains to be established. Recently, the data set has been complemented by new studies reporting an increase in lung cancer incidence in women treated with radiation for breast cancer [195,196].

In both humans and animals, delayed effects of radiation exposure are pulmonary fibrosis, the replacement of normal tissue with connective tissue fibers, and carcinogenesis. The induction of pulmonary fibrosis *versus* the induction of lung cancer appears to be a function of dose, with carcinogenesis requiring a much smaller dose [187]. A report by Williams *et al.* provides an extensive guide to animal model selection for radiation fibrosis in addition to other radiation-induced malignancies [11]. This review summarizes three models of radiation-induced lung cancer employing whole body irradiations and targeted thoracic exposures in C3H, BALB/c and RF mice. Table 4 summarizes the strains and methodologies of induction.

**Table 4.** Induction of lung cancer in mice with low-LET ionizing radiation.

Malignancy	Mouse Strain	Age	Sex	Mode of Induction	Latency	Spontaneous Frequency	Induced Frequency	Ref.
Lung Cancer	C3H (C3H/HeSlc)	6 weeks	Male	2 fractions of 7.5 Gy to the thorax 12 h apart	12 months	3.5–9.5%	40%	[190, 191]
Lung Cancer	RFM (RFM/Un)	10–12 weeks	Female	9 Gy to thorax	9 months	~28%	87%	[193, 194]
Lung Cancer	BALB/c (BALB/c/An)	12 weeks	Female	2 Gy TBI	12 months	~12%	~37%	[195, 196]

### 3.3.1. C3H Mouse

C3H/He mice have a low spontaneous frequency of lung tumors and moderate sensitivity to radiation-induced lung tumorigenicity [197]. While the highest frequency of induction at ~62% is observed with a 7.5 Gy thorax irradiation followed by three 3 Gy whole body irradiations at 3-month intervals, it is potentially irrelevant to lung radiation carcinogenesis in humans. A more clinically relevant scenario is a two-fraction irradiation at 7.5 Gy with a 12-hour interval between the irradiations. This exposure scenario results in a ~40% induction in males irradiated at 6-weeks of age. After a 12-month latency, treated mice tend to develop alveologenic adenomas and adenocarcinomas; tubular- or papillary-form tumors are rarely observed [198]. In a series of dose-response studies, Hashimoto and colleagues showed that tumor incidence following a single WBI increases up to 5.0 Gy and then begins to decrease, supporting a previously suggested model of competitive dynamics between inductive and suppressive effects of radiation [199].

Night irradiations are much more potent inducers of RI-LT in C3H mice than exposures during the day. To achieve the same tumor frequency as that seen at night with a 1.25 Gy irradiation a 5 Gy irradiation is required during the day [198]. Diurnal variations have been also reported in responses to cancer therapy in man as well and have been the basis for a clinical study [200]. C3H appears to be the optimal choice for ionizing radiation-induced lung carcinogenesis with its low spontaneous and moderate induction frequencies. Coggle and colleagues suggested that induction with thoracic irradiations is the preferred method [187] because it is clinically more relevant and reduces the incidence of other tumors in the animal that can contribute to lethality.

### 3.3.2. RF Mouse

Lung adenoma is inducible with ionizing radiation in both male and female RFM/Un mice when they are exposed at 10–12-week old [201,202]. Following a single irradiation with 9.0 Gy to the thorax roughly 87% of female RFM/Un mice develop lung cancer within 6–9 months with an average of 1.8 tumors per mouse. With a dose of 10.0 Gy 54% of male RFM/Un develop the same malignancy with a tumor multiplicity of 0.8 tumors per mouse within 11 months. However, there is a relatively high incidence of spontaneous lung carcinogenesis, at 28% in females and ~32% in males over the course of their lifespan [201,202].

### 3.3.3. BALB/c Mouse

A single TBI dose of 2.0 Gy at 12 weeks of age with a high dose rate (0.35 Gy/min) administered to a female BALB/c/An mouse, on average, results in a 37% induction of lung adenocarcinoma. The rate of spontaneous lung adenocarcinoma is between 11–14% [203]. Fractionation at 2.0 Gy per dose does not increase the incidence of lung carcinoma when compared to a single acute exposure at low dose-rates [204].

### 3.3.4. Lung Cancer-Associated Molecular Pathologies

The effects of the dose, dose-rate, fractionation and radiation quality on lung carcinogenesis in the mouse have been studied extensively, but the underlying molecular pathologies were more difficult to investigate until the recent emergence of genetically engineered mice (GEM). Most molecular pathologies identified in GEM are yet to be correlated with molecular pathologies observed in inbred animals [199,201–205]. Some data have been retroactively extrapolated from radiation studies involving 40,000 B6CF1 hybrid mice (C57BL/6 females × BALB/c male) conducted at Argonne National Laboratory between 1971 and 1986 [206,207]. Genetic material extracted from lung tissues preserved in paraffin and amplified with PCR from animals with adenocarcinomas and controls revealed that a significant percentage of animals with either radiation-induced or spontaneous lung adenocarcinoma have deletions of *Rb*, a tumor suppressor. Zhang and Woloschack reported that 97% of samples with *Rb* deletions also carried *p53* deletions and concluded that *p53* mutations may be one of the predominant mutations leading to radiation-induced lung carcinogenesis in B6CF1 mice [207]. Additionally, the same methodology has uncovered a high rate of point mutations in the *K-ras* gene in spontaneous (75%) irradiation-induced (50%) mouse lung adenocarcinomas [208].

Salient features of human lung tumors, be they carcinogen-induced or spontaneous, are also shared by murine lung cancers with alterations in *p53*, *K-ras*, and *Rb* among others [209–211]. *p53* is a tumor suppressor and cell cycle regulator, commonly known as the “guardian of the genome”, is either deleted or mutated in 80% of primary lung tumors [212–215]. Its loss is associated with poor clinical outcome [209]. It is thought that *p53* antitumor activity is tightly linked to apoptosis induction [216]. Retinoblastoma protein (*Rb*) and its associated pathway is another tumor suppressor mechanism that is either directly or indirectly inactivated in a variety of tumors, including a 90% rate in human small cell carcinomas [217,218]. *Rb* is involved in the regulation of cell cycle progression from G<sub>1</sub> to S [219]. Proto-oncogene *K-ras*, involved in cell differentiation, growth, and apoptosis [220], is mutated in 20–30% of human lung adenocarcinomas [221]. Activated *K-ras* is also associated with poor clinical prognosis [222]. Table 5 summarizes the relevant molecular pathologies linked to IR lung cancer.

The data on the underlying molecular and pathophysiological basis of radiation-induced lung cancer in animal models is rather lacking, but nevertheless, the use of these inbred models can be valuable in testing therapeutic agents against secondary cancers in man. Further research into the mechanisms of induction and promotion of IR-induced lung carcinogenesis in inbred mice has the potential to uncover novel therapeutic targets for preventing secondary neoplastic malignancies in man following radiation therapy. Genetically engineered mice mimicking human cancers, such as *K-ras* knockout mouse model of lung adenocarcinoma [12], are very useful and sophisticated models but are potentially self-limiting

and biased. These animals are predisposed to develop only a certain type of malignancy along a designated progression route and do not allow for the study of alternative mechanisms of carcinogenesis. If radiation-induced lung carcinogenesis does not follow the pre-programmed initiation and progression in a certain GEM employed, then the studies using these mice are not of general use and therapies based on these models might not be effective. Using inbred mice, however, may present a more unbiased approach to these “discovery” studies.

**Table 5.** Molecular pathologies associated with radiation-induced lung cancer.

Mouse Strain	Malignancy	Molecular Pathology	Role in Cancer	Ref.
B6CF1	Lung Adenocarcinoma	— <i>Rb</i> deletions/point mutations	Tumor suppressor; cell cycle progression control from G <sub>1</sub> to S —Inactivated in 90% small cell carcinomas	[207, 217–219]
		— <i>p53</i> deletions/point mutations	Tumor suppressor; cell cycle regulator and apoptosis inducer Deleted or mutated in 80% of primary lung tumors and other cancers	[209, 212–216]
		— <i>K-ras</i> point mutations	Proto-oncogene; cell growth and differentiation Mutated <i>RAS</i> found in 20–30% of lung adenocarcinoma	[208, 220–222]

### 3.4. Radiation-Induced Breast Cancer

Early compelling data linking radiation and breast cancer have been gathered from the Japanese female survivors of the atomic bomb attacks, females subjected to diagnostic fluoroscopes in Massachusetts tuberculosis sanatoria, and women treated for postpartum mastitis in New York [5]. In fact, in the Japanese atomic bomb survivors breast carcinoma presents the greatest radiation-induced increase in relative risk among all solid tumors [4]. The Massachusetts study demonstrated that females exposed to over a hundred diagnostic X-rays over the years were 80% more likely to develop breast tumors [223]. More reports are constantly emerging, implicating radiation therapy in secondary breast cancers. All of these studies demonstrate dependency on age during exposure. Up to 35% of women treated with radiation for Hodgkin’s disease at an early age developed breast cancer by the age of forty. Bhatia and Sankila studies approximated secondary radiation-induced breast cancer latency to over 10 years following radiation exposure [224,225]. Stovall and colleagues reported that an absorbed dose of >1Gy to the contralateral breast during radiotherapy is linked to a high risk of secondary *de novo* contralateral breast cancer (CBC) [226]. Risk for CBC was also linked with the reproductive history of a patient: women who have never given birth or became pregnant after the first diagnosis and subsequent radiation therapy were more likely to develop CBC than matched controls [227].

Ionizing radiation is a well-established etiological agent of both rodent and human breast cancer [190,203,228–233]. Despite the fact that mammary cancer mouse models are somewhat dissimilar from human breast cancers—low frequency of hormonal dependence of the tumor and carcinomas originating in the alveolar tissue—they are nonetheless valuable in studying

chemotherapeutic preventative and therapeutic agents in addition to modeling the underlying molecular pathology [230]. The BALB/c mouse has been used extensively as a model of mammary cancer either with cancer either being induced with a TBI or through the implantation of irradiated tissues into syngenic mice [234]. Table 6 summarizes the most commonly used BALB/c models.

**Table 6.** Induction of breast cancer in mice with low-LET ionizing radiation.

Malignancy	Mouse Strain	Age	Sex	Mode of Induction	Latency	Spontaneous Frequency	Induced Frequency	Ref.
Breast Cancer	BALB/c	12 weeks	Female	2.0 Gy exposure (TBI)	~24 months	8%	22%	[235]
Breast Cancer	BALB/c orthograft	12 weeks	Female	1.0 Gy TBI of donor cells	10 weeks	<1%	* Dysplasia ~75% * Tumors ~25%	[236]
Breast Cancer	BALB/c chimera	12 weeks	Female	4.0 Gy TBI of host	6 weeks	~19%	~81%	[237–240]

\* Dependent on the passage status of the donor cells.

#### 3.4.1. BALB/c Whole-Body Exposure Model

Original studies on BALB/c females whole-body irradiated with gamma rays have shown an increase in mammary carcinogenesis, from a background frequency of around 8% to about 22% within the mouse’s lifetime. To induce mammary adenocarcinoma, BALB/c females are irradiated at 12-weeks of age with a total dose of 2.0 Gy at a relatively high dose-rate of ~0.35 Gy/min; irradiation with the same total dose but a much smaller dose-rate of 0.083 Gy/day results in roughly half of the high dose-rate frequency at ~13% [203]. In fact, even a dose of 0.25 Gy but at the high dose-rate of 0.35 Gy/min induces mammary tumors in roughly 20% of animals [204]. Irradiation does not change latency but rather affects the incidence of breast adenocarcinomas. Prior to the appearance of tumors, hyperplastic lesions in the ductal dysplasia are detected 12–14 months after IR exposure [235]. Sensitivity to radiation-induced breast adenocarcinoma in the BALB/c female has been attributed to polymorphisms of *Prkdc*, a DNA-dependent protein kinase involved in DNA repair and post-IR cell signaling [241]. This model, however, is plagued by ovarian tumors detected in over 90% of autopsied mice [203].

#### 3.4.2. BALB/c Syngenic Transplant Model

A great leap forward in the field of breast cancer biology was made in 1959 when DeOme and colleagues introduced a murine orthograft model of breast cancer. The model involves clearing of the fat pad in 3-week-old female virgin mice, followed by a transplant of a 1mm duct fragment from a donor mouse containing hyperplastic lesions [236,242]. Ethier and Ullrich successfully adapted this model from the original C3H mice to BALB/c and later extensively used it to demonstrate strain



sensitivity differences and the associated molecular mechanism [236,243–245]. Additionally, Barcellos-Hoff and colleagues employed this model to further revolutionize the cancer research field demonstrating the importance of tissue microenvironment in breast carcinogenesis [237–240].

In the “cell dissociation assay” or the *in vitro/in vivo* model employed by Ethier and Ullrich, virgin donor BALB/c females are TBI irradiated with a total dose of 1.0 Gy at 12-weeks of age, then their mammary tissues are removed at 24 hours post-exposure. Single-cell suspensions of  $10^4$  cells, prepared from these donor animals, are then injected into 3-week-old virgin BALB/c females whose mammary fat pad had been removed. At 10 weeks following the procedure, the mice are sacrificed and the outgrowths are removed and analyzed for pathologies in the ductal architecture. Normal outgrowths have 2–3 terminal ducts that are capped by end buds in the fat pad and resemble anatomically correct ducts. Abnormal outgrowths have up to 10 or more terminal ducts capped with hyperplastic end buds and are assigned an arbitrary classification I–III, with Class III being the most severe [244,246,247].

In a series of elegant experiments, Ullrich and colleagues demonstrated that T cells from the irradiated donor harvested at different time points after irradiation, passaged *in vitro*, and transplanted into unirradiated recipient mice develop either dysplasia or adenocarcinomas depending on the time of harvesting or the number of passages in culture prior to implantation. Cells harvested at 52 weeks post-IR and injected into recipient host tend to regenerate dysplastic outgrowths at a high rate (3 in 4) and develop into tumors (1 in 4) while cells harvested at 1–16 weeks develop into normal outgrowths unless they have undergone extensive *in vitro* passaging. Dysplasia and tumors resembled *in situ* tumorigenesis with leukocyte infiltrations and angiogenesis [235].

Barcellos-Hoff and Ravi capitalized on this model and have established a radiation chimera model of their own [248] in which the fat pads of BALB/c mouse hosts are cleared at 3-weeks of age and the mice themselves are TBI irradiated with 4.0 Gy at 10–12-weeks of age. Three days later these hosts are subsequently transplanted with immortalized but non-malignant, unirradiated COMMA-D mouse epithelial cells from midpregnant BALB/c females [249]. At 6 weeks post-IR, the cells injected into irradiated host have 81% tumor penetrance as compared to 19% in the unirradiated host. Alternatively, a  $1\text{ mm}^3$  fragment of the formed epithelia from a wildtype donor or a donor primed for neoplastic development can be transplanted into the irradiated host whose mammary fat pads have been cleared [250]. This syngenic model demonstrates that radiation-induced changes in the stromal microenvironment contribute to carcinogenicity [248].

#### 3.4.3. Breast Cancer-Associated Molecular Pathologies

Cell lines established from female BALB/c donors irradiated with 1.0 Gy and harvested at 4 weeks (EF42) or 16 weeks (EF137) were used in early studies to examine molecular pathologies leading to tumorigenesis. Reduced or absent *Rb* protein was detected in EF42 after 11 passages and in EF137 after only 6 passages in culture. Mutant *p53* was detected in 95% after >20 passage and 1–5% in passages 6–10 suggesting that it is an early transformation event in preneoplastic cells. Additionally, following 20 passages in culture angiogenesis is often detected [235]. Ethier and Ullrich reported that injecting a larger number of cells results in a less frequent and less pronounced dysplasia as compared to an injection with fewer cells [244,246]. This observation suggests that replicative stress might be contributing to a faster and more prominent progression to ductal dysplasia as in the case with TL.

Barcellos-Hoff and colleagues have linked rapid remodeling of the microenvironment observed in the irradiated mammary gland to changes in the extracellular matrix and latent Transforming Growth Factor Beta (TGF-β) expression [237,251–253] and later showed that it accelerates tumor progression [250]. TGF-β is involved in regulating a variety of cell processes including cell cycle control, apoptosis and cell differentiation among others [252,254]. Radiation-induced activation of TGF-β has been additionally implicated in cell fate decisions and influence DNA-repair kinetics in an ATM-dependent manner [255,256].

The radiation chimera model is able to capture salient features of breast cancer that are thought to arise after irradiation, despite the fact that, unlike in the case of human malignancy, the transplanted epithelium itself has not been irradiated. Human breast cancer associated with radiation exposure has been shown to initiate in the ducT cells that often infiltrate the rest of the breast tissue [5] similarly to the way mammary cancer arises in the transplantation models. Barcellos-Hoff and colleagues have also reported that tumors arising from transplanted epithelium lack functional *p53* protein and are estrogen receptor (ER) negative [250], akin to those observed in women with breast cancer who have been previously irradiated [257]. *Rb* deficiencies observed by Ullrich and Preston in neoplastic ducT cells have also been reported in human breast cancer tumors and correlated with a highly invasive tumor phenotype [258]. Table 7 summarizes relevant molecular pathologies in radiation-induced breast cancer studies.

**Table 7.** Molecular pathologies associated with radiation-induced breast cancer.

Mouse Strain	Malignancy	Molecular Pathology	Role in Cancer	Ref.
		—Reduction or loss of <i>Rb</i>	Tumor suppressor; cell cycle progression control from G <sub>1</sub> to S Inactivated in 90% small cell carcinomas	[235,258]
BALB/c	Mammary Adenocarcinoma	— <i>p53</i> mutation	Tumor suppressor; cell cycle regulator and apoptosis inducer Among the key mutations in breast cancer initiation	[235,250, 257]
		—TGF-β expression	Cell cycle control; apoptosis; cell differentiation Linked to pro-tumorigenic microenvironment	[245, 251–256]

#### 4. Conclusions

An ideal mouse model of radiation-induced carcinogenesis would have a low spontaneous background frequency of the desired malignancy, would not co-develop cancers at alternative sites, would have a short latency period and would have tumors that are nearly identical to corresponding human disease in their onset, progression and underlying pathology. Such a perfect model, however, does not exist and we are therefore forced to compromise on some of these features. While we can, perhaps, compromise on the latency of the cancers and the frequencies of inductions, we cannot afford to compromise on the molecular and pathophysiological similarities to human radiation-induced

malignancies that these models must mimic. Much work in the field of radiation oncology remains to be done in order to develop more accurate recapitulations of human radiation-induced cancers. Today we are still at the stage where we still have difficulty discerning radiation-induced secondary cancers from primary tumors in men because the molecular signatures of each type remain to be established. Relating these molecular signatures to tumors that arise in mice following IR is yet another degree of difficulty.

Murine models presented within the scope of this review are most often a compromise on background frequencies and rates of induction, but they do demonstrate strong molecular and phenotypic correlations to salient features of the human cancers they are meant to represent. This enables these models to be rightfully employed to test the extent of therapeutic benefits of candidate drugs against radiation-induced carcinogenesis.

## References

1. *Seer Cancer Statistics Review, 1975–2009 (Vintage 2009 Populations)*; Howlader, N., Noone, A.M., Krapcho, M., Neyman, N., Aminou, R., Altekruse, S.F., Kosary, C.L., Ruhl, J., Tatalovich, Z., Cho, H., Mariotto, A., Eisner, M.P., Lewis, D.R., Chen, H.S., Feuer, E.J., Cronin, K.A., Eds.; National Cancer Institute: Bethesda, MD, USA, 2012.
2. Ringborg, U.; Bergqvist, D.; Brorsson, B.; Cavallin-Stahl, E.; Ceberg, J.; Einhorn, N.; Frodin, J.E.; Jarhult, J.; Lamnevik, G.; Lindholm, C.; *et al.* The swedish council on technology assessment in health care (SBU) systematic overview of radiotherapy for cancer including a prospective survey of radiotherapy practice in sweden 2001—Summary and conclusions. *Acta oncologica* **2003**, *42*, 357–365.
3. Prasanna, P.G.; Stone, H.B.; Wong, R.S.; Capala, J.; Bernhard, E.J.; Vikram, B.; Coleman, C.N. Normal tissue protection for improving radiotherapy: Where are the gaps? *Transl. Cancer Res.* **2012**, *1*, 35–48.
4. Fajardo, L.F.; Berthrong, M.; Anderson, R.E. *Radiation Pathology*; Oxford University Press: New York, 2001; p. 454.
5. Hall, E.J.; Giaccia, A.J. *Radiobiology for the Radiologist*, 7th ed.; Wolters Kluwer Health/Lippincott Williams & Wilkins: Philadelphia, PA, USA, 2012.
6. Zelefsky, M.J.; Fuks, Z.; Leibel, S.A. Intensity-modulated radiation therapy for prostate cancer. *Semin. Radiat. Oncol.* **2002**, *12*, 229–237.
7. de Arruda, F.F.; Puri, D.R.; Zhung, J.; Narayana, A.; Wolden, S.; Hunt, M.; Stambuk, H.; Pfister, D.; Kraus, D.; Shaha, A.; *et al.* Intensity-modulated radiation therapy for the treatment of oropharyngeal carcinoma: The memorial sloan-kettering cancer center experience. *Int. J. Radiat. Oncol. Biol. Phys.* **2006**, *64*, 363–373.
8. Kim, K.; Damoiseaux, R.; Norris, A.J.; Rivina, L.; Bradley, K.; Jung, M.E.; Gatti, R.A.; Schiestl, R.H.; McBride, W.H. High throughput screening of small molecule libraries for modifiers of radiation responses. *Int. J. Radiat. Biol.* **2011**, *87*, 839–845.
9. Rubin, P. *Cured I—Lent: Late Effects of Cancer Treatment on Normal Tissues (Medical Radiology/Radiation Oncology)*; Springer: Berlin, Germany, 2008; p. 140.

10. Ryan, J.L.; Krishnan, S.; Movsas, B.; Coleman, C.N.; Vikram, B.; Yoo, S.S. Decreasing the adverse effects of cancer therapy: An NCI workshop on the preclinical development of radiation injury mitigators/protectors. *Radiat. Res.* **2011**, *176*, 688–691.
11. Williams, J.P.; Brown, S.L.; Georges, G.E.; Hauer-Jensen, M.; Hill, R.P.; Huser, A.K.; Kirsch, D.G.; Macvittie, T.J.; Mason, K.A.; Medhora, M.M.; *et al.* Animal models for medical countermeasures to radiation exposure. *Radiat. Res.* **2010**, *173*, 557–578.
12. Jackson, E.L.; Willis, N.; Mercer, K.; Bronson, R.T.; Crowley, D.; Montoya, R.; Jacks, T.; Tuveson, D.A. Analysis of lung tumor initiation and progression using conditional expression of oncogenic *K-ras*. *Gene. Develop.* **2001**, *15*, 3243–3248.
13. Frese, K.K.; Tuveson, D.A. Maximizing mouse cancer models. *Nat. Rev. Cancer* **2007**, *7*, 645–658.
14. Hall, E.J.; Giaccia, A.J. *Radiobiology for the Radiologist*, 6th ed.; Lippincott Williams & Wilkins: Philadelphia, PA, USA, 2006; p. 546.
15. Little, M.P.; Weiss, H.A.; Boice, J.D., Jr.; Darby, S.C.; Day, N.E.; Muirhead, C.R. Risks of leukemia in japanese atomic bomb survivors, in women treated for cervical cancer, and in patients treated for ankylosing spondylitis. *Radiat. Res.* **1999**, *152*, 280–292.
16. Preston, D.L.; Kusumi, S.; Tomonaga, M.; Izumi, S.; Ron, E.; Kuramoto, A.; Kamada, N.; Dohy, H.; Matsuo, T.; Matsui, T.; *et al.* Cancer incidence in atomic bomb survivors. Part III. Leukemia, lymphoma and multiple myeloma, 1950–1987. *Radiat. Res.* **1994**, *137*, S68–S97.
17. Weiss, H.A.; Darby, S.C.; Doll, R. Cancer mortality following X-ray treatment for ankylosing spondylitis. *Int. J. Cancer* **1994**, *59*, 327–338.
18. Weiss, H.A.; Darby, S.C.; Fearn, T.; Doll, R. Leukemia mortality after X-ray treatment for ankylosing spondylitis. *Radiat. Res.* **1995**, *142*, 1–11.
19. Wakeford, R.; Kendall, G.M.; Little, M.P. The proportion of childhood leukaemia incidence in great britain that may be caused by natural background ionizing radiation. *Leukemia* **2009**, *23*, 770–776.
20. Boice, J.D., Jr.; Engholm, G.; Kleinerman, R.A.; Blettner, M.; Stovall, M.; Lisco, H.; Moloney, W.C.; Austin, D.F.; Bosch, A.; Cookfair, D.L.; *et al.* Radiation dose and second cancer risk in patients treated for cancer of the cervix. *Radiat. Res.* **1988**, *116*, 3–55.
21. Noshchenko, A.G.; Bondar, O.Y.; Drozdova, V.D. Radiation-induced leukemia among children aged 0–5 years at the time of the chernobyl accident. *Int. J. Cancer* **2010**, *127*, 412–426.
22. Ivanov, V.K.; Tsyb, A.F.; Gorsky, A.I.; Maksyutov, M.A.; Rastopchin, E.M.; Konogorov, A.P.; Korelo, A.M.; Biryukov, A.P.; Matyash, V.A. Leukaemia and thyroid cancer in emergency workers of the chernobyl accident: Estimation of radiation risks (1986–1995). *Radiat. Environ. Biophys.* **1997**, *36*, 9–16.
23. Ivanov, V.K.; Gorskii, A.I.; Tsyb, A.F.; Khaut, S.E. Incidence of post-chernobyl leukemia and thyroid cancer in children and adolescents in the briansk region: Evaluation of radiation risks. *Vopr. Onkol.* **2003**, *49*, 445–449.
24. Ivanov, V.K.; Gorski, A.I.; Maksyutov, M.A.; Vlasov, O.K.; Godko, A.M.; Tsyb, A.F.; Tirmarche, M.; Valenty, M.; Verger, P. Thyroid cancer incidence among adolescents and adults in the briansk region of russia following the chernobyl accident. *Health Phys.* **2003**, *84*, 46–60.

25. Preston, D.L.; Pierce, D.A.; Shimizu, Y.; Cullings, H.M.; Fujita, S.; Funamoto, S.; Kodama, K. Effect of recent changes in atomic bomb survivor dosimetry on cancer mortality risk estimates. *Radiat. Res.* **2004**, *162*, 377–389.
26. Little, M.P.; Wakeford, R.; Tawn, E.J.; Bouffler, S.D.; Berrington de Gonzalez, A. Risks associated with low doses and low dose rates of ionizing radiation: Why linearity may be (almost) the best we can do. *Radiology* **2009**, *251*, 6–12.
27. Tomonaga, M. Leukaemia in nagasaki atomic bomb survivors from 1945 through 1959. *Bull. WHO* **1962**, *26*, 619–631.
28. Little, M.P.; Wakeford, R.; Kendall, G.M. Updated estimates of the proportion of childhood leukaemia incidence in great britain that may be caused by natural background ionising radiation. *J. Radiol. Prot.* **2009**, *29*, 467–482.
29. Upton, A.C.; Wolff, F.F.; Furth, J.; Kimball, A.W. A comparison of the induction of myeloid and lymphoid leukemias in X-irradiated RF mice. *Cancer Res.* **1958**, *18*, 842–848.
30. Wolman, S.R.; McMorrow, L.E.; Cohen, M.W. Animal model of human disease: Myelogenous leukemia in the RF mouse. *Am. J. Pathol.* **1982**, *107*, 280–284.
31. Resnitzky, P.; Estrov, Z.; Haran-Ghera, N. High incidence of acute myeloid leukemia in SJL/J mice after X-irradiation and corticosteroids. *Leuk. Res.* **1985**, *9*, 1519–1528.
32. Major, I.R.; Mole, R.H. Myeloid leukaemia in X-ray irradiated CBA mice. *Nature* **1978**, *272*, 455–456.
33. Major, I.R. Induction of myeloid leukaemia by whole-body single exposure of CBA male mice to X-rays. *Brit. J. Cancer* **1979**, *40*, 903–913.
34. Seki, M.; Yoshida, K.; Nishimura, M.; Nemoto, K. Radiation-induced myeloid leukemia in C3H/He mice and the effect of prednisolone acetate on leukemogenesis. *Radiat. Res.* **1991**, *127*, 146–149.
35. Chia, R.; Achilli, F.; Festing, M.F.; Fisher, E.M. The origins and uses of mouse outbred stocks. *Nat. Genet.* **2005**, *37*, 1181–1186.
36. Festing, M.F. 25 Inbred Strains of Mice as Possible Candidates for a Multi-Strain Carcinogenesis Bioassay. 2005. Available online: [http://ntp.niehs.nih.gov/files/MouseStrains\\_Festing.pdf](http://ntp.niehs.nih.gov/files/MouseStrains_Festing.pdf) (accessed on 15 August 2012).
37. Ullrich, R.L.; Preston, R.J. Myeloid leukemia in male RFM mice following irradiation with fission spectrum neutrons or gamma rays. *Radiat. Res.* **1987**, *109*, 165–170.
38. Furth, J. Recent experimental studies on leukemia. *Physiol. Rev.* **1946**, *26*, 47–76.
39. Cole, R.K.; Furth, J. Experimental studies on the genetics of spontaneous leukamia in mice. *Cancer Res.* **1941**, *1*, 957–965.
40. Upton, A.C.; Jenkins, V.K.; Conklin, J.W. Myeloid leukemia in the mouse. *Ann. N. Y. Acad. Sci.* **1964**, *114*, 189–202.
41. Upton, A.C.; Buffett, R.F.; Furth, J.; Doherty, D.G. Radiation-induced dental death in mice. *Radiat. Res.* **1958**, *8*, 475–479.
42. Azumi, J.I.; Sachs, L. Chromosome mapping of the genes that control differentiation and malignancy in myeloid leukemic cells. *Proc. Natl. Acad. Sci. USA* **1977**, *74*, 253–257.

43. Hayata, I.; Ishihara, T.; Hirashima, K.; Sado, T.; Yamagiwa, J. Partial deletion of chromosome No. 2 in myelocytic leukemias of irradiated C3H/He and RFM mice. *J. Nat. Cancer Inst.* **1979**, *63*, 843–848.
44. Morgan, C. Hiroshima, nagasaki and the RERF. *Am. J. Pathol.* **1980**, *98*, 843–856.
45. Haran-Ghera, N.; Ben-Yaakov, M.; Peled, A.; Bentwich, Z. Immune status of SJL-J mice in relation to age and spontaneous tumor development. *J. Nat. Cancer Inst.* **1973**, *50*, 1127–1135.
46. Dunn, T.B. Normal and pathologic anatomy of the reticular tissue in laboratory mice, with a classification and discussion of neoplasms. *J. Nat. Cancer Inst.* **1954**, *14*, 1281–1433.
47. Haran-Ghera, N.; Kotler, M.; Meshorer, A. Studies on leukemia development in the SJL/J strain of mice. *J. Nat. Cancer Inst.* **1967**, *39*, 653–661.
48. Haran-Ghera, N.; Krautghamer, R.; Lapidot, T.; Peled, A.; Dominguez, M.G.; Stanley, E.R. Increased circulating colony-stimulating factor-1 (CSF-1) in SJL/J mice with radiation-induced acute myeloid leukemia (AML) is associated with autocrine regulation of AML cells by CSF-1. *Blood* **1997**, *89*, 2537–2545.
49. Haran-Ghera, N.; Resnitzky, P.; Krautghamer, R.; Tartakovsky, B. Multiphase process involved in radiation induced murine AML. *Leukemia* **1992**, *6*, 123S–125S.
50. Haran-Ghera, N.; Trakhtenbrot, L.; Resnitzky, P.; Peled, A. Preleukemia in experimental leukemogenesis. *Haematol. Blood Trans.* **1989**, *32*, 243–249.
51. Trakhtenbrot, L.; Krauthgamer, R.; Resnitzky, P.; Haran-Ghera, N. Deletion of chromosome 2 is an early event in the development of radiation-induced myeloid leukemia in SJL/J mice. *Leukemia* **1988**, *2*, 545–550.
52. Tartakovsky, B.; Goldstein, O.; Krautghamer, R.; Haran-Ghera, N. Low doses of radiation induce systemic production of cytokines: Possible contribution to leukemogenesis. *Int. J. Cancer* **1993**, *55*, 269–274.
53. Cadman, E.C.; Capizzi, R.L.; Bertino, J.R. Acute nonlymphocytic leukemia: A delayed complication of hodgkin's disease therapy: Analysis of 109 cases. *Cancer* **1977**, *40*, 1280–1296.
54. Coleman, C.N.; Williams, C.J.; Flint, A.; Glatstein, E.J.; Rosenberg, S.A.; Kaplan, H.S. Hematologic neoplasia in patients treated for hodgkin's disease. *N. Engl. J. Med.* **1977**, *297*, 1249–1252.
55. Pedersen-Bjergaard, J.; Philip, P.; Pedersen, N.T.; Hou-Jensen, K.; Svejgaard, A.; Jensen, G.; Nissen, N.I. Acute nonlymphocytic leukemia, preleukemia, and acute myeloproliferative syndrome secondary to treatment of other malignant diseases. II. Bone marrow cytology, cytogenetics, results of hla typing, response to antileukemic chemotherapy, and survival in a total series of 55 patients. *Cancer* **1984**, *54*, 452–462.
56. Scholl, S.M.; Bascou, C.H.; Mosseri, V.; Olivares, R.; Magdelenat, H.; Dorval, T.; Palangie, T.; Validire, P.; Pouillart, P.; Stanley, E.R. Circulating levels of colony-stimulating factor 1 as a prognostic indicator in 82 patients with epithelial ovarian cancer. *Brit. J. Cancer* **1994**, *69*, 342–346.
57. Hakala, A.; Kacinski, B.M.; Stanley, E.R.; Kohorn, E.; Puistola, U.; Risteli, J.; Risteli, L.; Thomas, C.; Kaupillaa, A. Macrophage colony stimulating factor (CSF-1), a clinically usefully tumor arker in endometrial adenocarcinoma: Comparison with CA125 and aminoterminal of type III procollagen. *Amer. J. Obstet. Gynecol.* **1994**, *173*, 112–119.

58. Scholl, S.M.; Lidereau, R.; de la Rochefordiere, A.; Le-Nir, C.C.; Mosseri, V.; Nogues, C.; Pouillart, P.; Stanley, F.R. Circulating levels of the macrophage colony stimulating factor CSF-1 in primary and metastatic breast cancer patients. A pilot study. *Breast Cancer Res. Treat.* **1996**, *39*, 275–283.
59. Toy, E.P.; Chambers, J.T.; Kacinski, B.M.; Flick, M.B.; Chambers, S.K. The activated macrophage colony-stimulating factor (CSF-1) receptor as a predictor of poor outcome in advanced epithelial ovarian carcinoma. *Gynecol. Oncol.* **2001**, *80*, 194–200.
60. Festing, M.F.; Blackmore, D.K. Life span of specified-pathogen-free (MRC category 4) mice and rats. *Lab. Animals* **1971**, *5*, 179–192.
61. Yoshida, K.; Inoue, T.; Nojima, K.; Hirabayashi, Y.; Sado, T. Calorie restriction reduces the incidence of myeloid leukemia induced by a single whole-body radiation in C3H/He mice. *Proc. Natl. Acad. Sci. USA* **1997**, *94*, 2615–2619.
62. Yoshida, K.; Hirabayashi, Y.; Watanabe, F.; Sado, T.; Inoue, T. Caloric restriction prevents radiation-induced myeloid leukemia in C3H/HeMs mice and inversely increases incidence of tumor-free death: Implications in changes in number of hemopoietic progenitor cells. *Exp. Hematol.* **2006**, *34*, 274–283.
63. Yoshida, K.; Nemoto, K.; Nishimura, M.; Seki, M. Exacerbating factors of radiation-induced myeloid leukemogenesis. *Leuk. Res.* **1993**, *17*, 437–440.
64. Hayata, I.; Seki, M.; Yoshida, K.; Hirashima, K.; Sado, T.; Yamagiwa, J.; Ishihara, T. Chromosomal aberrations observed in 52 mouse myeloid leukemias. *Cancer Res.* **1983**, *43*, 367–373.
65. Ban, N.; Kai, M.; Kusama, T. Chromosome aberrations in bone marrow cells of C3H/He mice at an early stage after whole-body irradiation. *J. Radiat. Res.* **1997**, *38*, 219–231.
66. Coupland, L.A.; Jammu, V.; Pidcock, M.E. Partial deletion of chromosome 1 in a case of acute myelocytic leukemia. *Cancer Genet. Cytogenet.* **2002**, *139*, 60–62.
67. Finger, L.R.; Kagan, J.; Christopher, G.; Kurtzberg, J.; Hershfield, M.S.; Nowell, P.C.; Croce, C.M. Involvement of the TCL5 gene on human chromosome 1 in T-cell leukemia and melanoma. *Proc. Natl. Acad. Sci. USA* **1989**, *86*, 5039–5043.
68. Rithidech, K.N.; Cronkite, E.P.; Bond, V.P. Advantages of the CBA mouse in leukemogenesis research. *Blood Cells Mol. Dis.* **1999**, *25*, 38–45.
69. Rithidech, K.; Dunn, J.J.; Bond, V.P.; Gordon, C.R.; Cronkite, E.P. Characterization of genetic instability in radiation- and benzene-induced murine acute leukemia. *Mutat. Res.* **1999**, *428*, 33–39.
70. Mole, R.H.; Major, I.R. Myeloid leukaemia frequency after protracted exposure to ionizing radiation: Experimental confirmation of the flat dose-response found in ankylosing spondylitis after a single treatment course with X-rays. *Leuk. Res.* **1983**, *7*, 295–300.
71. Smith, I.E.; Powles, R.; Clink, H.M.; Jameson, B.; Kay, H.E.; McElwain, T.J. Early deaths in acute myelogenous leukemia. *Cancer* **1977**, *39*, 1710–1714.
72. Rithidech, K.N.; Bond, V.P.; Cronkite, E.P.; Thompson, M.H. A specific chromosomal deletion in murine leukemic cells induced by radiation with different qualities. *Exp. Hematol.* **1993**, *21*, 427–431.
73. Rithidech, K.; Dunn, J.J.; Roe, B.A.; Gordon, C.R.; Cronkite, E.P. Evidence for two commonly deleted regions on mouse chromosome 2 in gamma ray-induced acute myeloid leukemic cells. *Exp. Hematol.* **2002**, *30*, 564–570.

74. Rithidech, K.; Bond, V.P.; Cronkite, E.P.; Thompson, M.H.; Bullis, J.E. Hypermutability of mouse chromosome 2 during the development of X-ray-induced murine myeloid leukemia. *Proc. Natl. Acad. Sci. USA* **1995**, *92*, 1152–1156.
75. Bouffler, S.D.; Meijne, E.I.; Morris, D.J.; Papworth, D. Chromosome 2 hypersensitivity and clonal development in murine radiation acute myeloid leukaemia. *Int. J. Radiat. Biol.* **1997**, *72*, 181–189.
76. Cleary, H.; Boulton, E.; Plumb, M. Allelic loss on chromosome 4 (Lyr2/TLSR5) is associated with myeloid, B-lympho-myeloid, and lymphoid (B and T) mouse radiation-induced leukemias. *Blood* **2001**, *98*, 1549–1554.
77. Giotopoulos, G.; McCormick, C.; Cole, C.; Zanker, A.; Jawad, M.; Brown, R.; Plumb, M. DNA methylation during mouse hemopoietic differentiation and radiation-induced leukemia. *Exp. Hematol.* **2006**, *34*, 1462–1470.
78. Jawad, M.; Giotopoulos, G.; Fitch, S.; Cole, C.; Plumb, M.; Talbot, C.J. Mouse bone marrow and peripheral blood erythroid cell counts are regulated by different autosomal genetic loci. *Blood Cells Mol. Dis.* **2007**, *38*, 69–77.
79. Dekkers, F.; Bijwaard, H.; Bouffler, S.; Ellender, M.; Huiskamp, R.; Kowalczyk, C.; Meijne, E.; Suttmuller, M. A two-mutation model of radiation-induced acute myeloid leukemia using historical mouse data. *Radiat. Environ. Biophys.* **2011**, *50*, 37–45.
80. Alexander, B.J.; Rasko, J.E.; Morahan, G.; Cook, W.D. Gene deletion explains both *in vivo* and *in vitro* generated chromosome 2 aberrations associated with murine myeloid leukemia. *Leukemia* **1995**, *9*, 2009–2015.
81. Cook, W.D.; McCaw, B.J.; Herring, C.; John, D.L.; Foote, S.J.; Nutt, S.L.; Adams, J.M. PU.1 is a suppressor of myeloid leukemia, inactivated in mice by gene deletion and mutation of its DNA binding domain. *Blood* **2004**, *104*, 3437–3444.
82. Silver, A.; Moody, J.; Dunford, R.; Clark, D.; Ganz, S.; Bulman, R.; Bouffler, S.; Finnon, P.; Meijne, E.; Huiskamp, R.; *et al.* Molecular mapping of chromosome 2 deletions in murine radiation-induced aml localizes a putative tumor suppressor gene to a 1.0 cm region homologous to human chromosome segment 11p11-12. *Genes Chromosomes Cancer* **1999**, *24*, 95–104.
83. Moreau-Gachelin, F.; Tavitian, A.; Tambourin, P. Spi-1 is a putative oncogene in virally induced murine erythroleukaemias. *Nature* **1988**, *331*, 277–280.
84. Scott, E.W.; Simon, M.C.; Anastasi, J.; Singh, H. Requirement of transcription factor PU.1 in the development of multiple hematopoietic lineages. *Science* **1994**, *265*, 1573–1577.
85. Simon, M.C.; Olson, M.; Scott, E.; Hack, A.; Su, G.; Singh, H. Terminal myeloid gene expression and differentiation requires the transcription factor PU.1. *Curr. Topics Microbiol. Immunol.* **1996**, *211*, 113–119.
86. McKercher, S.R.; Torbett, B.E.; Anderson, K.L.; Henkel, G.W.; Vestal, D.J.; Baribault, H.; Klemsz, M.; Feeney, A.J.; Wu, G.E.; Paige, C.J.; *et al.* Targeted disruption of the PU.1 gene results in multiple hematopoietic abnormalities. *EMBO J.* **1996**, *15*, 5647–5658.
87. Kastner, P.; Chan, S. PU.1: A crucial and versatile player in hematopoiesis and leukemia. *Int. J. Biochem. Cell. Biol.* **2008**, *40*, 22–27.



88. Suraweera, N.; Meijne, E.; Moody, J.; Carvajal-Carmona, L.G.; Yoshida, K.; Pollard, P.; Fitzgibbon, J.; Riches, A.; van Laar, T.; Huiskamp, R.; *et al.* Mutations of the PU.1 Ets domain are specifically associated with murine radiation-induced, but not human therapy-related, acute myeloid leukaemia. *Oncogene* **2005**, *24*, 3678–3683.
89. Mueller, B.U.; Pabst, T.; Osato, M.; Asou, N.; Johansen, L.M.; Minden, M.D.; Behre, G.; Hiddemann, W.; Ito, Y.; Tenen, D.G. Heterozygous PU.1 mutations are associated with acute myeloid leukemia. *Blood* **2002**, *100*, 998–1007.
90. Joo, M.; Park, G.Y.; Wright, J.G.; Blackwell, T.S.; Atchison, M.L.; Christman, J.W. Transcriptional regulation of the cyclooxygenase-2 gene in macrophages by PU.1. *J. Biol. Chem.* **2004**, *279*, 6658–6665.
91. Rosenbauer, F.; Wagner, K.; Kutok, J.L.; Iwasaki, H.; le Beau, M.M.; Okuno, Y.; Akashi, K.; Fiering, S.; Tenen, D.G. Acute myeloid leukemia induced by graded reduction of a lineage-specific transcription factor, PU.1. *Nat. Genet.* **2004**, *36*, 624–630.
92. Metcalf, D.; Dakic, A.; Mifsud, S.; di Rago, L.; Wu, L.; Nutt, S. Inactivation of PU.1 in adult mice leads to the development of myeloid leukemia. *Proc. Natl. Acad. Sci. USA* **2006**, *103*, 1486–1491.
93. Walter, M.J.; Park, J.S.; Ries, R.E.; Lau, S.K.; McLellan, M.; Jaeger, S.; Wilson, R.K.; Mardis, E.R.; Ley, T.J. Reduced PU.1 expression causes myeloid progenitor expansion and increased leukemia penetrance in mice expressing PML-RAR $\alpha$ . *Proc. Natl. Acad. Sci. USA* **2005**, *102*, 12513–12518.
94. Hirouchi, T.; Takabatake, T.; Yoshida, K.; Nitta, Y.; Nakamura, M.; Tanaka, S.; Ichinohe, K.; Oghiso, Y.; Tanaka, K. Upregulation of *c-Myc* gene accompanied by PU.1 deficiency in radiation-induced acute myeloid leukemia in mice. *Exp. Hematol.* **2008**, *36*, 871–885.
95. Peng, Y.; Brown, N.; Finnon, R.; Warner, C.L.; Liu, X.; Genik, P.C.; Callan, M.A.; Ray, F.A.; Borak, T.B.; Badie, C.; *et al.* Radiation leukemogenesis in mice: Loss of PU.1 on chromosome 2 in CBA and C57BL/6 mice after irradiation with 1 GeV/nucleon <sup>56</sup>Fe ions, X rays or gamma rays. Part I. Experimental observations. *Radiat. Res.* **2009**, *171*, 474–483.
96. Steidl, U.; Rosenbauer, F.; Verhaak, R.G.; Gu, X.; Ebraldidze, A.; Otu, H.H.; Klippel, S.; Steidl, C.; Bruns, I.; Costa, D.B.; *et al.* Essential role of jun family transcription factors in PU.1 knockdown-induced leukemic stem cells. *Nat. Genet.* **2006**, *38*, 1269–1277.
97. Finnon, R.; Brown, N.; Moody, J.; Badie, C.; Olme, C.H.; Huiskamp, R.; Meijne, E.; Suttmuller, M.; Rosemann, M.; Bouffler, S.D. Flt3-ITD mutations in a mouse model of radiation-induced acute myeloid leukaemia. *Leukemia* **2012**, *26*, 1445–1446.
98. Plumb, M.; Cleary, H.; Wright, E. Genetic instability in radiation-induced leukaemias: Mouse models. *Int. J. Radiat. Biol.* **1998**, *74*, 711–720.
99. Boulton, E.; Cleary, H.; Papworth, D.; Plumb, M. Susceptibility to radiation-induced leukaemia/lymphoma is genetically separable from sensitivity to radiation-induced genomic instability. *Int. J. Radiat. Biol.* **2001**, *77*, 21–29.
100. Morgan, W.F. Is there a common mechanism underlying genomic instability, bystander effects and other nontargeted effects of exposure to ionizing radiation? *Oncogene* **2003**, *22*, 7094–7099.
101. Busuttill, R.A.; Rubio, M.; Dolle, M.E.; Campisi, J.; Vijg, J. Oxygen accelerates the accumulation of mutations during the senescence and immortalization of murine cells in culture. *Aging Cell* **2003**, *2*, 287–294.

102. Ban, N.; Kai, M. Implication of replicative stress-related stem cell ageing in radiation-induced murine leukaemia. *Brit. J. Cancer* **2009**, *101*, 363–371.
103. Hirouchi, T.; Akabane, M.; Tanaka, S.; Braga-Tanaka, I., 3rd; Todate, A.; Ichinohe, K.; Oghiso, Y.; Tanaka, K. Cell surface marker phenotypes and gene expression profiles of murine radiation-induced acute myeloid leukemia stem cells are similar to those of common myeloid progenitors. *Radiat. Res.* **2011**, *176*, 311–322.
104. Darakhshan, F.; Badie, C.; Moody, J.; Coster, M.; Fannon, R.; Fannon, P.; Edwards, A.A.; Szluinska, M.; Skidmore, C.J.; Yoshida, K.; *et al.* Evidence for complex multigenic inheritance of radiation aml susceptibility in mice revealed using a surrogate phenotypic assay. *Carcinogenesis* **2006**, *27*, 311–318.
105. Schottenfeld, D.; Fraumeni, J.F. *Cancer Epidemiology and Prevention*, 3rd ed.; Oxford University Press: Oxford, UK, 2006; p. 1392.
106. Hartge, P.; Smith, M.T. Environmental and behavioral factors and the risk of non-hodgkin lymphoma. *Cancer Epidemiol. Biomarkers Prev.* **2007**, *16*, 367–368.
107. Boice, J.D., Jr. Radiation and non-hodgkin's lymphoma. *Cancer Res.* **1992**, *52*, 5489s–5491s.
108. Scientific Committee on the Effects of Atomic Radiation in United Nations. *Sources and Effects of Ionizing Radiation: United Nations Scientific Committee on the Effects of Atomic Radiation: Unscear 2000 Report to the General Assembly, with Scientific Annexes*; United Nations: New York, USA, 2000.
109. Adami, H.-O.; Hunter, D.J.; Trichopoulos, D. *Textbook of Cancer Epidemiology*; Oxford University Press: Oxford, UK, 2002; p. 599.
110. Richardson, D.B.; Sugiyama, H.; Wing, S.; Sakata, R.; Grant, E.; Shimizu, Y.; Nishi, N.; Geyer, S.; Soda, M.; Suyama, A.; *et al.* Positive associations between ionizing radiation and lymphoma mortality among men. *Amer. J. Epidemiol.* **2009**, *169*, 969–976.
111. Waalkes, M.P.; Ward, J.M. *Carcinogenesis*; Raven Press: New York, NY, USA, 1994; p. 478.
112. Okumoto, M.; Nishikawa, R.; Imai, S.; Hilgers, J. Genetic analysis of resistance to radiation lymphomagenesis with recombinant inbred strains of mice. *Cancer Res.* **1990**, *50*, 3848–3850.
113. Pattengale, P.K.; Taylor, C.R. Experimental models of lymphoproliferative disease. The mouse as a model for human non-hodgkin's lymphomas and related leukemias. *Am. J. Pathol.* **1983**, *113*, 237–265.
114. Pattengale, P.K.; Frith, C.H. Immunomorphologic classification of spontaneous lymphoid cell neoplasms occurring in female BALB/c mice. *J. Nat. Cancer Inst.* **1983**, *70*, 169–179.
115. Pattengale, P.; Leder, A.; Kuo, A.; Stewart, T.; Leder, P. Lymphohematopoietic and other malignant neoplasms occurring spontaneously in transgenic mice carrying and expressing MTV/myc fusion genes. *Curr. Topics Microbiol. Immunol.* **1986**, *132*, 9–16.
116. Kaplan, H.S.; Brown, M.B.; Paull, J. Influence of postirradiation thymectomy and of thymic implants on lymphoid tumor incidence in C57BL mice. *Cancer Res.* **1953**, *13*, 677–680.
117. Okumoto, M.; Nishikawa, R.; Imai, S.; Hilgers, J. Resistance of STS/A mice to lymphoma induction by X-irradiation. *J. Radiat. Res.* **1989**, *30*, 135–139.
118. Okumoto, M.; Nishikawa, R.; Takamori, Y.; Iwai, Y.; Iwai, M.; Tsubura, Y. Endogenous Type-C viral expression during lymphoma development in irradiated NFS mice. *Radiat. Res.* **1985**, *104*, 153–165.

119. Kaplan, H.S. Radiation-induced lymphoid tumors of mice. *Acta-Unio Internationalis Contra Cancrum* **1952**, *7*, 849–859.
120. Boniver, J.; Humblet, C.; Rongy, A.M.; Delvenne, C.; Delvenne, P.; Greimers, R.; Thiry, A.; Courtoy, R.; Defresne, M.P. Cellular aspects of the pathogenesis of radiation-induced thymic lymphomas in C57 BL mice (review). *In vivo* **1990**, *4*, 41–43.
121. Mori, N.; Takamori, Y. Development of nonthymic lymphomas in thymectomized NFS mice exposed to split-dose X-irradiation. *J. Radiat. Res.* **1990**, *31*, 389–395.
122. Saito, Y.; Ochiai, Y.; Kodama, Y.; Tamura, Y.; Togashi, T.; Kosugi-Okano, H.; Miyazawa, T.; Wakabayashi, Y.; Hatakeyama, K.; Wakana, S.; *et al.* Genetic loci controlling susceptibility to gamma-ray-induced thymic lymphoma. *Oncogene* **2001**, *20*, 5243–5247.
123. Meier, H.; Myers, D.D.; Huebner, R.J. Differential effect of a synthetic polyribonucleotide complex on spontaneous and transplanted leukemia in mice. *Life Sci. II* **1970**, *9*, 653–659.
124. Brues, A.M. Radiation as a carcinogenic agent. *Radiat. Res.* **1955**, *3*, 272–280.
125. Muto, M.; Sado, T.; Hayata, I.; Nagasawa, F.; Kamisaku, H.; Kubo, E. Reconfirmation of indirect induction of radiogenic lymphomas using thymectomized, irradiated B10 mice grafted with neonatal thymuses from Thy 1 congenic donors. *Cancer Res.* **1983**, *43*, 3822–3827.
126. Humblet, C.; Greimers, R.; Boniver, J.; Defresne, M.P. Stages in the development of radiation-induced thymic lymphomas in C57 BL/Ka mice: Preleukemic cells become progressively resistant to the tumor preventing effects of a bone marrow graft. *Exp. Hematol.* **1997**, *25*, 109–113.
127. Reichert, W.; Buselmaier, W.; Vogel, F. Elimination of X-ray-induced chromosomal aberrations in the progeny of female mice. *Mutat. Res.* **1984**, *139*, 87–94.
128. Newcomb, E.W.; Steinberg, J.J.; Pellicer, A. Ras oncogenes and phenotypic staging in N-methylnitrosourea- and gamma-irradiation-induced thymic lymphomas in C57BL/6J mice. *Cancer Res.* **1988**, *48*, 5514–5521.
129. Amari, N.M.; Meruelo, D. Murine thymomas induced by fractionated-x-irradiation have specific T-cell receptor rearrangements and characteristics associated with day-15 to -16 fetal thymocytes. *Mol. Cell Biol.* **1987**, *7*, 4159–4168.
130. Hogarth, P.M.; Henning, M.M.; McKenzie, I.F. Alloantigenic phenotype of radiation-induced thymomas in the mouse. *J. Nat. Cancer Instit.* **1982**, *69*, 619–626.
131. Hogarth, P.M.; Edwards, J.; McKenzie, I.F.; Goding, J.W.; Liew, F.Y. Monoclonal antibodies to the murine Ly-2.1 cell surface antigen. *Immunology* **1982**, *46*, 135–144.
132. McMorrow, L.E.; Newcomb, E.W.; Pellicer, A. Identification of a specific marker chromosome early in tumor development in gamma-irradiated C57BL/6J mice. *Leukemia* **1988**, *2*, 115–119.
133. Takabatake, T.; Kakinuma, S.; Hirouchi, T.; Nakamura, M.M.; Fujikawa, K.; Nishimura, M.; Oghiso, Y.; Shimada, Y.; Tanaka, K. Analysis of changes in DNA copy number in radiation-induced thymic lymphomas of susceptible C57BL/6, resistant C3H and hybrid F1 mice. *Radiat. Res.* **2008**, *169*, 426–436.
134. Sasaki, M. Current status of cytogenetic studies in animal tumors with special reference to nonrandom chromosome changes. *Cancer Genet. Cytogenet.* **1982**, *5*, 153–172.

135. Brathwaite, O.; Bayona, W.; Newcomb, E.W. *p53* mutations in C57BL/6J murine thymic lymphomas induced by gamma-irradiation and N-methylnitrosourea. *Cancer Res.* **1992**, *52*, 3791–3795.
136. Tomita, N. BCL2 and MYC dual-hit lymphoma/leukemia. *J. Clin. Exp. Hematop.* **2011**, *51*, 7–12.
137. Newcomb, E.W.; Corominas, M.; Bayona, W.; Pellicer, A. Multistage carcinogenesis in murine thymocytes: Involvement of oncogenes, chromosomal imbalances and T cell growth factor receptor. *Anticancer Res.* **1989**, *9*, 1407–1415.
138. Mao, J.H.; Wu, D.; Perez-Losada, J.; Nagase, H.; DelRosario, R.; Balmain, A. Genetic interactions between pten and *p53* in radiation-induced lymphoma development. *Oncogene* **2003**, *22*, 8379–8385.
139. Liu, C.; Li, B.; Cheng, Y.; Lin, J.; Hao, J.; Zhang, S.; Mitchel, R.E.; Sun, D.; Ni, J.; Zhao, L.; *et al.* Mir-21 plays an important role in radiation induced carcinogenesis in BALB/c mice by directly targeting the tumor suppressor gene Big-h3. *Int. J. Biol. Sci.* **2011**, *7*, 347–363.
140. Lewis, B.P.; Shih, I.H.; Jones-Rhoades, M.W.; Bartel, D.P.; Burge, C.B. Prediction of mammalian microRNA targets. *Cell* **2003**, *115*, 787–798.
141. Santos, J.; Perez de Castro, I.; Herranz, M.; Pellicer, A.; Fernandez-Piqueras, J. Allelic losses on chromosome 4 suggest the existence of a candidate tumor suppressor gene region of about 0.6 cm in gamma-radiation-induced mouse primary thymic lymphomas. *Oncogene* **1996**, *12*, 669–676.
142. Cleary, H.J.; Boulton, E.; Plumb, M. Allelic loss and promoter hypermethylation of the p15INK4b gene features in mouse radiation-induced lymphoid—but not myeloid—leukaemias. *Leukemia* **1999**, *13*, 2049–2052.
143. Cleary, H.J.; Wright, E.; Plumb, M. Specificity of loss of heterozygosity in radiation-induced mouse myeloid and lymphoid leukaemias. *Int. J. Radiat. Biol.* **1999**, *75*, 1223–1230.
144. Okano, H.; Saito, Y.; Miyazawa, T.; Shinbo, T.; Chou, D.; Kosugi, S.; Takahashi, Y.; Odani, S.; Niwa, O.; Kominami, R. Homozygous deletions and point mutations of the *Ikaros* gene in gamma-ray-induced mouse thymic lymphomas. *Oncogene* **1999**, *18*, 6677–6683.
145. Shimada, Y.; Nishimura, M.; Kakinuma, S.; Okumoto, M.; Shiroishi, T.; Clifton, K.H.; Wakana, S. Radiation-associated loss of heterozygosity at the *Znfn1a1* (*Ikaros*) locus on chromosome 11 in murine thymic lymphomas. *Radiat. Res.* **2000**, *154*, 293–300.
146. Shinbo, T.; Matsuki, A.; Matsumoto, Y.; Kosugi, S.; Takahashi, Y.; Niwa, O.; Kominami, R. Allelic loss mapping and physical delineation of a region harboring a putative thymic lymphoma suppressor gene on mouse chromosome 12. *Oncogene* **1999**, *18*, 4131–4136.
147. Herranz, M.; Santos, J.; Salido, E.; Fernandez-Piqueras, J.; Serrano, M. Mouse *p73* gene maps to the distal part of chromosome 4 and might be involved in the progression of gamma-radiation-induced T-cell lymphomas. *Cancer Res.* **1999**, *59*, 2068–2071.
148. Melendez, B.; Malumbres, M.; Perez de Castro, I.; Santos, J.; Pellicer, A.; Fernandez-Piqueras, J. Characterization of the murine *p19(ARF)* promoter cpg island and its methylation pattern in primary lymphomas. *Carcinogenesis* **2000**, *21*, 817–821.
149. Malumbres, M.; Perez de Castro, I.; Santos, J.; Fernandez Piqueras, J.; Pellicer, A. Hypermethylation of the cell cycle inhibitor p15INK4b 3'-untranslated region interferes with its transcriptional regulation in primary lymphomas. *Oncogene* **1999**, *18*, 385–396.

150. Payne, K.J.; Dovat, S. *Ikaros* and tumor suppression in acute lymphoblastic leukemia. *Crit. Rev. Oncogenesis* **2011**, *16*, 3–12.
151. Gutierrez, A.; Kentsis, A.; Sanda, T.; Holmfeldt, L.; Chen, S.C.; Zhang, J.; Protopopov, A.; Chin, L.; Dahlberg, S.E.; Neuberg, D.S.; *et al.* The BCL11B tumor suppressor is mutated across the major molecular subtypes of T-cell acute lymphoblastic leukemia. *Blood* **2011**, *118*, 4169–4173.
152. Kominami, R. Role of the transcription factor BCL11B in development and lymphomagenesis. *Proc. Jpn. Acad. B* **2012**, *88*, 72–87.
153. Kaghad, M.; Bonnet, H.; Yang, A.; Creancier, L.; Biscan, J.C.; Valent, A.; Minty, A.; Chalon, P.; Lelias, J.M.; Dumont, X.; *et al.* Monoallelically expressed gene related to *p53* at *1p36*, a region frequently deleted in neuroblastoma and other human cancers. *Cell* **1997**, *90*, 809–819.
154. Pei, J.H.; Luo, S.Q.; Zhong, Y.; Chen, J.H.; Xiao, H.W.; Hu, W.X. The association between non-hodgkin lymphoma and methylation of *p73*. *Tumour Biol.* **2011**, *32*, 1133–1138.
155. Gronbaek, K.; de Nully Brown, P.; Moller, M.B.; Nedergaard, T.; Ralfkiaer, E.; Moller, P.; Zeuthen, J.; Guldberg, P. Concurrent disruption of p16INK4a and the *ARF-p53* pathway predicts poor prognosis in aggressive non-hodgkin's lymphoma. *Leukemia* **2000**, *14*, 1727–1735.
156. Mangani, D.; Roberti, A.; Rizzolio, F.; Giordano, A. Emerging molecular networks in burkitt's lymphoma. *J. Cell Biochem.* **2012**, *114*, 35–38.
157. Pear, W.S.; Aster, J.C.; Scott, M.L.; Hasserjian, R.P.; Soffer, B.; Sklar, J.; Baltimore, D. Exclusive development of T cell neoplasms in mice transplanted with bone marrow expressing activated notch alleles. *J. Exp. Med.* **1996**, *183*, 2283–2291.
158. Lopez-Nieva, P.; Santos, J.; Fernandez-Piqueras, J. Defective expression of *Notch1* and *Notch2* in connection to alterations of *c-Myc* and *Ikaros* in gamma-radiation-induced mouse thymic lymphomas. *Carcinogenesis* **2004**, *25*, 1299–1304.
159. Piskorowska, J.; Gajewska, M.; Szymanska, H.; Krysiak, E.; Quan, L.; Grygalewicz, B.; Skurzak, H.M.; Czarnomska, A.; Pienkowska-Grela, B.; Demant, P. Susceptibility loci and chromosomal abnormalities in radiation induced hematopoietic neoplasms in mice. *J. Rad. Res.* **2011**, *52*, 147–158.
160. Davila, M.; Foster, S.; Kelsoe, G.; Yang, K. A role for secondary V(D)J recombination in oncogenic chromosomal translocations? *Advan. Cancer Res.* **2001**, *81*, 61–92.
161. Marculescu, R.; Le, T.; Bocskor, S.; Mitterbauer, G.; Chott, A.; Mannhalter, C.; Jaeger, U.; Nadel, B. Alternative end-joining in follicular lymphomas' t(14;18) translocation. *Leukemia* **2002**, *16*, 120–126.
162. Marculescu, R.; Le, T.; Simon, P.; Jaeger, U.; Nadel, B. V(D)J-mediated translocations in lymphoid neoplasms: A functional assessment of genomic instability by cryptic sites. *J. Exp. Med.* **2002**, *195*, 85–98.
163. Kominami, R.; Niwa, O. Radiation carcinogenesis in mouse thymic lymphomas. *Cancer Sci.* **2006**, *97*, 575–581.
164. Kaplan, H.S. The role of radiation on experimental leukemogenesis. *Natl. Cancer Inst. Monogr.* **1964**, *14*, 207–220.
165. Sado, T.; Kamisaku, H.; Kubo, E. Bone marrow-thymus interactions during thymic lymphomagenesis induced by fractionated radiation exposure in B10 mice: Analysis using bone marrow transplantation between Thy 1 congenic mice. *J. Radiat. Res.* **1991**, *32*, 168–180.

166. Boniver, J.; Humblet, C.; Rongy, A.M.; Delvenne, C.; Delvenne, P.; Greimers, R.; Thiry, A.; Courtoy, R.; Defresne, M.P. Cellular events in radiation-induced lymphomagenesis. *Int. J. Radiat. Biol.* **1990**, *57*, 693–698.
167. Kaplan, H.S.; Hirsch, B.B.; Brown, M.B. Indirect induction of lymphomas in irradiated mice. IV. Genetic evidence of the origin of the tumor cells from the thymic grafts. *Cancer Res.* **1956**, *16*, 434–436.
168. Kaplan, H.S.; Carnes, W.H.; Brown, M.B.; Hirsch, B.B. Indirect induction of lymphomas in irradiated mice. I. Tumor incidence and morphology in mice bearing nonirradiated thymic grafts. *Cancer Res.* **1956**, *16*, 422–425.
169. Kaplan, H.S.; Brown, M.B.; Hirsch, B.B.; Carnes, W.H. Indirect induction of lymphomas in irradiated mice. II. Factor of irradiation of the host. *Cancer Res.* **1956**, *16*, 426–428.
170. Muto, M.; Kubo, E.; Sado, T. Development of prelymphoma cells committed to thymic lymphomas during radiation-induced thymic lymphomagenesis in B10 mice. *Cancer Res.* **1987**, *47*, 3469–3472.
171. Little, J.B. Radiation carcinogenesis. *Carcinogenesis* **2000**, *21*, 397–404.
172. Redpath, J.L.; Gutierrez, M. Kinetics of induction of reactive oxygen species during the post-irradiation expression of neoplastic transformation *in vitro*. *Int. J. Radiat. Biol.* **2001**, *77*, 1081–1085.
173. Tamura, Y.; Maruyama, M.; Mishima, Y.; Fujisawa, H.; Obata, M.; Kodama, Y.; Yoshikai, Y.; Aoyagi, Y.; Niwa, O.; Schaffner, W.; *et al.* Predisposition to mouse thymic lymphomas in response to ionizing radiation depends on variant alleles encoding metal-responsive transcription factor-1 (*Mtf-1*). *Oncogene* **2005**, *24*, 399–406.
174. Maruyama, M.; Yamamoto, T.; Kohara, Y.; Katsuragi, Y.; Mishima, Y.; Aoyagi, Y.; Kominami, R. *Mtf-1* lymphoma-susceptibility locus affects retention of large thymocytes with high ros levels in mice after gamma-irradiation. *Biochem. Biophys. Res. Commun.* **2007**, *354*, 209–215.
175. Lichtlen, P.; Wang, Y.; Belser, T.; Georgiev, O.; Certa, U.; Sack, R.; Schaffner, W. Target gene search for the metal-responsive transcription factor *Mtf-1*. *Nucleic Acids Res.* **2001**, *29*, 1514–1523.
176. Sun, L.; Goodman, P.A.; Wood, C.M.; Crotty, M.L.; Sensel, M.; Sather, H.; Navara, C.; Nachman, J.; Steinherz, P.G.; Gaynon, P.S.; *et al.* Expression of aberrantly spliced oncogenic *Ikaros* isoforms in childhood acute lymphoblastic leukemia. *J. Clin. Oncol.* **1999**, *17*, 3753–3766.
177. Sun, L.; Crotty, M.L.; Sensel, M.; Sather, H.; Navara, C.; Nachman, J.; Steinherz, P.G.; Gaynon, P.S.; Seibel, N.; Mao, C.; *et al.* Expression of dominant-negative *Ikaros* isoforms in T-cell acute lymphoblastic leukemia. *Clin. Cancer Res.* **1999**, *5*, 2112–2120.
178. Ruiz, A.; Jiang, J.; Kempfski, H.; Brady, H.J. Overexpression of the *Ikaros* 6 isoform is restricted to t(4;11) acute lymphoblastic leukaemia in children and infants and has a role in B-cell survival. *Brit. J. Haematol.* **2004**, *125*, 31–37.
179. Mullighan, C.G.; Miller, C.B.; Radtke, I.; Phillips, L.A.; Dalton, J.; Ma, J.; White, D.; Hughes, T.P.; Le Beau, M.M.; Pui, C.H.; *et al.* BCR-ABL1 lymphoblastic leukaemia is characterized by the deletion of *Ikaros*. *Nature* **2008**, *453*, 110–114.

180. Tsuji, H.; Ishii-Ohba, H.; Katsube, T.; Ukai, H.; Aizawa, S.; Doi, M.; Hioki, K.; Ogiu, T. Involvement of illegitimate V(D)J recombination or microhomology-mediated nonhomologous end-joining in the formation of intragenic deletions of the *Notch1* gene in mouse thymic lymphomas. *Cancer Res.* **2004**, *64*, 8882–8890.
181. Weng, A.P.; Ferrando, A.A.; Lee, W.; Morris, J.P.T.; Silverman, L.B.; Sanchez-Irizarry, C.; Blacklow, S.C.; Look, A.T.; Aster, J.C. Activating mutations of *Notch1* in human T cell acute lymphoblastic leukemia. *Science* **2004**, *306*, 269–271.
182. Zuurbier, L.; Petricoin, E.F., 3rd; Vuerhard, M.J.; Calvert, V.; Kooi, C.; Buijs-Gladdines, J.G.; Smits, W.K.; Sonneveld, E.; Veerman, A.J.; Kamps, W.A.; *et al.* The significance of PTEN and AKT aberrations in pediatric T-cell acute lymphoblastic leukemia. *Haematologica* **2012**, *97*, 1405–1413.
183. Mulligan, C.S.; Best, O.G.; Mulligan, S.P.; Consortium on Chronic Lymphocytic Leukaemia Australian Research. The precursor of chronic lymphocytic leukemia. *N. Engl. J. Med.* **2009**, *360*, 2575–2576.
184. Okuda, T.; Shurtleff, S.A.; Valentine, M.B.; Raimondi, S.C.; Head, D.R.; Behm, F.; Curcio-Brint, A.M.; Liu, Q.; Pui, C.H.; Sherr, C.J.; *et al.* Frequent deletion of p16INK4a/MTS1 and p15INK4b/MTS2 in pediatric acute lymphoblastic leukemia. *Blood* **1995**, *85*, 2321–2330.
185. Lopez-Nieva, P.; Vaquero, C.; Fernandez-Navarro, P.; Gonzalez-Sanchez, L.; Villa-Morales, M.; Santos, J.; Esteller, M.; Fernandez-Piqueras, J. EPHA7, a new target gene for 6q deletion in T-cell lymphoblastic lymphomas. *Carcinogenesis* **2012**, *33*, 452–458.
186. Carbone, D. Smoking and cancer. *Amer. J. Med.* **1992**, *93*, 13S–17S.
187. Coggle, J.E.; Lambert, B.E.; Moores, S.R. Radiation effects in the lung. *Environ. Health Perspect.* **1986**, *70*, 261–291.
188. Griem, M.L.; Kleinerman, R.A.; Boice, J.D., Jr.; Stovall, M.; Shefner, D.; Lubin, J.H. Cancer following radiotherapy for peptic ulcer. *J. Nat. Cancer Instit.* **1994**, *86*, 842–849.
189. Darby, S.C.; Doll, R.; Gill, S.K.; Smith, P.G. Long term mortality after a single treatment course with X-rays in patients treated for ankylosing spondylitis. *Brit. J. Cancer* **1987**, *55*, 179–190.
190. Preston, D.L.; Ron, E.; Tokuoka, S.; Funamoto, S.; Nishi, N.; Soda, M.; Mabuchi, K.; Kodama, K. Solid cancer incidence in atomic bomb survivors: 1958–1998. *Radiat. Res.* **2007**, *168*, 1–64.
191. Egawa, H.; Furukawa, K.; Preston, D.; Funamoto, S.; Yonehara, S.; Matsuo, T.; Tokuoka, S.; Suyama, A.; Ozasa, K.; Kodama, K.; *et al.* Radiation and smoking effects on lung cancer incidence by histological types among atomic bomb survivors. *Radiat. Res.* **2012**, *178*, 191–201.
192. Travis, L.B. Therapy-associated solid tumors. *Acta Oncologica* **2002**, *41*, 323–333.
193. Travis, L.B.; Gospodarowicz, M.; Curtis, R.E.; Clarke, E.A.; Andersson, M.; Glimelius, B.; Joensuu, T.; Lynch, C.F.; van Leeuwen, F.E.; Holowaty, E.; *et al.* Lung cancer following chemotherapy and radiotherapy for hodgkin’s disease. *J. Nat. Cancer Instit.* **2002**, *94*, 182–192.
194. Travis, L.B.; Curtis, R.E.; Boice, J.D., Jr. Late effects of treatment for childhood hodgkin’s disease. *N. Engl. J. Med.* **1996**, *335*, 352–353.
195. Prochazka, M.; Granath, F.; Ekbohm, A.; Shields, P.G.; Hall, P. Lung cancer risks in women with previous breast cancer. *Eur. J. Cancer* **2002**, *38*, 1520–1525.

196. Kirova, Y.M.; Gambotti, L.; de Rycke, Y.; Vilcoq, J.R.; Asselain, B.; Fourquet, A. Risk of second malignancies after adjuvant radiotherapy for breast cancer: A large-scale, single-institution review. *Int. J. Radiat. Oncol. Biol. Phys.* **2007**, *68*, 359–363.
197. Endoh, D.; Suzuki, A.; Kuwabara, M.; Satoh, H.; Sato, F. Circadian variation in lung tumor induction with X-rays in mice. *J. Radiat. Res.* **1987**, *28*, 186–189.
198. Hashimoto, N.; Endoh, D.; Kuwabara, M.; Satoh, H.; Sato, F. Induction of lung tumors in C3H strain mice after single or fractionated irradiation with X-rays. *J. Vet. Med. Sci.* **1994**, *56*, 493–498.
199. Hashimoto, N.; Endoh, D.; Kuwabara, M.; Satoh, H.; Sato, F. Dose and dose-splitting effects of X-rays on lung tumour induction in mice. *Int. J. Radiat. Biol.* **1990**, *58*, 351–360.
200. Focan, C. Chronobiological concepts underlying the chronotherapy of human lung cancer. *Chronobiol. Int.* **2002**, *19*, 253–273.
201. Yuhas, J.M.; Walker, A.E. Exposure-response curve for radiation-induced lung tumors in the mouse. *Radiat. Res.* **1973**, *54*, 261–273.
202. Ullrich, R.L.; Jernigan, M.C.; Adams, L.M. Induction of lung tumors in rfm mice after localized exposures to X rays or neutrons. *Radiat. Res.* **1979**, *80*, 464–473.
203. Ullrich, R.L. Tumor induction in BALB/c female mice after fission neutron or gamma irradiation. *Radiat. Res.* **1983**, *93*, 506–515.
204. Ullrich, R.L.; Jernigan, M.C.; Satterfield, L.C.; Bowles, N.D. Radiation carcinogenesis: Time-dose relationships. *Radiat. Res.* **1987**, *111*, 179–184.
205. Coggle, J.E. The role of animal models in radiation lung carcinogenesis. *Radiat. Environ. Biophys.* **1991**, *30*, 239–241.
206. Grahn, D.; Lombard, L.S.; Carnes, B.A. The comparative tumorigenic effects of fission neutrons and cobalt-60 gamma rays in the B6CF1 mouse. *Radiat. Res.* **1992**, *129*, 19–36.
207. Zhang, Y.; Woloschak, G.E. *Rb* and *p53* gene deletions in lung adenocarcinomas from irradiated and control mice. *Radiat. Res.* **1997**, *148*, 81–89.
208. Zhang, Y.; Woloschak, G.E. Detection of codon 12 point mutations of the *K-ras* gene from mouse lung adenocarcinoma by “enriched” PCR. *Int. J. Radiat. Biol.* **1998**, *74*, 43–51.
209. Tuveson, D.A.; Jacks, T. Modeling human lung cancer in mice: Similarities and shortcomings. *Oncogene* **1999**, *18*, 5318–5324.
210. Salgia, R.; Skarin, A.T. Molecular abnormalities in lung cancer. *J. Clin. Oncol.* **1998**, *16*, 1207–1217.
211. Sekido, Y.; Fong, K.M.; Minna, J.D. Progress in understanding the molecular pathogenesis of human lung cancer. *Biochim. Biophys. Acta* **1998**, *1378*, F21–59.
212. D’Amico, D.; Carbone, D.; Mitsudomi, T.; Nau, M.; Fedorko, J.; Russell, E.; Johnson, B.; Buchhagen, D.; Bodner, S.; Phelps, R.; *et al.* High frequency of somatically acquired *p53* mutations in small-cell lung cancer cell lines and tumors. *Oncogene* **1992**, *7*, 339–346.
213. Hensel, C.H.; Xiang, R.H.; Sakaguchi, A.Y.; Naylor, S.L. Use of the single strand conformation polymorphism technique and PCR to detect *p53* gene mutations in small cell lung cancer. *Oncogene* **1991**, *6*, 1067–1071.
214. Takahashi, T.; Takahashi, T.; Suzuki, H.; Hida, T.; Sekido, Y.; Ariyoshi, Y.; Ueda, R. The *p53* gene is very frequently mutated in small-cell lung cancer with a distinct nucleotide substitution pattern. *Oncogene* **1991**, *6*, 1775–1778.



215. Sameshima, Y.; Matsuno, Y.; Hirohashi, S.; Shimosato, Y.; Mizoguchi, H.; Sugimura, T.; Terada, M.; Yokota, J. Alterations of the *p53* gene are common and critical events for the maintenance of malignant phenotypes in small-cell lung carcinoma. *Oncogene* **1992**, *7*, 451–457.
216. Symonds, H.; Krall, L.; Remington, L.; Saenz-Robles, M.; Lowe, S.; Jacks, T.; van Dyke, T. *P53*-dependent apoptosis suppresses tumor growth and progression *in vivo*. *Cell* **1994**, *78*, 703–711.
217. Sherr, C.J.; McCormick, F. The *Rb* and *p53* pathways in cancer. *Cancer cell* **2002**, *2*, 103–112.
218. Olsson, A.Y.; Feber, A.; Edwards, S.; Te Poele, R.; Giddings, I.; Merson, S.; Cooper, C.S. Role of E2F3 expression in modulating cellular proliferation rate in human bladder and prostate cancer cells. *Oncogene* **2007**, *26*, 1028–1037.
219. Das, S.K.; Hashimoto, T.; Shimizu, K.; Yoshida, T.; Sakai, T.; Sowa, Y.; Komoto, A.; Kanazawa, K. Fucoxanthin induces cell cycle arrest at G0/G1 phase in human colon carcinoma cells through up-regulation of p21WAF1/Cip1. *Biochim. Biophys. Acta* **2005**, *1726*, 328–335.
220. Vojtek, A.B.; Der, C.J. Increasing complexity of the ras signaling pathway. *J. Biol. Chem.* **1998**, *273*, 19925–19928.
221. Califano, R.; Landi, L.; Cappuzzo, F. Prognostic and predictive value of *K-ras* mutations in non-small cell lung cancer. *Drugs* **2012**, *72*, 28–36.
222. Bongiorno, P.F.; Whyte, R.I.; Lesser, E.J.; Moore, J.H.; Orringer, M.B.; Beer, D.G. Alterations of *K-ras*, *p53*, and *erbB-2/neu* in human lung adenocarcinomas. *J. Thorac. Cardiovasc. Surg.* **1994**, *107*, 590–595.
223. Boice, J.D., Jr.; Preston, D.; Davis, F.G.; Monson, R.R. Frequent chest X-ray fluoroscopy and breast cancer incidence among tuberculosis patients in massachusetts. *Radiat. Res.* **1991**, *125*, 214–222.
224. Bhatia, S.; Robison, L.L.; Oberlin, O.; Greenberg, M.; Bunin, G.; Fossati-Bellani, F.; Meadows, A.T. Breast cancer and other second neoplasms after childhood hodgkin’s disease. *N. Engl. J. Med.* **1996**, *334*, 745–751.
225. Sankila, R.; Garwicz, S.; Olsen, J.H.; Dollner, H.; Hertz, H.; Kreuger, A.; Langmark, F.; Lanning, M.; Moller, T.; Tulinius, H. Risk of subsequent malignant neoplasms among 1,641 hodgkin’s disease patients diagnosed in childhood and adolescence: A population-based cohort study in the five nordic countries. Association of the nordic cancer registries and the nordic society of pediatric hematology and oncology. *J. Clin. Oncol.* **1996**, *14*, 1442–1446.
226. Stovall, M.; Smith, S.A.; Langholz, B.M.; Boice, J.D., Jr.; Shore, R.E.; Andersson, M.; Buchholz, T.A.; Capanu, M.; Bernstein, L.; Lynch, C.F.; *et al.* Dose to the contralateral breast from radiotherapy and risk of second primary breast cancer in the wecare study. *Int. J. Radiat. Oncol. Biol. Phys.* **2008**, *72*, 1021–1030.
227. Brooks, J.D.; Boice, J.D., Jr.; Stovall, M.; Reiner, A.S.; Bernstein, L.; John, E.M.; Lynch, C.F.; Mellemkjaer, L.; Knight, J.A.; Thomas, D.C.; *et al.* Reproductive status at first diagnosis influences risk of radiation-induced second primary contralateral breast cancer in the wecare study. *Int. J. Radiat. Oncol. Biol. Phys.* **2012**.
228. Thomas, D.B.; Rosenblatt, K.; Jimenez, L.M.; McTiernan, A.; Stalsberg, H.; Stemhagen, A.; Thompson, W.D.; Curnen, M.G.; Satariano, W.; Austin, D.F.; *et al.* Ionizing radiation and breast cancer in men (United States). *Cancer Causes Control* **1994**, *5*, 9–14.

229. Ronckers, C.M.; Erdmann, C.A.; Land, C.E. Radiation and breast cancer: A review of current evidence. *Breast Cancer Res.* **2005**, *7*, 21–32.
230. Imaoka, T.; Nishimura, M.; Iizuka, D.; Daino, K.; Takabatake, T.; Okamoto, M.; Kakinuma, S.; Shimada, Y. Radiation-induced mammary carcinogenesis in rodent models: What's different from chemical carcinogenesis? *J. Radiat. Res.* **2009**, *50*, 281–293.
231. Medina, D. The preneoplastic phenotype in murine mammary tumorigenesis. *J. Mammary Gland Biol. Neoplasia.* **2000**, *5*, 393–407.
232. Finerty, J.C.; Binhammer, R.T.; Schneider, M.; Cunningham, A.W. Neoplasms in rats exposed to single-dose total-body X radiation. *J. Nat. Cancer Instit.* **1953**, *14*, 149–157.
233. Shellabarger, C.J.; Cronkite, E.P.; Bond, V.P.; Lippincott, S.W. The occurrence of mammary tumors in the rat after sublethal whole-body irradiation. *Radiat. Res.* **1957**, *6*, 501–512.
234. Medina, D. Of mice and women: A short history of mouse mammary cancer research with an emphasis on the paradigms inspired by the transplantation method. *Cold Spring Harb. Perspect. Biol.* **2010**, *2*, a004523, doi: 10.1101/cshperspect.a004523.
235. Ullrich, R.L.; Preston, R.J. Radiation induced mammary cancer. *J. Radiat. Res.* **1991**, *32*, 104–109.
236. Deome, K.B.; Faulkin, L.J., Jr.; Bern, H.A.; Blair, P.B. Development of mammary tumors from hyperplastic alveolar nodules transplanted into gland-free mammary fat pads of female C3H mice. *Cancer Res.* **1959**, *19*, 515–520.
237. Barcellos-Hoff, M.H. Radiation-induced transforming growth factor beta and subsequent extracellular matrix reorganization in murine mammary gland. *Cancer Res.* **1993**, *53*, 3880–3886.
238. Barcellos-Hoff, M.H. The potential influence of radiation-induced microenvironments in neoplastic progression. *J. Mammary Gland Biol. Neoplasia.* **1998**, *3*, 165–175.
239. Barcellos-Hoff, M.H. How tissues respond to damage at the cellular level: Orchestration by transforming growth factor-[1] (tgf-[1]). *BJR Suppl.* **2005**, *27*, 123–127.
240. Barcellos-Hoff, M.H. Integrative radiation carcinogenesis: Interactions between cell and tissue responses to DNA damage. *Semin. Cancer Biol.* **2005**, *15*, 138–148.
241. Yu, Y.; Okayasu, R.; Weil, M.M.; Silver, A.; McCarthy, M.; Zabriskie, R.; Long, S.; Cox, R.; Ullrich, R.L. Elevated breast cancer risk in irradiated BALB/c mice associates with unique functional polymorphism of the *prkdc* (DNA-dependent protein kinase catalytic subunit) gene. *Cancer Res.* **2001**, *61*, 1820–1824.
242. DeOme, K.B.; Miyamoto, M.J.; Osborn, R.C.; Guzman, R.C.; Lum, K. Detection of inapparent nodule-transformed cells in the mammary gland tissues of virgin female BALB/cfC3H mice. *Cancer Res.* **1978**, *38*, 2103–2111.
243. Ethier, S.P.; Ullrich, R.L. Factors influencing expression of mammary ductal dysplasia in cell dissociation-derived murine mammary outgrowths. *Cancer Res.* **1984**, *44*, 4523–4527.
244. Ethier, S.P.; Ullrich, R.L. Detection of ductal dysplasia in mammary outgrowths derived from carcinogen-treated virgin female BALB/c mice. *Cancer Res.* **1982**, *42*, 1753–1760.
245. Ethier, S.P.; Adams, L.M.; Ullrich, R.L. Morphological and histological characteristics of mammary dysplasias occurring in cell dissociation-derived murine mammary outgrowths. *Cancer Res.* **1984**, *44*, 4517–4522.

246. Ethier, S.P.; Ullrich, R.L. Induction of mammary tumors in virgin female BALB/c mice by single low doses of 7,12-dimethylbenz[a]anthracene. *Jo. Nat. Cancer Instit.* **1982**, *69*, 1199–1203.
247. Ullrich, R.L.; Bowles, N.D.; Satterfield, L.C.; Davis, C.M. Strain-dependent susceptibility to radiation-induced mammary cancer is a result of differences in epithelial cell sensitivity to transformation. *Radiat. Res.* **1996**, *146*, 353–355.
248. Barcellos-Hoff, M.H.; Ravani, S.A. Irradiated mammary gland stroma promotes the expression of tumorigenic potential by unirradiated epithelial cells. *Cancer Res.* **2000**, *60*, 1254–1260.
249. Danielson, M. Hemodynamic effects of diuretic therapy in hypertension. *Acta pharmacol. Toxicol.* **1984**, *54*, 33–36.
250. Nguyen, D.H.; Oketch-Rabah, H.A.; Illa-Bochaca, I.; Geyer, F.C.; Reis-Filho, J.S.; Mao, J.H.; Ravani, S.A.; Zavadil, J.; Borowsky, A.D.; Jerry, D.J.; *et al.* Radiation acts on the microenvironment to affect breast carcinogenesis by distinct mechanisms that decrease cancer latency and affect tumor type. *Cancer cell* **2011**, *19*, 640–651.
251. Barcellos-Hoff, M.H.; Brooks, A.L. Extracellular signaling through the microenvironment: A hypothesis relating carcinogenesis, bystander effects, and genomic instability. *Radiat. Res.* **2001**, *156*, 618–627.
252. Barcellos-Hoff, M.H.; Park, C.; Wright, E.G. Radiation and the microenvironment—Tumorigenesis and therapy. *Nat. Rev. Cancer* **2005**, *5*, 867–875.
253. Barcellos-Hoff, M.H.; Medina, D. New highlights on stroma-epithelial interactions in breast cancer. *Breast Cancer Res.* **2005**, *7*, 33–36.
254. Alberts, B. *Molecular Biology of the Cell*, 5th ed.; Garland Science: New York, NY, USA, 2008.
255. Andarawewa, K.L.; Paupert, J.; Pal, A.; Barcellos-Hoff, M.H. New rationales for using tgfbeta inhibitors in radiotherapy. *Int. J. Radiat. Biol.* **2007**, *83*, 803–811.
256. Andarawewa, K.L.; Erickson, A.C.; Chou, W.S.; Costes, S.V.; Gascard, P.; Mott, J.D.; Bissell, M.J.; Barcellos-Hoff, M.H. Ionizing radiation predisposes nonmalignant human mammary epithelial cells to undergo transforming growth factor beta induced epithelial to mesenchymal transition. *Cancer Res.* **2007**, *67*, 8662–8670.
257. Castiglioni, F.; Terenziani, M.; Carcangiu, M.L.; Miliano, R.; Aiello, P.; Bertola, L.; Triulzi, T.; Gasparini, P.; Camerini, T.; Sozzi, G.; *et al.* Radiation effects on development of HER2-positive breast carcinomas. *Clin. Cancer Res.* **2007**, *13*, 46–51.
258. Arima, Y.; Hayashi, H.; Sasaki, M.; Hosonaga, M.; Goto, T.M.; Chiyoda, T.; Kuninaka, S.; Shibata, T.; Ohata, H.; Nakagama, H.; *et al.* Induction of ZEB proteins by inactivation of *Rb* protein is key determinant of mesenchymal phenotype of breast cancer. *J. Biol. Chem.* **2012**, *287*, 7896–7906.

© 2013 by the authors; licensee MDPI, Basel, Switzerland. This article is an open access article distributed under the terms and conditions of the Creative Commons Attribution license (<http://creativecommons.org/licenses/by/3.0/>).

## References

1. Hall, E.J.; Giaccia, A.J., Radiobiology for the radiologist. 7th ed.; Wolters Kluwer Health/Lippincott Williams & Wilkins: Philadelphia, 2012; p p.
2. Hershman, J.M.; Okunyan, A.; Rivina, Y.; Cannon, S.; Hogen, V., Prevention of DNA double-strand breaks induced by radioiodide-(131)i in frtl-5 thyroid cells. *Endocrinology* **2011**, 152, 1130-1135.
3. Williams, D., Cancer after nuclear fallout: Lessons from the chernobyl accident. *Nature reviews. Cancer* **2002**, 2, 543-549.
4. Bozhok, Y.; Greenebaum, E.; Bogdanova, T.I.; McConnell, R.J.; Zelinskaya, A.; Brenner, A.V.; Zurnadzhly, L.Y.; Zablotska, L.; Tronko, M.D.; Hatch, M., Na cohort study of thyroid cancer and other thyroid diseases after the chernobyl accident: Cytohistopathologic correlation and accuracy of fine-needle aspiration biopsy in nodules detected during the first screening in ukraine (1998-2000). *Cancer* **2009**, 117, 73-81.
5. Miller, A.C.; Stewart, M.; Rivas, R., DNA methylation during depleted uranium-induced leukemia. *Biochimie* **2009**, 91, 1328-1330.
6. Miller, A.C.; McClain, D., A review of depleted uranium biological effects: In vitro and in vivo studies. *Reviews on environmental health* **2007**, 22, 75-89.
7. Kurz, E.U.; Lees-Miller, S.P., DNA damage-induced activation of atm and atm-dependent signaling pathways. *DNA repair* **2004**, 3, 889-900.
8. Lavin, M.F.; Kozlov, S., Atm activation and DNA damage response. *Cell cycle* **2007**, 6, 931-942.
9. Gatti, R.A.; Tward, A.; Concannon, P., Cancer risk in atm heterozygotes: A model of phenotypic and mechanistic differences between missense and truncating mutations. *Molecular genetics and metabolism* **1999**, 68, 419-423.
10. Gatti, R.A.; Berkel, I.; Boder, E.; Braedt, G.; Charmley, P.; Concannon, P.; Ersoy, F.; Foroud, T.; Jaspers, N.G.; Lange, K., et al., Localization of an ataxia-telangiectasia gene to chromosome 11q22-23. *Nature* **1988**, 336, 577-580.
11. Gatei, M.; Young, D.; Cerosaletti, K.M.; Desai-Mehta, A.; Spring, K.; Kozlov, S.; Lavin, M.F.; Gatti, R.A.; Concannon, P.; Khanna, K., Atm-dependent phosphorylation of nibrin in response to radiation exposure. *Nature genetics* **2000**, 25, 115-119.
12. Modesti, M.; Hesse, J.E.; Gellert, M., DNA binding of xrcc4 protein is associated with v(d)j recombination but not with stimulation of DNA ligase iv activity. *The EMBO journal* **1999**, 18, 2008-2018.

## **CONCLUSION**

## CONCLUSION

The first goal of this dissertation was to optimize the DEL high throughput assay (DEL HTS) for drug discovery screening of small molecule libraries to uncover drugs that protect and mitigate radiation-induced lethality and genomic instability. The second goal was to develop and characterize the lead radiation mitigator molecule, Yel002, identified in DEL high throughput screening for commercialization as a “stockpile” therapy for use in nuclear and radiological accidents to prevent mass casualties due to acute radiation syndrome (ARS).

The original plate-based DEL assay was adapted to microwell format for high throughput assessment of carcinogenic potential in novel chemical entities by my colleagues Dr. Hontzeas and Dr. Hafer. This new assay was proposed as a screening tool for radiation-modulating compounds from large collections of commercially available drug-like molecules such as the Asinex™ targeted library. DEL HTS screening project was a part of a larger effort of UCLA’s Center for Medical Countermeasures against Radiation (CMCR) established in 2005 with the purpose of generating novel chemotherapies for prophylaxis and treatment of radiation injuries. The newly optimized, yeast-based DEL high throughput screen presented a novel approach to identifying potential drugs against radiation toxicity. To our best knowledge, it is the only screen that simultaneously assesses molecule’s ability to modulate radiation-induced cell death and its genomic stability – the two main consequences of radiation exposure in biological systems.

We found that in yeast, akin to mammalian cells, sensitivity to radiation varies with the stages of the cell cycle. Yeast cells were the most sensitive to radiation-induced cell death and DNA-deletion (DEL events) during the lag and exponential growth phases

(mostly S/G2) of the cell cycle. Interestingly, the effect of cell cycle phase on survival was different than its effect on DNA-deletions – survival was less affected by the phase than genomic instability. Additionally, protection against radiation genotoxicity offered by L-ascorbic acid and DMSO was only significant in dividing cells. These findings have modified the DEL HTS screening protocol to add an additional cell phase synchronization step. Looking back at the detected rise in sensitivity in S/G2 phase in RS112 cells triggered a post-factum epiphany – perhaps it is not the rise in sensitivity but a rise in the detection of DNA damage. Genomic instability in the DEL assay is measured as product of a homologous recombination (HR), a reversion to a functional His3 gene per 10,000 surviving cells. During the S/G2 phase the predominant DNA repair mechanism is HR and thus a rise in the number of registered DEL events might simply mean an increase in HR products for the same amount of DNA damage sustained during other phases of the cell cycle. Simply put, more damage is detected because cell preferentially repairs the damage in way that generates more His3 revertants. Alternatively, the number of increased DEL events following irradiation in S/G2 might be due to the relaxed state of the DNA molecule that makes it more susceptible to damage in the first place, as some literature suggests.

Next, before we set out to screen thousands of small molecule compounds we validated DEL high throughput's ability to detect radiation-induced damage and the effects of bona fide radiation-modulating compounds. The DEL HTS assay effectively demonstrated a dose-response relationship between increasing radiation doses and radiation-induced cell killing and DEL events.

Armed with the optimized DEL HTS assay we have screened over 5,000 compounds from the Asinex™ target library of biologically active compounds before we uncovered

Yel002 and validated it in a modified plate-based DEL Assay. Because the targeted libraries were optimized for “druggability,” transition into a mouse model did not necessitate extensive preliminary toxicity studies. We also knew that Yel002 did not demonstrate overt toxicities in cells from concurrent in vitro experiments conducted in the laboratory of Dr. William McBride. However, we still proceeded with a small pilot study to assess potential side effects of Yel002 and five other hit molecules at doses exceeding our projected therapeutic dose of 75mg/kg. No side effects were registered and we proceeded first to test the 6 hit molecules’ capacity to protect against radiation-induced lethality. In this study the selected compounds were injected at -24 hr and -1 hr prior to lethal irradiation (LD100/30). Aside from a small increase in radiation death latency the effects were minimal. However, when we have attempted to administer the compounds on a mitigation therapy protocol at +1 hr and +24 hrs, Yel002 and Yel002 have demonstrated remarkable success and rescued ~66% of lethally-irradiated animals. Yel002 eventually became the lead molecule ahead of Yel001 because Yel002 demonstrated a better mitigation capacity when administered on the protracted administration schedule where the first injection is administered at 24 hrs following ionizing radiation (IR) exposure with additional injections at 48, 72, 96, an 120 hours.

It is important to note that Dr. Mike Jung enabled all Yel002 experiments described in this thesis aside from the initial screening studies. Neither Yel002 nor Yel001 were available from the manufacturer of the screening libraries and thus all of the compounds had to be synthesized de novo at UCLA. Throughout the years we have relied on Dr. Jung and his chemical synthesis laboratory not only for supply of Yel002 but also for the structural analogs constructed based on Yel001’s and Yel002’s structures. One of these



analogs, CJ010 is another potent radiation mitigator and will be further explored and developed in the very near future.

We validated the activity of the structural analogs in the plate-based DEL assay but not in the in vivo models, therefore it is possible that these analogs might have activity in mammalian systems. We relied on the yeast-based high throughput and plate-based assays for the identification of radiation-mitigating compounds with the assumption that modulation of radiation response in a cell is a strictly conserved mechanism from simple eukaryotes to higher mammals. While it is certainly true that for example pathways like DNA repair are remarkably similar, some small changes are still present even in the most highly conserved protein homologues. Thus, it is possible that an analog that might have efficacy in a mammalian cell will not have any in a yeast cell due to a minor variation in the binding protein target.

We demonstrated that Yel002 reduces radiation-induced lethality in the hematopoietic syndrome dose range by accelerating the recovery of the hematopoietic and immune system components. We believe that Yel002 prevents cell death (apoptosis or necrosis) and replicative senescence in the hematopoietic stem cells and the more differentiated progenitors. The fact that Yel002 mitigates survival when administered at 24 hrs after irradiation is also consistent with the onset of apoptosis during the same time. We arrived at this conclusion by looking at the prevention of IR-induced senescence in primary human keratinocytes with corresponding molecular profile to support it and at increased survival of murine lymphoblast cells after irradiation. Further studies are necessary to definitively demonstrate mitigation of apoptosis, necrosis, and replicative senescence in the bone marrow cells.

Additionally, we were able to show that Yel002 mitigates radiation-induced DNA damage and prevents radiation leukemogenesis in mice. In the study that demonstrated that Yel002 reduces DNA damage in thyroid cells the source of radiation was radioactive iodine isotope I-131, a common fallout product following a nuclear accident or bomb detonation. These two very important aspects of Yel002's activity set it above any currently reported radiation mitigator therapies because it mitigates both the early and the late radiation effects. Furthermore, ability to mitigate IR-induced carcinogenesis might enable Yel002's application in a clinical setting as an agent against secondary cancers often experienced by radiotherapy patients in remission.

On the cellular level Yel002 appears to act via the PI3K/Akt pathway. Our protein microarray assays examining protein level changes and phosphorylation state, and gene expression analyses have converged on this particular pathway following incubation with Yel002 in murine lymphocytes. This multifaceted pathway has been implicated in a variety of diseases including cancer and type 2 diabetes and directs cell fate in response to receptor stimulation. Depending on its downstream substrates, PI3K/Akt may act in either pro-survival, in pro-apoptotic, or in a pro-senescence manner. Because we observed across the board increase in survival, we naturally gravitated towards the hypothesis that Yel002 affects the pro-survival aspect of the PI3K/Akt signaling cascade with the precise target within the pathway remaining to be determined.

Some of the first necessary experiments to definitively implicate PI3K pathway will include using PI3K kinase inhibitor (e.g. BEZ235, LY294003, BYL719 and others). If indeed PI3K is important for survival, then cells co-incubated with Yel002 will not survive above the control levels in CFC assays. Following validation studies activation of the Akt cascade

and its substrates can be probed with Western Blotting (WB) with the same inhibitor and Yel002 treatment in irradiated and non-irradiated cells. Confirmed affected proteins might then be sequentially silenced with either RNA interference assays (e.g. shRNA) or with commercially available inhibitors if such exist.

In conclusion, our screening and early drug development efforts have produced an effective radiation mitigator Yel002 that is currently being explored as a potential stockpile countermeasure against radiation by the Biomedical Advanced Research and Development Authority (BARDA) with the Office of the Assistant Secretary for Preparedness and Response in the U.S. Department of Health and Human Services. Many additional studies are still ahead of Yel002's FDA approval for its use as a radiation mitigator in the field and hospital setting in response to public health radiological emergency. However, we are hopeful that the development of Yel002 might open many new possibilities in the field of radiation mitigation – maybe in a therapeutic setting or as a research tool to uncover new signaling cascades that mediate radiation responses in cells and tissues.